Understanding the role of Post-translational modifications of human non-histone chromatin protein PC4

A Thesis submitted for the degree of

Doctor of Philosophy

By

Pallabi Mustafi

To

Molecular Biology and Genetics Unit

Jawaharlal Nehru Centre for Advanced Scientific Research

Jakkur, Bangalore-560064, India

February, 2021

Dedicated to My Parents

Table of contents

2.1.3. Whole cell extract preparation

2.1.4. DNA isolation

2.1.5. RNA isolation

2.1.5.1.RNA extraction from mammalian cells

2.1.5.2.RNA extraction from Patient samples

2.1.6. Nucleic Acid estimation

2.1.7. Estimation of protein concentration

2.1.8. Agarose gel electrophoresis

2.1.9. SDS-Polyacrylamide gel electrophoresis (SDS-PAGE)

2.1.10. Western blot analysis

2.1.11.Real time quantitative RT-PCR

2.2. Cloning

2.2.1. Sub-cloning

2.2.2. Site-directed mutagenesis

2.3. Protein Purification

2.3.1. C-terminal His-tagged PC4purification

2.3.2. Purification of acetylation defective PC4 mutants

2.3.3. Purification of bacterial expressed untagged PC4

2.3.4. Purification of bacterial expressed untagged Phospho-defective PC4 mutants and phosphomimic PC4

2.3.5. Purification of His-tagged human somatic linker histone H1 variants

2.4.7. Dot blot assay

2.4.8. Isothermal Calorimetry

2.5. Protocol for different in vivo assays

2.5.1. Active chromatin and heterochromatin isolation

2.5.2. Nuclear fractionation

2.5.3. Micrococcal Nuclease (MNase) assay

2.5.4. Chromatin immunoprecipitation assay (ChIP)

2.5.5. Indirect Immunocytochemistry

2.5.6. Fluorescence activated cell sorting (FACS)

2.5.6.1.Cell cycle analysis by FACS

2.5.6.2.Cell Sorting by FACS

2.5.7. Hematoxylin and Eosin (H&E) staining

2.5.8. Immunohistochemistry

2.5.9. Immuno-pull down

2.5.9.1 M2 agarose pull down to study interacting partners

2.5.9.2.M2 agarose pull down from chromatin fraction

2.5.9.3.Pull down using purified PC4K26-28ac and purified PC4 antibody to study interacting partners

2.5.10 Cell Synchronization for studying PC4 acetylation across cell cycle

2.5.10.1.G0/G1 block

2.5.10.2.G1/S block

3.1.3 Determination and validation of CKII phosphorylation sites of PC4

3.1.4 Casein Kinase II mediated phosphorylation of PC4 is critical for its interaction with linker histone H1

3.1.5 Quantitative Estimation of interaction of Phosphorylated PC4 with linker H1

3.1.6 Phosphorylation of PC4 mediates its interaction with somatic linker H1 variants

3.1.7. Interactions of Phosphomimic PC4 (PM-PC4) with linker histone H1 in vitro

3.1.8 Phosphomimic PC4 interaction with different domains of linker histone H1

3.1.9 Phosphorylation of PC4 mediates its interaction with linker histone H1 in cells

3.1.10 Phosphomimic PC4 promotes condensation of a reconstituted nucleosomal array

3.1.10.1 Determining concentration of Phosphomimic-PC4 (PM-PC4) mediating nucleosomal compaction

3.1.10.2 PM-PC4 begins to induce compaction at a lower concentration than unmodified PC4

3.1.10.3 Phosphomimic PC4 bound nucleosomal array achieves higher sedimentation coefficient value indicating greater compaction

3.2.3.2 PC4 K26 28ac antibody specifically probes the acetylated PC4 in vitro

3.2.3.2 PC4 K26 28ac antibody specifically probes the acetylated PC4 in cells

3.2.4 Acetylation of PC4 across cell cycle

3.2.4.1 Localisation of acetylated PC4 during cell cycle

3.2.4.2 Acetylation of PC4 reduces upon mitosis

3.2.4.3 Acetylated PC4 is not associated with chromatin upon mitotic arrest

3.2.5 Lysine 26 and 28 residues in PC4 gets acetylated by p300 in vivo

3.2.5.1 Acetylation of PC4 reduces upon treatment with p300 specific inhibitor

3.2.5.2 Acetylation of PC4 reduces upon silencing p300

3.2.5.3 Acetylation of PC4 increases upon treatment with a p300 specific activator

3.2.6 PC4K26,28ac antibody specifically pulls down PC4 from cells

3.2.7 Studying the occupancy of Acetylated PC4 at PC4 target gene promoters

3.2.8 Acetylation of PC4 in oral cancer cells

3.2.9 Acetylated PC4 interacts with elongating RNA polymerase II

3.2.10 Studying the levels of PC4 acetylation in oral cancer patient samples

DECLARATION

I hereby declare that this thesis entitled "Understanding the role of Post-translational modifications of human non-histone chromatin protein PC4" is an authentic result of investigations carried out by me at the Molecular Biology and Genetics Unit, Jawaharlal Nehru Centre for Advanced Scientific Research, Bangalore, India under the supervision of Prof. Tapas K. Kundu and that this work has not been submitted elsewhere for the award of any degree or diploma.

In keeping with the general practice of reporting scientific observations, due acknowledgement has been made whenever the work described has been based on the findings of other investigators. Any omission, which might have occurred by oversight or misjudgement, is regretted.

Date: Feb, 8, 2021

Place: Bangalore

Pallabi Mustafi

Pallabi Mustafi

जवाहरलाल नेहरु उन्नत वैज्ञानिक अनुसंधान केन्द्र
(मान्यता प्राप्त विश्वविद्यालय)
JAWAHARLAL NEHRU CENTRE FOR ADVANCED SCIENTIFIC RESEARCH
(A Deemed University)
जक्कूर, बेंगलूर - 560 064, भारत / Jakkur P.O., Bengaluru - 560 064. INDIA

Prof. Tapas K. Kundu
Transcription and Disease Laboratory
Molecular Biology and Genetics Unit
Jawaharlal Nehru Centre for Advanced Scientific Research
Bangalore-560064
India

CERTIFICATE

This is to certify that the work described in this thesis entitled, **"Understanding the role of Posttranslational modifications of human non-histone chromatin protein PC4"**, is the result of investigation carried out by Ms. Pallabi Mustafi in the Molecular Biology and Genetics Unit, Jawaharlal Nehru Centre for Advanced Scientific Research (A Deemed University), Bangalore-560064, India, under my supervision, and the results presented in this thesis have not previously formed the basis of any other diploma, degree or fellowship.

Date: Feb 8, 2021
Place: Bangalore 64

Prof. Tapas K. Kundu

Acknowledgement

I would like to begin with immense appreciation and pleasure the contribution of my mentor Prof. Tapas K. Kundu because of whom this Thesis work has seen the light of the day. I acknowledge his contribution in this journey of five years in shaping my scientific and worldly outlook towards life. His rigour and perspectives has helped me in stimulating my interest towards science and in having bigger dreams and intrigued the planning to achieve the same. His training not only enables you to plan and perform bench work, but helps you do develop as a confident individual to be involved in scientific organizational work and mediating scientific interaction and he teaches you to grab every opportunity that helps you be a better scientist. His involvement in community services like taking forward science not only to the international podium through successful collaborations, but also popularizing science by taking it to the school kids of some of the remotest villages of India has been really inspiring and makes you realize your responsibility as a scientific member of this country. I thank him for giving me an opportunity to work in collaborations and the freedom to lead my own project as well as constantly guiding me on the way. He has helped me in building my scientific temper as well as how to manage lab issues and take up responsibilities in times of crisis. I take this opportunity to express my heartfelt gratitude towards him for this enriching experience of my life.

It gives me great pleasure in acknowledging Prof. Ranga Uday Kumar, in taking the extra step of managing the responsibility of our lab in the absence of Prof. Kundu. His critical insight to our work not only during our MBGU work presentations but also during our lab meetings have been really helpful. I also acknowledge the all the MBGU and NSU faculties Prof. M.R.S. Rao, Prof. Anand, Prof. Ranga, Prof. Hemalatha Balram, Prof. Kaustuv Sanyal, Prof. Maneesha Inamdar, Prof.Namita Surolia, Dr.Ravi Manjithaya, Dr.Kushagra Bansal, Dr.James Chelliah and Dr.Sheeba Vasu for their excellent course work and the positive criticisms extended in the course of my research in terms of experimental designing, suggestions and feasibility of the outcome and with whom I interacted at various times during my stay in JNCASR and who have been kind enough in suggesting ways to improve the quality of my work. I owe my gratitude to Dr.N. Ravi Sundaresan (Indian Institute of Science) for the valuable suggestions during my comprehensive examination. I also thank Dr.Ravi Manjithaya for his contribution in instilling scientific curiosity and his meticulous planning of work has been a learning experience during my first lab rotation. I also thank Dr. Ramesh for teaching us the basic lab techniques and

helping in our early stages of MS in handling lab equipment that has helped us immensely in our later stages of research work.

I am thankful to my collaborator, Prof. Guohong Li, National laboratory of Bio-macromolecules, CAS Center for Excellence in Biomacromolecules, Institute of Biophysics, Chinese Academy of Science, Beijing, China for extending his immense support and contribution to my work and providing me an opportunity to work and learn in his laboratory. It is very difficult to find a very good scientist who is also an amazing human being like Prof. Li and I really cherish my brief association with him. I appreciate Mingli Hu in helping me in my experiments in a place where I had no clue about the language, and also all the lab members of Prof.Li especially, Ting, Yuting Liu for making my stay in China, so comfortable and enjoyable.

I would like to acknowledge Dr. Madhav Nilakanth Mugale, Sadan Pandey and Kaveri R.Washimkar for their contribution in carrying out IHC studies in oral cancer patient samples and I would like to acknowledge Dr.Azeem , from SDU, Kolar hospital by facilitating our work with patient samples that has been integral part of my thesis work.

I would like extend my sincere gratitude to all my college teachers specially my H.O.D, Dr.A.K. Mitra and Dr. Sudeshna Shyam Chowdhury for their constant encouragement to take up research in my future and instilling in me the interest for research early on during my bachelors by providing opportunities to work in projects and present in various seminars. I would also like to thank my school biology teacher Dr. Sucharita Chatterjee for building up my interest in the subject of biology and made me realize to pursue something for the love of it.

I would now like to acknowledge all my present and past labmates for making my stay in TDL a memorable experience. I would like to thank Dr.Karthigeyan, Dr.Parijat Senapati, Dr.Amrutha, Dr.Amit, Dr.Stephanie, Dr.Sweta, Dr.Arnab, Deepthi, Dr.Surabhi, Dr.Suchismita, Dr.Shilpa, Moumita, Smitha, Aditya, Akash, Siddharth, Raktim, Dr Sarmistha, Dr Manoj, Dr.Vanajakshi, Dr.Jagannath, Dr.Shrinka, Debanjan, Shubham, Vinay, Koyel, Padmalaya, Vishakah Nikitha, Taniya, Dharaneeshwar and Ila. A special thanks to Kruthi Gowda for keeping us away from the worries of the most of the official work and for her always ready to help attitude. I would like to thank Dr.Stephanie and Dr.Arnab for being such wonderful and helpful seniors who would not only help you with critical suggestions as well as with a positive attitude. I would like to thank Gowda ji and Sunil for making our life so easy

in the lab and keep our lab going on a daily basis. I would thank Sunil for his effort in bringing the patient samples from SDU, Kolar hospital and making our IHC work happen smoothly.

I owe my deepest gratitude to Dr.Arnab and Vinay, whom by all means I adore as friends and possess enormous respect from the deepest core of my heart. Their sense of worldly understanding had helped me sail through some of the roughest patches and grow both as a professional and a personal entity.

I would like to thank Dr.Suresh, Dr Sreedevi, Dr.Piyush and Dr.Gaurav for making stay in Autophagy lab during my first lab rotation an enjoyable and wonderful experience

My special thanks to all my batchmates Siddharth, Priya, Veena, Bhavna, Shubhangini, Krishnendu, Praveen, Aparna, Surabhi, Rima, Aditya, Yamini for all the lovely time that we have spent together during the course works. A special thanks to my Int.Ph.D batchmates Siddhrath, Veena and Bhavana for all the fun time we have spent together in the MS-lab and in NVSH and during the journey of Ph.D still being keeping our friendship tight. I would like to thank Disha, Deepak, Abhiroop, Dr.Vijay Jayram, Dr. Lakshmeeshah, Dr.Arnab, Dr.Divyesh, Dr.Raagesh, Dr.Ananya, Kushagra, Dr.Shantanu, Aishwarya Iyengar, Chitrang, Paramita, Suchismita, Preeti, Kuladeep, Chhavi, Rafi, Sambhavi, Ekashmi, Shambhu, Ankit, Rajarshi, Nikita, Badri, Swati for making my stay in JNC filled with wonderful memories at some point or the other. I would like to thank Utsa for all the engaging conversations we had on science, politics and food and the fun we had in organizing JNCASR Life Science Fest would be a lifetime experience to remember.

I would also like to thank some of my friends outside JNC, Ritam, Arnab, Pushpendu for always being there for me even being miles apart and always keeping up the positivity inside me.

I would like to thank Dr. Prakash for the animal facility, Dr.Suma for helping me with confocal imaging, Ms. Anita for sequencing, and Ms. Swaroopa and Dr. Narendra for the Flow Cytometry facility, which have been really helpful and necessary in shaping the present thesis. I acknowledge DST, and JNCASR for all the financial support for the Ph.D. programme.

I would like to express my heartfelt thanks to the Common Instrumentation Facility (CIF) of MBGU and JNCASR, admin, academic, purchase, library, complab, Dhanvantri and hostel facilities.

I would like to acknowledge scientists like Marie Curie, Rosalind Franklin for showing the courage, strength and perseverance that is exemplary to any young woman who aspires to be a scientist. I would also like to mention some woman leaders like Angela Merkel, Aung San Suu Ky and lives of Mother Teresa that has been truly inspirational to me as a woman and helped me learn the importance of good scientific vision and the importance of kindness and dedication.

Lastly, I would acknowledge those people for whom words would fall short: ‘My family’ for being the supporting pillars for me through all the ups and downs of my life. I would like to thank my sister who is like my second mother and also a friend and inspiration. I would also like to thank Debabrata Da and the apple of my eye, my cute bundle of joy, Hridaan. Finally, the two most important members of my life and my biggest support system, whom I can never acknowledge enough, Ma and Baba. Thanks to them for everything. I’ll always be grateful for having such wonderful and supportive parents. Thanks to my Ma for being the woman whom I’ll always look upto for my strength and who’ll always keep inspiring me to keep fighting and striving for better.

Abbreviations

µg- Microgram

µM- Micromolar

µm- Micrometre

ºC- Degree Celsius

ΔC - N-terminal globular domain

ΔN - C-terminal globular domain

ac- Acetylated

AcPC4 – Acetylated PC4

Ac mut – acetylation defective mutant

Ac mimic- acetylation mimic

APS- Ammonium persulfate

ATCC- American Type Culture Collection

ATP-Adenosine triphosphate

ChIP seq- Chromatin immunoprecipitation coupled to massively parallel DNA sequencing

CHX- Cycloheximide

CKII- Casien kinase 2

cm- Centimetre

CO_2- Carbon dioxide

CTD- C-terminal domain

DDR- DNA damage response

DMEM-Dulbecco's Modified Eagle medium

DMSO- Dimethyl sulfoxide

DTT- Dithiothreitol

EDTA- Ethylene diamine tetra acetate

EGTA- Ethylene glycol tetra acetate

EMSA- Electrophoretic mobility shift assay

FACS- Fluorescence activated cell sorting

FBS- Fetal bovine serum

FL -full length

HA- Haemaglutinin

HAT- Histone acetyltransferase

HDAC- Histone deacetylase

HP1 -Heterochromatin protein 1

IPTG- Isopropyl β-D thiogalactoside

KAT- Lysine acetyltransferase

kDa- KiloDalton

MTP5- Phosphodefective mutant

ng- Nanogram

NTD- N-terminal domain

Ni-NTA- Nickel Nitrilotriacetic acid

NP40- Nonidet P-40

O.D.600- Optical density at 600nm

ph- Phosphorylated

PAGE- Polyacrylamide gel electrophoresis

PBS- Phosphate buffer saline

PC4 -Human Positive co-activator 4

PM-PC4 – Phosphomimic PC4

PMSF- Phenyl methyl sulphonyl fluoride

PTM- Post translational modification

PVDF- Polyvinylidene fluoride

RA- Retinoic acid

RT- Reverse transcriptase

RT-Room temperature

siRNA- Silencing RNA

SDS- Sodium dodecyl sulphate

TBS- Tris buffered saline

TCF β1- T cell binding factor β1

TEMED- N, N, N', N'- tetramethyl ethylene diamine

TNBC- Triple negative breast cancer

Tris- tris-(hydroxymethyl)-aminomethane

w/v- Weight by volume

v/v- Volume by volume

Chapter 1: Introduction

Chapter outline

1.1 Eukaryotic Chromatin

The eukaryotic genome is a highly dynamic and complex nucleoprotein structure possessing a hierarchical order of chromatin organisation. The basic unit of the organisation is a nucleosome in which DNA is wrapped around histone octamer. The eukaryotic cell faces topological challenges of packaged genetic information as histone proteins mediated formation of nucleosome restrict access of DNA-binding transcription regulators to cis-regulatory DNA elements and the constant need to modulate gene expression in order to maintain cellular homeostasis (Clapier and Cairns, 2009). The highly dynamic nature of the eukaryotic genome and its transcriptional competency is achieved by diverse nuclear factors, including non-histone chromatin-associated proteins (CAPs), histone chaperones, ATP-dependent remodelling machinery, DNA methylation machinery, histone modifications and histone variants, enzymes that post-translationally modify chromatin proteins and the newly emerging role of RNA and RNA binding proteins. Eukaryotic chromatin displays structural dynamics at different hierarchical scales in a spatio-temporal manner. The basic unit of the chromatin, the nucleosome, follows the structural hierarchy from the 10nm filament to the 30nm filament which finally folds into the higher order chromatin structure of 100 to 400nm to accommodate in the nucleus (Figure 1.1). The dynamic nature of nucleosomes and higher order chromatin structure controls eukaryotic genome accessibility and thereby regulate DNA template dependent processes, like transcription, replication, recombination and repair. Technical progress has facilitated structural studies of nucleosomes and chromatin provided detailed insight into local chromatin organization and understanding of the functional and structural dynamics of nucleosomes and chromatin fibers.

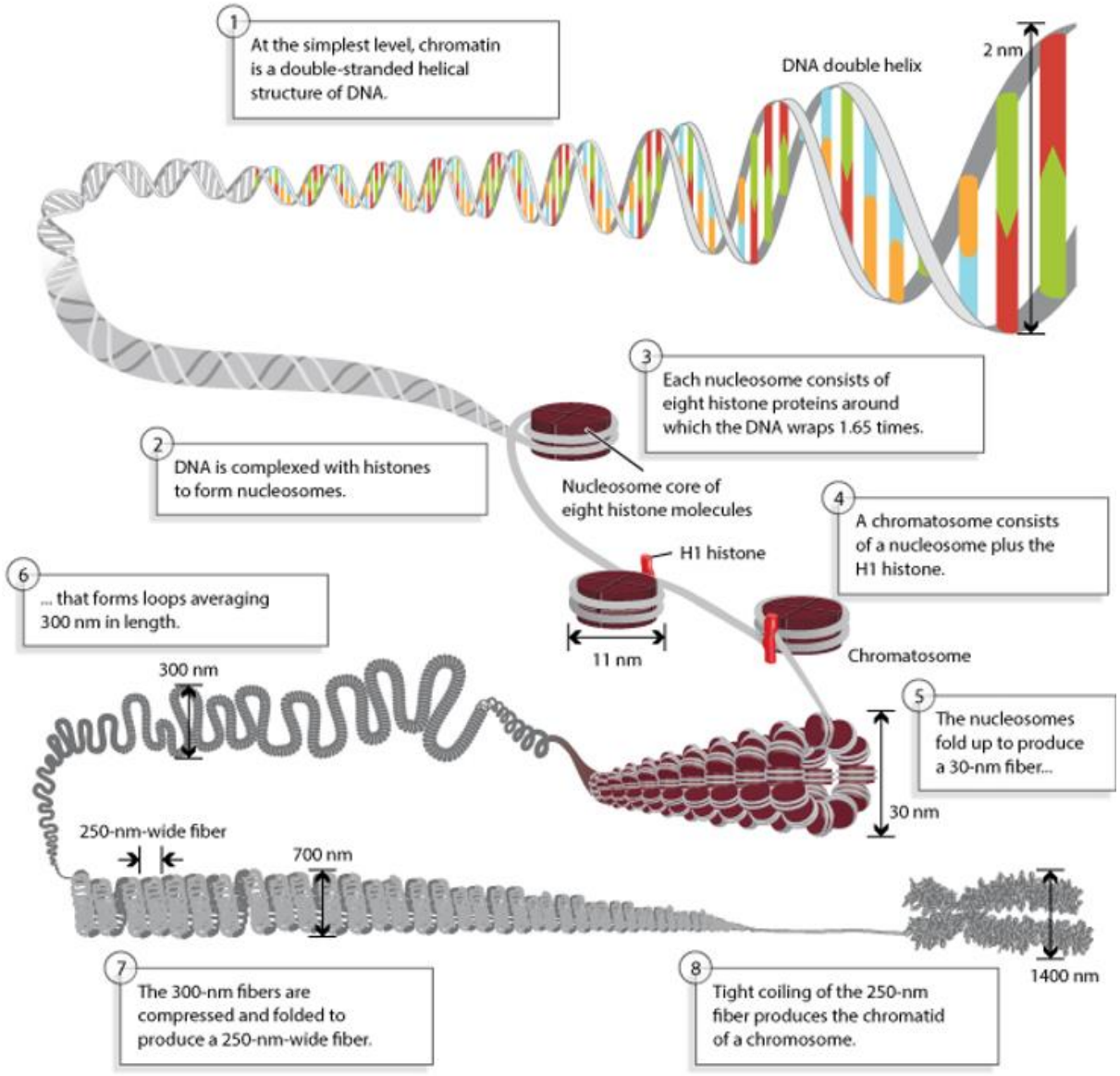

Figure1.1. The hierarchical organisation of the eukaryotic genome showing chromosomal DNA packaging inside nucleus with the help of positively charged histones starting from a basic nucleosome unit to a 30-nanometer chromatin fiber, which is further folded into loops averaging 300 nanometers in length. The chromatin loops are compressed and folded to produce a 250 nm-wide fiber, tightly coiled into the chromatid of a chromosome. (Figure adapted from Pierce, Benjamin. Genetics: A Conceptual Approach, 2nd ed, Nature Education ,2013).

Various crystal structures would represent just one possible state of the nucleosome and it is the incorporation of post-translational modifications (PTMs) and histone variants that potentiates a shift in the equilibrium between different structural states. This variability affects the compaction of the chromatin fibre and the interaction of nucleosomes with non-histone proteins. The nucleosome structure is stabilized by a multitude of protein–protein interactions within the histone octamer and through electrostatic and hydrogen bonds between protein and DNA over its entire length (Luger K at al., 1997, Davey CA,2002 and Rohs R et al., 2009). Majority of DNA–histone interactions occur between structured regions of the histones and DNA (Richmond TJ, Davey CA, 2003), whereas the flexible histone tails (the sites of most PTMs) extend away from nucleosomal DNA and are mainly involved in interaction with neighbouring nucleosomes or with nuclear factors (Luger K, Richmond TJ, 1998). *In vivo* studies revealed that histones turn over in a replication- and transcription-independent manner, and at a much more rapid rate than previously anticipated (Deal RB. et al., 2010 and Jamai A. et al., 2007); this, in turn, is at least in part determined by the intrinsic stability of the nucleosomes themselves. The stability of H2A.Z nucleosomes in response to variations in ionic strength have been studied (Hoch DA et la., 2007). The variant nucleosomes are shown to differ in their ability to be remodelled by the various ATP-dependent chromatin-remodelling factors (Goldman JA et al., 2010 and Angelov D et al., 2003).

The nucleosome organizing into chromatin fibres only results in modest changes in the rates of DNA exposure, suggesting that nucleosomes in chromatin fibres also undergo transient DNA breathing (Poirier MG, et al., 2008). More recently, single-molecule FRET approaches have identified an open state of the nucleosome during salt-dependent nucleosome assembly and disassembly (Böhm V et al., 2011 and Tims HS et al., 2011) (Figure1.1.1) characterized by a partial

disruption of the interface between the H2A–H2B dimer and the (H3–H4)$_2$ tetramer while the H2A–H2B dimers remain attached to the DNA.

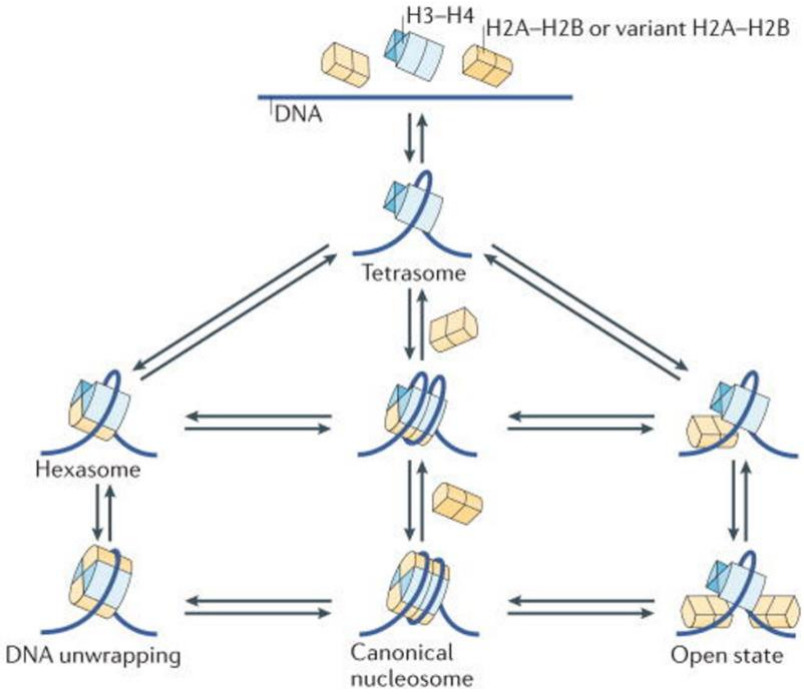

Figure1.1.1: Interchangeable structural states of nucleosome. These states include the tetrasome formed by the wrapping of ~80 bp DNA around an (H3–H4)2 tetramer, intermediates states forming Hexasomes (nucleosomes lacking one H2A–H2B heterodimer) during nucleosome assembly or disassembly and transcription. Structural transitions between these states are characterized either by the transient release of the DNA ends (DNA breathing) or by a transient opening of the interface between histone subcomplexes (open state). (Figure adapted from Karolin Luger K, Dechassa ML., Tremethick D J., 2012)

However, there are various contradictory interpretations of secondary chromatin structures which have been defined to produce chromatin fibres (30nm fibres) regulating all DNA- and chromosome dependent processes. Two competing models, the solenoid and zigzag arrangement of nucleosomes, have been proposed on the basis of *in vitro* data (Tremethick DJ., 2007) (1.1.2). The solenoid model depicted a one start model where consecutive nucleosomes interact with each other and follow a helical trajectory with bending of linker

DNA (Kruithof M, et al. 2009) whereas the 'two-start' zigzag structure shows two rows of nucleosomes forming a two-start helix so that alternate nucleosomes (for example, N1 and N3) become interacting partners, with relatively straight linker DNA (Dorigo B, et al., 2004) (Figure 1.1.2). The two stacks in a zig-zag model can further twist and coil producing different forms of the zigzag model.

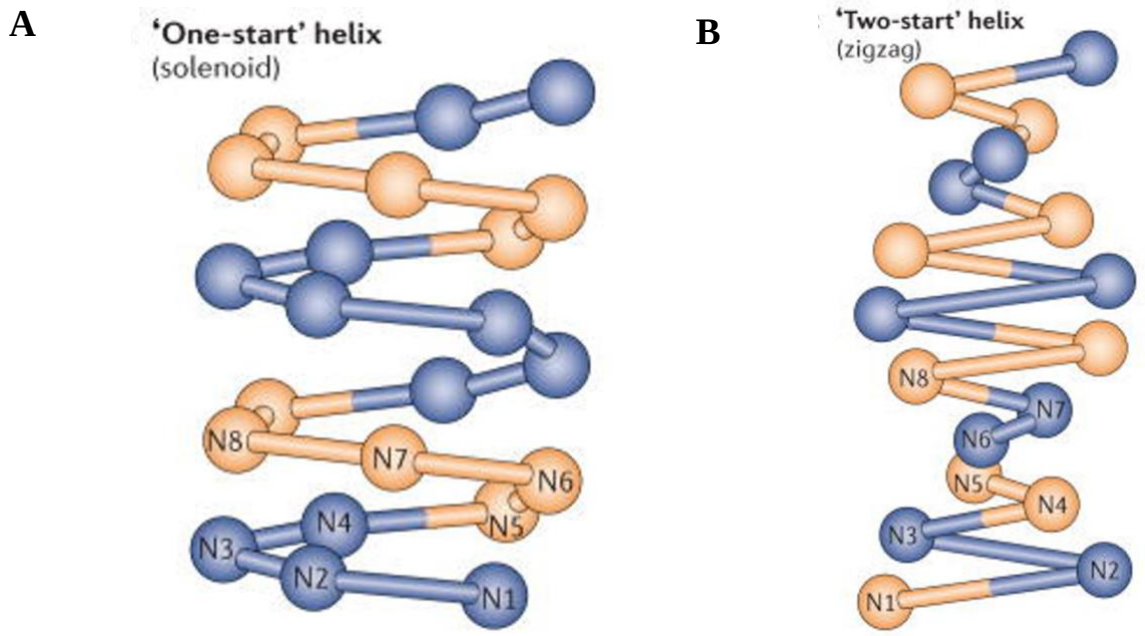

Figure1.1.2: Two models for chromatin secondary structure: (A).The solenoid model where the 30 nm chromatin fibre is an interdigitated one-start helix in which a nucleosome in the fibre interacts with its fifth and sixth neighbour nucleosomes (Robinson PJ, Rhodes D, 2006). (B) The zig-zag model implies interaction between alternate nucleosomes forming a two-start helix in which nucleosomes are arranged in a zigzag manner (Dorigo B et al., 2004). The two models differ in the trajectory and degree of bending of the DNA that connects two nucleosomes (linker DNA) (Li G, Reinberg D, 2011). (Figure adapted from Karolin Luger K, Dechassa ML., Tremethick D J., 2012).

Tertiary chromosome structure that is best represented as condensed metaphase chromosomes are believed to be the end point of chromatic compaction in dividing cells. Since recent studies question the existence of 30nm fibre *in vivo,* alternative models suggest less-ordered chromosome condensation process (Fussner E et al., 2011) where the arrangement of the metaphase chromosome is similar to a 'molten globule' state (Tremethick DJ, 2007, Fussner E et al., 2011 and Eltsov M, et al., 2008) arising from the interdigitation of over-crowded and irregularly folded nucleosomal arrays. Studies upon analysis of extended chromatin fibres (~50–100 times their normal interphase length) revealed that 10–40 kb regions of CenH3- and H2A-containing nucleosomes are interspersed with similar-sized domains of dimethylated H3 and H2A.Z occupying distinct 3D locations (Greaves IK et al., 2007). Studies using artificial segments of chromosomes created and tagged by the insertion of multiple copies of the lac operator sequence (Strukov YG, Belmont AS, 2009) have shown that there is no reproducibility in the lateral positions of the tagged sequences in mitotic chromosomes and positioning of these sequences differed even between sister chromatids (Strukov YG, Belmont AS, 2009). Therefore, eukaryotic chromatin both at the local level of chromatin fibre and at the global chromosomal level, does not exhibit structural uniformity and small, subtle changes by PTMs, histone variants and DNA sequence in chromatin primary structure yield dramatic effects in its large-scale organization significantly affecting nucleosome shape and stability and its protein surface.

1.2 Eukaryotic genome organization and chromatin compartmentalization

The spatial organization of eukaryotic chromatin profoundly determines their function. One of the ways is through membrane-mediated compartmentalization having distinct protein compositions. One of the newly emerging mechanism for regulating spatial organization is through membrane-less compartmentalisation

driven by phase separation. Recent studies show that reconstituted chromatin undergoes histone tail-driven liquid-liquid phase separation (LLPS) in physiologic salt and when microinjected into cell nuclei, producing dense and dynamic droplets. Chromatin protein linker H1 and Heterochromatin protein1α (HP1α) promote phase separation of chromatin forming dense liquid condesates regulating heterochromatinization (Gibson B A et al., 2019 and Larson A G et al., 2017). On the other hand, histone acetylation by lysine acetyltransferase p300 antagonises phase separation of the chromatin by dissolving liquid droplets and inhibiting their formation in nuclei (Gibson B A et al., 2019). Chromatin acetylation leads to formation of a new phase-separated state by binding to multi-bromodomain proteins, such as BRD4 with distinct physical properties. Thus, suggesting a new framework of eukaryotic genome organisation through intrinsic phase separation of the chromatin polymer (Gibson B A et al., 2019).

The chromosomes organise themselves on the basis of their functions, and adopt reproducible positions within the nucleus. There are fundamental differences in the spatial distribution of the genome and the two most common configurations are the Rabl configuration observed in rapidly dividing embryonic cells and the second type of global nuclear organisation is the non-overlapping discrete chromosome territories (Fung J C et al., 1996, Lee, K. K et al., 2001). The human genome consists of 3×109 nucleotides of DNA that is present in 46 chromosomes and each of the chromosomes is present in a distinct chromosomal territory having a distinct spatiotemporal domain (Figure1.2). The chromatin comprises of largescale chromatin domains such as euchromatin and the heterochromatin. The euchromatin comprise mostly of the open chromatin where transcription occurs. Even though heterochromatin mostly comprise the silenced chromatin foci correlating with more compact chromatin, evidence suggest that transcription also occurs in such regions (Gilbert N et al., 2004). The fraction of the human genome having an “open” chromatin structure originates from the most gene-rich

domains that may not necessarily be transcriptionally active but have the potential for transcription, given the right transcription factor environment (Gilbert N et al., 2004). The concept of transcription factories (TFs) is a newly evolved concept where active sites of both RNA polymerase II and III mediated transcription cluster and each factory consist of one type of polymerase but specific transcription factors that activate transcription of specific group of genes (Bartlett, J et al., 2006). Chromosome folding and position within the nucleus determines the exposure of different regions of the chromosome to these TFs. As observed in differentiated cells different chromosome territories form within the volume of the nucleus (Cremer T et al., 2006). Expressed genes localise within these territories in differentiated cells (Noordermeer D et al., 2008) with the most active genes being positioned between chromosome territories towards the interior of the nucleus where repressed regions located towards the nuclear periphery along with heterochromatin region (Cremer T et al., 2006, Kosak ST et al., 2002, Reddy KL et al., 2008, Reddy KL et al., 2006 and Mahy NL, Perry PE, Bickmore WA, 2002).

Recent advances in the technology have helped in the understanding that chromosomes are compartmentalised into discrete territories (Figure 1.2) and the expression of a particular gene is decide upon its location within a chromosome territory that determines the accessibility of different transcription and splicing machineries (Figure1.2) (Cremer T and Cremer C,2001). The topological model for gene regulation suggests (Cremer T and Cremer C,2001):

- The chromosomes occupying discrete territories contain chromosome arm and chromosome band domains
- The chromosome territories (CTs) have distinct nuclear localisations with different gene densities with gene-poor, mid-to-late replicating genes being

enriched in nuclear periphery and perinucleolar region whereas the gene-dense, early replicating chromatin being away from the periphery.

- Chromatin domains that contain DNA of ~1Mb are detectable in the interphase and non-cycling cells
- The interchromatin compartment (IC) also comprises of non-chromatin factors regulating transcription, splicing, DNA replication and repair and CT-IC model predicts a specific topological relationship between them regulating gene expressions.
- The gene positions within CTs determines their transcriptional status and gene silencing and activation on the other hand is regulated by the dynamic repositioning of the genes with respect to centromeric heterochromatin.

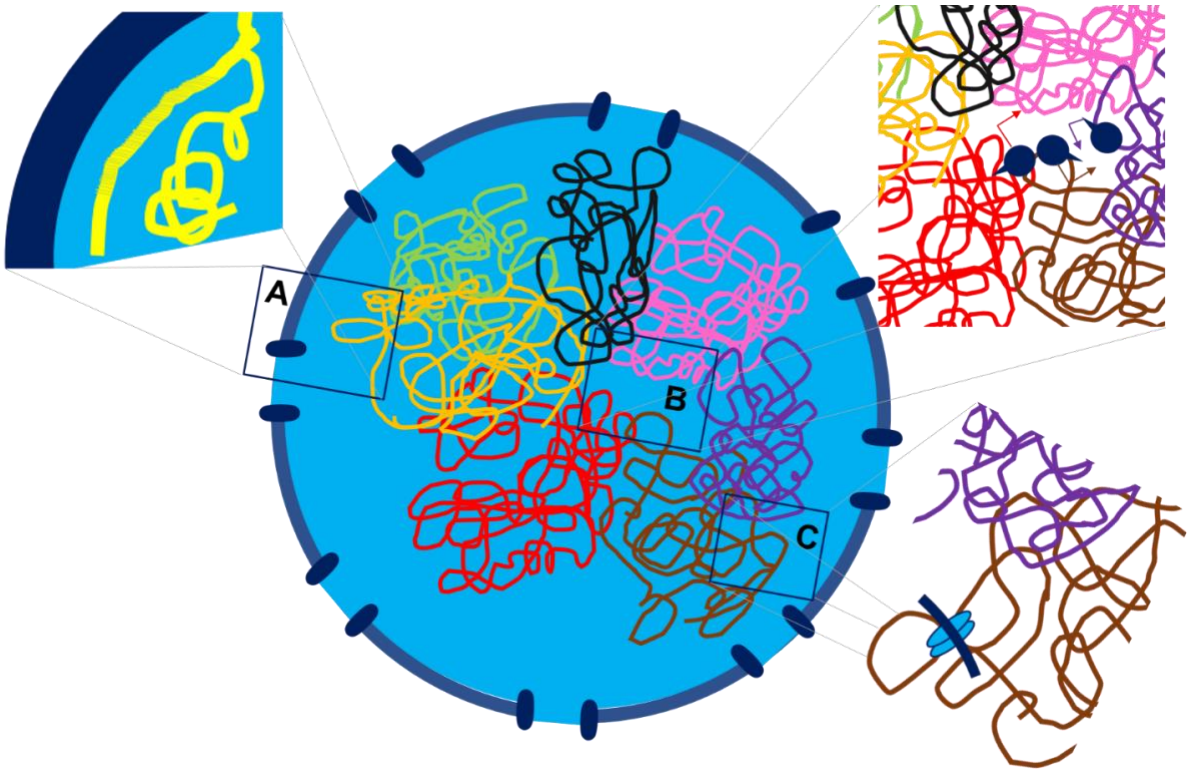

Figure 1.2: The spatial organization of the nucleus. Cartoon depiction of the spatial arrangement of different chromosome territories along with expanded view showing lamin-associated dense heterochromatin (hatched pattern) in region A, RNA polymerase II TF consisting of clusters of active genes from

different chromosomes in association with RNA polymerase II (blue) in region B and Intra-chromosomal loop mediated by CTCF (light blue ovals) in association with cohesin (deep blue ring) in region C.

Advanced chromosome capture methods such as 4C and HiC, highlights the importance of the chromatin loops as functional chromatin architecture and not random events (Bonev and Cavalli 2016). Bromo-deoxy-uridine (BrdU) pulse labelling of nuclei during early S phase coupled with 3D fluorescence imaging, has shown nearly 1,100 sites of DNA replication, called Replication Sites (RS), in NIH 3T3 cells (Ma et al., 1998). Each RS with an average size of 1million bases comprises of 5-6 replicon clusters that persist through several cell divisions (Jackson and Pombo, 1998 and Ma et al., 1998). With the help of 5C and Hi-C techniques, chromatin interactions have been shown to be spatially restricted into repeated chromatin domains (Dixon et al., 2012; Nora et al., 2012; Sexton et al., 2012). Studies reveal that chromatin interactions in human and mouse cells occur predominantly within domains of average size of 880Kb, similar to that of RS, known as Topologically Associated Domains, or TADs. TADs are generally stable like RS, with diverse cell types such as embryonic stem cells and fibroblasts sharing the majority of the TADs defined in each cell type. TADs represent a physical compartmentalization where two regions associate on average more frequently with each other than with regions outside the TAD (Dixon et al., 2012; Nora et al., 2012; Sexton et al., 2012) suggesting a property of "self -association" of regions within the TAD, and second, an "insulation" property between regions in neighbouring TADs. TADs are hierarchical in nature containing smaller "sub-TADs" (Phillips-Cremins et al., 2013; Rao et al., 2014), and loops at their most local level (Rao et al., 2014) or "insulation neighbourhoods" (Dowen et al., 2014; Ji et al., 2016). They are preserved in syntenic sequences (Dixon et al., 2012; Vietri Rudan et al., 2015) serving as the basic unit of chromosome folding (Dekker, 2014) regulating nuclear processes

that involve chromatin organization like transcription, DNA replication, and VDJ recombination (Hu et al., 2015; Lucas et al., 2014; Nora et al., 2012; Pope et al., 2014; Sanborn et al., 2015). Figure 1.2.1 shows the hierarchical folding of the eukaryotic genome reflecting the different layers of higher-order chromosome folding (Figure 1.2.1).

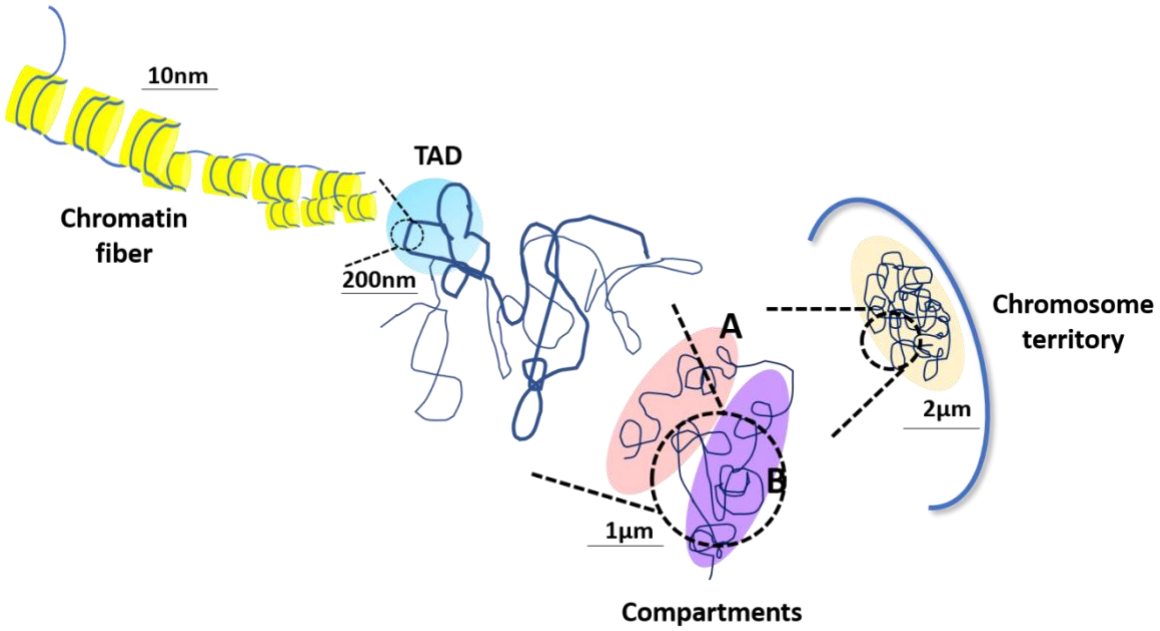

Figure 1.2.1: Schematic view of chromosome folding inside the nucleus. Chromatin packed at different nucleosome densities depending on gene regulation, folding at the submegabase scale into higher-order domains of preferential internal interactions termed as TADs. Chromatin segregation at the chromosomal scale into active "A" and repressed "B" compartments of interactions, reflecting preferential contacts between chromatin regions of the same epigenetic features. Chromosomes occupying individual space within the nucleus, forming chromosome territories.

The different mechanisms that shapes a chromatin polymer in the nucleus contributing to chromatin organization involves chromatin fiber movement through fractional Langevin motion (Dekker and Mirny, 2016) or fractal globule (Lieberman-Aiden et al., 2009), chromatin domains attraction through multiple

binding sites for certain diffusible molecules like large protein complex, or a chromatin-associated RNA, or an RNA/ protein complex (Barbieri et al., 2012) (Mele and Rinn, 2016) and insulation by specific sequence binding proteins factors or RNAs inducing topological constraints to the local chromatin fiber (Phillips-Cremins and Corces, 2013; Vietri Rudan and Hadjur, 2015). TAD formation occurs through an "attractive" force involving the Cohesin complex (Kagey et al., 2010; Phillips-Cremins et al., 2013; Seitan et al., 2013; Sofueva et al., 2013; Vietri Rudan and Hadjur, 2015; Watrin et al., 2016; Zuin et al., 2014). Recent evidence now suggests the role of Cohesin complex in mediating long range chromatin interactions between enhancers and promoters (Kagey et al., 2010; PhillipsCremins et al., 2013; Seitan et al., 2013; Sofueva et al., 2013; Zuin et al., 2014). Interestingly, chromosome territories repositioning can occur in diseases, and this might provide novel insights into disease mechanisms and deregulated gene expressions in pathophysiological conditions.

1.3 Chromatin and transcription

Chromatin is a dynamic functional organisation comprising of regions with variable gene expression that is determined by several factors. There two different states of the chromatin, one is transcriptionally active or the open chromatin called the euchromatin and the transcriptionally silenced or heterochromatin state that is mostly composed of closed and compact chromatin. The boundaries of euchromatin and heterochromatin region are composed of insulator elements. The theory regarding chromatin architecture that actively transcribed genes (constitutively expressing) or genes expressed under certain stimuli (being in poised state) are located on an open chromatin while silenced genes are located on closed chromatin loci is not entirely correct. Recent studies have shown that though there is a correlation between open chromatin structure and high gene

density, it doesn't necessarily corroborate with high gene expression. Transcriptionally active genes are also present in compact regions of the chromatin while silent genes are present in more open chromatin loci. The chromatin modification states determine the recruitment or removal of factors involved in regulating the gene expression. Different biochemical process that are essential for gene expression are not uniformly distributed within the nucleus and might constitute either stable assemblies that serve as factories for biochemical processes (Figure 1.3.1 A) or could be a product of transcription upon accumulation of RNA or proteins involved in post-transcriptional events (Figure 1.3.1 B) and they need not mutually exclusive. Gene movement to these sites represent different modes of transcriptional regulation (Figure 1.3.1).

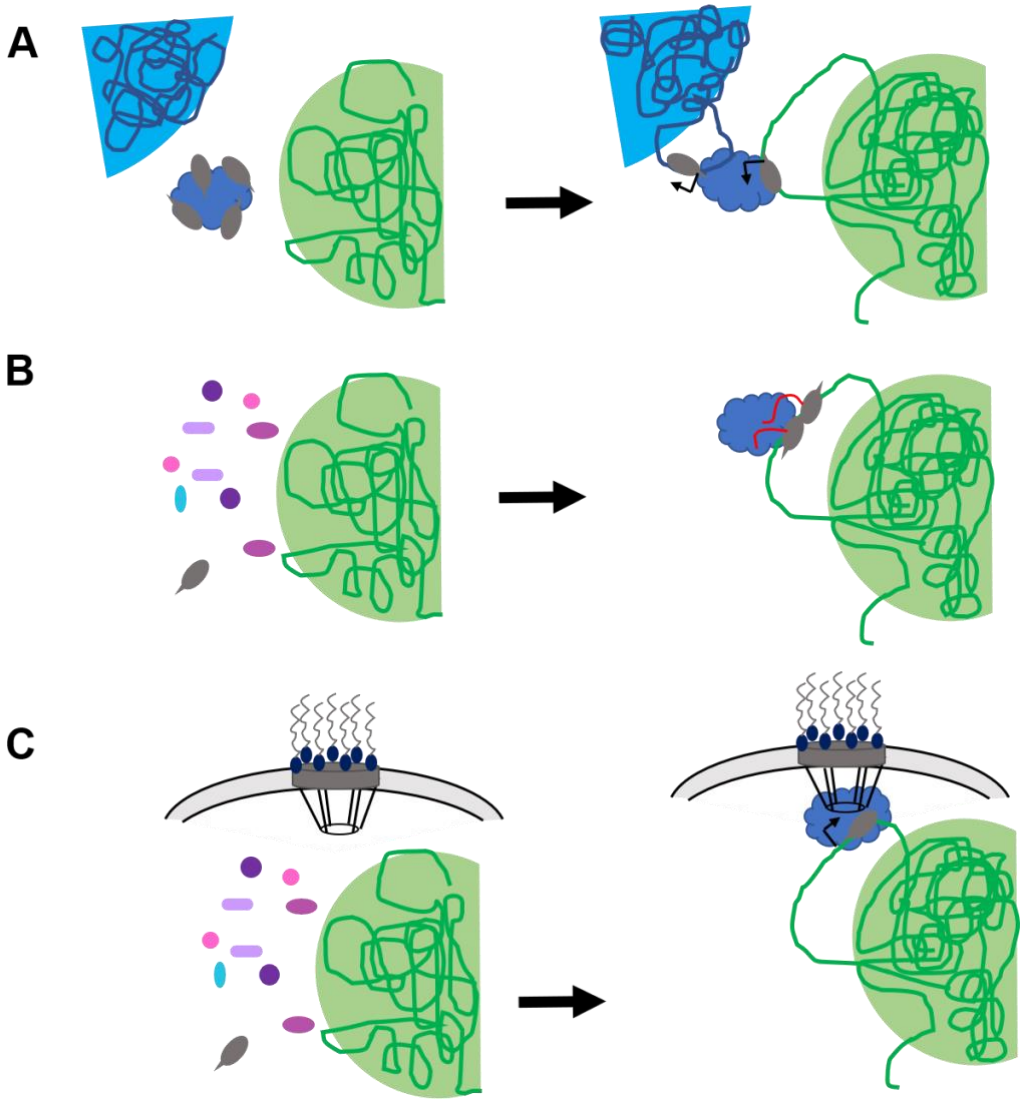

Figure 1.3.1. Different modes of spatial organization impacting transcription in the nucleus. (A) Chromosomes loop formation upon activation from respective territories to interact with a stable protein body (blue cloud) enriched for RNA polymerase II (grey). (B) de novo formation of a nuclear body at active transcription sites induced by mRNA synthesis (red). (C) Targeted gene movement to a nuclear pore complex serving as platform concentrating proteins (blue) and RNA polymerase II (gray) for transcription.

The chromatin modifications comprise both modifications of DNA as well as histone and non-histone components that form the epigenetic code. Both the

genetic and epigenetic code together determines the gene expression pattern (Figure 1.3.2). The epigenetic code includes the following:

- **DNA Methylation:** The DNA methylation may achieve silencing of gene by preventing transcription factors from binding to their cognate DNA binding sequence or recruiting methyl CpG binding proteins that in turn recruit corepressors to silence the chromatin.
- **Acetylation of histones and non-histone proteins:** The acetylation of histones is reversible and catalysed by Histone Acetyltransferases (HATs) and Deacetylases (HDACs). The HATs are also termed as Factor acetyltransferase (FATs) because they have a broad range of substrates including transcription factors, coactivators, histone chaperones etc. Reversible acetylation of these factors can lead to altered DNA binding ability as well as transition between open and closed chromatin structure. There is an interplay between factor acetylation, chromatin remodeling and histone chaperones in transcriptional regulation of genes.
- **Methylation of histone and non-histone proteins:** This modification has a greater half-life and therefore contributes to epigenetic memory. The site-specific Lysine (K) methylation is associated with both transcriptional activation as well as repression. The lysine methyltransferases are found to be associated with protein complexes. Suv39H1-mediated trimethylation of H3K9 leads to docking of HP1and is associated with heterochromatin assembly. The H3K4me3 is associated with increased transcription elongation and enhancer activity, which together lead to exceptionally high gene expression (Chen K et al., 2015). Some non-histone substrates of methyltransferases are linker histone H1 and p53. Ezh2 mediated methylation of H1 in mammalian cells has been implicated in transcriptional repression (Kuzmichev A et al., 2004). Studies on human CD4+ T cells have mapped 20 histone methylations of lysine and arginine

residues by chromatin immunoprecipitation followed by sequencing (ChIP-seq) (Barski et al. 2007). Data suggested that monomethylated H3K27, H3K9, H4K20, H3K79 and H2BK5 were linked to gene activation, while trimethylated H3K27, H3K9 and H3K79 were associated with gene repression.

- **Phosphorylation of histone and non-histone proteins:** Phosphorylation of histones is intricately linked to cell cycle arrest. Phosphorylation occurs in wide repertoire of non-histone proteins with distinct functional consequence that has been discussed later (1.7).
- **ADP Ribosylation:** Poly ADP ribose polymerase (PARP1) catalysing ADP ribosylation or PARylation of both histones and non-histone substrate is an interesting example of a non-histone protein having enzymatic activity. ADP ribosylation of histone H2A is important for its function in double stranded break repair. PARP1 itself gets ADP ribosylated causing dynamic chromatin alterations. This enzymatic process is required in various DNA repair pathways and in the maintenance of genomic stability. PARP-1 regulates gene expression by promoting exclusion of H1 and opening of chromatin near promoter region (Krishnakumar R. et al, 2008). SATB1 (matrix attachment region (MAR)-binding protein, special AT-rich sequence binding protein 1) is crucial for establishing higher order chromatin loop structures at the MHCI locus by directly interacting with PML (Pavan Kumar et al. 2007).
- **Ubiquitination:** Factors that are involved in telomere associated gene silencing have showed that monoubiquitination is required for methylation. Ubiquitination is also a reversible process as monoubiquitinated H2B can be deubiquitinated by the enzyme Ubp8, a component of the SAGA histone acetyltransferase complex required for transcription initiation (Henry K. W. et al.,2003 and Daniel, J. A., 2004). Ubiquitylation of histone H2B at lysine residue 120 (H2BK120ub) is an actively transcribed genome mark

which triggers several critical downstream histone modification pathways and changes in chromatin structure. Nucleosome stability is reduced or enhanced upon modulating levels of H2Bub1 and it regulates initiation by stabilizing nucleosomes positioned over the promoters of repressed genes reflected by an intrinsic difference in the property of chromatin assembled in the presence or absence of H2Bub1 (Chandrasekharan M. B., Huang F., and Sun Z., 2009).

- **Sumoylation:** Sumoylation are small ubiquitin related modifications involved in chromatin structure thus regulating gene expression. The four core histones get sumoylated which negatively regulates transcription (Shiio, Y., and Eisenman, R. N., 2003). Sumoylation is involved in Methyl CpG binding protein MBD1 and MCAF1 interaction inducing chromatin silencing (Uchimura, Y. et al., 2006).
- **Protein acylations:** Proteomics based approach have led to identification of acyl intermediates derived from acetyl-CoA (like succinylation, malonylation, propionylation and hydroxyl-butyrylation) and fatty acid derived myristoylation and crotonylation as novel modifications (Sabari BR. et al., 2017; Tan M. et al., 2011). With the help of *in vitro* labeling and peptide mapping by mass spectrometry, p300 and CREB-binding protein (CBP) of KAT3 family have been shown to catalyse lysine propionylation and lysine butyrylation of histones as well as non-histone protein p53 (Chen Y. et al., 2007). Butyryl CoA levels affect chromatin structure and regulate gene expression through butyrylation of chromatin or transcription components (Dutta R. *et al.* 2016) and by inhibiting KDACs, which would ultimately lead to increased acetylation (Steliou K. et al. 2012). Recent study discovers the relevance of crotonylation of H3K9 for robust transcriptional induction, along with H3K9 acetylation (Li Y. et al., 2016).

There are other modifications like biotinylation, formylation, citrullination, along with newly discovered which act on both histone and non-histone proteins leading to different functional consequences. Along with these modifications, very recently identified modifications like serotonylation of glutamine, at position 5 (Q5ser) of histone H3 upon serotonin secretion meditated by Tissue transglutaminase 2 (TGM2) in histone H3 tri-methylated lysine 4 (H3K4me3)-marked nucleosomes, results in H3K4me3Q5ser enrichment in euchromatin sensitive to cellular differentiation and permissive to gene expression (Farrelly LA.et al.,2019). Recently identified modification histone H3 glutamine 5 dopaminylation (H3Q5dop) has a specific role in cocaine-induced transcriptional plasticity in the midbrain exhibiting its function in a specific region of the brain that is ventral tegmental area (Lepack A. E. et al., 2020).

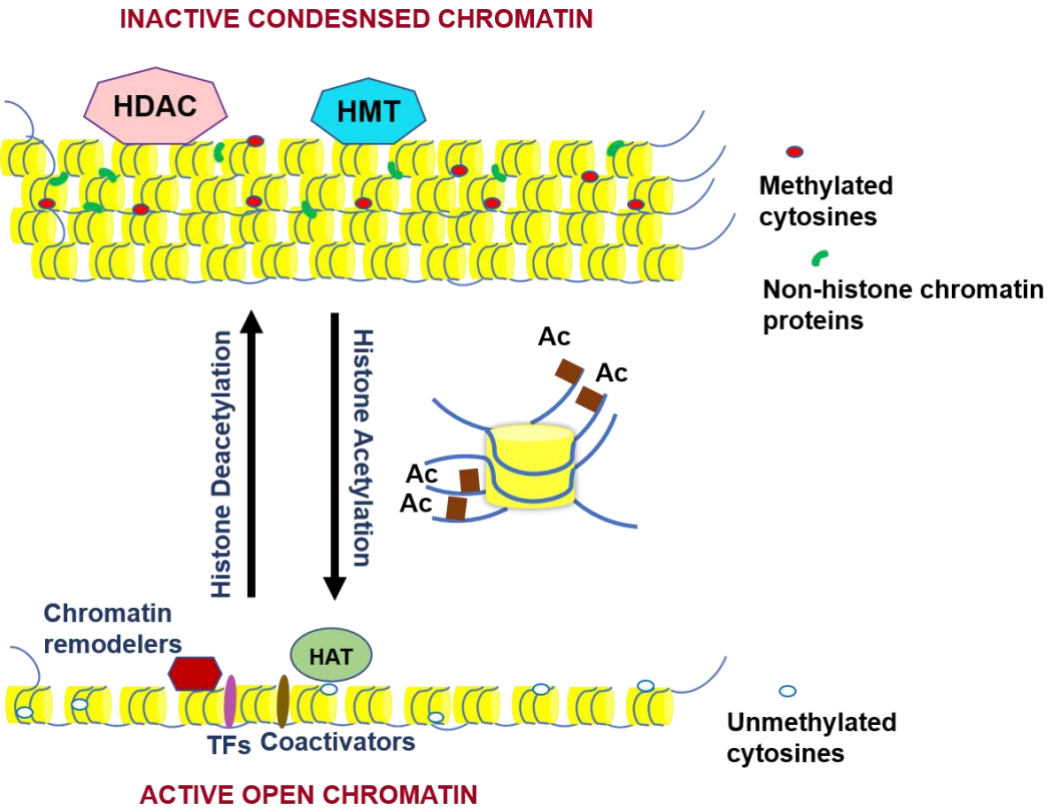

Figure 1.3.2. Chromatin dynamics mediated by different chromatin player regulating gene expression. Transcriptionally active open chromatin state is a in which the histone tails are acetylated by the Histone acetyltransferases (HATs).

Chromatin remodelers modulating chromatin landscape by positioning the nucleosomes making it accessible to TFs and coactivators. The inactive condensed heterochromatin state is often mediated by Histone methyltransferase (HMT) and deacetylation by Histone deacetylase (HDAC) proteins along with non-histone chromatin binding proteins making it inaccessible to the transcription machinery.

Non-histone proteins like Positive coactivator 4 (PC4) is involved in activator dependent transcription acting as coactivators or mediators for the transcription and initiation factors (Batta K et al., 2007). The non-histone chromatin proteins are critical players in the dynamic process of transcription through chromatin. The differential localisation of three heterochromatin protein 1 (HP1) isoforms in the nucleus; HP1α, HP1β and HP1γ, has functional implications in terms of heterochromatinization and gene expression (Eissenberg and Elgin,2000). HP1α specifically interact with PC4, to repress specific chromatin domains stands is an example of such functional interactions (Das C. et al.2010; Sikder S. et al. 2019). Non-histone protein regulating gene expression have implications in pathophysiological conditions as well. Linker histone H1 mediated gene expression has also been studied in stable T47D breast cancer shRNA inducible cell lines where different subsets of genes were affected upon knockdown of specific H1 subtypes (Sancho M et al., 2008). Linker H1 mediated gene expression also regulates important cellular process like embryogenesis and muscle differentiation (Lee H et al.,2004).

Growing evidence suggest phase separation mediating various cellular processes, including formation of classical membrane-less organelles, signaling complexes, the cytoskeleton, and numerous other supramolecular assemblies. Recent experimental studies show that chromatin proteins like linker H1 promote phase separation acting as scaffolds for phase separated heterochromatin domains and p300 mediated histone acetylation antagonizes chromatin phase separation, and

forms a new phase separated state in the presence of multi-bromodomain proteins, such as BRD4 forming nuclear chromatin subdomains distinct from the unmodified chromatin (Shakya A. et al., 2020 and Gibson B.A. et al., 2019). An interesting aspect of heterochromatin mediated gene repression by HP1 family shown by single-molecule DNA curtain assay is that it occurs through sequestration of compacted chromatin in phase-separated HP1 droplets, which are dissolved or formed by specific ligands on the basis of nuclear context (Larson A.G. et al, 2017). Phase separation mediated by protein forming liquid-like compartments may play a role in reducing the transcriptional noise regulating biological signal processing and control (Klosin A. et al., 2020).

1.4 Non-histone chromatin associated proteins (CAPs)

A number of studies have identified a large family consisting several sub families under its roof as chromosome-associated non-histone proteins (CAPs), each of them having a distinct mode of function in the organization of the higher order structure of the eukaryotic genome. The non-histone chromosomal proteins are defined as proteins excluding core histones that isolated together with DNA in purified chromatin and overlaps with the class of acidic nuclear proteins and contribute to the dynamicity of the chromatin. These proteins exhibit distinct chemical, physical and biological properties that are different from those of histones and show limited tissue specificity. A class of these proteins are involved in chromatin compaction and higher order chromatin organisation whereas some are involved in chromatin decompaction leading to an open chromatin structure activating transcription.

1.4.1.1 Role of different CAPs in chromatin organisation

The non-histone chromatin proteins are also multifunctional proteins and have diverse physiological functions that enables the otherwise inaccessible chromatin template available to various factors, inducing topological changes and functional

folding of the genome to facilitate chromatin template dependent functions like transcription (mentioned in the earlier section), DNA replication, DNA recombination and repair. Each family of CAP exhibit different mechanisms to regulate chromatin structure some of which are mentioned below.

1.4.1.1 Linker histone H1

The first identified non-histone chromatin protein involved in dynamic chromatin organisation is linker histone H1. H1 contains a short N-terminal tail (~20-35aa), a central globular domain (~70 aa) and a long, extremely basic C-terminal tail (CTD) (~100 aa). Linker histone H1 has large number of tissue specific variants regulating chromatin architecture. Linker histone H1 interacts with nucleosomes leading to compaction of the chromatin and restricting the accessibility of the chromatin binding sites to the regulatory factors (Wolffe, A. P. et al., 1997, Thomas, J. O.,1999, Zlatanova, J., Caiafa, P., and Van Holde, K., 2000 and Hizume, K., Yoshimura, S. H., and Takeyasu, K., 2005). There are two sub-populations of H1 with differential mobility interacting with the chromatin in dynamic fashion and rapid exchange of H1 occurs in euchromatin and heterochromatin regions (Misteli, T. et al., 2000 and Catez, F., Ueda, T., and Bustin, M.,2006). The nucleosome bound H1 termed as chromatosome were identified in the 1970s (Olins AL, Olins DE., 1974, Kornberg RD., 1974 and Simpson RT., 1978). From near-atomic resolution structure of the nucleosome core particle solved in 1997 (Luger K et al., 1997), indicating how the side chains of amino acids of core histones interact with DNA to various structural models of the chromatosome core particle proposed on the basis of Cryo-electron microscopy (Cryo-EM) studies. The first crystal structure of the linker histone H1 bound nucleosome using 167 bp of DNA and the globular domain of chicken H5 (Figure 1.4.1) shows that the globular domain binds on the nucleosome dyad and interacts with the linker DNA at both the entry and the exit sites of the nucleosome through interactions with occurring between positively charged Lys

and Arg residues of the globular domain and the phosphates of the DNA backbone in the nucleosome (Zhou BR, et al., 2015) (Figure 1.4.1). This structure was in agreement with the binding of the globular domain of mouse H1.0 and its mutants to chromatin *in vivo* (Brown DT et al., 2006). Later NMR and cryo-EM using longer linker DNA and H1.0 suggest that the tails of the linker histones and linker DNA in the chromatosome do not contribute to the binding mode between the nucleosome and the globular domain of the linker histone (Zhou BR. et al., 2016 and Bednar J. et al., 2017). However, later studies that measured the binding affinity from cryo-EM structure does imply that within a single chromatosome, the C-terminal tail of linker H1.0 prefers association with only one of the two available linker DNAs (Bednar J. et al., 2017, White AE. et al., 2016). Similar structural studies of chromatosome in D.melanogaster indicates an off dyad binding mode of linker H1 that appears to interact with one linker DNA (Zhou BR, et al., 2013). Subsequent studies identified five key residues in the globular domains of H5 and D. melanogaster H1 which determines the binding location of the globular domain in the chromatosome and thereby the different binding mode (on-dyad versus off-dyad binding) (Zhou BR, et al., 2013). Cryo-EM structure of a nucleosome array with linker histone variant H1.4 of 11 Å resolution indicates that the globular domain of H1.4 binds off the nucleosome dyad where tails of H1.4 were not largely visible indicating an unstable binding to linker DNA (Song F, et al., 2014). This was contrary to on dyad binding mode of globular domain of human H1.5, despite having the same amino acid sequence as that of H1.4 (Syed SH, et al., 2010 and Bednar J. et al., 2017). Thus, these structural studies indicate the relevance of PTMs and mutations in the globular domain of linker histone H1 on chromatin structure and function.

A newly discovered mode of linker histone H1 mediated chromatin organisation has been through linker H1 condensing into liquid-like droplets as shown in HeLa cell nuclei during the interphase stage of the cell cycle (Shakya A et al., 2020).

These droplets colocalized with DNA-dense regions thus mediating heterochromatinization. H1 form these, liquid like phase separated droplets where the nucleosome core particle maintains its structural integrity (Shakya A et al., 2020).

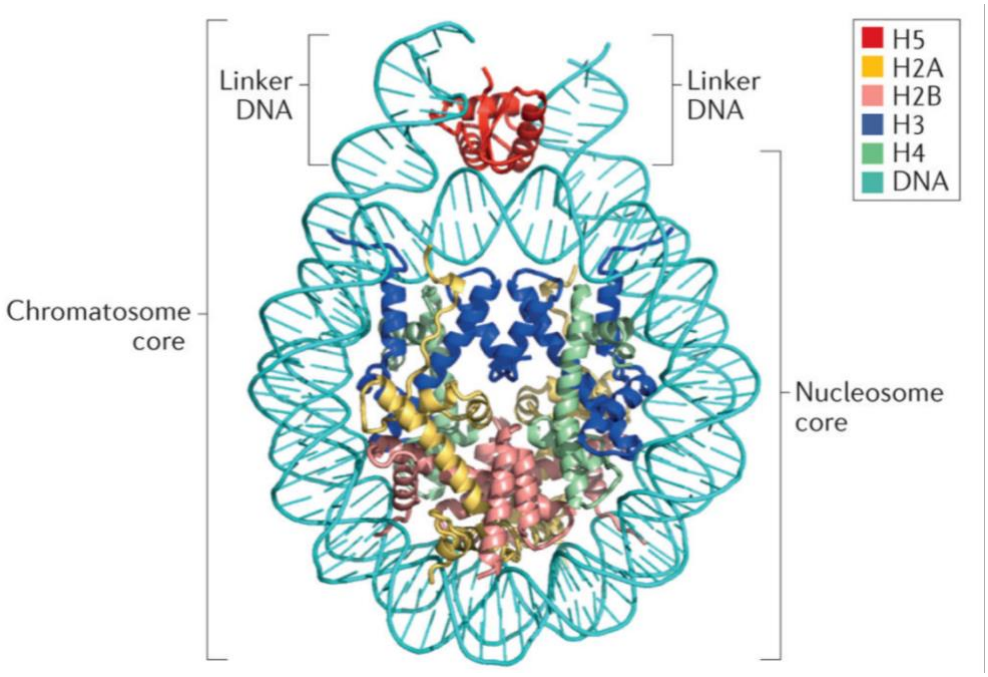

Figure 1.4.1: Crystal structure of chromatosome: The crystal structure of containing the nucleosome core particle with globular domain of chicken H5 (H1.0; shown in red) and fold regions of core histones (H2A, H2B, H3 and H4; all colour-coded) (Protein Data Bank identifier (PDB ID): 4QLC). This shows on dyad binding mode of the globular domain sitting on the nucleosome dyad and exhibiting interaction with both linker DNAs. (Figure adapted from Fyodorov D V., Zhou BR., Skoultchi A I., and Bai Y., 2018).

Role of linker histones in establishing 30nm chromatin fibers

Linker histone H1 is one of the most well studied chromatin proteins which stabilizes the nucleosomal core particle through direct binding. The exact position of H1 in the nucleosome and its precise interaction with linker DNA is still a matter of debate. One group with the help of cryo-electron microscopy (Cryo-EM), hydroxyl radical footprinting and nanoscale modelling develops a model

where the globular domain of H1 interacts with DNA minor groove located at the centre of nucleosome symmetrically contacting 10bp of linker DNA (Syed et al 2010) and other group based on the cryo-electron microscopy of *in vitro* reconstituted mammalian 30-nm fibers combined with fitting of the chicken histone H1 globular domain structure, indicates asymmetrical binding of H1 globular domain to the minor groove and contacting both linker DNA strand causing the nucleosome arrays to arrange into a twisted left-handed double helix with a zigzagged, two-start tetra-nucleosome as the repeating structural unit (Song et al., 2014) (Figure 1.4.2 A and B). Dimer formation by the globular domains of the linker histone between these tetra-nucleosome contributes to the twisted feature of the double helix which is in agreement with the previously proposed zigzag, two-start organization of the 30 nm chromatin fiber (Williams SP, et al., 1986 and Woodcock CL. et al., 2006) and is contradictory to the cryo-EM model obtained for the nucleosome array containing linker histone H5 in the presence of 1mM MgCl2 forming a single-start interdigitated nucleosome organization for the nucleosome array (Robinson PJ. et al., 2006).

Chromatin structural studies using stochastic optical reconstruction microscopy (STORM) enabled chromatin fiber visualization at the single-cell level in interphase stage, with a resolution of ~20 nm (Ricci MA et al., 2015). This study showed that nucleosome assembly occurs in discrete heterogeneous groups of varying sizes, termed ‘nucleosome clutches’ (Ricci MA et al., 2015). In different cells, like differentiated human fibroblasts contains larger clutches (~8 nucleosomes per clutch) whereas stem cells induced from fibroblasts contain smaller clutches (~4 nucleosomes per clutch). Greater association of linker histones in larger and denser clutches correlates with heterochromatin markers suggesting that linker histones H1 mediated chromatin folding forming 30 nm chromatin structures may exist as short fragments rather than as continuously folded fibers *in vivo* (Ricci MA et al., 2015). This observation is also consistent

with the recent findings using electron-microscopy-assisted nucleosome interaction capture crosslinking experiments in combination with mesoscale chromatin modelling (Grigoryev SA, et al., 2016) and small angle X-ray diffraction (Maeshima K. et al., 2014). *In vitro* assays have also observed formation of small clusters of nucleosome arrays primarily containing tetra-nucleosomes in force-stretched nucleosome arrays (Li W, et al., 2016).

Recent Cryo-EM studies from Dimitrov's group shows an intact 197bp nucleosome with full length H1 indicating a more compact conformation with reduced linker arm flexibility and that CTD which associates with only single linker is indispensable for this conformation (Bednar J, et.al., 2017) (Figure 1.4.2 C and D). This model suggests that the factors affecting the exit/entry angle of linker DNA could modulate the stability of H1 binding. The most recent crystal structure of a hexanucleosome with full length H1 reveals a two-start helix characterized by a flat zigzag arrangement of nucleosomes with uniform type II nucleosome stacking interfaces and a nucleosome packing density nearly half of that reported for 30-nm chromatin fibers, and a core-proximal linker DNA conformation resembling that of an H1-bound mononucleosome (Garcia-Saez et al., 2018). This study shows that how a flat chromatin fiber can switch conformation upon change in the ionic environment which reflect conformational fluctuations occurring *in vivo* during different regulatory process to allow chromatin to switch between different states of compaction in response to a change in the local environment. Studies in D. melanogaster shows that H1 depletion in larvae failed to develop into adults due to massively altered chromosome structure with loss of chromosome banding, lower levels of H3K9me2 and several Heterochromatin protein1(HP1) foci (Lu X et al., 2009). Triple H1 knockout in embryonic stem cells (ESCs) underlie the role of H1 in structural maintenance of heterochromatin (Cao K et al., 2013).

These structural studies do suggest one important aspect that nucleosome array structures are prone to environmental perturbations, employing non-invasive experimental methods such as NMR and cryo-EM in the absence of chemical crosslinking would be give us a better picture of the formation of higher order structures.

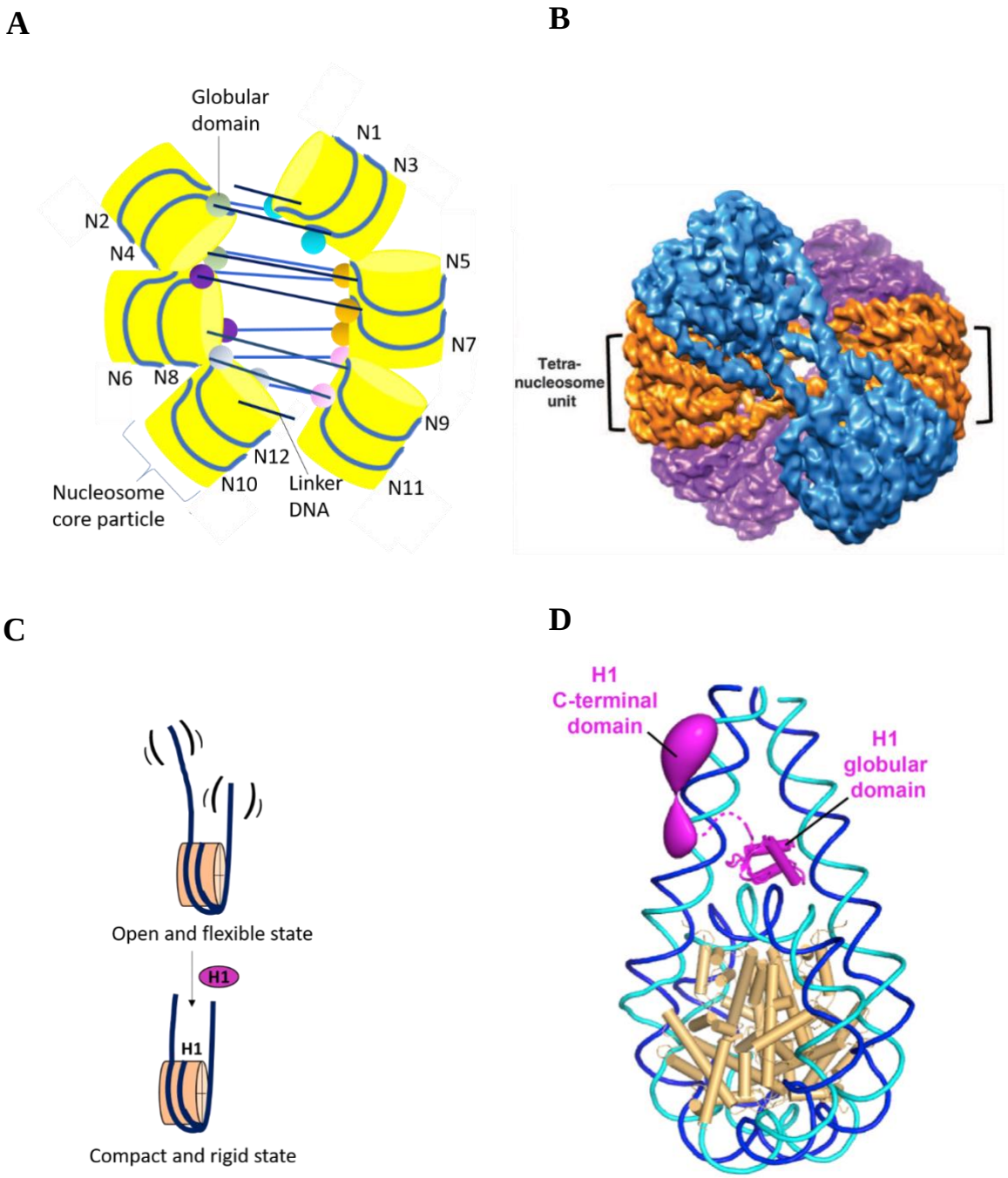

Figure 1.4.2: Role of linker histone H1 in chromatin folding. (A)Schematic model of the cryo-electron microscopy structure of the nucleosome array

condensed by human linker histone H1.4 showing the twisted double helix with tetra-nucleosomes as the structural unit. The globular domain of the linker histone in each nucleosome is mainly associated with one linker DNA interacting between neighbouring tetra-nucleosome units forming a dimer. (B) The 3D cryo-EM map of the 30-nm chromatin fibers reconstituted on 12 × 187 bp DNA with the three tetranucleosomal structural units highlighted by different colors (Figure adapted from Song et al., 2014). (C) Cartoon image illustrating the binding of linker histone H1 inducing the nucleosome to adopt a more compact and rigid conformation (D) Cryo-EM and crystal structure from Dimitrov's group showing that H1 globular domain interacts with core DNA on the dyad interacting with both DNA linkers whereas the C-terminal domain associates primarily with a single DNA linker (Figure modified from Bednar J et al., 2017).

Involvement of linker H1 in genome stability by regulating chromatin structure

Linker histone H1 binding to linker DNA pose an inhibition to DNA-binding proteins, including histone modifiers and transcription factors (Laybourn PJ, Kadonaga JT, 1991) whereas H1 bound nucleosome may block the translocation of processive, DNA-tracking enzymes, RNA and DNA polymerases and chromatin remodeling factors (Maier VK et al., 2008).

Chromatin structure defects observed upon elimination or reduction of linker histone affecting genome stability. Studies have shown that the non-essential S. cerevisiae homologue of H1, HHO1, is important for the suppression of DNA repair by homologous recombination (HR) and telomere maintenance through the recombination pathway (Downs JA et al., 2003). Studies in Drosophila have shown that H1 depletion derepresses transposable elements (Lu X, et al. 2013 and Vujatovic O, et al., 2012) thus accounting for the genomic instability observed in H1-depleted flies. Accumulation of extrachromosomal circular DNA originating from the rDNA gene cluster in larval imaginal disc and salivary gland cells

accumulate results due to enhanced recombination events and genomic rearrangements upon H1 knockdown (Vujatovic O, et al., 2012). Involvement of linker histone H1 in genome stability has also been shown in mouse ES cells where H1 depletion have led to increased number of telomeric sister chromatid exchange events and increase in telomere length (Murga M, et al., 2007). Upon DNA damage signaling, global chromatin fibre compaction occurs that protects the genome from additional lesions and this is further stabilized by the chromatin protein linker H1 (Hamilton C et al., 2011).

It is conceivable that these alternative mechanisms of H1 mediated chromatin functions and interactions are often subtype specific which shows tissue specific abundance.

Linker Histone variants

Different variants of linker histone variants may bind to the nucleosome in different modes associated with distinct structures of condensed nucleosome arrays or more condensed chromatin architecture which in turn regulates chromatin function**.** Linker histone H1 family contains 11 variants in humans and including seven somatic subtypes (H1.0, H1.1 to H1.5, and H1x), three testis-specific subtypes (H1t, H1T2 and HILS1) and one oocyte-specific subtype (H1oo) (Hergeth SP, Schneider R., 2015). H1.1 to H1.5 are expressed in a replication-dependent manner, whereas H1.0 and H1x are replication-independent and expressing in non-proliferating cells. H1.1 to H1.5, and H1x, are ubiquitously expressed whereas H1.0 accumulates in terminally differentiated cells. H1.0 (known as H5 in birds) leads to formation of highly condensed inactive chromatin, a characteristic feature of terminally differentiated cells like nucleated erythrocytes, comprising the majority of the H1 pool (Bates DL, Thomas JO., 1981). Below is the table (Table 1.4) showing the characteristics of human linker histone H1 variants.

Variant	Expression pattern	Genomic distribution pattern (Izzo A. et al, 2013)	Function	Knockout Phenotype
H1.1	Somatic	enriched in intergenic regions and at active chromosome 19; present at promoters	Functions apart from chromatin compaction through linker DNA binding not known	Not known
H1.2	Somatic	depleted in TSS of active genes, intergenic regions and CpG islands; enriched at LADs, enriched at chromosome X;	Maintenance of active gene transcription, recruitment of Cul4A ubiquitin ligase/PAF1 (Kim K. et al., 2013) H1.2S173p: active transcription (Zheng Y. et al., 2010). Repressor of p53-mediated transcription (Kim K. et al., 2008)	Cell cycle arrest in G1 (Sancho M et al.,2008), reduction in nucleosome spacing (Sancho M et al., 2008)
H1.3	Somatic	depleted in TSS of active genes,intergenic regions and CpG islands; enriched at LADs.	Inhibition of h19 noncoding RNA transcription (Medrzycki M. et al., 2014)	No significant difference (Sancho M et al., 2008)
H1.4	Somatic	depleted in TSS of active genes,intergenic regions and CpG islands; enriched at LADs.	H1.4K26me: heterochromatin formation via binding to HP1 and L3MBTL1 (Daujat S. et al.,2005, Trojer P. et al., 2007) H1.4K34ac: recruitment of TAF, active transcription (Kamieniarz K. et al., 2012) H1.4S172p, H1.4S187p: active transcription (Zheng Y. et al., 2010)	Deleterious effect with an increase in the subG1 peak (Sancho M et al., 2008)
H1.5	Somatic	depleted in TSS of active genes,intergenic regions and CpG islands; enriched at LADs.	Interacts with Msx1, repression of muscle cell differentiation, compaction (Lee H, Habas R, Abate-Shen C., 2004)	slight decrease of S phase (Sancho M et al., 2008) SIRT1 down-regulation and lower H3K9me2 level (Li JY et al.,2012
H1.6	Testis		forms less compacted chromatin compared to other H1 histone subtypes. Formation of more relaxed chromatin to promote chromatin architecture during meiosis, such as homologous recombination (Machida S. et al., 2016).	Not known
H1.7	Testis		normal spermatogenesis and male fertility. Required for proper cell restructuring and DNA condensation during the elongation phase of spermiogenesis (Tanaka H. et al., 2006)	Not known
H1.8	Oocyte		Expression of pluripotency genes in early embryos, Essential for meiotic maturation of germinal vesicle-stage oocytes. (Tanaka M. et al., 2001 and Hayakawa K. et al., 2014)	Impaired differentiation (Terme JM. et al.,2011) (IMR90) No significant difference (Sancho M et al., 2008)
H1.9	Testis			Not known
H1.10	Somatic	enriched in active chromatin	Mitotic progression (Takata H. et al., 2007)	Not known
H1.0	Somatic	enriched at the nucleolus	Replacement subtype in differentiated cells (Zlatanova J, Doenecke D., 1994)	Impaired differentiation of hESCs (Terme JM. et al.,2011), (IMR90) No significant difference (Sancho M et al., 2008)

Table 1.4: Characteristic of different Linker histone variants in humans.

The histone variants in mouse also have specific functions similar to humans. Triple knock out of H1.2, H1.3 and H1.4 have been shown to be embryonic lethal in mouse (Fan Y et al., 2003) and H1.5 regulates muscle differentiation (Lee H, Habas R, Abate-Shen C., 2004). A special histone variant H1.c is involved in heterochromatin formation in photoreceptors that has a reverse arrangement with heterochromatin being at the center of the nuclei and euchromatin at the periphery (Popova EY. et al., 2013). H1.7 and H1.8 being germ cell specific expression regulate sperm cell differentiation and embryogenesis respectively (Martianov I. et al., 2005 and Tanaka M. et al., 2001). The linker histone variants often show redundancy in terms of their chromatin compaction functions compensating for the knock-out of any of the variants. Despite that they have a context specific function where variations in their individual binding affinity to linker DNA and differences in their globular domains does account for their individual ability to carry out that specific function.

1.4.1.2 Heterochromatin Protein 1 (HP1) family

The Heterochromatin Protein 1 (HP1) is an yet another family of non-histone chromosomal protein involved in the establishment and maintenance of higher-order chromatin structures. It binds to methylated K9 of histone H3 (H3K9me) which is a mark for transcriptionally repressed chromatin. HP1 family consist of three distinct groups, HP1α encoded by CBX5, HP1β and HP1γ by CBX1 and CBX3 respectively. The conserved synteny among the HP1 proteins exhibit that their functions have been selected under stringent evolutionary pressures with each protein having distinct localization patterns. The functional diversity of HP1 is achieved by interacting with several different factors. H3K9 trimethylation by Suv39H1 acts as the docking site for HP1 recruitment whereas H3Serine10 phosphorylation by Aurora B Kinase influence the binding of HP1 during mitosis (Hirota, T. et al., 2005). Although H3K9me3 is necessary for HP1α recruitment but studies made it apparent that it is not sufficient to mediated heterochromatin

formation alone. Linker histone H1.4 impedes the binding of HP1α and this inhibition is partially relieved upon incorporation of both H2A.Z and H3K9me3 into the nucleosomal array (Ryan D.P. and Tremethick D.J., 2018). Studies suggest that there could be two modes by which HP1α may interact with nucleosomes; one mediated by linker DNA interactions and other through direct binding with nucleosome core that is facilitated in the presence of H2A.Z and H3K9me3 as secondary mode when linker DNA has been occluded by linker histone (Ryan D.P. and Tremethick D.J., 2018). HP1α binds to condensed higher order chromatin structure and alters chromatin fiber without crosslinking to them facilitated by nucleosomal surface created by H2AZ (Fan, J. Y. et al., 2004). HP1 proteins contain chromodomain binding to di- and trimethylated lysine 9 of histone H3 and C-terminal chromoshadow domain involved in homo/heterodimerisation and interaction with other proteins being separated by a variable linker region containing nuclear localisation sequence (Cao R et al., 2005 and Cao R et al., 2002). Knockout studies have shown that HP1β is associated with genome instability whereas depletion of HP1γ led to mitotic defects (Aucott R. et al, 2008 and Serrano A 2009). Studies in drosophila have shown that three isoforms exhibit differential binding to H3K9me with HP1 showing the strongest binding to the methylated H3K9 peptides, whereas HP1c presenting the weakest binding to the methylated peptides (Lee D.H. et al., 2019). HP1b and HP1c are localized to both the nucleus and cytoplasm whereas HP1a is only present in the nucleus (Lee D.H. et al., 2019).

Recent cryo-EM studies show the structural basis of heterochromatin formation by HP1 proteins which includes two H3K9me3 nucleosomes bridged by a symmetric HP1 dimer (Machida S. et al., 2018). The model depicts no direct interaction between linker DNA and HP1 thus allowing nucleosome remodeling by ATP-utilizing chromatin assembly and remodeling factor (ACF) (Machida S. et al., 2018). The chromoshadow domain dimer of HP1 is present in an accessible

location in the complex where the linker DNA between nucleosomes does not directly interact with HP1 (Machida S. et al., 2018). HP1 protein members are also involved in centromere stability and transcriptional regulation therefore deregulation of these proteins has often been prognostic signatures in several cancers.

HP1 members also exhibit functional interactions with other non-chromosomal proteins. HP1α interacts with Positive coactivator 4 to recruit REST-CoREST complex to repress neuronal gene expression in non-neuronal cells (Das C et al., 2010). Linker H1 acetylated at lysine 85 recruits HP1 facilitating chromatin compaction and dynamic mobilization of HP1 upon DNA damage (Li Y. et al., 2018). HP1 can promote transcriptional repression or activation depending on the chromatin context and its interacting partners. HP1 associate with transcription Initiation Factors (TIF) at the promoters to activate transcription through recruitment of coactivators and also play a role in stabilization of mRNAs. HP1 is recruited to the promoters of Cyclin E genes in association with Rb promoting histone methylation leading to gene repression. HP1 also interacts with corepressors like TIFß.

HP1β interacts with the histone methyltransferase (HMTase) Suv(3-9)h1 and is a component of both pericentric and telomeric heterochromatin (Aagaard L. et al., 2000, Wreggett K.A. et al., 1994 and Sharma G.G. et al., 2003). HP1β is involved in modulating chromatin silencing at the pericentric heterochromatin in a dosage-dependent manner (Festenstein R. et al., 1999) which is mediated by a dynamic association of the HP1β chromodomain with the tri-methylated Histone H3K9me3.

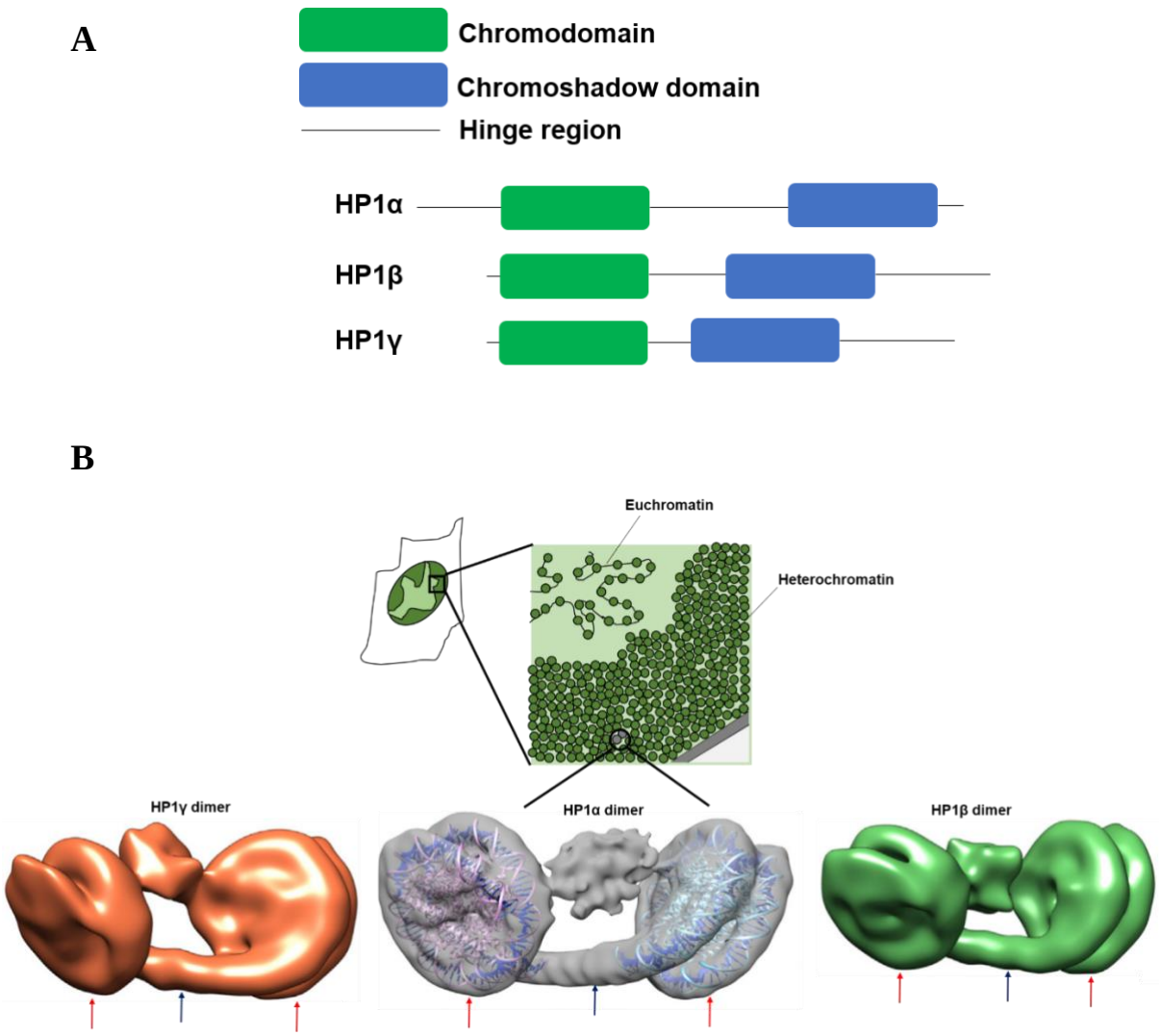

Figure 1.4.1.2.1: (A) Domain organisation of three isoforms of HP1 family. (B) HP1 mediated heterochromatin formation. Cryo-EM structure showing HP1 dimer bound nucleosome at 10A° resolution (Cryo-EM figure adapted from Machida S. et al.,2018) for each of the isoforms.

HP1 family mediating heterochromatinization through phase separation

Another very interesting aspect of heterochromatin mediated gene repression by HP1 family shown by single-molecule DNA curtain assay occurs through sequestration of compacted chromatin in phase-separated HP1 droplets, which are dissolved or formed by specific ligands on the basis of nuclear context (Narlikar G, 2017). HP1 mediates chromatin compaction through oligomerization between two phase-separated condensates (Figure1.4.2.2)

(Canzio D. et al., 2011, Canzio D. et al., 2013, Larson A. G. et al, 2017 and Strom, A. R. et al., 2017). Studies in Schizosaccharomyces pombe shows that compaction by its HP1 protein homolog Swi6 results in phase-separated liquid condensates increasing the accessibility and dynamics of buried histone residues within a nucleosome. Swi6 oligomers reshapes the nucleosome core by dynamically exposing buried nucleosomal regions facilitating multivalent interactions between nucleosomes, thus promoting phase separation (Sanulli S. et al., 2019). A very recent study in mouse fibroblasts reveals interesting and relevant features of pericentric heterochromatin with HP1 forming liquid droplets in living cells weakly and HP1 doesn't determine the size, global accessibility, and compaction of heterochromatin foci which lack a separated liquid HP1 pool. HP1 promotes formation of phase separated liquid droplets which are not stable inside the nucleoplasm. Thus, compaction of chromocenters is dependent on the presence of a strong activator that induces a switch-like transition, leading to decompaction of chromocenters abruptly (Erdel F. et al., 2020).

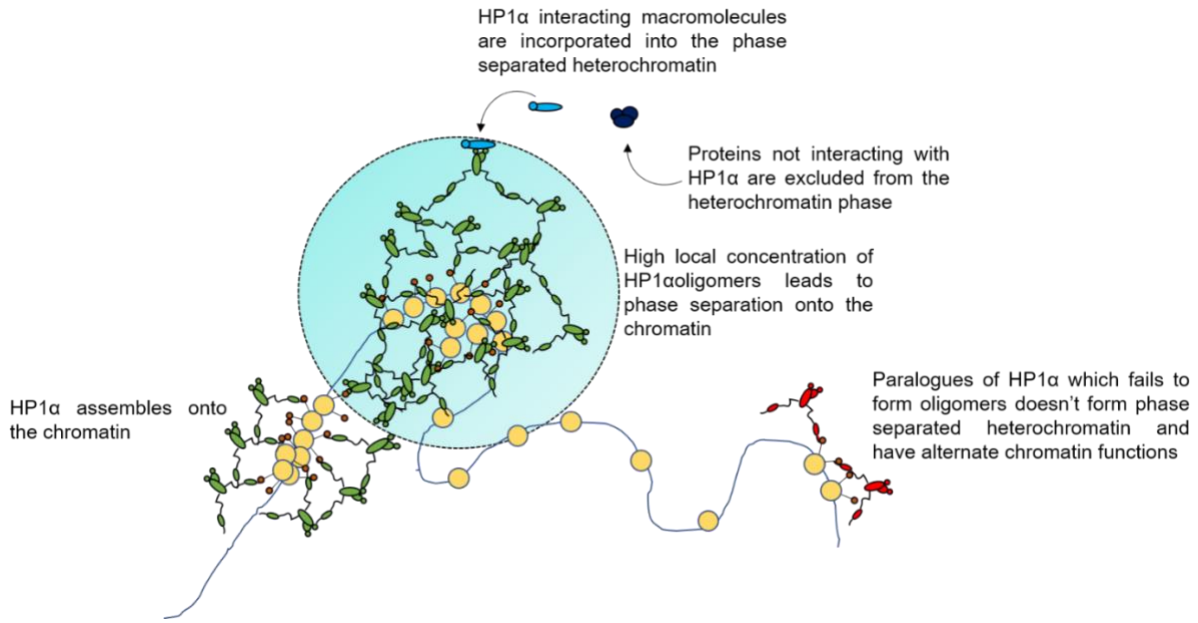

Figure 1.4.1.2.2. Model showing formation and regulation of phase separated heterochromatinization mediated by HP1α oligomers.

1.4.1.3 High Mobility Group (HMG) proteins

The High mobility group protein containing three families of proteins: HMGA, HMGB and HMGN each with their distinct binding to the chromatin, unique DNA-binding motifs, preferred binding substrates, changes induced in their substrates and subsequently different subsets of cellular processes they influence and functions. “High Mobility Group” or HMG proteins were termed so as they had unusual solubility properties, small size and rapid mobility upon electrophoresis compare to other chromatin proteins (Bustin M, Reeves R.,1996). HMG proteins are characterized by the presence of a long, negatively charged carboxy terminal tail regulating their functions (Bustin M, Reeves R.,1996, Gerlitz G. et al., 2009). This family is involved in embryonic development, transcriptional regulation and DNA repair modulation.

HMGA

The HMGA family has a canonical DNA-binding domain which is a palindromic amino motif called the ‘AT-hook’ binding preferentially to minor groove of short AT-rich stretches B-form DNA via recognition of structures (Reeves R et al., 1990). HMGA family exhibits a unique feature of intrinsic flexibility with disordered random coils to ordered secondary structure after binding to DNA (Huth JR et al.,1997) enabling formation of multi-subunit, stereospecific protein-DNA complexes of enhanceosomes (Merika M. et al., 2001) on AT-rich regions of the promoter regulating transcriptional activation (Fashena SJ, 1992 and Thanos D, 1995) (Figure 1.4.1.3.1). This class of HMG proteins possess the ability to bend, straighten, unwind and supercoil DNA substrates contributing to their ability to form enhanceosomes (Reeves R, 2001). Besides recognizing the structure of the narrow minor groove of A/T-rich DNA, HMGA proteins can bind to non-B-form DNAs with unusual structural features including : synthetic four-way and three-way junctions (Hill DA, Pedulla ML, Reeves R, 1999 and Hill DA, Reeves R, 1997), bent and supercoiled DNAs (Nissen MS, Reeves R,1995) base-

unpaired regions of A/T-rich DNA (Nissen MS, Reeves R,1995) and distorted or flexible regions of DNA on isolated nucleosome core particles (Pruss D. et al., 1994, Reeves R, Nissen MS, 1993 and Reeves R, Wolffe AP, 1996) (Figure 1.4.1.3.1). HMGA binding to nucleosomes induces localised rotational settings on surface of core particles not driven by ATP hydrolysis (Reeves R, Wolffe AP, 1996). HMGA1 being a key player in coordinating enhanceosome assembly/disassembly with transcriptional activation process by binding and straightening stretch A/T-residues located between two well-positioned nucleosomes on the IFN-β promoter (Reeves R., 2010) assisting recruitment of a number of transcription factors (IRF-1, p50, p65 and ATF-2/c-Jun) to an array of binding site on the naked DNA mediating enhanceosome formation (Yie J. et al., 1999). GCN5 histone acetyltransferase (HAT) is then recruited on enhanceosome surface acetylating histones on both of the adjacent nucleosomes and acetylating a specific residue (K71) of HMGA1 protein enhancing protein-protein interactions crucial for maintaining its stability during transcription (Merika M, Thanos D., 2001, Merika M. et al., 1998). HMGA proteins is associated with localized changes in chromatin/nucleosome structure altering cellular phenotype during transcriptional activation of both the IL-2 (Reeves R., 2010) and IL-2α (John S. et al., 1995 and John S, Robbins CM, Leonard WJ,1996) genes in activated lymphoid cells. HMGA1 has been implicated to play a role in 'remodeling' or removal of inhibitory nucleosomes in unstimulated T cells positioned on the recognition sites of regulatory key transcription factors. *In vitro* experiments showed HMGA1 to bind the A/T-stretch on the surface of the nucleosome as two different HMGA1 protein molecules bound to the two separate A/T-rich stretches in a direction-specific, "tail-to-tail" manner (Reeves R, Leonard WJ, Nissen MS. 2000). Several experimental evidences suggest that the function of the HMGA1 protein is to facilitate and assist remodeling of the inhibitory nucleosome by the BRG-1/SWI/SNF complex (Scaffidi P, Misteli T, Bianchi ME.2002). One of the hall marks of the positioned nucleosomes include

frequent overlapping of the binding sites for HMGA1 and the transcription factor involved and extending into the adjacent linker region.

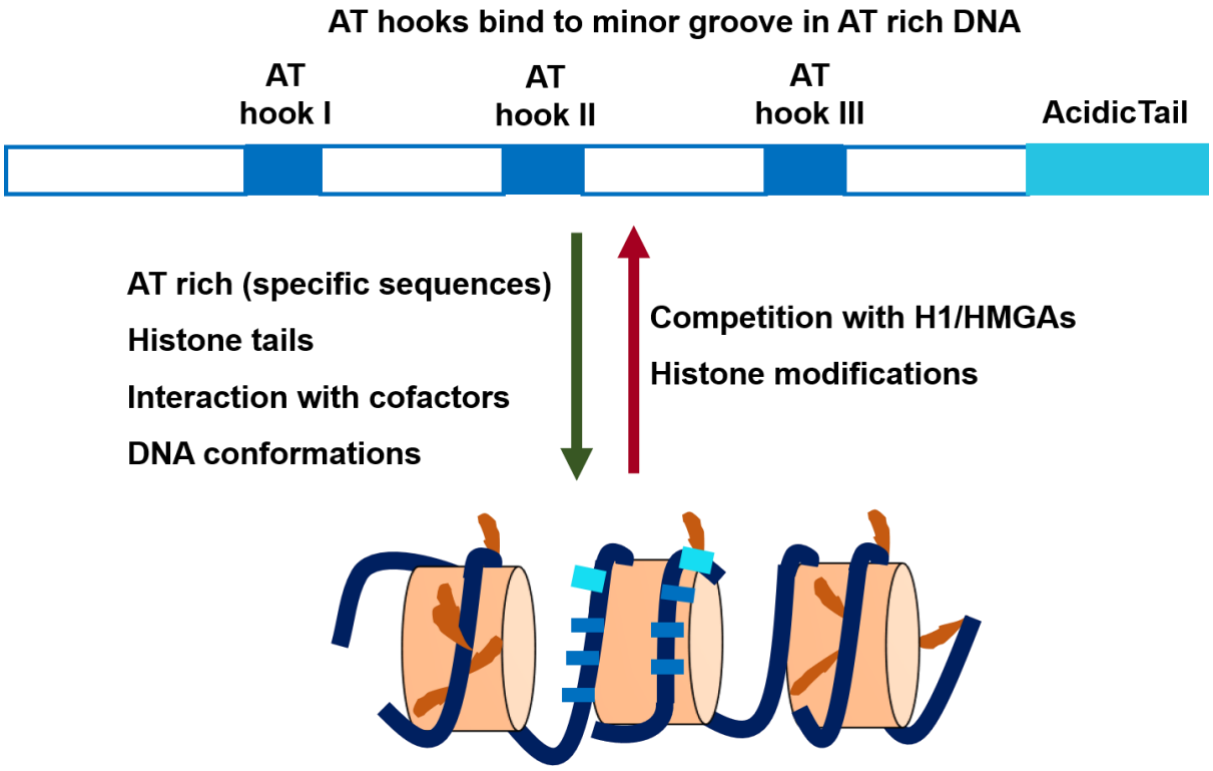

Figure1.4.1.3.1: Domain structure of HMGA and factors determining HMGA–chromatin interactions shown is a schematic diagram where AT hooks appear as deep blue rectangles. The factors indicated by green arrow promote HMGA interaction with chromatin, while those indicated by the red arrow promotes HMGA dissociation from chromatin.

HMGB

The second family of HMG proteins, HMGB plays roles in several nuclear processes like transcription, V(D)J recombination, DNA repair apart from being chromatin architectural proteins. HMGB proteins characterized by two tandem DNA binding regions called HMG box domains followed by a 30 amino acid long acidic tail (Thomas JO, 2001) binding to minor groove of B-form DNA introducing a 90° bend into the backbone and also to distorted DNA structures

like four-way junctions, bulges, kinks and modified DNA containing cisplatin adducts (Pil M., Lippard SJ.,1992). 80 amino acid long HMG box domains consist of three α-helices folded into an L-shaped configuration binding into the minor groove of DNA on its concave surface with limited or no sequence specificity (Thomas JO, Travers AA., 2001) (Figure 1.4.1.3.2). DNA bending induced by HMGB binding produces an allosteric transition structure facilitating the recognition and binding by other proteins during the formation of functional multiprotein-DNA complexes (Figure 1.4.1.3.2). Whereas HMGB binding to distorted DNA structures is analogous to enzymes which recognizes these molecular structures resembling transition states between reagents and products influencing the rate of formation of multiprotein-DNA complexes (Agresti A, 2003) (Figure 1.4.1.3.2). The ability of HMGB proteins to bind to nucleosome at the DNA entry/exit site (Bustin M, 2005) creating a more flexible structure as opposed to H1 bound nucleosomes facilitate recruitment of remodeling proteins (e.g., ACF/CHRAC) that induce nucleosome sliding, thus exposing previously blocked regions of DNA represents one of the mechanisms HMBG mediate transcriptional regulation (Bonaldi T et al., 2002) (Figure 1.4.1.3.2).

Several mechanisms attribute to HMGB participation in different cellular processes as transcription, replication, V(D)J recombination, DNA repair (Agresti A, Bianchi ME., 2003, Bianchi ME, Agresti A., 2005). EMSA studies also shows that HMGB is also involved in forming transcriptional repressor complex binding to TATA-binding protein (TBP) to form a stable HMG-1/TBP/TATA complex inhibiting assembly of preinitiation complex on gene promoters (Das D, 2001). Additional experimental evidences demonstrate that the accessory transcription factor TFIIA binding to TBP and displacing HMGB1 from the inhibitory HMGB1/TBP/TATA complex mediates formation of a stable preinitiation complex to form and promote the early stages of transcriptional initiation (Dasgupta A, Scovell WM., 2003). It also organizes and maintains

heterochromatin formation by binding to heterochromatic DZ4Z tandem repeat sequences in the subtelomeric region of human 4q35 in complex with nucleolin and YY1 (Gabellini D. et al., 2002). One of the very well characterized mechanism executed by HMGB is termed as 'hit-and-run' mode of action where HMGB proteins facilitate the stable binding of other transcription factors to their DNA recognition sites followed by dissociation from any ternary complex that is formed thus stably recruiting the protein onto its DNA substrate (Agresti A, Bianchi ME., 2003). Thus, HMGB functions transiently as a protein chaperone in such scenario. However, in certain cases, for example for BHLF-genes, HMGB mediates formation of an enhanceosome on its promoter and remains a stable part of the complex following transcriptional activation (Ellwood KB. et al., 2000). Other remarkable examples of HMGB1 chromatin bound complex formation is in apoptosis during which the dynamic movement of HMGB1 is completely arrested followed by chromatin condensation and fragmentation on a global scale (Scaffidi P, Misteli T, Bianchi ME., 2002). The plausible explanation for this has been suggested as either HMGB recognition and binding to hypoacetylated N-terminal histone tails found in heterochromatin or due to structural alterations resulting from histone deacetylation during heterochromatin formation (Agresti A, Bianchi ME., 2003). The implication for the HMGB tight binding to chromatin in apoptotic cells lies in the prevention of protein leakage out of dying cells that can trigger an inflammatory response (Bianchi ME, Manfredi A., 2004). Thus, HMGB proteins can impact both local as well global chromatin structure.

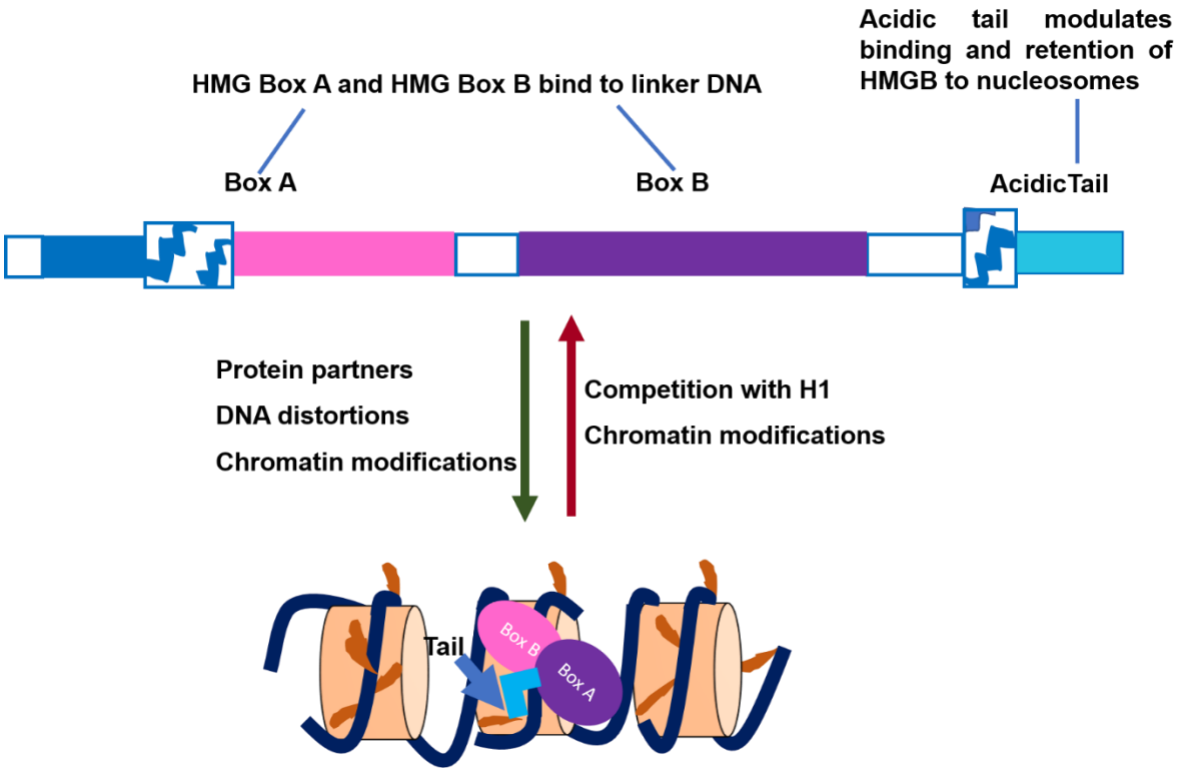

Figure1.4.1.3.2: Domain structure of HMGB and factors determining HMGB–chromatin interactions shown is a schematic diagram where 3 structural domains of HMG box A and HMG box B are indicated in pink and purple. The factors indicated by green arrow promote HMGB interaction with chromatin, while those indicated by the red arrow promotes HMGB dissociation from chromatin.

HMGN

HMGN family consisting primarily of five members (HMGN1, HMGN2, HMGN3a, HMGN3b and HMGN4) (Bustin M, 2001). The domain of HMGN proteins comprises three important functional regions: a bipartite nuclear localization signal (NLS), a 30 amino acid-long nucleosomal binding domain (NBD) and an acidic chromatin-unfolding domain (CHUD) (Bustin M., 2004) (Figure1.4.1.3.3). The levels of expression HMGN proteins are tightly linked to cellular differentiation exhibiting an inverse correlation between the level of HMGN proteins and the differentiation state of cell (Furusawa T et al., 2006 and Korner U et al., 2003). Such changes in HMGN observed during mouse

embryogenesis but not in continuously renewing cell types such as the basal kidney epithelium (Furusawa T. et al., 2006, Lehtonen S, Lehtonen E., 2001). Studies have shown that differentiation is inhibited upon HMGNs overexpression in cells (Furusawa T. et al.,2006, Pash JM, Alfonso PJ, Bustin M., 1993). HMGN proteins majorly function through the unfolding of higher-order-chromatin structure, thus, enhancing transcription, replication and DNA repair from chromatin templates (Bustin M., 2004). They facilitate chromatin unfolding by out-competing H1 for chromatin binding site and are highly mobile within the chromatin with residence-times ranging from 4 to 25 seconds (Catez F, 2002 and Phair RD, 2004). HMGN induces structural changes in chromatin by affecting the levels of post-translational modification in the tails of histone proteins (Reeves R., 2010) (Figure1.4.1.3.3). HMGN proteins exhibit tightly binding exclusively with nucleosome core particles, stabilizing their structure (Bustin M, Reeves R., 1996) (Figure1.4.1.3.3) and are the only non-histone proteins which bind specifically inside the nucleosome between the DNA gyres and the histone octamer core along with histone H3 and H2B tail being involved in the interaction (Bustin M., 2004). The mode of binding of HMGNs to chromatin is cell cycle dependent as HMGN1 and HMGN2 are distributed in distinct foci in interphase nuclei (Cherukuri S. et al., 2008). They enhance transcription acting as a genome-wide coactivator (Ding HF. et al, 1994 and Trieschmann L et al.,1995). Studies done in embryonic fibroblasts shows depletion of HMGN1 leads to both up and down-regulation of gene expression (Briger Y., et al., 2006), suggesting that specific subsets of genes may be differentially regulated by different HMGN proteins. Recent studies show that HMBN1 has role in enhancing DNA repair where Cockayne syndrome A and B proteins (CSA and CSB) cooperate to recruit HMGN1 and certain transcription factors to nucleotide excision repair (NER) complex to facilitate lesion removal and the re-initiation of transcription (Fouster M et al., 2006). Studies on embryonic fibroblasts from Hmgn1+/+ and Hmgn1−/− mice demonstrated that increase in the rate of heat shock-induced H3K14

acetylation in the Hsp70 promoter is mediated by HMGN1, assisting chromatin remodeling and thereby transcriptional activation induced by Hsp70 in the initial rounds (Belova GI. et al., 2008). HMGN1 is involved in chromatin decompaction facilitating Nucleotide excision repair (NER) proteins to access the damaged site thus repairing UV-induced lesions (Birger Y. et al.,2003 and West KL., 2004). HMGN proteins functions are influenced by extensive post-translational modifications that determines their mode of binding to chromatin. Phosphorylation of HMGN1 exhibits transient weakening of its chromatin binding ability facilitating kinases to subsequently access and phosphorylate the N-terminal tail of histone H3 thus contributing to 'histone code' modulation (Lim JH. et al., 2004).

Thus, collectively different studies highlight some distinct features of HMG family; one being that the proteins of each of HMG family member weakened the H1 binding to nucleosomes through dynamic competition for chromatin binding, second being that different HMG families do not compete with each other for chromatin binding instead functions synergistically competing with H1 binding for unique sites creating distinct protein complexes around different nucleosome linker DNAs.

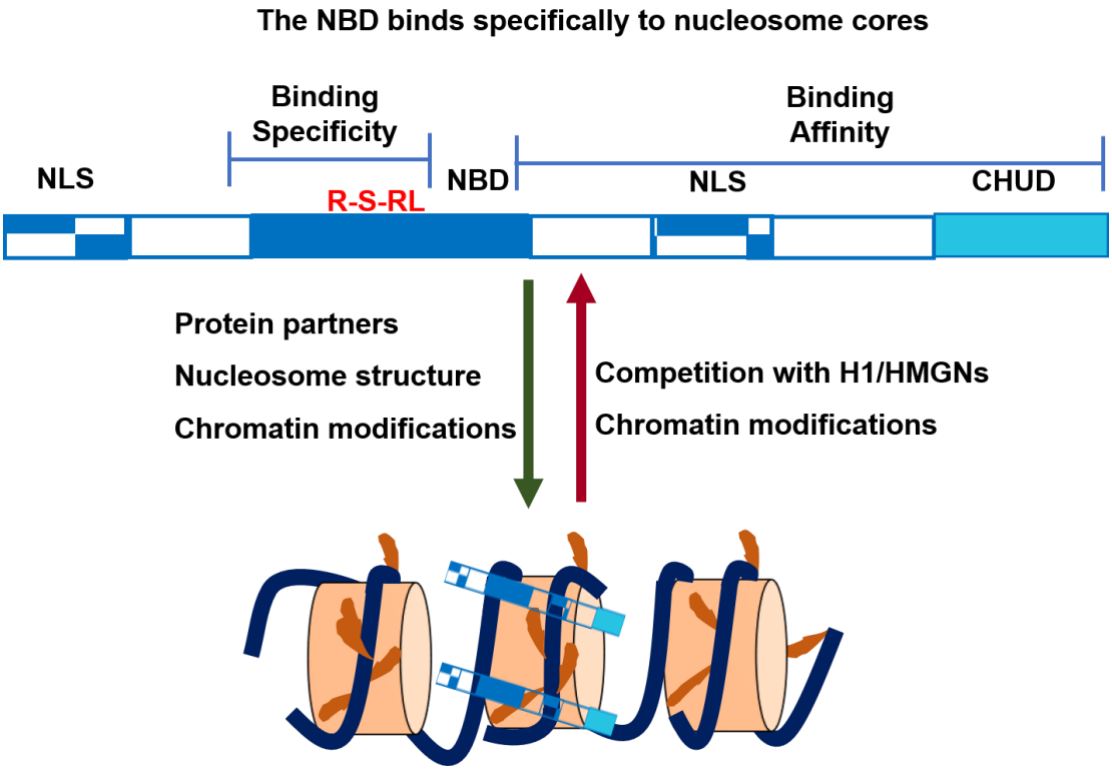

Figure1.4.1.3.3: Domain structure of HMGB and factors determining HMGB–chromatin interactions shown is a schematic diagram where the R-S-RL motif shown above the nucleosomal binding domain (NBD) denotes amino acid residues specifying HMGN interaction with nucleosome core particles. NLS denotes nuclear localization signal and CHUD denotes chromatin-unfolding domain. The factors indicated by green arrow promote HMGN interaction with chromatin, while those indicated by the red arrow promotes HMGN dissociation from chromatin.

1.4.1.4 Methyl CpG Binding protein 2 (MeCP2)

Methyl CpG binding protein 2 (MeCP2) is a member of a complex family of proteins, the methyl-CpG-binding domain (MBD) protein family binding to methylated cytosines, highly abundant in the adult brain establishing a link between DNA methylation and higher-order chromatin structure through interactions with chromatin modifiers (Nan, X., et al., 1998). MeCP2 located on

X chromosome is highly conserved in humans and has two isoforms; MeCP2 e1 (exon 1) and MeCP2 e2 (exon 2) that are differentially expressed in developing and post-natal mouse brains. The two isoforms have different amino termini as a result of alternative splicing and having different translational start sites. MeCP2 e1, the predominant isoform, expressing earlier than MeCP2 e2 in brain (Olson, C.O. et al., 2014) plays a role in neuronal maturation (Li, Y. et al., 2013) and responsible for Rett Syndrome (Fichou, Y et al., 2009, Saunders, C.J. et al., 2009 and Sheikh, T.I. et al., 2017). MeCP2 has two functionally characterized domains: the methyl-CpG binding domain (MBD) which specifically recognizes and binds 5-methylcytosine (5mC) and the transcriptional repression domain (TRD) which binds multiple transcriptional repressors mediating gene silencing as well as (Nan, X. et al., 1998, Lunyak, V.V et al., 2002, Kokura, K. et al., 2001, Suzuki, M. et al., 2003, Forlani, G. et al., 2010) multiple transcriptional activators activating gene expression (Schmidt A., Zhang H., Cardoso M C.,2020) (Fig.14.1.4.1). TRD has been narrowed down to the N-CoR/SMRT interacting domain in recent studies (NID) (Lyst, M.J. et al., 2013) (Figure 1.4.1.4.1)

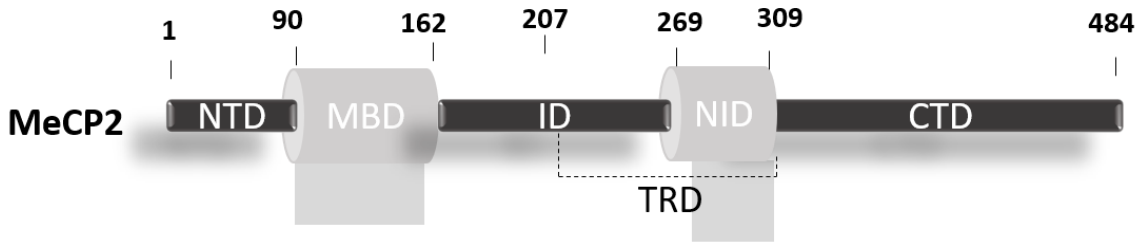

Figure 1.4.1.4.1: Domain organization of MeCP2 protein.

MeCP2 exhibits both methylation-specific and non-specific DNA binding that contribute to transcriptional repression and chromatin organization (Figure 1.4.1.4.2).

MeCP2 and chromatin fibers

MeCP2-mediated chromatin organization is responsible for MeCP2 mode of gene silencing (Georgel PT, Horowitz-Scherer RA, Adkins N, et al. 2003). Mutants of MeCP2 with a truncation in the AT hook 2 domain failed to induce high-order chromatin structures (Baker SA. et al., 2013) (Figure 1.4.1.4.2 A). Nikitina et al. showed that human MeCP2-e2 induces compaction of nucleosomal arrays containing 208bp long tandem repeats with 12 CpG units assembled with histones in a methylation independent manner with each MeCP2 molecule simultaneously binding to two different nucleosomes (Nikitina T. et al., 2007) (Figure 1.4.1.4.2 E). Mutant studies have shown that C-terminal portion of MeCP2 (from amino acids 295 to 486) is essential for its interaction with the chromatin. The methylation of CpGs increases the MeCP2-binding affinity for nucleosomes. MeCP2 forms similar architectural motif like linker histone H1 upon compacting tetra-nucleosomes. FRAP and fluorescence anisotropy assays studies shows that MeCP2 compete for nucleosome binding with H1 by strongly displacing them as they share common binding sites (Ghosh RP. et al., 2010). Abundance of MeCP2 in purified neuronal nuclei from mature brains is similar to that of histone octamers (Skene, PJ. et al., 2010) suggesting a compensatory role of neuronal MeCP2 for reduced amounts of H1 (Skene, PJ. et al., 2010 and Ghosh RP. et al., 2010). MeCP2 mediated gene silencing mechanism through higher order chromatin structure was identified for the imprinted Dlx5-Dlx6 (distal-less homeo box 5/6) locus in mouse brain (Horike S. et al., 2005).

MeCP2 and pericentric heterochromatin organization

Pericentric heterochromatin (PCH) characterized by specific epigenetic markers; DNA methylation, histone variants, hypoacetylation and methylation of H3-Lys9, HP1 protein recruitment aggregates forming chromocenters. MeCP2 is involved in PCH organization (Brero A. et al., 2005) (Figure 1.4.1.4.2 F) with increased MeCP2 expression and methylation of CpGs correlating in PCH during

myogenic differentiation. Overexpression studies using MeCP2-YFP revealed a negative correlation between MeCP2-YFP amount and chromocenter number. Later studies shown role of MeCP2 in the re-organisation of nucleoli in neurons showing higher number of small sized nucleoli in MeCP2-deficient mice (Brero A. et al., 2005). MeCP2 is involved in activity-dependent chromatin re-organization during postnatal neuronal maturation, which possibly acts through induction of chromocenter clustering (Singleton, MK. et al., 2011). Increased MeCP2 levels during neural differentiation leads to remarkable chromocenter clustering, whereas this PCH compaction was strongly impaired in MeCP2-null cells (Bertulat, B. et al. 2012). The missense RTT mutations of MeCP2 affects PCH binding and not the aggregation of heterochromatin organization (Agarwal, N. et al., 2011). Recent techniques of quantitative high-resolution imaging compared the differences in chromatin architecture in the brain from WT and Mecp2-null female mice (Linhoff MW. et al., 2015). Array tomography (AT) imaging shows increased heterochromatin compaction and a redistribution of trimethylated H4-Lys20 into PCH in MeCP2-null hippocampal neurons. The truncated MeCP2 protein coded for by the Mecp2tm1.1Jae (Chen, RZ. et al., 2001) lacking most of the MBD exhibits diffused distribution in brain nuclei contrary to the accumulated WT MeCP2 on PCH, suggesting a role of MBD domain in the binding with the chromocenters. Studies in both myoblasts differentiating into myotubes, and myoblasts ectopically expressing MeCP2 showed that the chromocenter clustering was associated with increased MeCP2 expression (Agarwal N. et al., 2007, Brero A. et al., 2005).

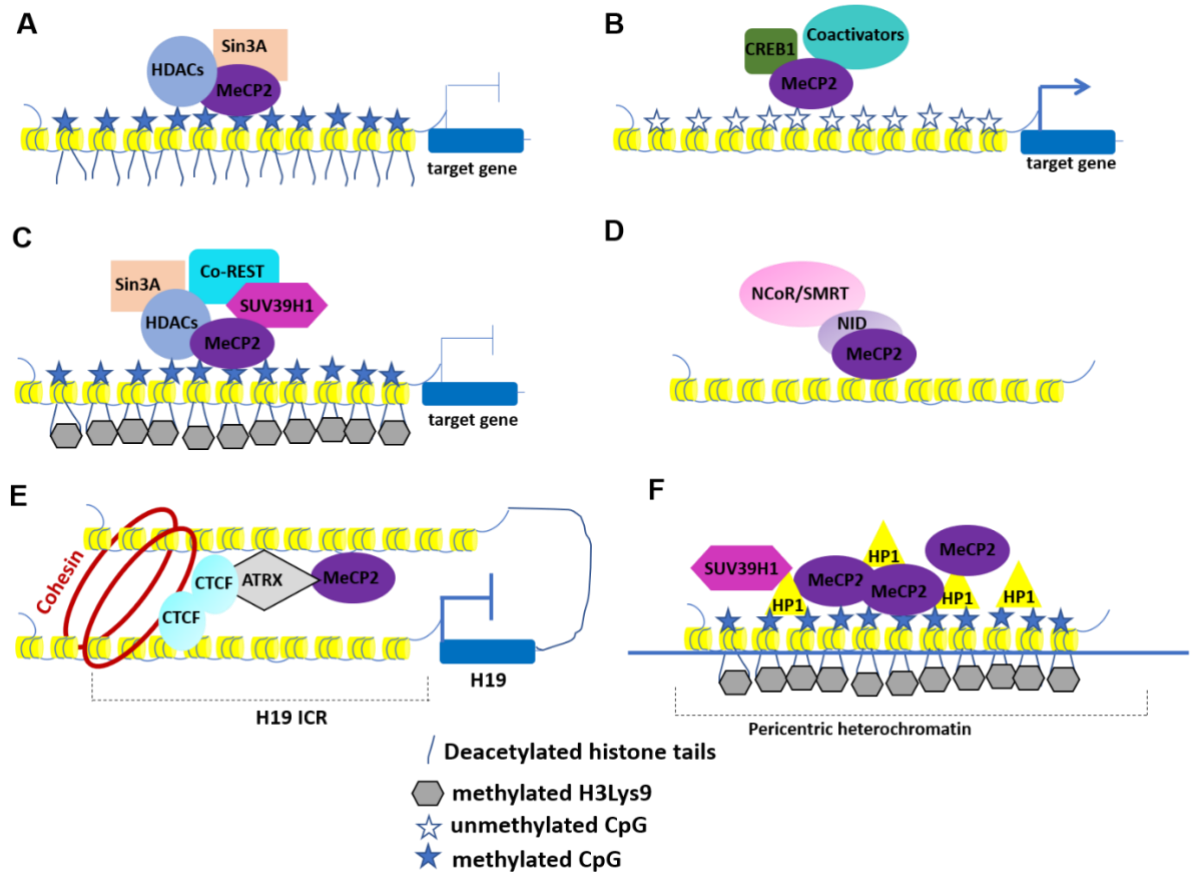

Figure 1.4.1.4.2: Different MeCP2 complexes with several molecular partners: (A) MeCP2 mediated transcriptional silencing through methylated CpGs binding and the recruitment of a HDAC-containing complex. (B) MeCP2 mediated transcriptional activation. (C) MeCP2 and CoREST mediated heterochromatinization leading to neuronal gene repression. (D) MeCP2 recruits the NCoR-SMRT co-repressor complex to chromatin by NID domain. (E) MeCP2, ATRX and cohesin bind the maternal allele of H19 ICR, and promote CTCF binding and formation of higher-order chromatin loops. (F) MeCP2 facilitates binding of HP1 on pericentric heterochromatin during myogenic differentiation.

1.4.1.5 DEK

DEK is an evolutionarily conserved protein implicated in the regulation of multiple chromatin-related processes (Sandén C., Gullberg U., 2015). DEK

which is discovered as chromosomal translocation in a subset of patients with myeloid leukemia (von Lindern et al., 1990; Soekarman et al., 1992); is a bona fide oncoprotein (Wise-Draper et al., 2009) and is associated with a number of different types of tumors (Riveiro-Falkenbach and Soengas, 2010). DEK is involved in determining the fate of stem and progenitor cells (Broxmeyer et al., 2012). DEK possess the property of DNA, chromatin, and histone binding as well as DNA-folding activities thus behaving as an architectural chromatin protein (Alexiadis et al., 2000; Waldmann et al., 2002, 2003; Kappes et al., 2004a, 2004b, 2008, 2011; Tabbert et al., 2006; Gamble and Fisher, 2007; Sawatsubashi et al., 2010). DEK, a nuclear phospho-protein, that remain associated with chromatin throughout all the stages of cell cycle (Kappes, F. et al., 2001) and present in both active and repressed chromatin foci. It undergoes oligomerization thus altering the chromatin structure in phosphorylation dependent manner. DEK can alter the DNA topology only in the chromatin and not with naked DNA and in presence of H2A-H2B dimer (Alexiadis, V. et al., 2000). *In vitro* DNA binding studies reveal DEK displays preferential binding to supercoiled and cruciform DNA (Waldmann et al., 2003). There are studies which indicate sequence-specific binding of human DEK (Hs-DEK) to DNA (Waidmann S. et al., 2014), and Drosophila melanogaster DEK (Dm-DEK) with the nuclear ecdysone receptor locus (Sawatsubashi et al., 2010). DEK regulates integrity of heterochromatin regions and can be attributed to its histone chaperone activity, although shown *in vitro* (Sawatsubashi et al., 2010; Kappes et al., 2011). DEK binds to supercoiled DNA and several DEK molecules cooperate to link separate DNA sites on the same or different DNA strand.

DEK's role as a chromatin protein regulates several important cellular processes such as DNA replication (Alexiadis et al., 2000), DNA double-strand break repair (Kappes et al., 2008; Kavanaugh et al., 2011), mRNA splicing (Le Hir et al., 2000,

2001; McGarvey et al., 2000; Soares et al., 2006), and transcriptional regulation (Sandén C., Gullberg U., 2015).

DEK as proto-oncogene

Due to DNA binding ability of DEK, it emerged as a novel class of DNA topology modulators making it a plausible target as well as effectors of pro-tumorigenic events. The DEK locus at chromosome 6p22.3 is amplified or reorganized in multiple cancer types. DEK's involvement in tumor is both at the transcriptional level and attributed to its post-translational modifications favoring cell transformation, by inhibiting cell differentiation and premature senescence. Recent reports suggest that DEK contributes to the resistance of malignant cells to apoptotic inducers (Kappes, F. et al., 2008) and upon knocking down DEK results in enhanced apoptosis and chemosensitivity of canine transitional cell carcinoma cells (Yamazaki H., et al., 2015). DEK also possess RNA binding ability and affect alternative splicing hinting at pleiotropic roles that this protein may exert in cancer cells (McGarvey, T. et al., 2000, Soares, LM. et al., 2006). Thus, the DNA binding ability that regulates its chromatin functions also establishes its role as a proto-oncogene.

1.4.1.6 Poly(ADP-ribose) polymerase 1(PARP1)

PARP1 is a nucleosome-binding architectural protein like the linker histone H1, promoting structural alterations in chromatin and modulating transcriptional responses (Krishnakumar R., Kraus WL., 2010). PARP-1 can alter nucleosome spacing and promote the compaction of nucleosomal arrays (Happel and Doenecke, 2009; Kim et al., 2004; Wacker et al., 2007) and elicits grossly similar alterations in chromatin structure *in vitro* like linker histone H1 (Kim et al., 2004; Wacker et al.,2007), but their effects on chromatin structure may vary *in vivo* (Kraus, 2008). PARP-1 competes with H1 compete for binding to nucleosomes (Kim et al., 2004) and exhibit a reciprocal pattern of binding at actively

transcribed promoters (Krishnakumar et al., 2008). PARP1 is a highly conserved chromatin protein and it consists of three main domains: an amino-terminal DNA-binding domain (DBD) that consists of zinc finger motifs, a BRCT domain-containing central auto-modification domain and a highly conserved carboxy-terminal catalytic domain (Ciccarone F., Zampieri M., Caiafa P.,2017) (Figure 1.4.1.6.1 A).

PARP-1 mediated PARylation and DNA Repair

PARP-1 is also a unique chromatin architectural protein possessing an intrinsic enzymatic activity that catalyses the polymerization of ADP-ribose units from donor NAD+ molecules on target proteins (D'Amours et al., 1999) (Figure 1.4.1.6.1 B). PARP-1 itself is the major substrate for PARylation *in vivo* through auto-modification besides, core histones, linker H1, and a variety of nuclear proteins involved in gene regulation, are also PARylated by PARP1 (D'Amours et al., 1999; Krishnakumar and Kraus, 2010) altering their function in an inhibitory manner (Kraus, 2008; Krishnakumar and Kraus,2010). PARylation of PARP-1 can inhibit its ability to bind nucleosomes (Kim et al., 2004; Wacker et al., 2007), while PARylation of components of the TLE1 corepressor complex can promote its dissociation from target gene promoters (Ju et al., 2004). PARP1 possess very low catalytic activity with PAR having an estimated half-life of up to several hours. Upon inducing DNA strand-break, PARP1 dimerizes at the site of break, activating its enzymatic function (Beneke S., 2012). PARylation metabolism increases as one of the early cellular responses upon exposure to genotoxic stress (Haince et al.,2007,2008) (Figure 1.4.1.6.1 B).

Upon DNA damage, PARP1 is rapidly recruited to sites of damage through its DNA-binding ability stimulating the covalent attachment of ADP-ribose units to Glu, Asp or Lys residues of acceptor proteins by a transesterification reaction (Ray Chaudhuri A., Nussenzweig A., 2017). Repeating units of ADP-ribose are attached through 2′,1′′-O-glycosidic ribose–ribose bonds forming long polymers

chains of PAR containing branches every 20–50 ADP ribose units (Ray Chaudhuri A., Nussenzweig A., 2017) (Figure 1.4.1.6.1 B). Proteins involved in the DNA damage repair and in DNA metabolism interact with PARP proteins via binding to PAR through non-covalent interactions, recruiting it to DNA damage sites (Krietsch, J. et al., 2013) (Figure 1.4.1.6.1 C). Target protein exhibit non-covalent interactions with PARP-1 contain PAR-binding modules, such as PAR-binding consensus motifs (PBMs), PAR-binding zinc finger motifs (PBZs), macrodomain folds, WWE domains and many other modules (Krietsch, J. et al., 2013, Teloni, F. & Altmeyer, M., 2016). The prompt turnover of PAR is critical for mediating efficient DNA repair (Ray Chaudhuri A., Nussenzweig A., 2017) (Figure 1.4.1.6.1).and defective PAR catabolism aften results in increased DNA damage that are deleterious for cells (Ray Chaudhuri, A. et al., 2015, Ray Chaudhuri A., Nussenzweig A., 2017). Studies have revealed that recruitment of X-ray repair cross-complementing protein 1 (XRCC1), a core factor for single strand break repair is PARP1 dependent (Hanzlikova, H. et al., 2017, Ray Chaudhuri A., Nussenzweig A., 2017). Recent studies have shown that PARP1 is involved in the initial steps of damage recognition in global genome nucleotide excision repair (GG-NER), a dominant sub-pathway of nucleotide excision repair (NER). DDB2-stimulated PARylation of histones by PARP1 results in the recruitment of the chromatin-remodelling helicase amplified in liver cancer protein 1 (CHD1L) through its PAR-binding domains that is required for the repair of UV lesions (Pines, A. et al., 2012).

PARP1 also acts as a sensor of DNA double-strand breaks (DSB) facilitating DSB repair (Ray Chaudhuri A., Nussenzweig A., 2017). Studies of PARP1 deficiency or inhibition have shown repair proteins such as phosphorylated histone H2AX, p53 and structural maintenance of chromosomes protein 1 (SMC1), which are targeted to DSBs by the apical DDR kinase ataxia telangiectasia mutated (ATM) (Haince, J. F. et al., 2007). PARP1 recruits the DNA damage sensors meiotic recombination 11 (MRE11) and Nijmegen

breakage syndrome protein 1 (NBS1) to sites of DSBs (Haince, J. F. et al., 2008) and early recruitment of MRE11 in homologous recombination (HR) by PARP1 leads to DNA-end processing and helps in DNA repair-pathway choice by channelling the repair of DSBs towards HR (Hochegger, H. et al., 2006).

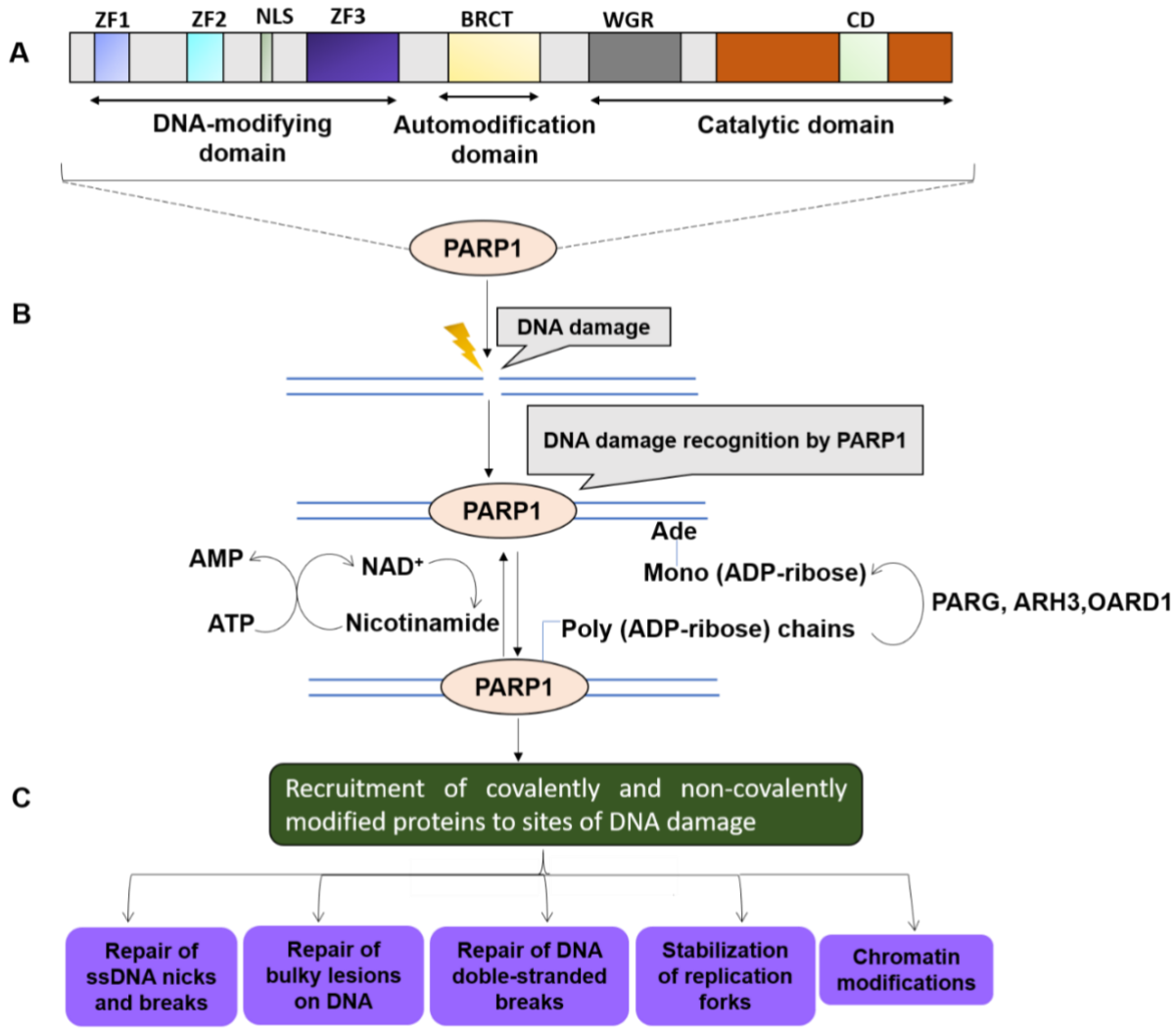

Figure 1.4.1.6.1: The biochemical functions of PARP1 in DNA damage repair. (A) The domains of PARP1are shown. (B)PARP1 detects DNA damage through its DNA binding domain (DBD), activating synthesis of poly (ADP-ribose) (PAR) chains mainly on itself but also on some of its target proteins. NAD+, used as substrate for PARylation is replenished in the cells from nicotinamide, using ATP. PAR chains are rapidly catabolized by PAR glycohydrolase (PARG), ADP-ribosylhydrolase 3 (ARH3) and O-acyl-ADP-

ribose deacylase 1 (OARD1) to release mono (ADP-ribose). (C) PARylation of PARP1 and other target proteins, both covalently and non-covalently, results in the recruitment of multiple proteins that have roles in different aspects of DNA damage repair.

PARP1 as chromatin modulator during DNA Damage Repair

PARP1 mediated DNA repair response necessitates involvement of PARP1 in the modulation of chromatin structure to facilitate the repair process. PARP1 can facilitate nucleosome disassembly by PARylating histones, resulting in chromatin relaxation (Figure 1.4.1.6.2) (Messner, S. et al., 2010, Poirier, G. G. et al., 1982) required for the recruitment of multiple chromatin remodeller to ensure chromatin accessibility for repair (Figure 1.4.1.6.2). Recruitment of remodellers like ALC1 by PARP-1 at DNA damage sites results in nucleosome repositioning and increased accessibility of DNA repair factors (Ahel, D. et al., 2009, Gottschalk, A. J. et al., 2009). Loss of PARP1 or ALC1 sensitises cells to DNA-damaging agents due to delayed repair (Pines, A. et al., 2012, Ahel, D. et al., 2009 (Figure 1.4.1.6.2). Another remodelling complex component SWI/SNF-related matrix-associated actin-dependent regulator of chromatin subfamily A member 5 (SMARCA5), is also recruited to DSBs in a PARP1-dependent manner (Smeenk, G. et al., 2013) and it interacts with the PARylated E3 ubiquitin ligase RING finger protein 168 (RNF168) thus playing role in NHEJ repair pathway (Figure 1.4.1.6.2). CHD2 is another example of a chromatin remodeler that is recruited by PARP-1 to DSBs which triggers the deposition of the histone variant H3.3 at these sites resulting in chromatin relaxation, thus promotes efficient repair by NHEJ (Luijsterburg, M. S. et al., 2016) (Figure 1.4.1.6.2). Besides chromatin remodelers, translocation of transcription factors like NR4A (a member of the nuclear orphan receptors) to DSBs occurs after PARP1 relaxes the chromatin relaxation (Figure 1.4.1.6.2) inducing its phosphorylation by DNA protein kinase Cs and facilitates DNA repair (Malewicz, M. et al., 2011). Following DNA

damage, transcription repression complexes are recruited to damage sites by PARP-1 like the nucleosome remodeling and deacetylase (NuRD) complex proteins CHD4 and metastasis-associated protein1 (MTA1) (Ray Chaudhuri A., Nussenzweig A., 2017) and members of Polycomb repressive complex 1 (PRC1) (Chou, D. M. et al., 2010) leading to gene silencing (Figure 1.4.1.6.2). Thus, PRAP-1 modulates local chromatin structure at DNA damage sites both through opening of the chromatin by evicting the nucleosomes and recruiting chromatin remodelers as well as by repressing the transcriptional activity at the DNA damage sites to prevent clashes between DNA repair and transcription machineries (Figure 1.4.1.6.2).

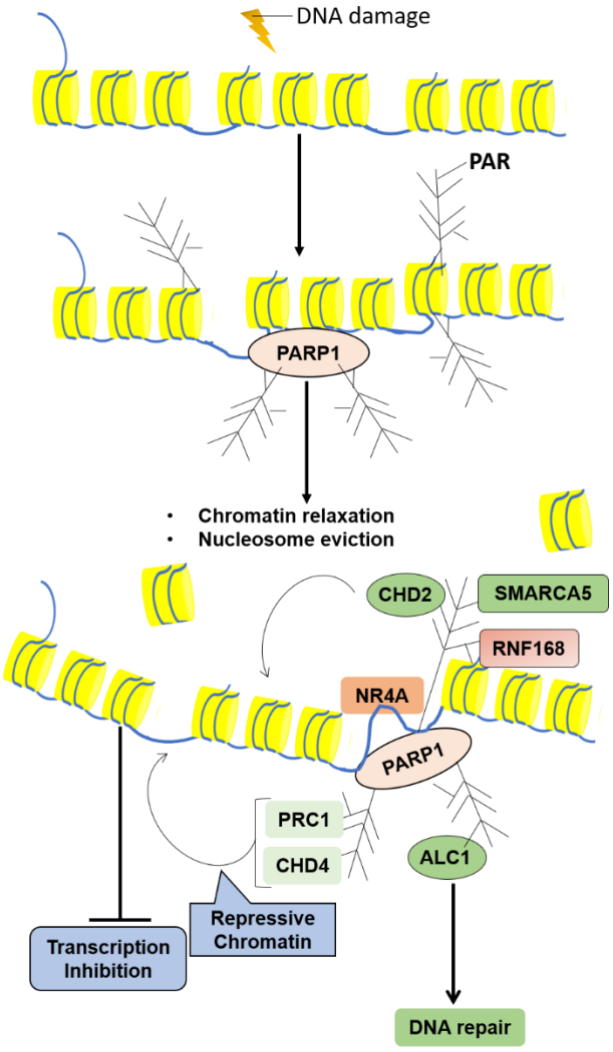

Figure 1.4.1.6.2: PARP-1 induced Chromatin changes mediating DNA repair.

1.4.1.7 Myeloid and erythroid nuclear stage specific protein (MENT)

Myeloid and erythroid nuclear stage specific protein (MENT) is another abundant nuclear protein that is developmentally regulated and found in terminally differentiated avian blood cells belonging to the serine protease inhibitor family. The protein has a Reactive Centre Loop (RCL) that helps in its oligomerisation (Springhetti, E. M. et al., 2003) required for its role in chromatin condensation. It binds to the chromatin through an AT-hook domain within the M-loop region (Springhetti, E. M. et al., 2003). MENT forms a zipper like structure bridging the DNA molecules similar to histone H1 by bringing together the nucleosomal linkers in close proximity (Fig. 1.4.1.7 B). MENT is capable of inhibiting the papain-like cysteine proteases, cathepsins V and L (Ong PC. Et al., 2009).

MENT as a potent chromatin remodelling protein is responsible for heterochromatin spreading and controlling terminal cell differentiation in avian erythrocytes (Grigoryev SA et al., 1992) with an interhelical extension termed the M-loop region primarily responsible for its interaction with nucleosomal DNA, an area centred on the D- and E-helices (McGowan S. et al., 2006). Several studies suggest a relationship between the inhibitory activity of MENT and its role in condensing chromatin: (Silverman GA et al., 2001) protease inhibition by MENT attributes to chromatin rearrangements *in vivo* (Ong PC. Et al., 2009); (2) cathepsin V, a nuclear protease regulating transcription factor CDP/CUX, has been rendered susceptible to MENT inhibition in the presence of DNA (Ong PC. et al., 2009); and (3) MENT is able to form protein-protein bridges, mediated by the RCL, that may be important for chromatin remodelling function (McGowan S. et al., 2006). Studies have shown that the distribution of MENT protein was opposite to that of acetylated core histones but correlated with that of histone H3 di-methylated at lysine 9 (H3K9me2) and ectopic MENT expression in NIH 3T3 cells caused a large-scale and specific remodelling of chromatin marked by

H3K9me2 with MENT colocalizing with H3me2K9 both in chicken erythrocytes and NIH 3T3 cells (Istomina, N.E. et al., 2003) (Fig. 1.4.1.7 A). Thus, such studies suggest that histone H3 modification at lysine 9 directly regulates chromatin condensation by recruiting MENT to chromatin in a spatially constrained manner separating active genes by gene boundary elements and histone hyperacetylation (Istomina, N.E. et al., 2003) (Fig. 1.4.1.7 A).

MENT initiates a bipartite mechanism leading to chromatin repression in granulocyte binding to linker DNA entry–exit segments bringing them to close apposition in a linker region (Grigoryev 2001) followed by interactions mediated by the RCL β-strand between adjoining molecules (McGowan et al. 2006) facilitating the protein oligomerization thus bridging laterally self-associated chromatin fibers and forming strongly compacted chromatin states (Fig. 1.4.1.7 B). MENT mediated chromatin condensation might be locally enhanced by other proteins, such as linker and core histones (Fig. 1.4.1.7 B). Studies validate the fact that heterochromatin spreading depends on the changing levels of the MENT (Grigoryev and Woodcock 1998) or the linker histone composition (Koutzamani et al. 2002) in distinct chromatin regions.

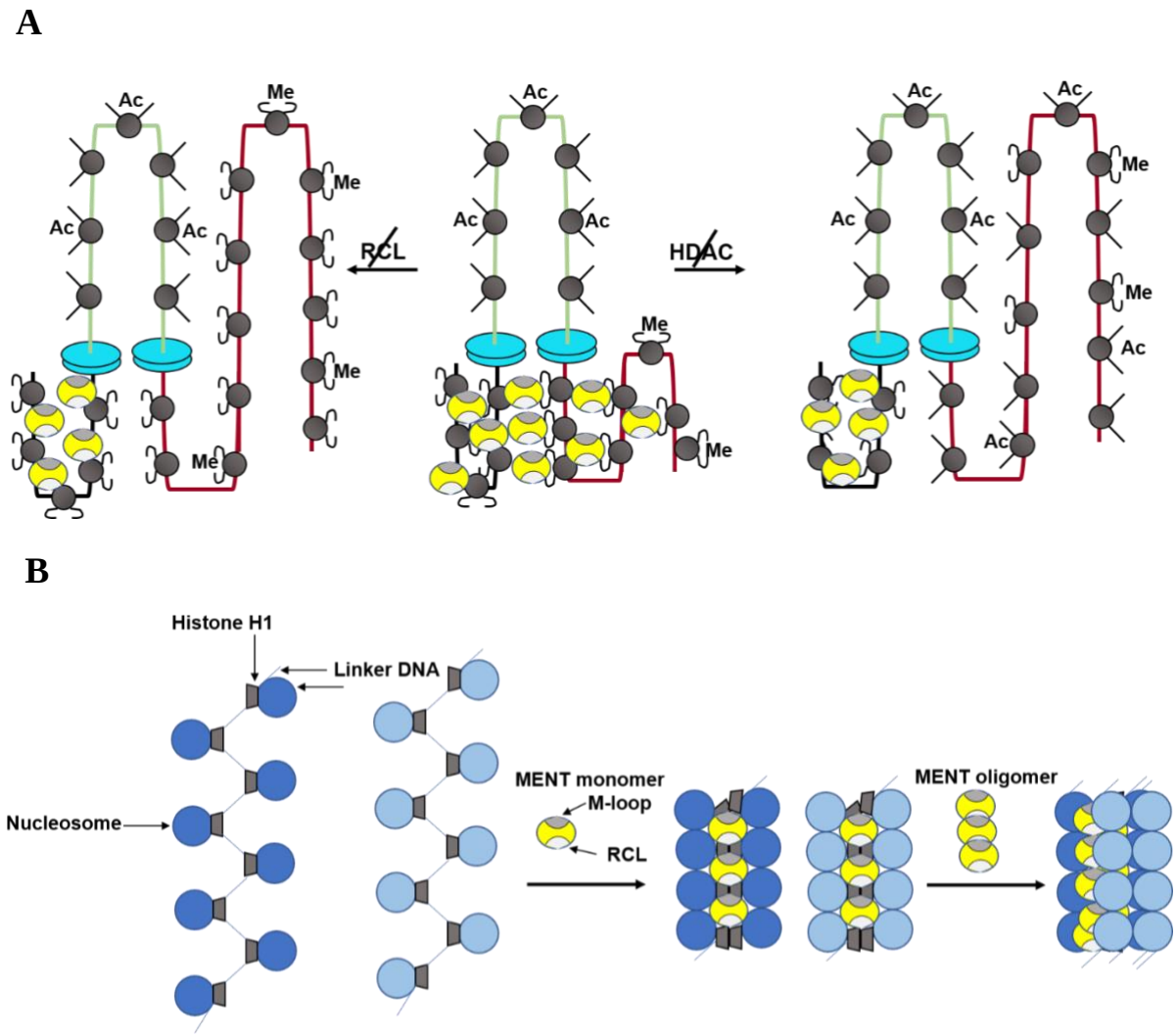

Figure 1.4.1.7: (A). A model representing MENT mediated chromatin condensation regulated by histone modifications, and gene boundary elements. MENT (yellow) binding simultaneously to constitutive heterochromatin (black) and silenced euchromatin (red) marked by H3K9me2. MENT exhibits cooperative binding to chromatin bridging between chromatin fibers bringing euchromatin containing methylated H3 close to constitutive heterochromatin, thus causing chromatin condensation. A hyperacetylated chromosomal domain (green) is insulated from MENT spreading by boundary elements (blue disks) creating hyperacetylated regions blocking MENT spreading from the domain flanks. (Right structure) Histone deacetylase (HDAC) inhibitors increase the acetylation level of non-centromeric chromatin, interfering with MENT-histone

interactions, and promoting MENT binding to constitutive heterochromatin. (Left structure) Mutations in RCL domain of MENT disrupt its interaction with H3K9me2 bound chromatin and promotes MENT binding to constitutive heterochromatin. (B) Model showing the two-step formation of compacted chromatin fibers initiated by binding of MENT-monomers to DNA followed by folding of the nucleosome arrays finally self-association of the chromatin fibers by MENT-oligomers.

1.4.2 Cross talk among CAPs and their functional consequence

Chromatin compaction is a multifaceted event which requires a coordinated functional interaction among the chromatin associated proteins. Along with the linker histone H1, several other proteins are known to bind to the DNA entry and exit site within a nucleosome forming a chromatosome like particle called CLiP. The strength of binding of the chromatin proteins at the DNA entry/exit site in a CLiP determines the accessibility of nucleosomal DNA to regulatory factors. The chromatin protein undergoes post-translational modifications which mediates functional interaction between these proteins. A very important example of such functional interaction is between the two key components of heterochromatin linker histone H1 and HP1-α. H1 upon phosphorylation by CDK2 doesn't interact with HP1-α leading to disassembly of higher order chromatin structure during interphase (Figure 1.4.2.1 B). H1 regulates HP1-α binding and heterochromatin formation (Hale, T. K., et al., 2006). Studies in D. melanogaster shows that H1 depletion in larvae failed to develop into adults due to massively altered chromosome structure with loss of chromosome banding, lower levels of H3K9me2 and several Heterochromatin protein1(HP1) foci (Lu X et al., 2009) (Figure 1.4.2.1 A). Depletion of H1 caused de-repression of more than 50% of transposable elements (TEs) located in the heterochromatin by interacting with histone methyltransferase Su(var)39 facilitating H3K9 methylation (LU X et al., 2013) and tethering it to heterochromatin providing a binding platform for HP1

(LU X et al., 2013 and Lu X, 2009). H1 and the HP1 protein interaction in mammals is thought to be subtype specific and dependent on a specific methylation of H1 (Nielsen AL ,2001, Daujat S, 2005, Trojer P ,2009) (Figure 1.4.2.1 A). HP1 members also exhibit functional interactions with other non-chromosomal proteins to mediate chromatin state. HP1α interacts with Positive coactivator 4 to recruit REST-CoREST repressor complex to silence neuronal gene expression in non-neuronal cells (Figure 1.4.2.1 B) (Das C et al., 2010).

There is a competition among the chromatin associated proteins for the binding to the chromatin and bring about dynamic changes in the chromatin organisation. PARP1 excludes H1 from the promoters of some PARP-1 regulated genes possibly by competing with H1 for binding to nucleosomes or by PARylating it (Krishnakumar, R. et al., 2008). During estrogen-induced transcription of TFF1, a PARP-1 target gene, PARP-1 promotes removal of H1 from its promoters as well as increases the levels of a chromosomal architectural protein HMGB1 to enhance transcription (Ju, B. G. et al., 2006). PARP-1- dependent PARylation of another abundant and ubiquitous non-histone protein DEK leads to its dissociation from the chromatin inducing transcription (Gamble MJ, Fisher RP.,2007). PARP-1 and SIRT-1 share an intriguing connection at the molecular level (Zhang, J., 2003) as increased levels of PARP-1 activity leads to depletion of NAD+ levels leading to reduction in HDAC activity of SIRT1 (Pillai, J. et al., 2005) on the other hand SIRT1 activation leads to loss of PARP-1 activity. PARP1's contribution in maintaining a transcriptional amenable landscape at the gene promoters by preventing demethylation at H3K4me3 and also facilitating exclusion of linker histone H1 (Krishnakumar and Kraus 2010). Other chromatin proteins like SATB1 (matrix attachment region (MAR)-binding protein, special AT-rich sequence binding protein 1) are involved in establishing higher order chromatin loop structures at the MHCI locus by directly interacting with PML (Pavan Kumar et al. 2007).

Several studies suggest that post-translational modifications of the chromatin proteins as well as the chromatin becomes a mediator of interactions between chromatin proteins like; linker histone H1 acetylated at lysine 85 recruits HP1 facilitating chromatin compaction and dynamic mobilization of HP1 upon DNA damage (Yinglu Li et al., 2018) (Figure 1.4.2.1 A iii).

The chromatin fluidity is a result of combinatorial action brought about by the histone chaperones and the ATP-dependent chromatin remodelers (Wright et al. 2016) resulting in the assembly and disassembly of the nucleosomes, to allow the course of RNA Pol II along the DNA template regulating gene expression. Histone chaperones mediating deposition or eviction of either canonical histone subunits or non-canonical histone variants also comprise chromatin proteins having functions besides their nucleosomal activity. Histone chaperones regulate histone metabolism, DNA replication, transcription, repair and maintenance of genome integrity (Venkatesh and Workman 2015). Similarly remodeling factors comprises chromatin binding proteins interacting to facilitate transcription, by attributing to changes in nucleosome architecture in order to facilitate the recruitment of RNA Pol II at the promoters of active genes. The A-T rich sequence present at the upstream of the transcribed region maintains a nucleosome-depleted region (NDR) with the help of chromatin remodelers like the RSC complex (Erkina et al. 2010; Talbert and Henikoff 2017) and SWR-dependent incorporation of the H2A.Z variant into the nucleosomes flanking the NDR takes place promotes transcription initiation. In higher eukaryotes, the H3.3 variant exchange takes place at enhancers, which results in increased incorporation of H2A.Z at the gene promoters. The sequence underlying the DNA template in the NDRs often exhibit binding sites for different chromatin factors to interact that ensures the binding of other factors/proteins to mediate the transcription of the gene.

Crosstalk among CAPs occurs at various levels and reflects a very perplexed relationship among them that is yet to be explored.

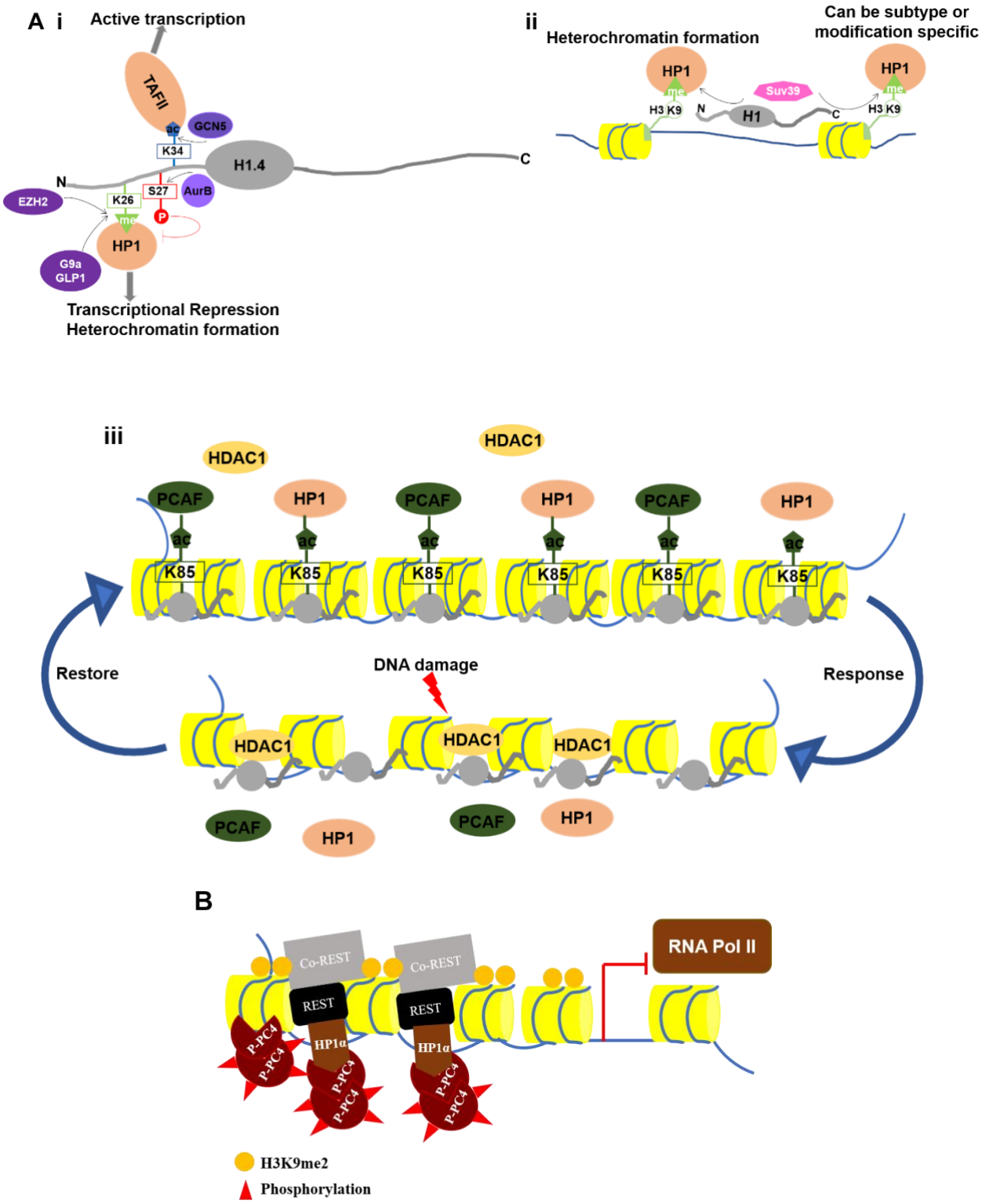

Figure 1.4.2: Implications of crosstalk between chromatin proteins (A) Interaction between two chromatin protein linker histone H1 and HP1 mediated by post-translational modifications in a subtype specific manner regulating different chromatin template-dependent functions in varying physiological

contexts. (B) PC4 interacts with HP1α to recruit REST-CoREST repressor complex onto neuronal genes to silence their expression in non-neuronal cells (Das, C. et al., 2010).

1.4.3. Regulation of epigenetic state by CAPs

The non-histone proteins often regulate the chromatin state by mediating the recruitment of different epigenetic modifiers: readers, writers and erasers onto the chromatin either by direct or via indirect interactions. Absence of some non-histone proteins like PC4 leads to the opening of the genome resulting in global hyperacetylation (Sikder et al.,2019). KAT3b or p300 specific histone acetylation signature seems to be upregulated in PC4 knockdown cells, which are involved in transcriptional regulation. PC4 interacts with histones which triggers chromatin modifications during Luteinizing hormone receptor (LHR) transcriptional activation. Treating breast cancer cells MCF-7 with Trichostatin A (TSA) reveals that PC4 interacts with acetylated H3.3 leading to LHR transcription. Knocking down of PC4 in MCF7 cells lead to decreased histone H3 acetylation and reduced H3.3 occupancy at LHR promoter thereby lower LHR promoter activity despite of TSA treatment which increases H3 and H3.3 protein expression (Zhao P et al., 2018). Transcription factors like p53 or histone chaperones like NPM1 mediated autoacetylation of CBP and p300 mediate such hyperacetylations in pathophysiological conditions such as oral cancer (Kaypee S et al.,2018 and Kaypee S et al.,2018). Other cellular factor that can modulate enzymatic activity of p300 under different signalling cues like the Notch signalling coactivator, MAML1, which interacts with the autoinhibitory domain, CH3 of p300, to enhance p300 autoacetylation and Notch pathway gene expression (Hansson et al. 2009). Under apoptotic conditions the metabolic enzyme GAPDH is S-nitrosylated and translocated to the nucleus upon interacting with the E3 ubiquitin ligase, Siah1. GAPDH, an abundant nuclear protein, also induces p300 autoacetylation inducing apoptosis upon nitric oxide

signalling (Sen N et al. 2008). Apart from being inducers of p300 mediated autoacetylation, non-histone proteins have also been reported to inhibit p300 autoacetylation such as Twist1 (Hamamori et al. 1999) and Polycomb protein of the PRC1 complex which binds to the un-acetylated autoinhibitory loop on CBP inhibiting CBP-mediated histone acetylation (Tie et al. 2016). Thus, direct modulation of p300 activity by these cellular factors can not only alter the epigenetic landscapes but can also shape the p300/CBP-mediated transcriptional network regulating important cellular functions and homeostasis.

Non-histone proteins controlling the epigenetic state of the chromatin often determines the fate in cellular differentiation. Depletion of Linker H1, which is intrinsically required in the regulation of germline stem cells (GSCs) in Drosophila ovary, leads to premature differentiation of GSCs through activation of the key differentiation factor bam and augmentation of H4 lysine 16 acetylation (H4K16ac). Further studies have revealed that overexpression of MOF reduces H1 association on chromatin thus H1 promotes GSC self-renewal by antagonizing MOF function (Sun J, 2015). H1 linker histone also plays a key role in regulating both DNA methylation and histone H3 methylation at the H19 and Gtl2loci in mouse ES cells by interfering with binding of theSET7/9 histone methyltransferase to the imprinting control regions inhibiting chromatin activation by methylation mark on histoneH3 lysine 4 (Yang SM, 2013). Linker H1 physically interacts with the histone methyltransferase Su(var)39 tethering it to heterochromatin, thus facilitating methylation of H3K9 (Lu X, 2013) and providing a binding platform for HP1 (Lu X, 2009). HP1 protein family which is known to be involved in gene silencing through heterochromatinization has also been shown to be required for gene expression. Recent report suggests that HP1α is specifically required for myogenic gene expression in myoblasts. Depletion of HP1α which binds to the genomic region of myogenic genes surprisingly increases H3K9me3 at these sites and binding of JHDM3A, a H3K9 demethylase to these genomic regions in myoblasts is dependent on its interaction with HP1α

(Sdek P.,2013). HP1 α interacts with another non-histone protein PC4 maintaining a repressed state of the chromatin and recruiting REST-CoREST repressor complex to repress neural gene expression in non-neuronal cells (Das C et al.,2010). H1 and the HP1 protein interaction in mammals is thought to be subtype specific and dependent on a specific methylation of H1 (Nielsen AL ,2001, Daujat S, 2005, Trojer P ,2009). Triple H1 knockout in embryonic stem cells (ESCs) underlie the role of H1 in structural maintenance of heterochromatin (Cao K et al., 2013).

HMG family of proteins also exhibits example of regulating the epigenetic modifications of histones like HMGN1 modulates the phosphorylation of histone H3 by binding to nucleosome and preventing the kinases from phosphorylating H3 either by steric hindrance or through conformational changes in histone tail thus Hmgn1−/− cells have elevated levels of H3S10p (Lim JH, 2004). HMGN1 also enhances H3K14ac by stimulating HAT activity optimising cellular response to heat shock (Lim JH et al, 2005). It also affects H3K9me and H3K9ac affecting transcription (Jenuwein T, Allis CD,2001 and Jim JH, 2004). PARP1 itself acts as an epigenetic modulator of chromatin by carrying out Poly (ADP-ribosyl) ation of histones that is associated with an extended and open chromatin conformation to drive the access of DNA repair factors to the damaged chromatin (Caiafa 2013). PARP-1 participates regulates DNA methylation in unmethylated regions of chromatin by controlling the DNA methylation pattern and protecting genomic DNA from full methylation (Guastafierro T. et al., 2013). It also regulates DNA methylation acting as pro-inflammatory enzyme deregulating the pattern of DNA methylation and histone deacetylase SIRT1 thus helping in ageing process (Cantó et al. 2013). We present a model depicting how different non-histone proteins regulates the epigenetic modifications of the chromatin regulating different chromatin functions.

One of the ways by which DNA methylation-mediated transcriptional repression occurs is through the binding of methylated DNA at CpG islands by proteins like

MeCP2 through their methyl binding domain (MBD) (Hendrich B, Bird A 1998). These proteins regulate gene repression by inducing a repressed chromatin state by facilitating chromatin modifiers like HDACs, methyltransferases chromatin-silencing factors, which increase chromatin condensation (Ballestar E Pile 2001 and Fujita N 2003) (Fig.1.4.3). During neuronal differentiation MeCP2 levels increases and is critical for maturation and maintenance of neurons (Cohen DR, 2003, Jung BP 2003 and Kishi N, 2004). It contains a transcriptional repression domain (TRD) that mediates its links with the histone modifications and co-repressors (Della Ragione, 2012) (Fig.1.4.3), a nuclear localization signal (NLS) that imports part of the total protein into the nucleus and a C-terminal domain that is involved in the interactions with DNA and its protein partners (Bienvenu T 2006).

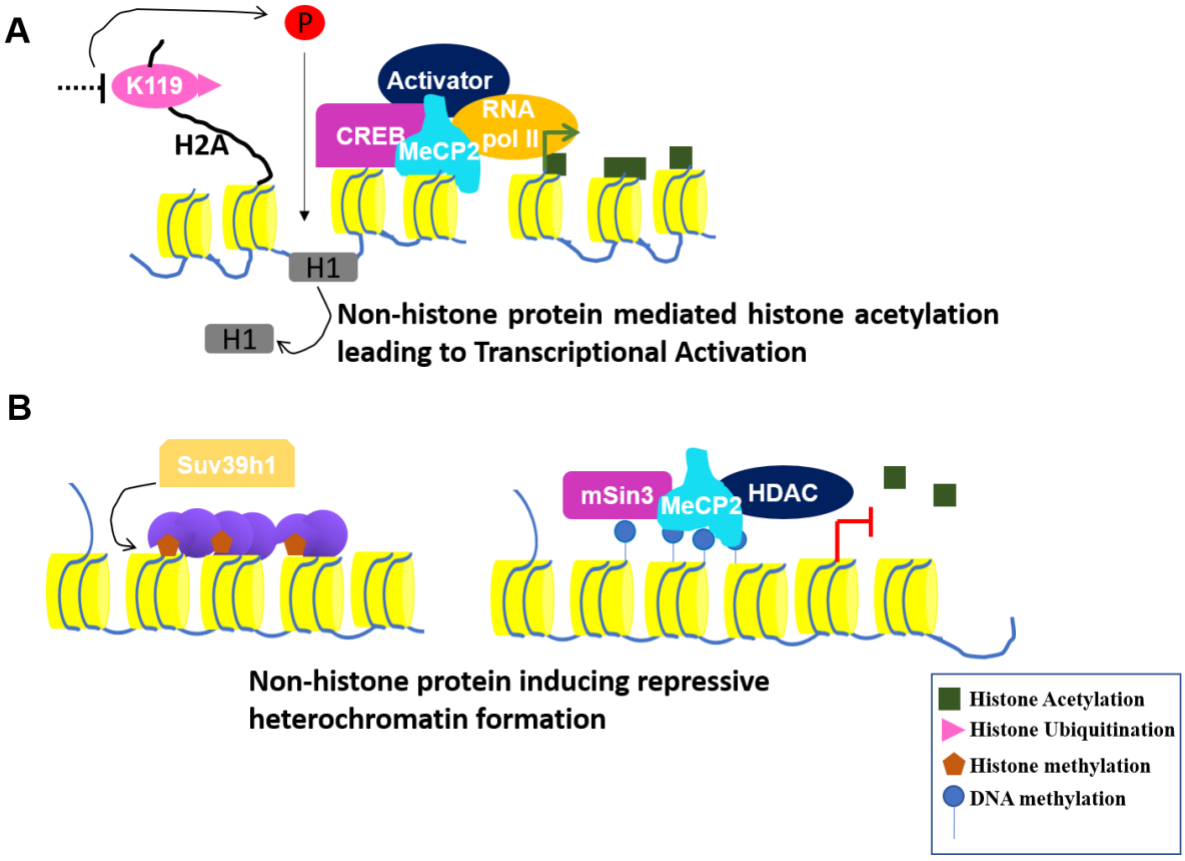

Figure 1.4.3: Different modes of regulation of the chromatin modification state by non-histone chromatin proteins. (A) MeCP2 mediated recruitment of

activator complex leading to histone acetylation facilitating transcription. Inhibition of ubH2A leads to phosphorylation of linker histone H1 which favours enhanced chromatin dissociation of this histone thus affecting transcription. (B) Non-histone chromatin proteins: MeCP2 and HP1 mediated repressive histone marks leading to a heterochromatin state.

1.4.4. Implication of CAPS in pathophysiological conditions: Cancer

The chromatin proteins are often deregulated in terms of their expression, function, post-translational modifications in various types of cancer. There are also several reports suggesting mutations in these proteins thereby disrupting the normal functions of the cell and promoting tumorigenesis. In this review we shall highlight the involvement of some of them in cancer.

Studies in breast cancer T47D cells shows that H1 could be a player in establishing lamina associated domains in normal cells thus regulating LAD rearrangement in cancer cells due to different prevalence of H1 variants within these domains. The relative abundance of H1.0, H1X variants at promoters suggests that promoter occupancy by H1 variants other than H1.2 is more permissive for transcription regulation in breast cancer cells (Millán-Ariño L. et al, 2014). H1.5 exhibits low expression level in benign prostate epithelial cells and low-grade cancer cells whereas in higher grade or even the expression level of H1.5 greatly increased (Khachaturov V, 2014). The same is observed for H1.5 in pulmonary neuroendocrine tumors (Hechtman JF, 2013). On the other hand, H1.0 level is anti-correlated with the presence of the proliferating cell marker Ki67, particularly in high grade cancer cells (Kostova NN, 2005). H1 expression profiling in ovarian cancer shows that H1°, H1.1, H1.4 and H1x are significantly reduced in expression, whereas H1.3 has drastically increased expression in ovarian adenocarcinomas compared with adenomas (Medrzycki M, 2014).

Studies in glioma samples also shows that lower levels of H1.0 in grade III-IV gliomas compared to grade II cancers and thus H1.0 downregulation plays a role in improving patient survival rate (Gabrovsky et al., 2013) quite similar to what is seen in case of less aggressive breast tumors expressing high levels of H1.0 (Kostova et al., 2005). Different histone variants exhibit different expression pattern that are signatures for specific cancer types and has distinct mechanism of actions contributing to tumorigenesis. For instance, in ovarian cancer cell line OVCAR-3, H1.3 represses the oncogenic non-coding RNA H19 mRNA by binding to its imprinting control region, increasing DNA methylation and preventing the insulator protein CTCF from binding to its cognate sites thus controlling cell growth and proliferation (Medrzycki et al., 2014). Other histone variants like H1.4 and H1.2 have a strong impact on cell survival of T47D cells as depletion of H1.2 causes G1 arrest and slows down proliferation and exhibit specific binding pattern across the genome (Sancho et al., 2008 and Sancho et al., 2008).

Heterochromatin protein1 is another important family of proteins that play role in cancer through their regulation of the centromere, telomere stability, and gene regulation. Decreased levels of HP1 often correlates with poor prognosis and increased levels with a reduction in metastasis as seen in case colon cancer where increased levels of HP1α reduces metastasis. Colon cancer cells expressing express gastrin-releasing peptide (GRP) and its receptor (GRPR) upregulate HP1α promoting a differentiated state while limiting proliferation and spread (Ruginis T, 2006). HP1ϒ appears to play a role in ovarian cancer progression through inhibition a heat shock protein 90 (HSP90) inhibitor (Maloney A, 2007). HP1α plays a causal role in breast cancer regulating cell invasion. It is down-regulated in highly invasive/metastatic cells relative to poorly invasive/non-metastatic cells with 95%of metastatic cells showing decreased levels of HP1α compared to primary breast cancer tumors (Kirschmann DA,2000). HP1α mediated cancer cell invasion is regulated by its interaction ability with other

proteins (Norwood LE, 2006) and acts like a metastasis suppressor that regulate metastasis without altering tumor growth (Steeg PS,2003). Besides their role in inhibiting cancer progression, they proteins might have deleterious effects as well. HP1 proteins are normally not detected in neutrophil granulocytes and very rarely detected in eosinophil granulocytes but in acute phase of acute myeloid leukaemia patients and chronic myeloid leukaemia (CML) patients elevated levels of all three HP1 proteins and H3K9me were detected in the granulocytes (Lukasova E,2005 and Popova EY, 2006). H3K9 demethylation by JMJD2A JMJD2B and JMJD2C results in decreased chromatin association of all three HP1 isoforms and this demethylase activity might be targeted to specific foci in esophageal and prostate cancers (Cloos PA ,2009). HP1 protein are also regulated by microRNAs and this has implications in cancer progression for instance miR-30a, a tumor-suppressive microRNA that targets HP1γ, specifically suppress the growth of colorectal cancer in mouse xenograft models (Liu M. et al, 2015).

Data available from different studies reveal that loss of any HMG leads to detectable phenotypic changes that are not compensated even by members of the same HMG family. The members of the HMG superfamily affect developmental processes making its role in cancer quite plausible. HMGA expression is developmentally regulated and Hmga1-/- mice suffer from cardiac hypertrophy and haematological malignancies due to an HMGA-dependent downregulation of the insulin receptor (Fusco A., Fedele M, 2007). HMGA overexpression is a hallmark of several malignant and benign tumors that are listed in the table. HMGA1's role in EMT helps in its function in tumor progression and metastasis (Reeves R, 2001) and HMGA2 controls epithelial differentiation, tumor invasiveness and metastasis being a mediator of TGF- β signalling (Fusco A., Fedele M., 2007). HMGA2 gene undergo rearrangements involving 12q13-15 chromosomal translocations which is most common in benign tumors of mesenchymal origin (Fusco A., Fedele M., 2007) leading to overexpression of HMGA2 which is sufficient to induce benign tumors in mice (Fusco A., Fedele

M., 2007). HMGAs interact with nuclear factors like (NF)-κB (Merika M,2001) and the tumor suppressors p53 (Fusco A., Fedele M., 2007) or pRB (Fusco A., Fedele M., 2007) regulating gene expressions in cancer and inhibits nucleotide excision repair increasing genome instability (Reeves R, and Adair JE,2005). HMGA proteins also exhibited antiproliferative effect in case of lymphoproliferative disorders (Fusco A., Fedele M., 2007). Like HMGA, HMGB proteins are upregulated in colon, breast, gastric and gastrointestinal cancer cells (Muller S,2004 and Kuniyasu H,2003). Extracellular HMGB binds to RAGE (receptor for advanced glycation end products) and other membrane receptors enhancing cell migration, tumor growth and metastasis (Taguchi A,2000). Studies show that incidence of tumors in Hmgn1-/- mice is almost twice that of wild-type mice which could be due to faulty DNA repair in these cells making them hypersensitive to UV and ionizing radiation (Birger Y 2003 and Birger Y, 2005). The hypersensitivity of Hmgn1-/- mice to ionizing radiation could be attributed to impaired ability to activate the G2-M checkpoint (Birger Y, 2005), leading to increased genomic instability and cancer. With the help of an unbiased genome wide screening for unmutated genes that drive tumorigenesis has identified MeCP2 as novel oncogene and X-chromosome region where MeCP2 resides is significantly amplified in 18% of cancers overexpressing MeCP2 (Neupane M,2016). KRASG12C-addicted cell line after KRAS downregulation shows growth rescue by MeCP2 and activated KRAS rescues growth of MECP2-addicted cell line after MECP2 downregulation (Neupane M,2016). MeCP2 interaction with epigenetically modified 5-hydroxymethylcytosine has been shown to be required for tumorigenic transformation (Neupane M,2016). Like other chromatin proteins MeCP2 is also regulated by micro-RNAs having implications in cancer growth. miR-638 targets MeCP2 facilitating gastric cancer cell proliferation and inducing cell-cycle progression through activation of the MEK1/2–ERK1/2 signalling pathway by upregulating CpG islands of G-protein-coupled receptor kinase-interacting protein 1 (GIT1) (Zhao LY et al.,2017).

Involvement of other chromatin proteins in different cancer has been enlisted in the table 1.4.4 below:

Cancer Type	Protein	Mutation	Altered level	Tissue/cell type/cell line	Reference
Ovarian	H1.3		Increased	Malignant adenocarcinoma	Medrzycki M,2012
Ovarian	H1.0, H1.1, H1.4 and H1x		Decreased	Malignant adenocarcinoma	Medrzycki M,2012
	H1.0		Decreased	transformation of mouse NIH 3T3 fibroblasts cells by c- Ha-rasVal12	Laitinen, J.,1995
Melanoma	H1.0		Decreased	Patient samples	Torres CM.,2016
Liver	H1.0		Decreased	Patient samples	Torres CM.,2016
Kidney	H1.0		Decreased	Patient samples	Torres CM.,2016
Follicular lymphoma	H1.2, H1.3, H1.4, H1.5	Recurrent Mutation		Patient samples	Hongxiu Li,2014 and Okosun, 2014
chronic lymphocytic leukemia (CLL)	H1.5	Recurrent Mutation		Pheripheral blood primary CLL patients	Landau and Wu, 2013
diffuse large B-cell lymphoma (DLBCL)	H1.2, H1.4, H1.8	Recurrent Mutation		Patients with primary tumor	Lohr et al., 2012
Colorectal cancer	H1.5	Recurrent Mutation		Patient	Sjoblom et al., 2006
Invasive breast cancer	H1.10		Increased	Patient sample database	Paolo Scaffidi, 2016
Invasive breast cancer	H1.2		Decreased	Patient sample database	Paolo Scaffidi, 2016
Prostate adenocarcinoma	H1.1		Increased	LNCaP cells	Kendra A. Williams,2018
Breast cancer	H1.0, H1.6		Increased	Patient sample database	Wang T, 2019
Lung cancer	H1.0, H1.6		Increased	Patient sample database	Wang T, 2019
Glioma	H1.5		Not changed but its Phosphorylation level decreased	$Ras^{G12V/Y40C}$ transfected A172 cells	Sang B, 2019

Breast	HP1α		Decreased	MDA-MB-231 and MCF7 breast cancer cell lines	Kirschmann DA,2000
Brain	HP1α		Decreased	Multiple types of embryonal brain tumors	Pomeroy SL,2002
Colon	HP1α		Decreased	HCT116 colon cancer cell line Caco-2 and Ht-29 colon cancer cell lines	Ruginis T,2006 and Espada J, 2004
Leukemia	HP1α, β, ϒ		Decreased	Peripheral blood leukocytes	Lukasova E, 2005 and Popova EY,2006
Ovarian	Hp1ϒ		Decreased	A2780 ovarian cancer cell line	Maloney A ,2007
Papillary thyroid carcinoma	HP1α		Decreased	Papillary thyroid carcinoma tissue	Wasenius VM,2003
Breast	HP1β		Increased	Poorly differentiated breast tumors and MCF-7 cells	Lee YH, 2015
Colon	HP1β		Decreased	DLD-1, HCT-15, LoVo colon cancer cell	Yi SA , 2014
Osteosarcoma	HP1ϒ		Increased	MG63 osteosarcoma cells	Ma C., 2019
NSLC	HP1ϒ		Increased	Patient samples	Chang SC., 2018
Myelo-lymphoid	HMGA 1		*Hmga1*$^{+/-}$ and knockout	Mouse	Fedele M,2006
hormone- or prolactin-secreting pituitary adenomas	HMGA 1		Increased	Mouse	Fedele M.2005
natural killer lymphomas; lymphoid	HMGA 1		Increased	Mouse	Xu Y, 2004
Pituitary	HMGA 2		Increased	Mouse	Fedele M., 2006
benign mesenchymal	HMGA 2		Increased	Mouse	Zaidi MR, 2006
Lymphoma	Truncated HMGA 2		Increased	Mouse	Baldassarre G, 2001
Lipoma and Lipomatosis	Truncated HMGA 2		Increased	Mouse	Fedele M, 2001

Breast	HMGA 1		Increased	Human patient samples	Adair JE,2005 and Reeves R., 2001
Thyroid	HMGA 1		Increased	TPC-1 and BC-PAP) and anaplastic (ARO) cancer cells	Frasca F, 2006 and Pierantoni GM, 2016
Breast	HMGB1		Increased	Mouse	Muller S., 2004
Colon	HMGB1		Increased	Colo320 and WiDr carcinoma cells	Kuniyasu H, 2003
Lung	Extracel lular HMGB1			Lewis lung carcinoma cells and mouse	Taguchi A, 2000
Uterine leiomyoma	HMGN 2		Knock out	Patient samples	Polito P,1999
Malignant tumor	HMGN 1		Knock out	ϒ irradiated mouse and SV40-transformed MEF cells	Birger Y, 2009
Colon	HMGN 2		Decreased	Human colon cancer cells	Okamura S, 1999
TNBC, lung adenocarcinoma , lung squamous, haed and beck, cervical, liver, stomach, uterine	MeCP2	amplified	Increased	TCGA database, *KRAS*^{G12C}-addicted cell line and MeCP2 addicted cell line	Neupane M., 2016
Gastric cancer	MeCP2		Increased	Patient samples, BGC-823, AGS, MKN-45, SGC-7901 and GES-1 cells, mouse	Zhao LY., 2017
Pancreatic ductal carcinoma	DEK		Increased	Patient samples and Panc-1, CFPAC-1, AsPC-1, SW1990, BxPC-3, MIAPaCa-2,	Zhao T, 2019
Colorectal	DEK		Increased	Patient samples	Lin L., 2013
Keratinocytes	DEK		Increased	WT and Knock out MEFs and near-diploid human keratinocyte cell line (NIKS)	Matrka MC., 2015

Table 1.4.4: Role of Non-histone chromatin proteins in different cancers

1.5. Human positive co-activator 4(PC4): a multifunctional protein

Human PC4 (positive cofactor 4) initially described as a factor required to stimulate reconstituted basal transcription *in vitro* (Ge and Roeder 1994) is an evolutionarily conserved DNA binding protein of 127 amino acids. The human positive coactivator 4 (PC4), purified from the upstream stimulatory activity (USA) fraction, is a highly abundant in nucleus playing diverse roles in the cellular context.

1.5.1. Structural organisation of PC4

PC4 has an unstructured N-terminal domain (1-62 residues) and a highly structured C-terminal domain (62-127 residues). There are two Serine rich Acidic domains (SEAC, separated by Lysine rich domains (LYS) from residues (Wertern S, 1998) having the double stranded DNA binding ability which overlaps with its coactivation domain. The C-terminal domain possess the single stranded DNA binding ability and the dimerization domain. The crystal structure of PC4 C-terminal domain (at 2.8Å resolution) reveals that the biological unit is a dimer with two ssDNA binding channels running in opposite direction to each other (Brandsen J, 1997). Each of the monomers consist of a curved four stranded anti-parallel ß sheet followed by a 45º kink α helix (Brandsen J, 1997). The residues 22-87 have the double stranded DNA binding ability which overlaps with its coactivation domain. The residues 63-127 possess the single stranded DNA binding ability and the dimerization domain. The N-terminal domain is on the other hand is unstructured and is subjected to different posttranslational modifications in the SEAC as wells as lysine rich domain.

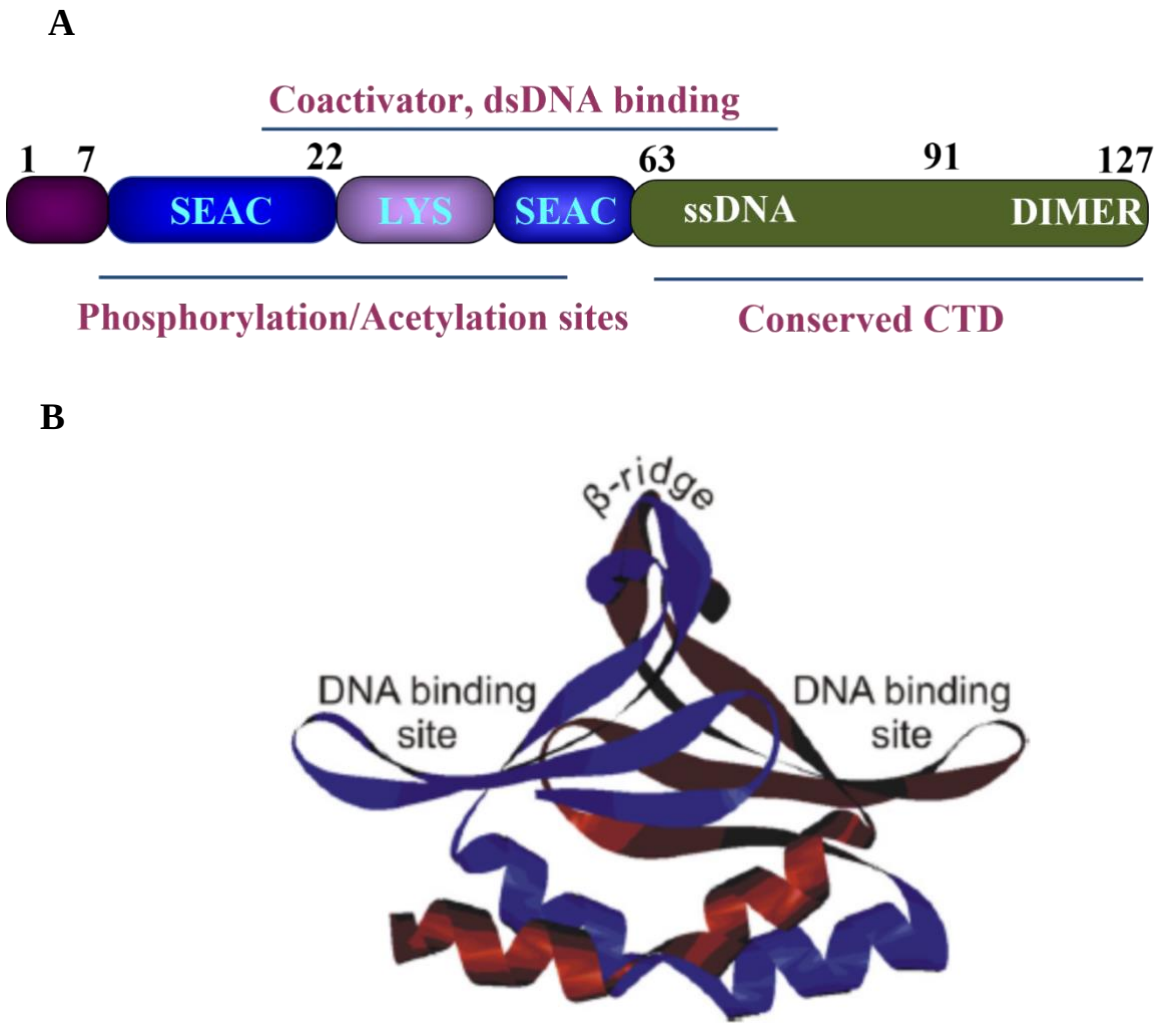

Figure 1.5.1.: (A) Schematic Representation of the different domains of Human Positive coactivator 4 PC4 indicating each of their function. (B) Crystal structure of the DNA-binding domain of a PC4 dimer with the monomers colored in red and blue. The DNA-binding sites and the -ridge are labelled (PDB code 1PCF (Figure adapted from Brandsen, J., Werten, S. et al., 1997).

1.5.2. Role of PC4 in transcription

PC4 facilitates activator dependent transcription by RNA pol II through direct interactions with the general transcription factors as well as other transcriptional activators like p53, Tat, BRCA1, AP2 (Banerjee S. et al., 2004, Haile D. et al.,1999, Kannan P et al., 1999 and Holloway., 2000). PC4 can interact with free or DNA bound TFIIA and TBP component of the basal transcription machinery

(Kaiser K., 1995) but not with TBP-TFIIB or free TFIIB or TBP alone in the absence of TFIIA (Ge and Roeder 1994). PC4 associates with TFIID and TFIIA and binds to the promoter to initiate activator dependent transcription (Malik S.,1998). Besides its role as an activator PC4 have also been reported to repress basal transcription initiation in the absence of TBP associated factors (TBP) and TFIIH. Studies have shown that yeast homolog SUB1 is a functional component of the Preinitiation complex (PIC) (Sikorski TW. et al., 2011) and mediates selection of the transcription start site (TSS) (Braberg H. et al., 2013). Sub1's recruitment to promoters by TFIIB and Rpb4/7 occurs during pre-initiation, where it supports CDK8-Mediator complex (Akoulitchev et al., 2000; Garcia et al. 2010), to maintain the PIC in a stable but inactive conformation (open), in association with TFIIE and TFIIH (Garcia et al. 2010; Sikorski et al., 2011) like the human homolog PC4. PC4 is shown to interact with TFIIE during the initiation–elongation transition to stabilize the melted promoter (Akimoto et al. 2014).

Initial studies have shown association of Sub1 predominantly with gene promoters (Sikorski TW. et al., 2011, Calvo O, Manley JL., 2005) but recent evidences also indicate its involvement in transcription elongation (Garcia A, Collin A, Calvo O., 2012, Garcia A. et al.,2010) as SUB1 can be localized within coding regions in a transcription-dependent manner affecting RNAPII levels associated to genes during the entire transcription cycle. SUB1 has been co-purified from the same fraction as the elongation factor Spt5, which regulates the elongation rate and promotes splicing (Garcia A, Collin A, Calvo O., 2012). During the transition to elongation, Sub1, most likely via its C-terminal domain remain attached to RNAPII through Rpb7(Garavis M. et al., 2017) thus joining the elongation complex by stabilizing Spt5-Rpb1 association with DNA, because in the absence of Sub1, Spt5-Rpb1 interaction decreases (Garcia A, Collin A, Calvo O., 2012).

PC4 interaction with CstF64 indicates its role in polyadenylation and transcription termination (Calvo O.,2001). PC4 also possess DNA bending ability suggesting probable mechanism for activation of p53 mediated transcription by providing a better substrate besides direct interaction with p53 itself (Batta K., 2007). Sub1 interacts with Rna15, evolutionary conserved in human cells suggesting displaying anti-terminator function by inhibiting Rna15 function thus preventing premature termination of prem-RNAs (Calvo O, Manley JL.,2001). SUB1 influence pre-mRNA processing, while interacting with the stalk of RNAPII (Chen CY. et al., 2009, Ujvari A, Luse DS., 2006) and depleting Sub1 renders an unstable Spt5-RNAPII complex which in turn could alter the recruitment and function of the component of the cleavage factor I (CFI)complex.

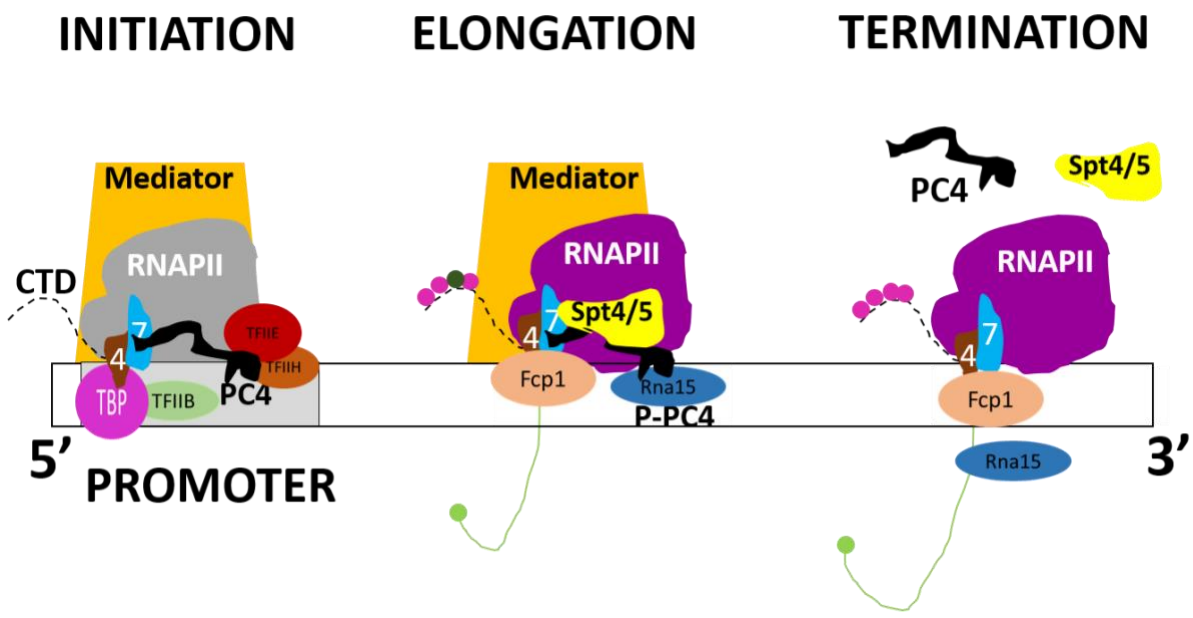

Figure1.5.2.1: A model showing involvement of Sub1 role during the whole transcription cycle. Phosphorylation states of RNAPII along the cycle are represented with different colors, along with SUB1 phosphorylation.

PC4 regulating CTD phosphorylation of RNAPII

Recent studies provide evidence for direct interaction of SUB1 with RNAPII stalk domain formed by the Rpb4 thus being involved in the modulation of C-terminal domain (CTD) phosphorylation levels (Allepuz Fuster et al. 2014; Garcia et al. 2010; Hanes 2014). Studies suggest that a functional Rpb4/7 heterodimer is required for Sub1 recruitment to gene promoters and maintained stably associated with RNAPII along with additional factors like Fcp1 and a full-length Rpb1-CTD (Garavis et al. 2017). Absence of SUB1 leads to an increase in the recruitment and activity of the CTD-Ser2 kinase Ctk1 during elongation (Garcia et al. 2010) thus, supporting role of SUB1 in modulating CTD-Ser2P levels. Thus, Sub1exhibiting functional interactions with factors like Rpb4/7, Fcp1, and the CTD gives a clue about how Sub1 can participate in the entire transcription cycle and regulate at least CTD-Ser2 phosphorylation (Figure1.5.2.2). Sub1 negatively regulates Kin28 recruitment and kinase activity, favouring Srb10 kinase activity and negatively influencing CTDSer5 phosphorylation by Kin28 (Garcia et al. 2010). Consistently, human PC4 also the ability to inhibit RNAPII phosphorylation *in vitro* by Cdk-1, Cdk-2, and Cdk-7 (mammalian Kin28 orthologue) (Schang et al. 2000) which is regulated by phosphorylation, as unphosphorylated PC4 displayed the kinase inhibitory activity, whereas phosphorylated PC4 was devoid of it (Jonker et al. 2006; Malik et al. 1998). Evidence suggesting Sub1 has genetical and functional interaction with Mediator Head and Cdk modules (Dettmann et al. 2010; Garcia et al. 2010) and it might influence CTD kinase recruitment via effects on the Mediator-CDK8 (Srb10) complex, while interacting with Rpb4/7 as well (Akoulitchev et al. 2000; Garcia et al. 2010; Ohkuni and Yamashita, 2000). Thus, different mechanisms could mediate Sub1's role in regulating Ser5 and Ser2 phosphorylation levels, but likely with a common interaction target, Rpb4/7(Calvo and Manley 2005; Garavis et al. 2017; Garcia et al., 2010) (Figure1.5.2.2).

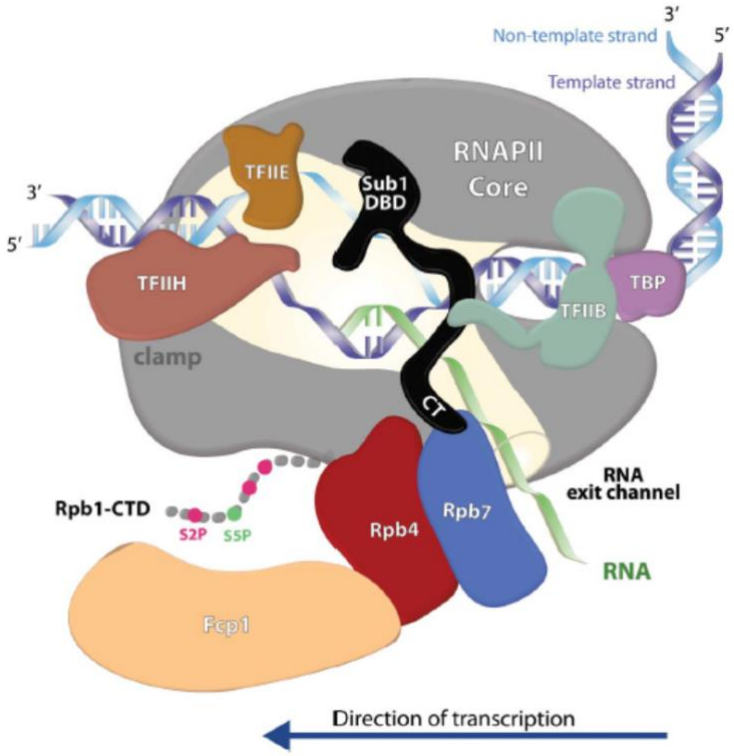

Figure 1.5.2.2: Schematic model depicting hypothetical localization of Sub1 bound to the promoter at the junction between single- and double-stranded DNA through its DNA Binding Domain. This model supports the reported interaction of Sub1 with TFIIB, TFIIE, TFIIH and Rpb4/7 contacting with the nascent RNA. (Figure adapted from Calvo O, 2017).

Role of PC4 in RNA pol III transcription

Besides its role during the entire transcription cycle of RNA polII, evidence from genome wide studies showed that Sub1, binds to all Pol III-transcribed genes and the rDNA gene locus (Tavenet et al.,2009). Interesting studies have shown that Sub1 localized in all the genes related to the protein synthesis machinery (ribosomal RNAs, tRNAs and ribosomal protein genes), in growing cells. These genes are in transcriptionally repressed state in the stationary phase. SUB1 behave as an effector of RNA polymerase III because it is required for an optimal reactivation of transcription upon recovery from starvation (Acker et al. 2014). Deletion studies showed correlation with a decrease in RNAPIII transcription efficiency without affecting the cell growth rate in the exponential phase (Tavenet

et al. 2009). Sub1 stimulates both transcription initiation and re-initiation *in vitro* and interacts with RNAPIII transcription factors (Tavenet et al. 2009) same as the human homolog PC4 playing a role in RNAPIII transcription termination and re-initiation (Wang and Roeder 1998).

1.5.3 PC4 as a chromatin organizer

Despite extensive studies on the role of PC4 in transcription, PC4 is also a bona fide component of the chromatin, highly abundant in the nucleus playing critical role in chromatin condensation. PC4 is associated with the chromatin throughout the cell cycle stages and broadly distributed on metaphase chromosome in punctuate manner except at the centromeric region. PC4 interacts with the core histones that might be crucial for PC4 mediated chromatin condensation (Das. C. et al., 2006) (Figure1.5.3C). PC4's direct interaction with histones, with a distinct preference for histone H3 and H2B could be essential for PC4 mediated chromatin condensation (Das. C. et al., 2006). Studies have shown that knockdown of PC4 dramatically alters heterochromatin organization of the genome, with increased H3K9 (histone H3 at lysine residue 9)/14 acetylation, H3K4 trimethylation and reduced H3K9 di-methylation (Das C, et al., 2010). PC4 has been shown to mediate a repressive chromatin state and heterochromatin gene silencing through its interaction with HP1α, REST/NRSF (RE1-silencing transcription factor/neuron-restrictive silencer factor) and Co-REST at the promoters of neural genes in nonneuronal cells (Das C, et al., 2010). PC4 may maintain the fidelity of segregation during the mitotic and cytokinesis events that occur during cell division as knockdown of PC4 exhibits numerous spindle pole organization defects (monopolar or multipolar) and delayed, unequal, retained or multilobed errors (Dhanasekaran K, et al., 2016) (Figure 1.5.3A and B). A recent report suggests that PC4 orchestrates chromatin structure and gene expression in mature B cells (Ochiai K et al., 2020) which comply with the findings that show knockdown of PC4 expression causes a drastic decompaction leading to open

conformation of the chromatin, altered nuclear architecture, defects in chromosome segregation and changed epigenetic landscape (Sikder S. et al., 2019) (Figure1.5.3 A and B).

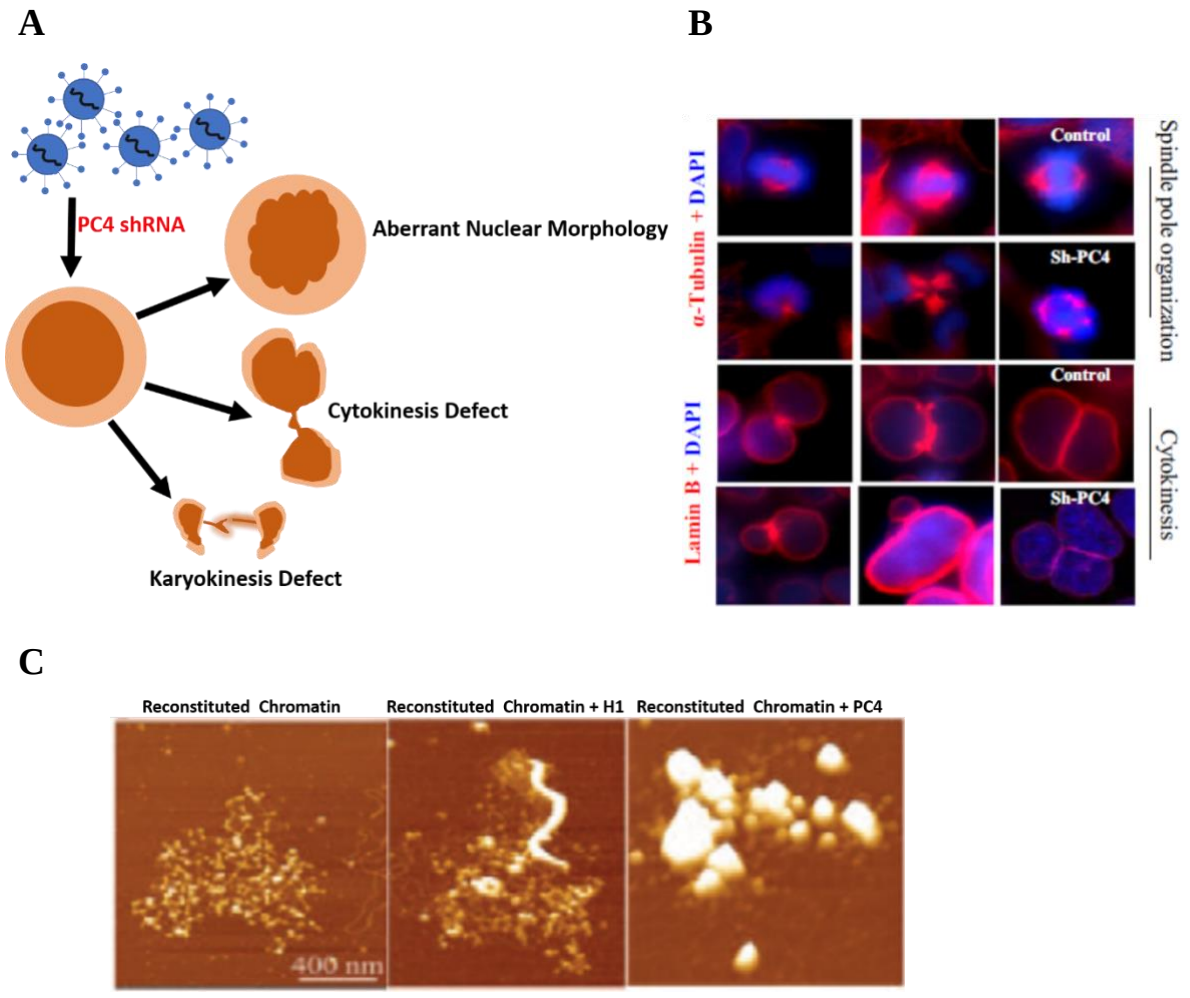

Figure 1.5.3: PC4 as chromatin organizer: (A)The essentiality of PC4 in maintaining chromatin architecture is implicated by the severity of the defects observed upon knocking down PC4 . These defects include abnormal nuclear morphology , cytokinetic and mitotic defects.(B) Studies led by Dhanasekaran et al., shows defects in spindle organization and cytokinesis after indirect immunostaining with a-tubulin and lamin B (Figure adapted from Dhanasekaran K., et al., 2016).(C) AFM imaging shows 106-kbp reconstituted chromatin: when

incubated with histone H1 forms fiber like structures and upon incubation with PC4 forms distinct globular domains (Figure adapted from Das C. et al., 2006).

1.5.4 Role of PC4 in DNA Replication and repair

PC4 has been reported to influence SV40 origin of replication by forming a complex with Human single stranded DNA binding (HSSB) protein on ssDNA and corroborates T-antigen mediated unwinding of DNA (Pan, Z. et al., 1996). PC4 prevents mutagenesis and oxidative DNA damage through its involvement in transcription coupled repair by binding to multifunctional DNA repair protein XPG (Pan, Z. et al., 1996). There are evidences showing PC4 as an activator of Non-homologous end joining (NHEJ) and double stranded DNA repair activity (Batta, K., et al., 2009). PC4 has been shown to accumulate rapidly at the DNA damage sites in the mammalian cells and enhances joining of the non-complementary DNA ends stimulating double strand break rejoining *in vivo*. PC4 might play similar roles in DNA repair like that of replication protein A (RPA) (Mortusewicz, O. et al., 2008). Studies provide evidence for PC4 recruitment to hydroxyurea (HU)-stalled replication forks, and its ssDNA binding thus suppress spontaneous DNA damage. PC4 depletion shows significant reduction in homologous recombination repair efficiency. PC4's accumulation sites co-localize with RPA at stalled forks and it increases upon RPA depletion, suggesting compensatory mechanisms in binding ssDNA to promote genome stability, especially at sites of replication-transcription collisions (Mortusewicz O., Evers B., Helleday T., 2016). Studies have demonstrated PARylation independent recruitment of PC4 to laser-induced DNA damage sites along with γH2AX. PC4 exhibits high turnover at DNA damages sites compared to other repair factors such as RPA and proliferating cell nuclear antigen (PCNA) indicating involvement of PC4 in the early response to DNA damage initiating or facilitating the subsequent steps of DNA repair (Mortusewicz, O. et al., 2008).

Studies further validate the implications of PC4 in NHEJ repair as depletion of PC4 increases radiosensitivity of non-small cell lung cancer (NSCLC) by downregulating the expression of XLF transcriptionally (Zhang T., et al. 2018). PC4 also plays a role in choice of DNA repair pathway as shown in DT40 chicken B cell model where clustered DNA lesions are formed at Ig loci via the action of activation-induced deaminase and ablation of PC4 results in significant disruption of gene conversion (GC) in gene conversion (GC)-active cells and reducing the overall mutation rate while simultaneously increasing the transversion mutation ratio in GC inactive cells (Caldwell RB. et al., 2016).

1.5.5 PC4 in the maintenance of genome stability

PC4 has emerged as an important protein that is required for the maintenance of the nuclear shape and integrity. Besides role of Sub1 and PC4 in protecting DNA from oxidative damage (Wang et al. 2004; Yu et al. 2016) and participate in DNA repair (Batta et al. 2009; Mortusewicz et al. 2008, 2016; Yu and Volkert 2013) PC4 attributes to genome integrity by regulating several other processes such as autophagy (Sikder S. et al., 2019) and chromosome segregation during mitosis, spindle assembly (Dhanasekaran K. et al., 2016) as well as suppressing G4 DNA mediated structures (Lopez C R. et al., 2017). Deletion of Sub1 resulted in elevated mutagenesis caused by cytosine deamination, particularly at gene promoters, suggesting that Sub1 protects ssDNA from mutations during transcription initiation when dsDNA is partially melted (Lada et al. 2015). Thus, PC4 helps in the maintenance of the open transcription bubble when binding to the non-template strand (Sikorski et al. 2011). PC4's involvement in the activation of p53 makes it a conceivable suppressor of tumour activity (Banerjee et al. 2004; Batta and Kundu 2007; Batta et al. 2009; Kishore et al. 2007).

G-quadruplex or G4 DNA, a non-B secondary DNA structure comprising of a stacked array of guanine-quartets formed during various genotoxic insults disrupting important process such as transcription, replication amplifying the

potential for genome instability (Lopez C R. et al., 2017). Evidence suggests that upon Sub1-disruption, genome instability linked to co-transcriptionally formed G4 DNA in Top1-deficient cells is significantly augmented and the human homolog PC4 is also sufficient to suppress G4-associated genome instability. SUB1/PC4 binding to G4DNA could be mediated by the physical and genetic interaction with the G4-resolving helicase Pif1 (Lopez C R. et al., 2017). Pif1 had been previously involved in the suppression of genome instability caused by G4-forming sequence (Paeschke et al. 2013; Ribeyre et al. 2009). Subsequent studies showed that PC4 alone is not able to unfold G4 and that PC4 regions responsible of ssDNA-binding are the same as those involved in G4 binding (Griffn et al. 2017) (Figure 1.5.4B). Further biochemical and docking results suggest a model where a PC4 homodimer could interact with a partly unpaired duplex, accommodating the G4-folded G-rich strand in one binding site and its complementary C-rich ssDNA strand in the other that can impart higher stability to the G4 and ssDNA structures bound to PC4 (Griffn et al. 2017) (Figure 1.5.4B). This novel function of PC4 in rendering stability of G4 DNA along with recent studies showing knockdown of PC4 causing a drastic de-compaction, altered nuclear architecture (Figure 1.5.4A), defects in chromosome segregation and changed epigenetic landscape (Sikder S. et al., 2019) reveal multiple facets of this protein and multiple questions about their involvement in different regulatory process involving DNA, RNA secondary structures and chromatin.

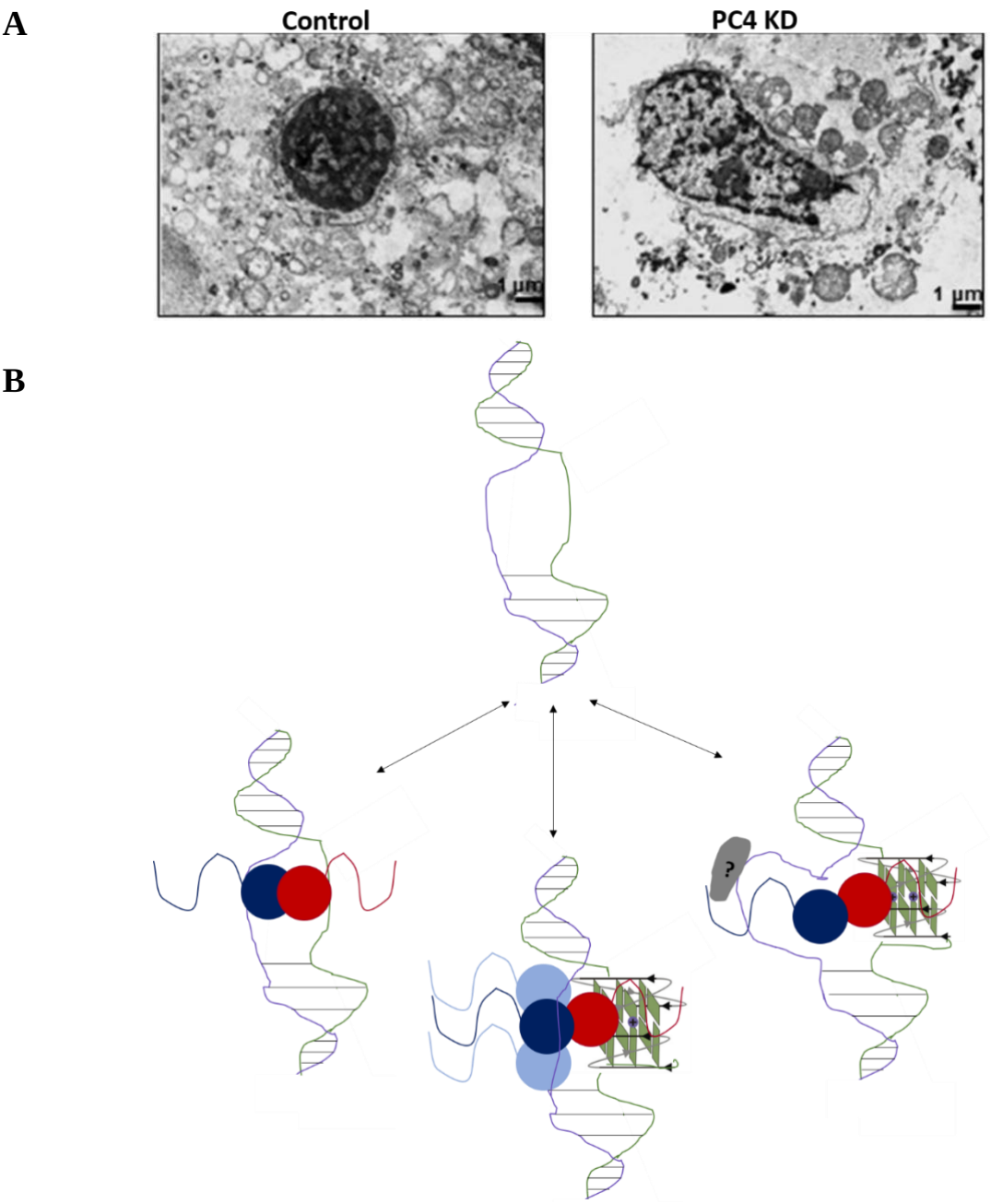

Figure 1.5.5: Implications of PC4 in maintaining genome stability. (A) Electron micrographs from control versus PC4 knockdown cells showing that PC4 knockdown cells have lost the integrity of the nucleus and displayed distorted nuclear shape (Figure adapted from Sikder S. et al., 2019). (B) Multiplex model depicting DNA recognition by PC4 and thereby stabilizing ssDNA and G4DNA within the context of melted dsDNA.

1.5.6 PC4 in differentiation and Pluripotency

PC4 is absolutely critical for life, because its absence leads to embryonic lethality and it imparts regulation in the differentiation process and pluripotency.

1.5.6.1 Neurogenesis

A novel role of PC4 has been shown through conditional brain knock-out (PC4f/fNestin-Cre) studies in mice which were smaller in size with decreased nocturnal activity (Swaminathan A et al., 2016). Interestingly knocking out PC4 exhibited a severe deficit in spatial memory extinction, with unaltered acquisition and long-term retention (Swaminathan A et al., 2016). This defect corresponds to the dysregulated expression of several neural function-associated genes, on the promoters of which PC4 was consistently found to localize. These observations indicate that PC4 could also contribute neuronal plasticity. It would be interesting to see what other differentiation pathways could be regulated by this chromatin protein in brain as well as in other organs.

1.5.6.2 Stem cell

An integrated transcriptomic analysis of mouse spermatogonial stem cells (SSCs) which can spontaneously dedifferentiate into embryonic stem cell (ESC)-like cells without ectopic expression of reprogramming factors, have identified 53 genes as putative pluripotency regulatory factors (Jo J., et al., 2016). This study further showed that one of the candidate genes among these 53 is PC4 which can enhance the efficiency of somatic cell reprogramming by promoting pluripotency marker gene expression like Oct4, Sox2, Nanog and Klf4 and repressing somatic cell marker expression (Jo J., et al., 2016). Further investigating the effect of Pc4 overexpression on genome-wide transcriptional regulation in mESCs by performing RNA sequencing (RNA-seq) analysis showed that upon PC4 overexpression they detected 88 up-regulated genes and 253 down-regulated genes with at least 4-fold differences from those and out of 88 up-regulated genes, 55 genes and out of 253 down-regulated genes, 70 genes encoded miRNAs (Jo

J., et al., 2016). These results suggest that PC4 could be a major transcriptional regulator of miRNAs. RNA-seq data showed that PC4 stimulates bone morphogenic protein 4 (Bmp4) expression and BMP signalling, which has an important role in the initiation stage of mouse iPSC reprogramming (Samavarchi-Tehrani P, et al., 2010). PC4 might also regulate the late or stabilization phase of reprogramming through the expression of Gbx2 (Tai CI, Ying QL, 2013) and Lifr in LIF/STAT3 signalling, which is required for the maturation phase of reprogramming (Tang Y, Tian XC,2013) and several genes associated with the late or stabilization phase such as Lefty2 (Golipour A, et al.,2012), Dppa2, Dppa4 and Gdf3 (Buganim Y, Faddah DA, Jaenisch R., 2013).

The majority of down-regulated genes upon PC4 overexpression are involved in the suppression of MEF marker genes such as Thy1, Postn (Buganim Y., Faddah D.A., Jaenisch R., 2013), Cd44, Snail1/2, Zeb2 (David L., Polo J.M., 2014), Nfix, Prrx1 and Tgfb3 (Yang C.S., Lopez C.G., Rana T.M., 2011). PC4 enhances OSKM-mediated reprogramming efficiency and can induce spontaneous somatic cell reprogramming via up-regulation of key pluripotency genes.

1.5.7 Role of PC4 in autophagy

A Recent finding has revealed another novel function of this multifunctional abundant chromatin protein PC4 which further validates its role in maintaining genome stability and cell survival. PC4 being important for nuclear integrity and chromosome compaction, knocking down of this protein harboured a range of nuclear and chromosomal defect, but strangely this study shows how these defects do not induce cellular death but results in enhanced cellular proliferation and one of the possible mechanisms that was found is through enhanced autophagic activity (Sikder S. et al., 2019). Another interesting observation made in this study shows that PC4 depletion confers significant resistance to gamma irradiation which further induced autophagy in these cells. Chromatin accessibility studies along with gene expression and ChIP confirmed that indeed

autophagy is the key mechanism behind this radiation resistance in the absence of PC4 (Sikder S. et al., 2019). This study thus revealed an unexplored role of chromatin architecture in mediating a cell survival process as autophagy during stress conditions such as radiation (Sikder S. et al., 2019).

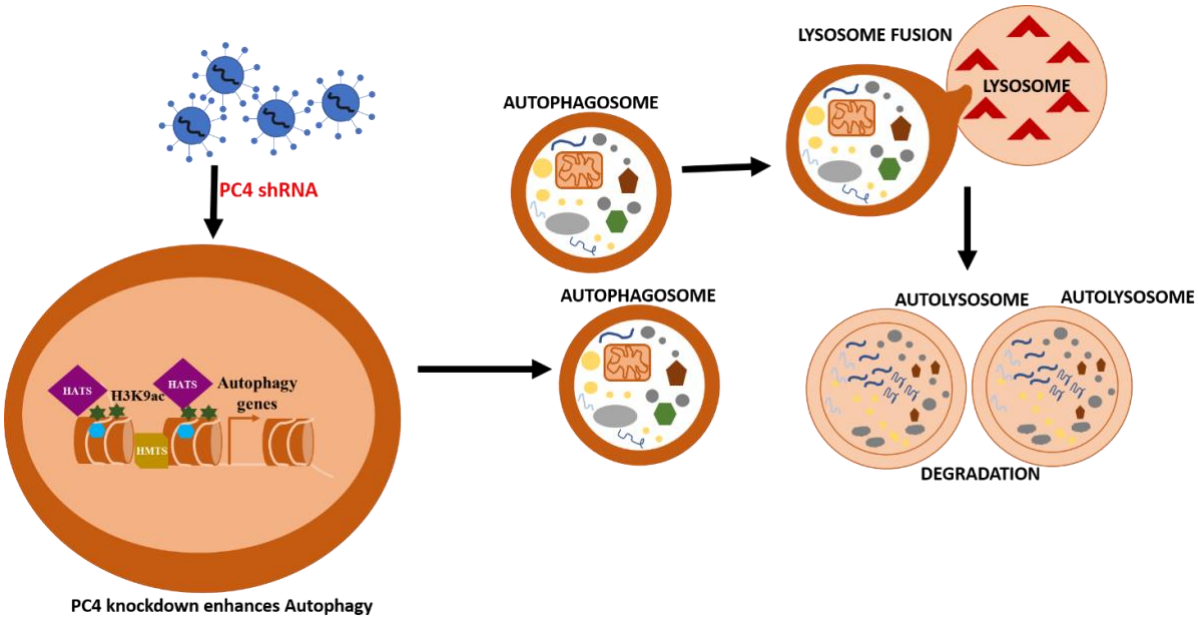

Figure 1.5.7: Model depicting PC4 as a negative regulator of autophagic process. Knocking down of PC4 enhances autophagy gene expression and thereby inducing autophagosome formation as well as autophagic flux.

1.6. Post-translational modifications of PC4

PC4 undergoes extensive posttranslational modifications which might lead to different functional consequences. Most of the posttranslational modifications occur at the N-terminal domain of PC4. The two well studied modifications that will be discussed here is acetylation and phosphorylation which forms the foundation of the study carried out in this thesis and how these modifications can act as a regulatory switch for different functions of PC4.

1.6.1 Phosphorylation

PC4 contains large number of phosphorylating serine residues within the two serine rich acid tracts and is a substrate for both casein kinase II, CKII and Protein kinase C (PKC) as shown *in vitro* but *in vivo* hyperphosphorylation is mostly mediated by CKII (Ge, H., Zhao, Y., Chait, B. T., and Roeder, R. G.,1994). There are seven predicted phosphorylation sites by CKII at the SEAC domain of PC4 (Ge, H., Zhao, Y., Chait, B. T., and Roeder, R. G.,1994). TFIIH and TAFII250 subunit of TFIID can also phosphorylate PC4 in the PIC and this can stimulate promoter escape as shown in response to GAL4-VP16 (Fukuda A. et al., 2004). Phosphorylation negatively regulates its transcriptional coactivation function (Ge, H., Zhao, Y., Chait, B. T., and Roeder, R. G.,1994) and inhibits binding of PC4 to VP16 as shown in an *in vitro* transcription assay. Subsequent studies by Jonker et al., has revealed that the phosphorylation status of unstructured N-terminal domain of the transcriptional cofactor PC4 differentially influences the various biochemical functions performed by the structured core of PC4. The ability to bind ssDNA is slightly enhanced by phosphorylation of one serine residue, which is not augmented by further phosphorylation and presence of at least two phosphoserines decreases DNA-unwinding activity and binding to the transcriptional activator VP16 (Jonker H R A, et al., 2006). It also reveals that phosphorylation gradually decreases the binding affinity for dsDNA. MS and NMR further validated the fact that up to eight serine residues are progressively phosphorylated towards the N-terminus, which gradually changes the environmental in the C-terminal direction of the following lysine rich region and within the structured core (Jonker H R A, et al., 2006). Later studies have shown that CKII mediated phosphorylation of PC4 inhibits p300 mediated acetylation of PC4 and it inhibits its double stranded DNA binding ability as well as abolishes its ability to activate p53function (Kumar B. R., Swaminathan V., Banerjee S., and Kundu T. K.,2001 and Batta K and Kundu T.K., 2007).

A recent finding by Dhanasekaran K. et al., PC4 to be hyperphosphorylated during mitosis and Aurora A and B to be responsible behind this that might impart a function of PC4 outside the nucleus upon nuclear envelope breakdown. PC4 associates with Aurora A and Aurora B and undergoes phosphorylation and in turn activates both Aurora A and B to sustain optimal kinase activity to maintain the phosphorylation gradient for the proper functioning of the mitotic machinery (Dhanasekaran K. et al., 2016). These observations are further strengthened when the mitotic defects observed upon PC4 depletion are rescued only by the catalytically active Aurora kinases, but not the kinase-dead mutants or by the phosphodeficient mutant of PC4 (Dhanasekaran K. et al., 2016).

Since phosphorylation imparts negative regulation to its cofactor function and gradual phosphorylation alters the environment masking its coactivator and DNA binding domain, it would be interesting to further investigate the structural alterations caused upon phosphorylation that could probably regulate its chromatin association and transcription regulation function.

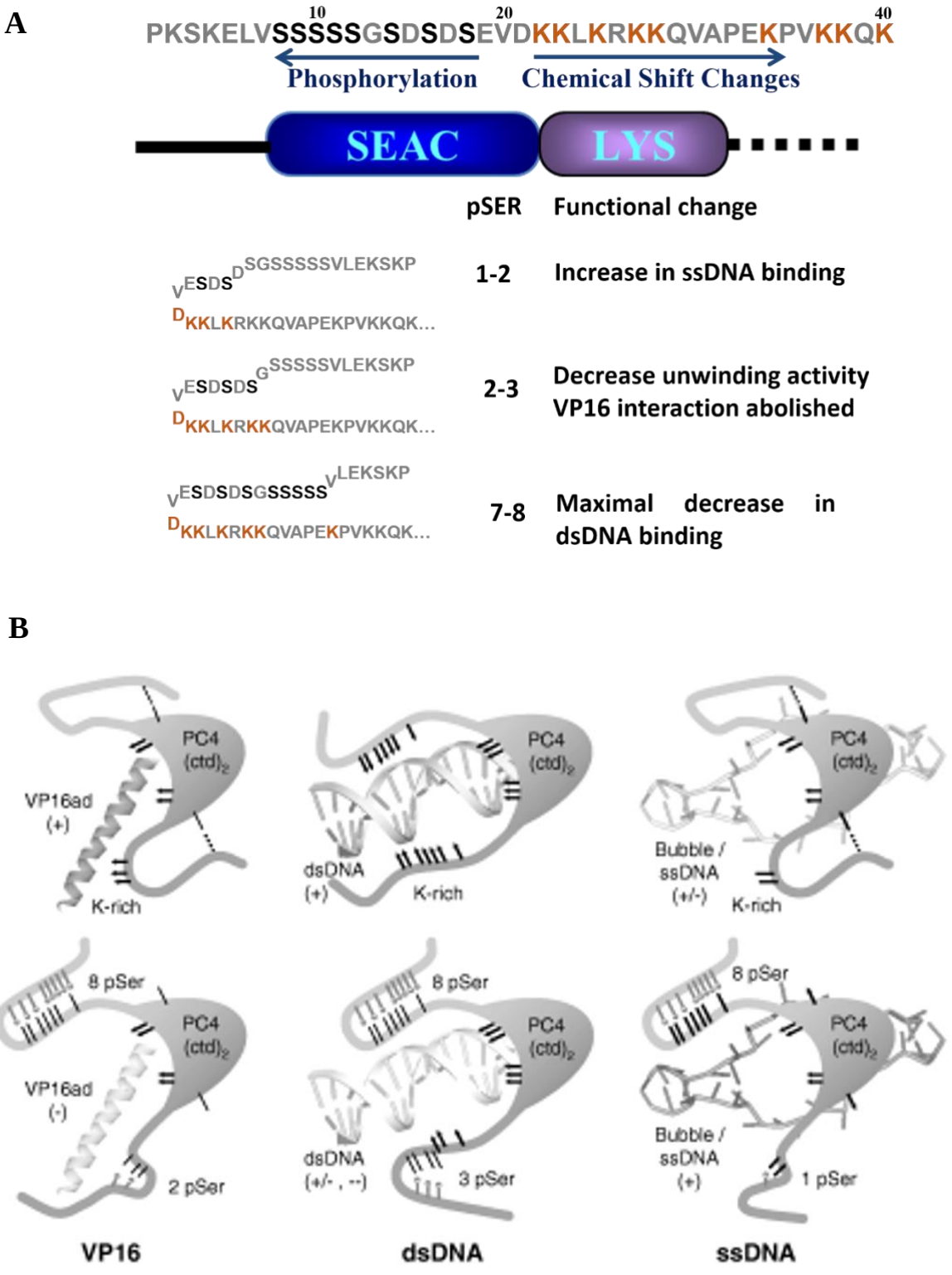

Figure 1.6.1: (A) Gradual phosphorylation changes the biochemical properties of PC4 through gradual masking of the functional lysine-rich region by the phosphoserines. (B) Schematic representation of PC4 binding to dsDNA, ssDNA

and VP16 activation domain (ad) influenced by phosphorylation depicting how the interaction is repressed gradual serine phosphorylation (phosphoserines are represented as grey lines with a dot) (Figure adapted from Jonker H.R.A et al., 2006).

1.6.2 Acetylation

Over the last decade proteomic analysis has shown non-histone proteins to constitute a major part of the acetylome in mammalian cells. Acetylation has often been associated with factor activation. PC4 being an important example of this as it interacts with TFs like p53 enhancing p53 mediated transcription upon acetylation by p300 (Banerjee S, 2004 and Batta K. and Kundu T.K., 2007). Acetylation of PC4 enhances its DNA-binding ability whereas phosphorylation of PC4 negatively regulates the acetylation (Batta K and Kundu T.K., 2007), thus showing an intriguing case for phosphorylation-mediated inhibition of acetylation, since in most scenario phosphorylation exerts positive effects on acetylation of the same proteins (Warnock LJ, 2005). Acetylation of PC4 induces the expression of p53-responsive genes and thereby enhances p53-dependent apoptosis (Batta K et al., 2007).

The intrinsic DNA-bending property of PC4 which contributes to one of the important functional components in its enhancement of p53 function is enhanced upon acetylation as shown by ligation-mediated circularization assays unlike the Phosphorylated PC4 which fails to bend DNA. Thus, acetylation of PC4 could be an inducing factor for its coactivator function and activating TFs as p53 (Batta K. and Kundu T.K., 2007).

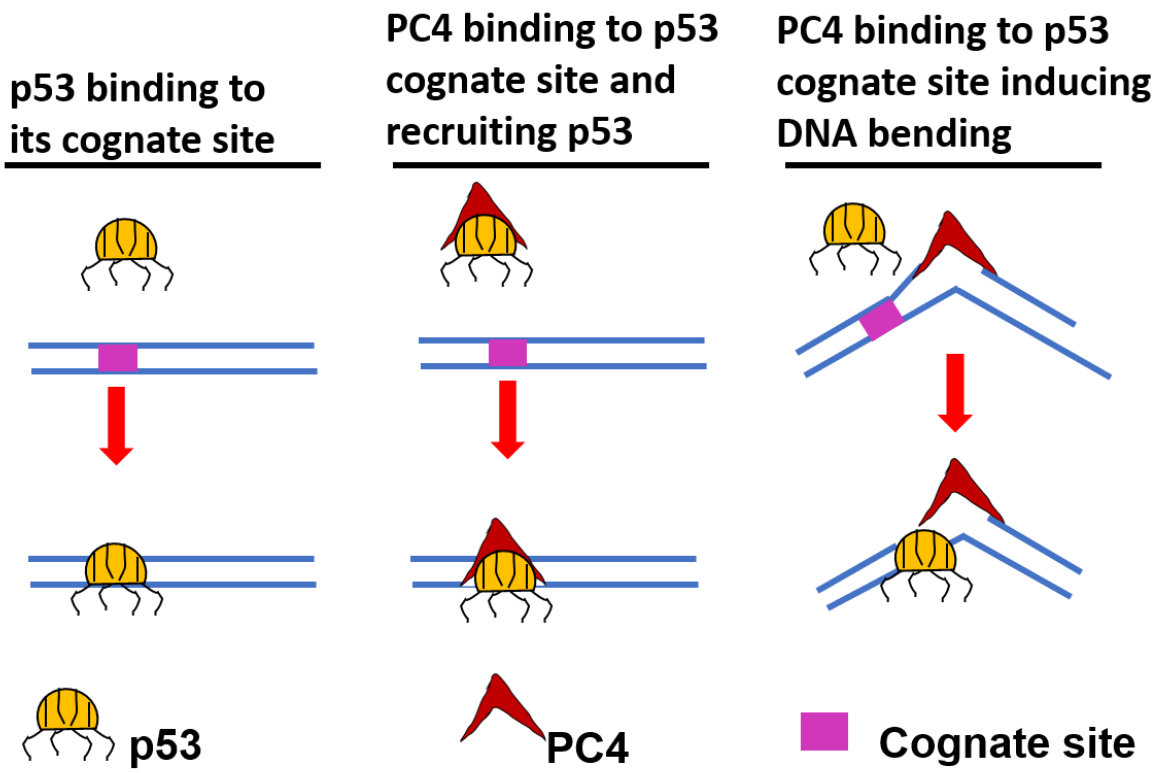

Figure 1.6.2: Model depicting PC4 mediated DNA bending enhancing the binding of p53 to its cognate site and thereby activating p53 function (Figure modified from Batta K and Kundu T.K., 2007).

1.6.3. Cross-talk between two modifications

Evidence till date have shown quite clearly that PC4 abolishes double stranded DNA binding ability, its coactivator function as well as its ability to activate other TFs like p53 whereas PC4 upon acetylation induces DNA bending and enhanced double stranded DNA binding ability which in turn enhances its ability to mediate p53 activation. These observations are quite indicative of the opposite functions being mediated by these two modifications and the observation that phosphorylation of PC4 also inhibits its acetylation by p300 further adds to the reciprocal nature of these two modifications in regulating PC4. The gradual masking model (Figure1.6.1) displays a picture of a plausible cross talk between phosphorylation of serine rich residues and the lysine rich domain. Gradual phosphorylation of serine residues within the first serine rich acidic tract changes

the charge environment on the following lysine rich region masking its interaction with DNA binding and coactivation domain at the C-terminus.

1.7 Phosphorylation and Chromatin Compaction

Phosphorylation of histones has been a nodal regulator of chromatin compaction during important cellular processes as mitosis, meiosis and apoptosis. Histone H3 phosphorylation is involved in chromatin relaxation and regulation of gene expression, as well as associated with chromosome compaction during mitosis and meiosis. H3 phosphorylation at T3, S10, T11 and S28 within the N-terminal tail of H3 are associated with chromosome condensation and segregation. The patterns of H3S10 and H3S28 phosphorylation in early mitosis, occurs at the onset of chromosome condensation during prophase (Goto H et al., 1999). Histone H3 is also phosphorylated on threonine 3 during mitosis by Haspin, a mitotic chromatin-associated kinase (Dai J, Higgins JM, 2005, Rossetto D., Avvakumov N., Côté J., 2012) and becomes highly enriched at inner centromeric regions on prometaphase and metaphase chromosomes, while its level decreases during anaphase, disappearing completely from decondensed chromosomes (Dai J, Higgins JM, 2005). Haspin plays a role in sister chromatin cohesion during mitosis, and its function appears to be mediated, at least in part, by phosphorylated H3T3.

H4S1phosphorylation has been observed during fruit fly and mouse spermatogenesis (Rossetto D., Avvakumov N., Côté J., 2012). S10 residues of both H2B and H3 are phosphorylated during meiotic chromosome condensation and disappear during meiotic divisions (Ahn SH, Henderson KA, Keeney S, Allis CD, 2005) whereas H4S1 phosphorylation appears later in meiosis and increases in post-meiotic cells (Rossetto D., Avvakumov N., Côté J., 2012) and might have role in chromatin compaction during later stages of meiosis (Rossetto D., Avvakumov N., Côté J., 2012). Linker histone H1 phosphorylation is also

regulated in a cell cycle-dependent manner (Rossetto D., Avvakumov N., Côté J., 2012) mediated by CDC2/CDK2 kinases (Rossetto D., Avvakumov N., Côté J., 2012). H1 phosphorylation appears to be associated with chromatin decondensation rather that chromatin condensation (Roth SY, Allis CD, 1992). H1 phosphorylation by CDK2 disrupt its binding with HP1, resulting in chromatin destabilization and efficient cell-cycle progression (Hale TK, Contreras A, Morrison AJ, Herrera RE, 2006).

Earlier studies demonstrated that phosphorylation of the N-terminal tail of histone H2B was essential for apoptosis-induced chromatin condensation (Rossetto D., Avvakumov N., Côté J., 2012) S14 of H2B was identified as the phosphorylated residue in apoptotic mammalian cells (Rossetto D., Avvakumov N., Côté J., 2012). Phosphorylation of H2AXS139 in mammals have been found to function in apoptosis (Rossetto D., Avvakumov N., Côté J., 2012). H2AX phosphorylation increases upon DNA fragmentation and apoptosis (Rossetto D., Avvakumov N., Côté J., 2012) and Mst1 has been identified as the kinase responsible for apoptotic H2AX phosphorylation (Rossetto D., Avvakumov N., Côté J., 2012). H2BS14 phosphorylation colocalises with γH2AX at the nuclear periphery following induction of apoptosis by death receptor agonists such as TRAIL or Fas-Ligand, or by treatment with staurosporine (Solier S et al., 2009). Another histone phosphorylation mark H3T45 phosphorylation was observed to occur during apoptosis as the target of the PKCδ kinase in normally cycling human cells (Hurd PJ et al., 2009) which increased in apoptotic cells. This phosphorylation event occurs concomitantly with or shortly after DNA nicking, and the kinetics of its appearance closely resembles those of caspase-3 activation probably influencing chromatin condensation during apoptosis.

1.8 Chromatin and Cancer

There has been extensive research concerning epigenetic changes that occur during carcinogenesis mainly devoted to understanding two important epigenetic processes: regional DNA hypermethylation and alterations in the chromatin components of DNA packaging which are linked to one another to dynamically alter epigenetic regulation of gene transcription from the earliest to the latest steps of tumor progression (Feinberg AP, Ohlsson R, Henikoff S, 2006, Herman JG, Baylin SB., 2003 and Jones PA, Laird PW.,1999).

The emerging picture of the role of chromatin in cancer is multifaceted and involves a complex interplay of chromatin-modifying enzymes and chromatin proteins. There are diverse mutations in genes involved in histone lysine methylation pathways associated with human cancer (Van Rechem C, Whetstine JR. 2014). There are reports of alterations in chromatin itself, such as histone H3.3 Lys27-to-methionine mutations that are highly specific to a single cancer type and occurs only in paediatric glioma (Morgan MA., Shilatifard A., 2015). Whereas there are mutations of related pathway component genes such as MLL3, MLL4, and UTX within the COMPASS (complex of proteins associated with Set1) family associated with a range of cancers, implying a broader tumor suppressor role (Morgan MA., Shilatifard A., 2015). Cancer genomic studies suggest co-occurrence as well as mutual exclusivity of mutations between related cancer types.

1.8.1 Chromatin structural changes in cancer

A large body of evidence implicates enhancer malfunction in cancer, and the molecular mechanisms of this process is yet to be elucidated (Herz et al. 2014). An interesting example of mis-regulation of enhancer chromatin is the classical chromosomal translocation in Burkitt's lymphoma that places the c-Myc gene under the regulation of the immunoglobulin heavy chain enhancer, thus boosting

its expression in B cells, resulting in lymphomagenesis. Acute myeloid leukaemia also exhibits chromosomal translocation near the GATA2 and EVI1 genes revealing that this inversion enables GATA2 enhancer to inappropriately activate EVI1 expression (Morgan M.A. and Shilatifard A., 2015).

Besides methylation abnormalities that are detected earlier, there are chromatin events, such as altered posttranslational histone modifications, chromatin remodelling, and nuclear positioning of genes, that precedes the DNA methylation process in cancers (Brock et al., 2007). The CpG islands are unmethylated and constitute actively transcribed chromatin where the nucleosome is less tightly wrapped, and the nucleosomes are arranged by remodelling factors into a linear array providing for an open configuration allowing access to the transcriptional machinery (Bird A.,2002 and Bird AP, Wolffe AP., 1999) whereas the chromatin structure is reversed in DNA associated with densely methylated CpG islands in gene promoter regions (Bird A.,2002 and Bird AP, Wolffe AP., 1999) where DNA is tightly wrapped in the nucleosome, and multiple nucleosomes are compacted into a higher order structure, forming closed, repressive local chromatin configuration (Bird A.,2002 and Bird AP, Wolffe AP., 1999). Thus, the nucleosome structure is a result of the states of chromatin balance involving differing ratios of active and repressive histone modifications (Briggs SD, Xiao T, Sun ZW, et al.,2002, Fischle W, Wang Y, Allis CD., 2003 and Jenuwein T, Allis CD., 2001) (Figure 1.8.1A).

Treatment of cancer cells with select type I and II inhibitors of HDACs has not been successful in stimulating re-expression of tumor suppressor genes in tumor cells with densely methylated promoter regions (Brock et al., 2007). Reports suggest that DNA demethylation agents could cause the loss of certain transcriptional-silencing marks, such as H3K9me2, and restores back transcriptional-activation marks, such as acetylation of K9 and K14 of H3 and H3K4me (Brock et al., 2007). Therefore, when administered in low dose

following treatment with HDAC inhibitors, there is synergistic effect promoting gene re-expression (Brock et al., 2007).

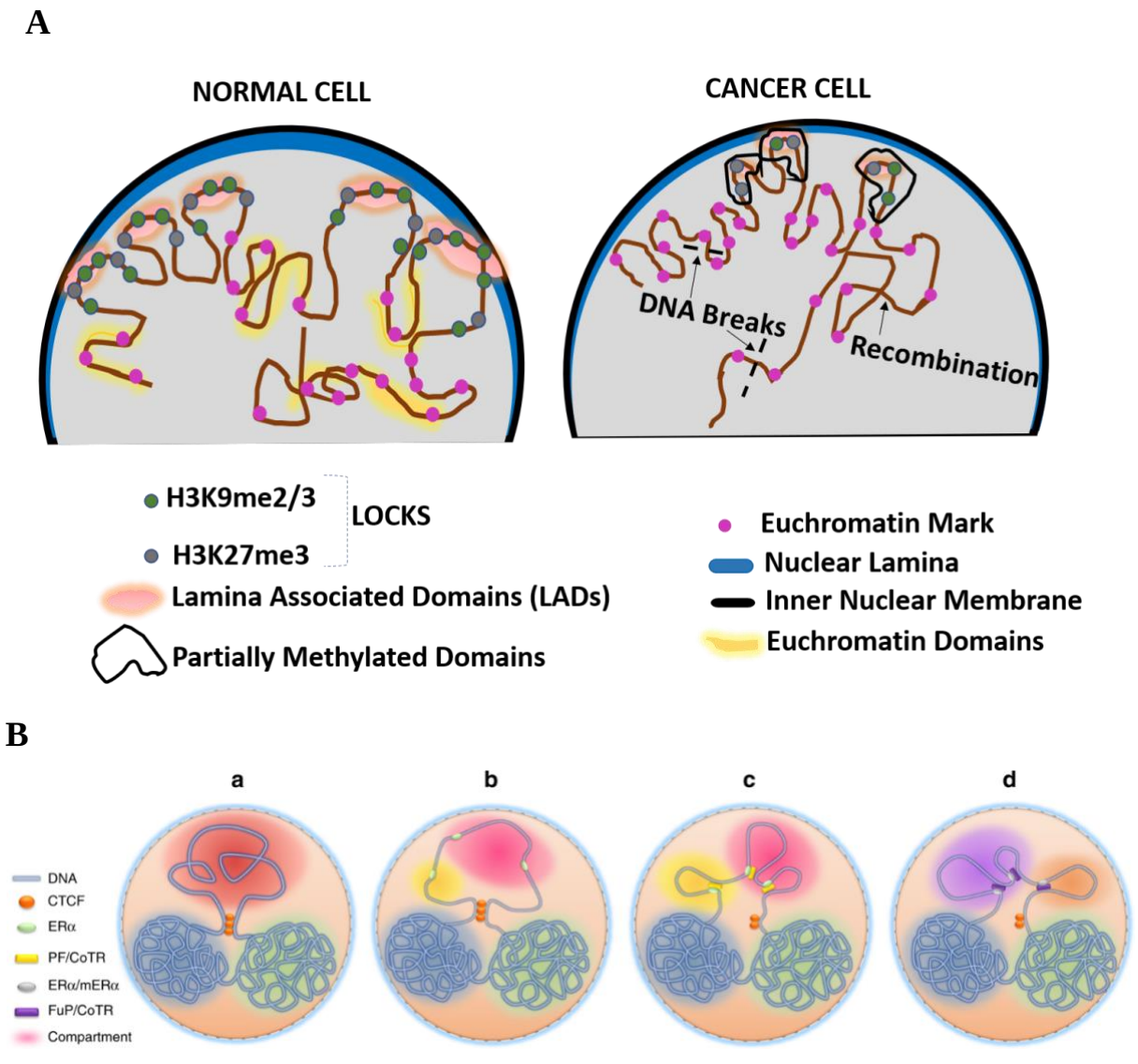

Figure 1.8.1: (A) **Chromatin rearrangement in the cancer nuclei**. In normal differentiated cells, heterochromatin is organized in the nuclear periphery by binding to the nuclear lamina proteins (in blue) and is organized into LADs (light red) whereas the active domains are tagged by euchromatin histone marks (magenta circles). Cancer cells display nuclear chromatin rearrangement with decreased lamin expression in the lamina, increased euchromatinization, and significant loss of LADs and LOCKs. (B) **A proposed model for dynamic 3D chromatin architecture.** a−c Constitutive estrogen stimulation in breast cancer

cells enhances stronger ERα activity recruiting its distal regulatory machinery and mobilizing highly dynamic gene looping. d. In acquired ER α resistant breast cancer cells, increased crosstalk between ERα and other signal transduction pathways results in altered chromatin reorganization (Figure adapted from Zhou Y. et al., 2019).

1.8.2 Maintenance of genome stability through heterochromatin

The heterochromatin state maintains genomic stability at multiple levels. Numerous examples like in mice doubly mutant for the H3K9 methyltransferases Suv39h1 and Suv39h2 lacking H3K9 methylation at pericentric heterochromatin, exhibit aneuploidy and male germline meiosis defects, and developing B-cell lymphoma (Peters et al. 2001). Mutations of heterochromatin HP1 protein disrupt genomic stability through both aberrant centromere and telomere function and Flies with HP1 mutations display defective chromosome segregation as well as telomere fusions (Morgan M.A. and Shilatifard A., 2015). Amplification of SETDB1 may play a role in development of human cancer (Morgan M.A. and Shilatifard A., 2015). Maintenance of histone hypoacetylation is also important for heterochromatin function which is reflected in the study showing that the treatment of cells with the class I and II histone deacetylase inhibitor trichostatin A (TSA) results in loss of HP1 binding to pericentric regions and re-localization of these domains to the nuclear periphery (Morgan M.A. and Shilatifard A., 2015). SIRT6 is frequently deleted in human cancer, and a conditional mutant mouse model revealed it to act as a tumor suppressor in an intestinal cancer model (Morgan M.A. and Shilatifard A., 2015). Studies have also showed how KDM4A amplification in human cancers results in focal copy number gains during DNA replication (Morgan M.A. and Shilatifard A., 2015).

1.9 PC4 and Cancer

PC4 being a multifunctional protein involved in DNA repair, genome stability and interacting with several transcription factors like tumor suppressor p53, it is not surprising that PC4 has been reported to be deregulated in several cancers. PC4 binds to the promoters of many oncogenes like Myc, PLK1, BUB1 regulating their expression and its effect can be mitigated by knocking down the oncogenes (Chakravarthi BV. et al., 2016). PC4 is regulated by microRNAs having implications in cancer like miR-101 suppresses PC4 which is often lost in prostate cancer leading to PC4 overexpression (Chakravarthi BV. et al., 2016). Besides regulating gene expression which contribute to cancer progression it is also involved in DNA damage repair pathways like nonhomologous end joining (NHEJ) by regulating expression of repair factors like XRCC4-like factor (XLF) (Zhang T ,2018). Knockdown of PC4 downregulated the expression of XLF in esophageal squamous cell carcinoma and increased radiosensitivity of non-small cell lung cancer (NSCLC) cells (Zhang T 2018 and Qian D, 2014). PC4 being a chromatin component modulates the chromatin epigenetic state which in turn regulates processes like autophagy contributing to radiation sensitivity of cells (Sikeder S et al., 2019) making it a potential therapeutic target for chemo-resistant patients. It interacts with other chromatin components like H3.3 inducing its acetylation regulating TSA-induced Lutenizing hormone receptor (LHR) gene transcription in breast cancer cells (Zhao P.,2018). PC4 knockdown reduces H3.3 enrichment reducing LHR promoter activity in TSA treated MCF-7 cells (Zhao P.,2018). There are also reports of PC4 being upregulated in patient derived osteosarcoma tissues with poorer overall survival and advanced clinic pathological tumour staging (Hu X., Zhang C., et al., 2017). Depleting PC4 in the highly metastatic osteosarcoma inhibits the propensity for lung metastasis through transcriptional suppression of matrix metallo-proteinases (MMPs) (Hu X., Zhang C., et al., 2017). PC4 does interacts with epigenetic modifiers like SMYD3 histone methyltransferase potentiating a group of genes whose

expression is linked to cell proliferation and invasion and thus depletion of PC4 leads to loss of SMYD3-mediated H3K4me3 regulating a distinct transcriptional program in cancer cells (Kim JM et al., 2015). Recent report suggests that PC4 was significantly upregulated in breast cancer and high PC4 expression positively correlated with metastasis and poor prognosis of patients. The gene sets of cell proliferation and Epithelial-Mesenchymal Transition (EMT) positively correlated with elevated PC4 expression. Consistently, loss of PC4 markedly inhibited the growth and metastasis of breast cancer both *in vitro* and *in vivo*. Mechanistically, PC4 exerted its oncogenic functions by directly binding to c-Myc promoters and inducing Warburg effect (Luo P. et al., 2019). PC4 mediates metabolic changes in cells promoting glycolysis through transcriptional activation of MYC oncogene facilitating breast cancer proliferation and metastasis (Luo P. et al., 2019). The same group also studied that loss of PC4 inhibits cell growth by suppressing c-Myc/P21 pathway and inducing cell cycle arrest at G1/S phase transition in androgen independent prostate cancer by promoting the expression of HIF-1α and activating β-catenin signalling (Luo P. et al., 2019). Most of the studies have shown PC4 to be upregulated and positively regulating tumorigenesis in most cancers but a recent report also suggests an alternate possibility of downregulation of PC4 mediating disease progression mediated by miR-29a inducing migratory as well as invasive properties in significant proportion of breast cancer patient samples and as well as in orthotopic breast cancer models (Sikder S., et al., 2019). This report indicates the role of PC4 in tumour suppression (Sikder S., et al., 2019). A recent study suggests that B-cell-specific PC4-deficient mice showing impaired production of antibody upon antigen stimulation indicating PC4 as a chromatin regulator of B cells and a possible therapeutic target adjoining IKAROS in B cell malignancies. PC4 overexpression was correlated with a poor outcome in pancreatic ductal adenocarcinoma patients. RNAi-mediated knockdown of PC4 expression in pancreatic ductal adenocarcinoma cell lines resulted in reduced cell proliferation

and tumor growth by inducing cell cycle arrest at the G1/S transition and suppressing the mTOR/p70s6k pathway (Su X et al., 2020).

The role of PC4 in different cancers has been listed in the table 1.9.

Cancer Type	Protein	Altered level	Tissue/cell-type/cell-line	Reference
Prostate	PC4	Increased	LnCap, VCaP, Du145, PC3 prostate cancer cells	BVSK Chakravarthi,2016 and Luo P, 2019
Breast	PC4	Increased/ Decreased	Primary breast cancer patient samples and MD-MB231 cells/ Patient samples, cell lines as well as orthotopic mouse model	Luo P, 2019 Sikder S. et al., 2019
NSCLC	PC4	Increased	Patient samples and A549, H1975, H460 and PC-9 cells	Zhang T., 2018
ESCC	PC4	Increased	Patient sample and Kyse30, Kyse140, Kyse410, Kyse510 and TE-1	Qian D, 2014
Colon	PC4	Increased	HCT116 colon cancer cell	Kim J M., 2015
Osteosarcoma	PC4	Increased	Patient derived osteosarcoma tissues	Hu X., Zhang C. et al., 2017
Pancreatic Ductal Adenocarcinoma	PC4	Increased	Patient sample and patient derived cell line	Su X et al., 2020

Table 1.9: Aberrant levels of PC4 in various cancers

1.10 Aberrant lysine acetylation in cancer with special emphasis in oral cancer

The extensive repertoire of post translational modifications (PTMs) on histone as well as non-histone proteins often dictate important cellular events such as gene expression, replication, cell cycle, DNA damage response, cell signaling pathways and metabolism. Particularly N-€-lysine acetylation has been identified

to play a pivotal role in various cellular processes and to be the key modification involved in the manifestation of pathophysiological conditions such as tumorigenesis. The dynamics of acetylation is regulated by lysine acetyltransferases (KATs) which are the 'writers' of this modification, bromodomain containing protein which are readers of this modification and lysine deacetylases (KDACs), the 'erasers' of acetylation.

Many studies have correlated alterations in histone acetylation as potential diagnostic or prognostic biomarkers in human diseases such as cancer (Struhl, 1998). In mouse ESCs, acetylation on H4K16 marks active enhancers and is involved in transcription regulation (Taylor et al., 2013). H4K16ac, along with H4K20me3, is often lost in cancers and is considered a universal hallmark for malignant transformation (Fraga et al., 2005). Alteration of histone acetylation patterns is also predictive of prognosis and recurrence, as in the case of prostate cancer, where hypoacetylation of histone H3 at K9, K18 and H4K16 strongly correlates with cancer recurrence (Seligson et al., 2005). Loss of H4K16ac serves as an early sign of breast cancer, and low levels of H3K9ac, H3K14ac and H4K12ac are prognostic of poor outcomes (Elsheikh et al., 2009). In non-small cell lung carcinoma (NSCLC), the reduction in H3K9ac is predictive of better survival while contrastingly, hypoacetylation at H2AK5 is correlated with poor prognosis (Barlesi et al., 2007). Hyperacetylation of H4K5, H4K8 and hypoacetylation of H4K12, H4K16 correlated with the progression of NSCLC (Van Den Broeck et al., 2008). Loss of H3K9 and K18 acetylation is predictive of better prognosis in glioma (Liu et al.,2010). The low levels of H3K18ac correlates with better survival in esophageal squamous cell carcinoma and poor survival in pancreatic adenocarcinoma patients (Manuyakorn et al., 2010; Tzao et al., 2009). The globular histone acetylation mark, H3K56ac, is often upregulated in cancers and undifferentiated cells (Das et al., 2009).

Hyperacetylation does seems to be an important property of tumorigenesis and similarly such observations are also reported in Oral cancer manifestation (Arif et al., 2010). Thus, hyperacetylation observed in cancers and justifies the necessity of epigenetic-based therapeutics as well as probing both its histone and non-histone substrates as prognostic marker for disease progression and exploring further therapeutic opportunities.

Several studies in oral cancer have shown how KAT p300 plays a crucial role in driving oral cancer progression by acetylating both its histone and non-histone substrates that drive oral cancer gene expression (Shandilya J. et al., 2009, Arif et al., 2010, Kaypee S. et al., 2018 and Kaypee S. et al., 2018) and how inhibition of p300 with small molecule modulators can rescue the tumor growth in xenografted tumor model of head and neck squamous cell carcinoma (HNSCC) and xenografted oral tumor growth (Selvi B R. et al., 2015 and Arif et al., 2010).

Acetylation of non-histone proteins:

Non-histone protein acetylation often forms a major contributing factor in tumor disease manifestation and progression. Acetylation adds properties of enhanced DNA binding to TFs like p53, STAT3, E2F1 (Gu and Roeder, 1997; Martinez-Balbas et al., 2000; Marzio et al., 2000; Yuan et al., 2005), this in turn could lead to increase in transactivation and gene expression by these proteins. Alternatively, acetylation could also decrease the DNA binding ability of certain proteins such as YY1, RelA, HMG proteins (Kiernan et al., 2003a; Lührs et al., 2002; Munshi et al., 1998; Yao et al., 2001). Acetylation can increase the transactivation potential of proteins such as AR, GATA proteins, MyoD (Boyes et al., 1998; Fu et al., 2000; Gaughan et al., 2002; Hayakawa et al., 2004; Polesskaya et al., 2000; Sartorelli et al., 1999; Yamagata et al., 2000), but also exhibit reverse effect by decreasing transactivation potential of other proteins such as ERα, and HIF1α (Jeong et al., 2002; Wang et al., 2001). Acetylation also

controls an important property of protein stability which increase upon acetylation, by blocking ubiquitination of the same lysine residues, thus preventing its proteosomal degradation, this has been observed in p53, cMyc, Smad7 (Grönroos et al., 2002; Ito et al., 2002; Patel et al., 2004). Although contrasting reports of acetylation decreasing stability, like acetylated DNMT1 has reduced stability and gets proteosomally degraded (Du et al., 2010). Acetylation of lysine residues creates new surfaces for interaction with other proteins as well as disrupting protein-protein interactions, as seen in the case of proteins such as Ku70, Hsp90 (Cohen et al., 2004; Kovacs et al., 2005). Another interesting regulatory phenomenon mediated by acetylation is the sub-cellular localization of proteins for example; SRY protein gets localized to the nucleus upon acetylation and consequently interacts with Importin-β (Thevenet et al., 2004), c-Abl acetylation leads to its nuclear to cytoplasmic delocalization (di Bari et al., 2006) and membrane localization of β-catenin (Iaconelli et al., 2015).

An important implication of this has been observed in oral cancer where acetylation of the non-histone substrate of p300, NPM1, makes it move from the nucleolus to the nucleoplasm leading to RNA Polymerase II-mediated transcription co-activation and gene expression promoting oral carcinogenesis (Shandilya et al., 2009).

Another interesting aspect is the contribution of acetylation of certain enzymes can alter their enzymatic activity; acetylation of ATM kinase by Tip60 increases its kinase activity (Sun et al., 2005) on the other hand, KDAC1 acetylation can lead to dampening of its deacetylase activity (Qiu et al., 2006), similarly, acetylation of PTEN reduces its phosphatase activity (Okumura et al., 2006). Often non-histone protein acetylation can fine tune this function as been observed for p300. p300 autoacetylation enhances its acetyltransferase activity (Thompson et al., 2004). p53 being a substate of p300 activates the acetyltransferase activity of p300 through the enhancement of p300 autoacetylation which then

accumulates near the transcription start sites. Abrogation of this interaction abolishes p300-mediated histone acetylation, suggesting a crucial role played by the activation in p53-mediated gene regulation. The Gain-of function mutant p53, known to impart aggressive proliferative properties in tumor cells, also activates p300 autoacetylation (Kaypee S. et al., 2018). Thus, reversal of gain-of-function properties of mutant p53 suggests that molecules targeting the p53-p300 interface may be good candidates for anti-tumor drugs specifically in oral cancer where such gain of function mutants are often reported along with p300 overexpression. The histone chaperone NPM1 which gets acetylated by p300 is hyperacetylated in oral cancer patients, also seems to be a specific inducer of p300 autoacetylation through a reversible binding between NPM1 and p300 which can modulate p300 acetyltransferase activity and this induction of p300 autoacetylation could be the cause of NPM1-mediated tumorigenicity (Kaypee S et al., 2018).

Thus, we see that aberrant acetylation to be an important feature of tumors, and oral cancer presents an intriguing model to explore the possibilities of the regulation mediation by KAT p300 through acetylation of its non-histone substrates (Table 1.10).

Protein	Lysine Residues acetylated	Enzymes Involved	Consequence/ Function	References
RelA	K218, K221, K310	p300/CBP, SIRT1	Increased DNA binding and recruitment of coactivators.	(Chen et al., 2002; Huang et al., 2009)
RelA	K122, K123	p300/CBP	Decreased DNA binding, Increased IκB binding	(Kiernan et al., 2003)
p50	K431, K440, K441	p300/CBP	Enhanced transcriptional activation.	(Deng and Wu, 2003)
STAT3	K685	p300/CBP	Increased DNA binding, transcriptional activation.	(Wang et al., 2005; Yuan et al., 2005; Zhuang, 2013)
WNT/β-catenin	K354	p300, SIRT1	Transcriptional activation of WNT target genes.	(García-Jiménez et al., 2014; Levy et al., 2004)
c-MYC	K143, K157, K275, K317, K323, and K371	p300	Reduced transcriptional activity; Negative regulation of MYC induced transformation in cancer	(Wasylishen et al., 2014; Zhang et al., 2005)

c-MYC	K149, K323, K417	PCAF/GCN5, TIP60	Increased stability.	Patel et al., 2004)
c-MYC	C-terminal domain	CBP	Increased stability.	(Vervoorts et al., 2003)
p53	K120	Tip60 and hMOF	Mediates expression of genes involved in DNA damage induced apoptosis.	(Sykes et al., 2006; Tang et al., 2006)
p53	C-Terminal	p300	Increased DNA binding and transcription	(Gu and Roeder, 1997)
p53	K117, K161, K162 K381 and K382	p300	Essential for p53 to mediate cell cycle arrest, apoptosis and senescence Interaction with PC4 coactivator	(Li et al., 2012) (Debnath S., Chatterjee S., et al.,2010)
p53	K382	CBP	Increases p53 affinity to CBP bromodomain and interaction with tandem bromodomains of TAF1.	(Li et al., 2007; Mujtaba et al., 2004)
ERα	K229, K299, K302 and K303	p300	Induces aberrant expression and proliferation of	(Wang et al., 2001)

			breast cancer cells.	
AR	K630, K632, K633	p300, PCAF	Enhanced transcriptional activation, promotes cancer cell growth	(Fu et al., 2003; Fu et al., 2000)
RFPL3	-	CBP	Upregulates hTERT activity and promotes cancer growth	(Qin et al., 2015)
Ku80	-	CBP	Promotes COX-2 expression and tumor growth.	(Xiao et al., 2015)
PTEN	K125, K128	PCAF, SIRT1	Control of growth factor signaling and gene expression.	(Okumura et al., 2006)
PTEN	K402	CBP, SIRT1	Modulates PTEN interaction with PDZ domain-containing proteins	(Ikenoue et al., 2008)
Notch-1	K2019,2039,2044, 2068	Tip60	Suppression of Notch-1 signaling.	(Kim et al., 2007)
Smad2	K19, K20, K39	p300/CBP	Modulates TGF-β and Activin responses.	(Tu and Luo, 2007)
Smad3	K378	p300/CBP	Positively regulates Smad3	(Inoue et al., 2007)

			mediated transcription.	
E2F1	K117, K120, K125	PCAF, HDAC1	Increased DNA-binding ability, activation potential and protein half-life. Leads to Increased cell proliferation.	(Martinez-Balbas et al., 2000) (Marzio et al., 200
p73a	K321,327,331	p300	Gets recruited to pro-apoptotic promoters and induces apoptosis.	(Costanzo et al., 2002)
FoxO1	K242, K245, K262	p300/CBP, PCAF, SIRT1	Diminishes DNA binding, reduces activity.	(Calnan and Brunet, 2008)
RUNX1	K24, K43	p300	Increases DNA binding ability.	(Wang et al., 2009)
NPM1	K212, K215, K229, K230, K257, K267 and K292	p300, SIRT1	Delocalizes to nucleoplasm, activates NPM1 mediated transcription.	(Shandilya et al., 2009)
HMGA1	K65, K71	CBP, PCAF	Modulates transcription of IFN-β upon viral infection.	(Munshi et al., 2001) (Munshi et al., 1998)
HMGB1	K2, K11	CBP	Acetylated upon LPS activation in monocytes and macrophages,	(Pasheva et al., 2004) (Sterner et al., 1979)

			triggers inflammation.	
YY1	K261-233	HDAC1	Suppresses DNA binding.	(Yao et al., 2001)
MATIIα	K81	p300, HDAC3	Destabilizes protein, leads to repression of cell growth.	(Yang et al., 2015)
DNMT-1	-	Tip60, HDAC1	Destabilization of DNMT1.	(Du et al., 2010)
MPP-8	K439	PCAF, SIRT1	Destabilizes MPP-8, inhibits EMT.	(Sun et al., 2015a)
Smad 7	K64, K70	p300	Increases protein stability.	(Grönroos et al., 2002) (Simonsson et al., 2005)
HIF-1α	K709	p300, HDAC1	Stabilizes protein, sensitizes cells to hypoxiainduced growth arrest.	(Geng et al., 2012)
E2F1	K117, K120, K125	PCAF, HDAC1	Increased DNA-binding ability, activation potential and protein half-life. Leads to Increased cell proliferation.	(Martinez-Balbas et al., 2000) (Marzio et al., 2000)
RAS	K104		Negative regulation of RAS oncogenicity.	(Yang et al., 2012)

			destabilization of the interactions with guanine nucleotide exchange factors	
pRB	K873, K874	p300, PCAF	Increased affinity to MDM2, hinders phosphorylation and cell cycle progression.	(Chan et al., 2001; Nguyen et al., 2004)
HDAC1	K218, 220, 432, 438, 439, and 441	p300, SIRT1	shows reduced deacetylation function. Loses ability to deacetylate p53, stabilizing p53 during heat stress.	(Qiu et al., 2006; Yang et al., 2015)
Beclin-1	K430, K437	p300, SIRT1	Inhibits autophagosome maturation	(Sun et al., 2015)
Snail	Snail K146, K187 CBP Switches Snail from being a repressor to an activator. (Hsu et al., 2014)	CBP	Switches Snail from being a repressor to an activator	(Hsu et al., 2014)
Tubulin	K40	HDAC6, SIRT2	Modulates organization of microtubule network.	Hubbert et al., 2002) (Matsuyama et al., 2002) (North et al., 2003)

Table 1.10: Non-histone protein acetylation and its consequence in cancer

1.11 Aim and Scope of the Study

The ordered three-dimensional organisation of the eukaryotic genome is designed and regulated such that it forms the foundation for various cellular process. The non-histone chromatin proteins form an integral part of the functional component of this genome and in regulating its dynamics. Human Positive Coactivator 4 (PC4) is a highly abundant nuclear protein that is crucial for genome integrity and exhibits its gene regulatory effects spanning from DNA repair, cell cycle, hypoxia, differentiation to autophagy. The several reports that reveal the role of PC4 in cancer manifestation and disease progression makes it even more necessary to tweak with the functionality of this protein that may provide opportunities for exploring therapeutic or diagnostic targets. PC4 initially was discovered as a transcriptional coactivator protein and later studies showed its extensive involvement in the transcription cycle by interacting with RNA pol II associated TFs like TFIIB and Rbp4/7 during pre-initiation, TFIIA and TFIID stabilizing PIC, with TFIIE during the initiation–elongation transition to stabilize the melted promoter as well as with elongation factor Spt5 and termination factor Cstf46 controlling elongation and termination steps as well (Garavís M., Calvo O., 2017 and Calvo O., 2018). PC4 regulates an intrinsic step during transcription by regulating RNA pol II CTD phosphorylation through genetical and functional interaction with Mediator Head and Cdk modules during preinitiation via Rpb4/7 and forms the nodal point of regulating processes involved in mRNA biogenesis (Garavís M., Calvo O., 2017 and Calvo O., 2018). This gives an intricate picture of how PC4 could be fine tuning the whole transcription process; given that it acts as a coactivator for a number of TFs like p53, NFκB that are involved in different signaling pathways implies how PC4 could be integrating environmental signals into appropriate cellular responses.

On the other hand, studies from our group have shown that knocking down PC4 disrupts the integrity of the nucleus, disrupts the chromosome segregation and

spindly assembly, inducing vesicular bodies to form and makes certain chromatin regions accessible indicating PC4 is also important in maintaining the genome, which is beyond its association with the transcriptional machinery. It does act as an important chromatin architect. The discovery of PC4 to be a chromatin protein inducing chromatin condensation forms one of the pillars of PC4's role a genome organizer.

As stated earlier, PC4 has a transcription regulation function as well as functions beyond transcription. So, there must be some regulatory switch within the cell that controls different aspects of PC4 under different cellular conditions. Post-translational modification often forms a major component leading to multifunctionality of single protein under different cellular contexts. It was thus quite compelling for us to explore the implications of different modifications of PC4 in cells. Soon after discovery of PC4, it was found to be enriched in the phosphorylated form in cellular extract and it was surprising to see that phosphorylated form of the protein negatively regulated its coactivator function. Mass spectrometric analysis combined with mutational analysis showed that majority of the sites getting phosphorylated *in vivo* where within the first serine rich acidic tract and Casein Kinase II, CKII was the kinase responsible for its phosphorylation. Subsequent studies proposed a model how phosphorylation could hinder the environment in the following lysine rich region and C-terminal domain involved in DNA biding and activation. Our group has also shown how phosphorylation abolishes PC4's dsDNA binding ability, DNA bending property as wells as p53 activation by PC4. These observations intrigued us that despite negatively regulating its coactivator function, there is such abundance of phosphorylated form of PC4 in the nucleus. Since PC4 is also a chromatin protein and crucial for maintenance of the genome, it is thus imperative for us to explore whether phosphorylation is important for this aspect of PC4. The discovery of PC4 as chromatin protein has stated that it could be mediated via its interaction

with core histones, specifically H3 and H2B and no interaction was reported with linker H1. We wanted to explore whether the phosphorylated form so abundantly present in the nucleus interacts with linker histone H1 and it was interesting to see H1 interacted only with phosphor form of the protein. This observation encouraged us further to study the chromatin condensation function of the phosphor-protein. A lot of observations stated PC4 being involved in different process like autophagy, neurogenesis by regulating gene expression, but exact mechanism of this regulation is not clear. Thus, it becomes imperative to study the implications of PTMs of a protein which can help us explain the observations seen upon its knockdown. Investigating the role of PC4 phosphorylation by CKII helps us to mechanistically explain the phenomenon of global chromatin decompaction and altered epigenetic landscape that is observed upon depleting PC4 that leads to alteration in specific gene expression. Our study unveils that hyperphosphorylation of the serine rich N-termini of PC4 is critical for its chromatin functions and the epigenetic state of the cell which translates into its gene expression regulatory effects, justifying the abundance of this form of PC4 that is present within cells and providing an additional axis to modulate its functions.

PC4's N terminus is interesting as it forms a hub for different modifications to occur to regulate its function. As stated above one such modification was phosphorylation occurring in its serine rich acidic tracts, but following first serine rich acidic tract is a lysine rich domain that undergoes acetylation. Studies from our group has shown p300 to be a prominent KAT that not only acetylates the protein but adds distinct properties to the acetylated PC4. The observation of acetylated PC4 to be a better dsDNA binding protein, a better DNA bending protein explains the enhanced p53 activation by acetylated PC4. These observations hint at the possibility of PC4 acetylation being a mediator for its co-activator function. We know that p300 is an important coactivator mediating

transcription through acetylating the chromatin including both histones and non-histone substrates. One of the well-studied, factor of p300 being p53 both Wildtype as well as mutants found in different cancers. p300 regulates p53 transcription as well its stability and interestingly acetylation of lysine 381 and 382 of p53 by p300 mediates its interaction with PC4. PC4 on the other hand is a global regulator of p53 mediating its gene expression. Putting together each of these dots, creates a possible picture of p300, PC4 and p53 to be part of one complex mediating transcription. Identification of several lysine residues of PC4 to be acetylated *in vivo* through mass spectrometric studies done earlier in our lab gave us leads to explore the implications of acetylated form of the protein by mutating those lysine residues. Several lysine mutants were generated and tested by Histone acetyl transferase (HAT) assay by p300 to see the sites critical for p300 mediated acetylation. In order to probe into the implications of p300 mediated acetylation of PC4 in transcription, raising a site-specific acetylation antibody is imperative. In this study we show that we succeed in raising a site-specific acetylation antibody against PC4 and has been validated through several assays for these sites being specific for p300 mediated acetylation. An interesting observation was to see that metaphase chromosome is devoid of acetylated PC4 and acetylated-PC4 was observed in interphase nucleus corresponding to its possible association with transcriptionally active regions present in the open chromatin. PC4 has been reported to be upregulated in several cancers and involved in regulating tumor genes such as Myc, MMPs, Bub1, p53, Lutenizing hormone receptor, XLF which contribute to cancer manifestation through several ways. On the other hand, aberrant acetylation is an important feature of several cancers including oral cancer, where p300 has been reported to be mediate hyperacetylation of both histones as well as non-histones as NPM1 which in turn regulate gene expression to promote tumorigenesis. Therefore, it is imperative to explore the various other non-histone substrates of p300 that could have implications in oral cancer manifestation. One of the prominent substrates is PC4

which has been implied to drive gene expression contributing to invasion, migration, proliferation, radiation resistance properties of several cancers. Thus, exploring p300 mediated acetylation of PC4 in oral cancer manifestation may provide new insights to various gene pathways being regulated to drive tumour progression as well as provide opportunities to develop new drug targets disrupting this acetylation process.

1.12 Thesis Objectives and Objective-Specific Relevance

Considering the above stated background knowledge, we laid down the objectives of the present thesis as follows:

1.12.1 Implications of CKII mediated phosphorylation of PC4 on its genome organizing function and thereby gene expression

In cells PC4 largely exists as a phosphor- protein. Casein Kinase II (CKII) is the dominant kinase responsible for its hyperphosphorylation at the N-terminal serine-rich region. Phosphorylation negatively regulates its double strand DNA binding and unwinding ability, co-activator function and its acetylation by p300. Despite the inhibitory effects of phosphorylation, the abundance of phosphorylated PC4 in cells intrigued us to investigate the functional implications of the phosphorylation. negatively regulate the coactivator function (Ge and Roeder.,1994 and Jonker H.R.A et.al., 2006). Till now, the functional consequence of phosphorylation of PC4 has been shown in the light of its cofactor binding properties where the positive charge of its lysine-rich region gets progressively masked by phosphoserines (Jonker H.R.A et.al., 2006). This study shows the physiological relevance of this protein modification in mediating PC4's chromatin functions. We started with series of serine mutants and

identified the serine residues critical for CKII mediated phosphorylation and interestingly, we found that CKII mediated phosphorylation of PC4 is critical for its interaction with linker histone H1. We explored the chromatin condensation ability of phospho-PC4 in an *in vitro* reconstituted nucleosomal array, which not only indicated phosphomimic PC4 to be a better chromatin condenser by itself but also complemented linker histone H1 in mediating further chromatin compaction. Cellular studies with ectopic overexpression of Flag tagged wild type, phospho-mimic and phospho-defective PC4 mutants in an endogenous PC4 knockdown background showed that phosphorylation is critical for its chromatin compaction ability. We further probed the implications of phosphorylation on the expression of neuronal genes repressed in non-neuronal cells via PC4 mediated heterochromatinization and some core autophagy genes and observed that the repression of neuronal and autophagy gene expression is indeed phosphorylation dependent. Collectively, our study unveiled that hyperphosphorylation of the serine rich N-termini of PC4 is critical for its chromatin condensation functions and thereby the underlying gene expression. Till date studies have shown PC4 to regulate gene expression by directly binding to the promoter of the genes (Sikder S. et al., 2019; Chakravarthi BVSK. et al., 2013; Luo P. et al., 2019) and interacting with transcription machinery throughout the transcription cycle (Calvo O, 2018) but this study shows for the first time that phosphorylated PC4 regulates gene expression by modulating chromatin state. It would be further interesting to look into structural mechanisms of PC4 mediated chromatin compaction by solving the cryo-EM structure of PC4 bound nucleosome and PC4 bound-chromatosome. This study is an important example of a post-translational modification like serine phosphorylation, switching the function of a transcriptional co-activator to a regulator of functional genome organisation that control the chromatin state and gene expression.

1.12.2 Implications of p300 mediated acetylation of PC4 regulating its coactivator function and probable role in cancer manifestation

Eukaryotic genome is organized as a highly dynamic nucleoprotein structure: which not only comprises of histones and DNA but also large number of non-histone chromatin associated proteins and RNA. As we discussed earlier the diverse functions of PC4 is reasonably brought about by its different post transcriptional modifications and interactions with several cellular proteins. We have shown that PC4 gets acetylated by lysine acetyltransferase p300 and identified the critical residues by conducting assays with different lysine defective mutants. Earlier studies have indicated that acetylation of PC4 by p300 enhances its dsDNA binding ability, DNA bending ability as well as its ability to activate p53 function which compelled us to explore the possibility of acetylated PC4 in regulating its transcriptional functions. We have identified the lysine residues which are the probable targets of p300 enzyme and raised the acetylation site specific antibody that enabled us to assign the cellular function of acetylated PC4. However, our recent screening suggests that PC4 could be acetylated by other lysine acetyltransferases in a context dependent manner, for example by KAT5A/Tip60 and its implications are currently being studied. In this study we tried investigating the cellular localization of acetylated PC4 using acetylation specific antibody along with PC4 localization across different chromosome stages through immunofluorescence which indicated that acetylated PC4 is present mostly in the interphase nucleus and it re-appears at the telophase stage and is completely absent from the metaphase chromosome whereas PC4 is present through different stages. Thus, indicating acetylated form of PC4 is associated with relatively active open chromatin. PC4 has been the driver for several oncogenes like Myc, Bub1, and genes involved in metastasis like MMPs and proliferation. The reports of PC4 being upregulated in several cancers along with the evidence of p300 being upregulated in oral cancers, led us to study this protein

acetylation oral cancer cells as well as patient samples. In oral cancer it has been shown that catalytically active p300 creates a hyperacetylated environment by acetylating both its histone and non-histone substrates, one of them being acetylated NPM1 which drives gene expression in oral cancer manifestation. Since PC4 has been shown to be over expressed in oral cancer cells as well as in patient samples, and it compelled us to explore the implications of acetylated PC4 in driving tumor gene expression. Thus, understanding PC4-p300 axis in mediating gene expression would provide us an additional opportunity to explore new drug targets or prognostic marker.

Chapter 2: Materials and Methods

Chapter outline

2.1 General Methods

2.1.1 Bacterial Transformation

Competent cells were thawed on ice for 10 mins. Approximately 100ng of plasmid DNA was added to it and was further incubated on ice for 30mins. A brief heat shock at 42ºC was given for 90 seconds and cells were immediately kept on ice for 5mins. 1ml LB was added and cells were grown in 37ºC shaker incubator for 45mins-1hour. Cells were pelleted down and plated on LB agar plates with suitable antibiotic for selection. Plated LB agar plates were kept in 37ºC incubator for 10-12 hours.

2.1.2 Preparation of bacterial competent cells

E. coli strains DH5α were inoculated overnight from respective frozen glycerol stocks in 5ml Luria Broth (LB; Himedia) media. The overnight culture was streaked on fresh LB agar plate and incubated at 37ºC for 8-10 hours. Single colony from the plate was inoculated in 500ml of medium A (10mM MgSO4 and 11mM glucose in LB) and was grown in 37ºC shaker incubator till OD600 reaches 0.3. Culture was cooled and pelleted at 4ºC, 4000rpm for 10mins. Pellet resuspended in 5ml ice cold medium A and again centrifuged for 10mins. Finally, pellet was resuspended in 25ml of storage buffer B (36% glycerol, 12mM MgCl2, 12% PEG-8000) and 100µl of cell suspension aliquots were frozen in liquid nitrogen and stored at -80ºC.

E. coli strains BL21 were streaked on a LB agar plate from thawed frozen stock, and cultured overnight at 37°C. About ten to twelve large (2-3 mm in diameter) colonies were isolated with a plastic loop, inoculated to 250 ml of SOB medium (2% Bacto tryptone/0.5% yeast extract/10 mM NaCl/2.5 mM KCI/10 mM MgCI2/10 mM MgSO4) in a 2-liter flask, and grown to an A6oo o of 0.6 at 18°C, with vigorous shaking (200-250 rpm). The flask was removed from the incubator

and placed on ice for 10 min. The culture was transferred to a 500ml centrifuge bottle and spun at 3000 rpm for 10 min at 4°C. The pellet was resuspended in 80ml of ice-cold Transformation Buffer (TB) (10 mM Pipes/55 mM MnCI2/15 mM CaC12/250mM KCI), incubated in an ice bath for 10 min, and spun down as above. The cell pellet was gently resuspended in 20 ml of TB, and DMSO was added with gentle swirling to a final concentration of 7%. After incubating in an ice bath for 10 min, the cell suspension was dispensed by 1-2 ml into tissue-culture cell-freezing tubes and immediately chilled by immersion in liquid nitrogen. The frozen competent cells were stored in -80ºC for without a detectable loss of competence.

2.1.3 Whole cell extract preparation

Cells were harvested by scraping following 1XPBS wash. Cells were collected and pellet down by centrifugation at 1000rpm for 3mins at 4ºC. Pellet was resuspended in 1X SDS dye and boiled at 90ºC for 15minutes and given a short spin before loading. Laemmli buffer: Cells were harvested and centrifuged at 2000rpm for 3minutes at 4ºC. Cell pellet was washed with cold 1X PBS and resuspended in 10 times packed volumes of cell pellet in laemmli buffer (0.125mM Tris-Cl, pH 6.8, 4% SDS, 20% Glycerol).5X SDS loading dye was added to samples and were boiled for 5minutes at 90ºC and later used for western blotting. For making RIPA lysate cells were harvested and lysed in RIPA buffer (20 mM Tris-HCl (pH 7.5) 150 mM NaCl, 1 mM Na2EDTA 1 mM EGTA 1% NP-40 1% sodium deoxycholate 2.5 mM sodium pyrophosphate 1 mM β-glycerophosphate 1 mM Na3VO4 1 µg/ml leupeptin) for 3hrs *at* 4ºC in end to end rotor and then spun at 13000rpm at 4ºC for 15mins to collect the supernatant as RIPA lysate.

2.1.4 DNA Isolation

Plasmid DNA extraction was done using Sigma mini and maxi prep kits according to the manufacturer's protocol. Briefly, overnight grown culture was pelleted and

resuspended till homogeneity in resuspension buffer. Alkaline lysis buffer was utilized to lyse the cells and followed by neutralizing the solution. Supernatant obtained was allowed to bind to the column through centrifugation. Following two washes of the column, bound DNA was eluted using TE buffer or water.

2.1.5 RNA isolation

2.1.5.1 RNA extraction from mammalian cells

Cells were rinsed with PBs and the lysed directly in 1ml of TRIZOL (Ambion) from 60mm dishes using cell scraper. 0.2 ml of chloroform per 1 ml of TRIZOL Reagent was added and the samples were vortexed vigorously for 15 seconds and incubate them at room temperature for 2 to 3 minutes. The samples were centrifuged at 12,000 x g for 15 minutes at 2 to 80°C. Following centrifugation, the RNA containing aqueous phase was collected from mixture containing phenol-chloroform phase, an interphase. The RNA was precipitated from the aqueous phase by mixing with isopropyl alcohol. 0.5 ml of isopropyl alcohol per 1 ml of TRIZOL Reagent was used. The samples were incubated for 10 minutes and centrifuged at 12,000 x g for 10 minutes at 4°C. The RNA forms an invisible gel-like pellet on the side and bottom of the tube after ethanol precipitation. The supernatant is completely removed and the RNA pellet is washed twice with 1ml of 75% ethanol. The RNA pellet is air-dried for 5-10 minutes dissolved in autoclaved milliQ water before measuring the concentration by Nanodrop. RNase free DNase I (NEB) treatment of the extracted RNA was carried out using 1µLof the enzyme for 10µg of RNA in presence of DNaseI buffer (NEB) at 37°C for 10mins followed by addition of 1ul of 0.5M EDTA and heat inactivation at 75°C

for 10 minutes. The DNaseI digested RNA was then subjected to ethanol precipitation before measuring the concentration at 260nm. The quality of the RNA was roughly assessed by A260/A280ratio. Further, the RNA was electrophoresed on a 1.2% agarose gel to check the quality of the RNA (Figure 2.1).

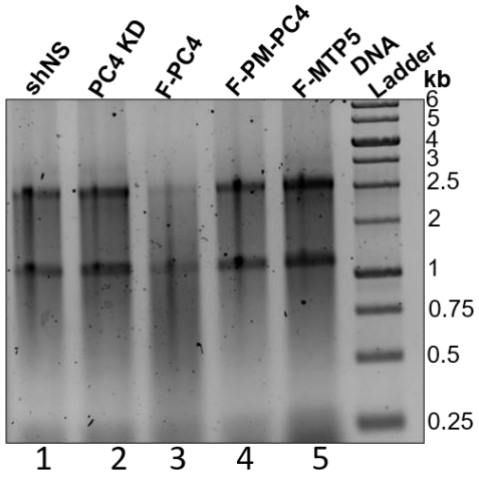

Figure 2.1: Lanes 1-5 represent the profile of 1µg of total RNA extracted from 5 different cells, resolved on a 1% agarose gel and visualized by EtBr staining.

2.1.5.2 RNA extraction from patient samples

RNA from patient samples were either obtained from paraffin-embedded tissues or from solid tumors stored in RNA Later solution at -80 degrees. For paraffin-embedded tissues first, deparaffinization was carried out by xylene method followed by Proteinase K digestion. For solid samples, it was crushed using a sterile mortar and pestle using liquid nitrogen. RNA Later was quickly blotted away using a solution with an absorbent lab wipe or paper towel, and then submerged the sample in RNA isolation lysis solution i.e. TRIZOL. The tissue was promptly homogenized after placing it in lysis/denaturation solution. The tissue samples were homogenized in 1 ml of TRIZOL reagent per 50 to 100 mg of tissue using KIMBLE dounce homogenizer (Sigma). The sample volume was not more than 10% of the volume of TRIZOL Reagent used for the

homogenization. To ensure efficient precipitation of the RNA the isopropanol step was done overnight. This was followed by ethanol wash and the pellet was dried similarly and dissolved in water. All the RNA extracted was analyzed through spectrophotometric analysis for absorbance at 260nm, 280 nm and 230nm. Pure RNA samples having A260/280 between 1.9-2.0 and A260/230 >1.7 were used for further gene expression analysis. The integrity of the RNA and its purity was measured by the absorbance 260/280nm, since the ratio was more than 1.5, presumably the RNA was substantially intact.

2.1.6 Nucleic Acid estimation

Nucleic acid concentration estimation was done using Nanodrop-1000 spectrophotometer (Thermo scientific) by measuring the absorbance of 1µL of DNA/RNA at 260nm wavelength where A260 of 1 corresponds to 50ng/µL. The purity of the sample was verified by A260/A280 ratios.

2.1.7 Estimation of Protein Concentration

Biorad protein estimation reagent was used to estimate protein concentration using manufacture's protocol. Known concentrations of BSA were used for plotting standard curve. A linear curve generated y absorbance values of known BSA concentrations was employed to assign concentration of the unknown protein samples. Recombinant protein concentration was estimated by running increasing concentrations of BSA along with protein of interest on SDS-PAGE gel.

2.1.8 Agarose Gel Electrophoresis

Electrophoresis was performed for detection, analysis and purification of DNA/RNA by using 0.8-1% agarose (Sigma) gel in 1X TBE (0.09 M Tris borate and 0.002 M EDTA) electrolyte. Samples were mixed with 6X loading buffer to make final concentration as 1X (for 1X- 0.25% Bromophenol Blue, 0.25%

Xylene cyanol in 40% Sucrose), loaded on the gel, electrophoresed at 150V in 1X TBE and stained in ethidium bromide solution (10μg/100 ml water) for 20 min. The stained nucleic acids were then visualized in the long wavelength UV lamp (Biorad), after destaining them with distilled water.

2.1.9 SDS-polyacrylamide gel electrophoresis (SDS-PAGE)

Purified Proteins and lysates were resolved according to their molecular weights in an SDS-PAGE. The resolving gels were made with either, 12 or 15% of acrylamide based on the resolution required in 0.375 M Tris-Cl (pH8.8), 0.1% SDS, 0.1% APS and 8% TEMED. The stacking gel composed of 5% acrylamide 0.375 M Tris-Cl (pH6.8), 0.1% SDS, 0.1% APS and 8% TEMED was layered on top of the resolving gel. Protein samples were prepared with 5X SDS sample buffer (for 1X- 50 mM Tris-HCl pH 6.8, 100 mM DTT, 0.1% Bromophenol blue, 10% Glycerol), and electrophoresed in Tris-glycine- electrophoresis buffer (25 mM Tris, 250 mM Glycine pH8.3, 0.1% SDS) after heating at 90°C for 5mins. To visualize the protein gel was stained with Coomassie Brilliant Blue (CBB) (45% MeOH, 10% glacial CH3COOH, 0.25% CBB), followed by destaining in Destaining solution (30% MeOH, 10% glacial CH3COOH).

2.1.10 Western blot analysis

The purified proteins or whole cell lysates were resolved by SDS-PAGE (denaturing PAGE) and equilibrated for 5mins in transfer buffer (25mM tris, 192mM glycine, 0.038% SDS and 20% MeOH) along with the methanol activated PVDF membrane (Millipore). Using a semidry western transfer apparatus (Biorad) the resolved proteins were transferred on to the PVDF membrane at 25 V, for 20-40 mins depending upon the molecular weight of the protein. After blocking the PVDF blots with either 5% skimmed milk solution or 2% BSA in PBS overnight at 4°C or at room temperature for 1 hr the blots were

probed with primary antibody diluted in 2.5% milk solution or 3% BSA according to the dilutions standardized for each protein in cell lysates, for a period of 8-12 hrs at 4°C depending on the affinity of the antibody. Further, after subjecting to washing with 1X PBS or PBST (PBS with 0.1% Tween 20), appropriate HRP conjugated secondary antibody solution was added and incubated for 1hr at room temperature, after which the blots were washed once again as mentioned earlier. The signal from expected protein of interest was developed using the Biorad Clarity chemiluminescence kit, as per the manufacturer's protocol. The blots were exposed in TMS (Kodak X-Ray films), for different time points and developed using GBX-Developer-Fixer Kit (Premiere Kodak reagents) or by using Biorad Chemidoc system.

2.1.11 Real time quantitative RT-PCR

Control or variously treated cells were harvested and lysed using TRIzol™ and total RNA was isolated and resolved on a 1% agarose gel to check for the integrity of the RNA to be subsequently used as template for complimentary DNA (cDNA) synthesis. The cDNA strand was prepared using oligo-dT23 (Sigma #O4387), M-MLV Reverse Transcriptase (Sigma #M1302) and RNaseOUT™ Recombinant Ribonuclease Inhibitor (Invitrogen™ Reagent #10777019) as per manufacturer's recommendations. This cDNA was used for real time PCR (RT-PCR) analysis using SYBR-Premix Ex Taq™ II (Tli RNaseH Plus) (Takara # RR820A) with 10pmol of specific primers (mentioned below) and different dilutions of the respective cDNAs. RT-PCR reactions were carried out in Step One Plus™ Real-Time PCR (Applied Biosystems) machine and amplification protocols were followed as indicated in the manufacturer's protocol. PCR conditions were standardized for each set of primers used. Fold expression change was calculated using ΔΔCt method using actin gene primers as internal control. Specificity and sensitivity of the primers was ascertained by melt curve analysis. The sequence for the different primers used for RT-PCR been shown in table 2.1.

Sl. No.	Gene Name	Forward Primer (5'-3')	Reverse Primer (5'-3')
1	β-Actin	AGATGTGGATCAGCAAGCAGGAGT	TCCTCGGCCACATTGTGAACTTTG
2	SCN2	GCTTTCTGATGTCATGATCTTGACTGTG	CGTGTAGCCATAGTTGGGGTTTCTACC
3	GAD1	GCGCCCCACAACGTACGATACC	CACCACTTCCAGGAGGAATTGC
4	M4	GGCCTCATGATTGCTGCTGCC	GGCTCTTGAGGAAGGCCAG
5	AMPKalpha1	GTCAAAGCCGACCCAATGATA	CGTACACGCAAATAATAGGGGTT
6	AMPKalpha2	CAGGCCATAAAGTGGCAGTTA	AAAAGTCTGTCGGAGTGCTGA
7	ULK1	GTCACACGCCACATAACAGA	CCATCAAGGTGATGAGGAAGAA
8	ULK2	CCCTCCCAAGTCTCATGTTTAG	TCTGATGTGGTTTCCTCTGATG
9	DRAM1	GTCAGCCGCCTTCATTATCT	CACTCTCTGGAGGTGTTGTTC
10	PC4	AGGTGAGACTTCGAGAGCCCTGT	TTCAGCTGGCTCCATTGTTCTGG

Table 2.1: Sequences for different qRT-PCR primers used for the genes mentioned

2.2 Cloning

2.2.1 Sub-cloning

For sub-cloning into bacterial and mammalian expression vectors, specific primers were used to amplify the various ORFs from the validated *E. coli* expression clones. Amplicons were purified by agarose gel extraction procedure and then the extracted DNA (2µg) was digested with the appropriate restriction enzymes (NEB) in their recommended compatible buffers. Similarly, the vector (2µg) was also digested under same conditions as the amplicons. The digested products were gel purified by agarose gel electrophoresis. Subsequently 1:3 or 1:5 molar ratio of vector to insert and maintaining 100-200ng total digested vector DNA was ligated at room temperature for 10-12 hrs using T4 DNA ligase (NEB). After ligation the total reaction mixture was transformed into *E. coli* (DH5α) and plated onto LB-agar containing the prescribed amount of the suitable antibiotic based on the selection marker gene present in the cloned vector. Individual colonies were amplified in LB broth and plasmid was isolated. Prior to expression these clones were verified by restriction digestion (Figure 2.2.1) to release the inserts of expected length and further corroborated by sequencing these clones individually.

A

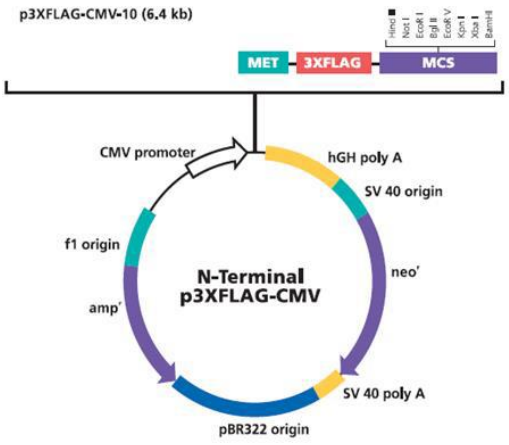

B

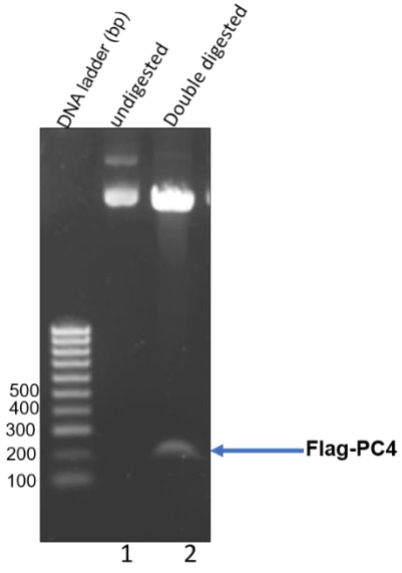

Figure 2.2.1: Clone confirmation of Flag-PC4. **A**. Vector map of p3XFlag-CMV10 used for cloning of Flag- PC4 mammalian expression construct. **B.** Confirmation of the respective clone of Flag-PC4 by double digestion of the clones with the restriction endonucleases HindIII and XbaI. The cloned insert has been represented by the blue arrow.

2.2.2 Site directed mutagenesis

To create various point mutants, primers were designed spanning the nucleotide coding for the desired residue to be mutated using the QuikChange Primer Design tool (Agilent), as per manufacturer's instructions. Briefly, the chosen expression plasmid containing the ORF was taken as template (50ng) and amplified using Pfu polymerase supplied with QuickChange II XL site directed mutagenesis kit (Agilent). The PCR product was incubated with Dpn1 for 2hrs at 37°C to digest the methylated template DNA and the digested product was then transformed into *E. coli* (XL10 Gold). Screening of the desired mutation was confirmed by sequencing (Figure 2.2.2).

The list of the different primers used for the present study has been enlisted in Table 2.2.2.

Sl. No.	Mutant generated	Forward Primer (5'-3')	Reverse primer (5'-3')
1	Untagged PC4S13D-S15D	ACCTCACTGTCAGAATCATCGCCATCAGAGCTTGAAGAAACAAGTTCCTTTGATTTAGG	CCTAAATCAAAGGAACTTGTTTCTTCAAGCTCTGATGGCGATGATTCTGACAGTGAGGT
2	Untagged PC4S13D-S15D- S17D S19D	CTTGTTTCTTCAAGCTCTGATGGCGATGATGATGACGATGAGGTTGACAAAAAGTTAAAGAGG	CCTCTTTAACTTTTTGTCAACCTCATCGTCATCATCATCGCCATCAGAGCTTGAAGAAACAAG
3	3X Flag tagged PC4S13D -S15D	ACCTCACTGTCAGAATCATCGCCATCAGAGCTTGAAGAAACAAGTTCCTTTGATTTAGG	CCTAAATCAAAGGAACTTGTTTCTTCAAGCTCTGATGGCGATGATTCTGACAGTGAGGT
4	3X Flag tagged PC4S13D S15D-S17D S19D	CTTGTTTCTTCAAGCTCTGATGGCGATGATGATGACGATGAGGTTGACAAAAAGTTAAAGAGG	CCTCTTTAACTTTTTGTCAACCTCATCGTCATCATCATCGCCATCAGAGCTTGAAGAAACAAG
5	3X Flag tagged PC4 K26R K28R	CTGGAGCAACTTGCTTTCTCCTCCTTAACTTTTTGTCAACCTCACT	AGTGAGGTTGACAAAAAGTTAAGGAGGAGAAAGCAAGTTGCTCCAG
6	3X Flag tagged PC4 K26Q K28Q	TTTTTCTGGAGCAACTTGCTTCTGCCTCTGTAACTTTTTGTCAACCTCACTGTCAG	CTGACAGTGAGGTTGACAAAAAGTTACAGAGGCAGAAGCAAGTTGCTCCAGAAAAA

Table 2.2.2: List of primer sequences used for site-directed mutagenesis.

A

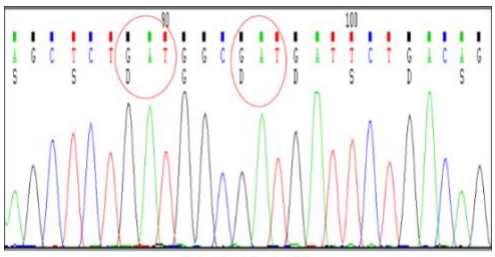

PC4S13D-S15D

B

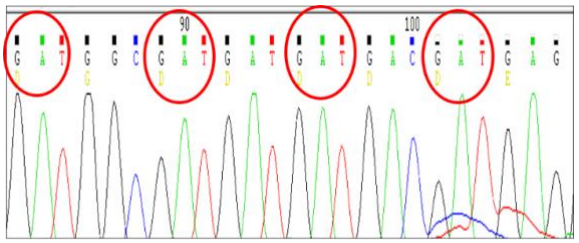

PC4S13D-S15D-S17D-S19D

C

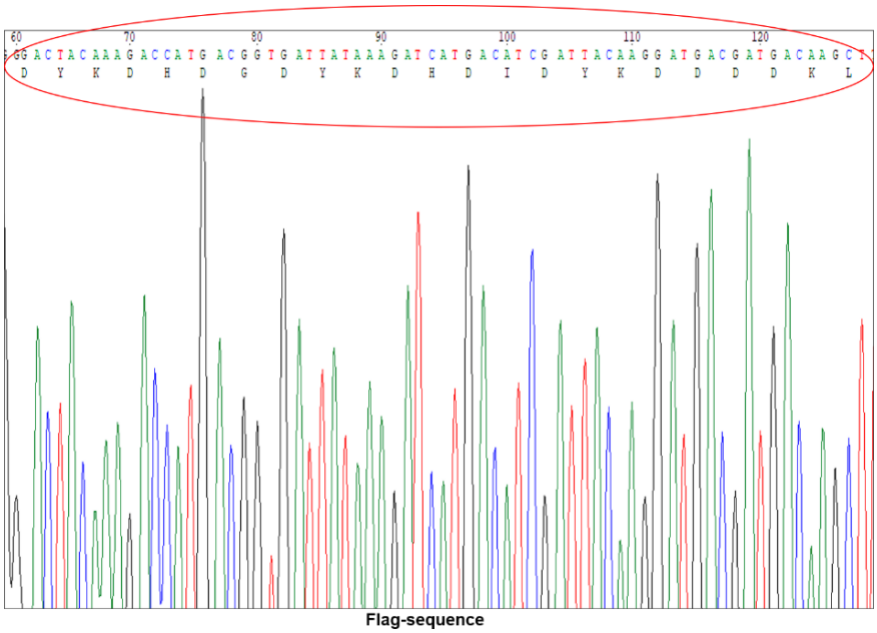

Flag-sequence

D

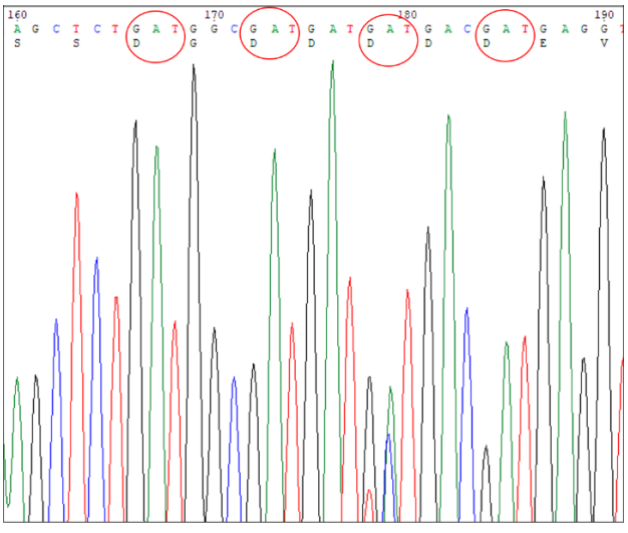

Flag-PC4S13D-S15D-S17D-S19D

Figure 2.2.2.1: Chromatogram highlighting the different point mutants generated for- A. Untagged PC4 S13D-S15D B. Untagged PC4 S13D-S15D-S17D-S19D; C. 3XFlag sequence of Flag tagged PC4 S13D-S15D-S17D-S19D; D. Flag tagged PC4 S13D-S15D-S17D-S19D. The mutated residues are circled in red.

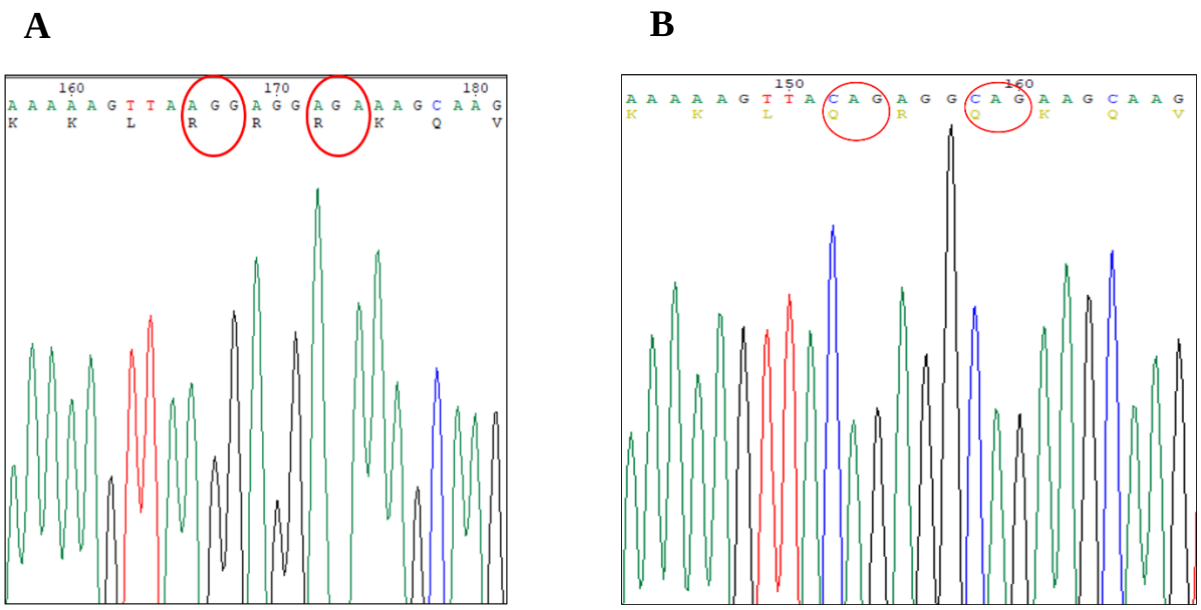

Figure 2.2.2.2: Chromatogram highlighting the different point mutants generated for- (A). Flag tagged PC4 K26R-K28R and (B). Flag tagged PC4 K26Q-K28Q. The mutated residues are circled in red.

2.3 Protein Purification

2.3.1. C-terminal His-tagged PC4 purification

E. coli BL21 cells were transformed with His6-PC4 expression vector. 100ml of LB medium containing 50µg/ml Kanamycin was inoculated from the transformed colony and grown overnight at 37ºC. This overnight culture was further inoculated into 900ml of Luria Bertani broth containing 50µg/ml Kanamycin and grown at 37ºC until the O.D. reaches 0.4 (O.D. 600). The culture was then induced with 0.4mM IPTG for 3hrs at 37ºC. The culture was then harvested and then homogenized in homogenization buffer (20mM Tris-HCl, 20% Glycerol,

2mM PMSF, 20mM EDTA,20mM Imidazole, 300mMKCl, 2mM βMe, 0.1% NP40) and then sonicated. Cleared lysate is obtained by centrifuging at 16,000 rpm at 4ºC for 30mins. The cleared lysate is then incubated with pre-equilibrated Ni-nitrilotriacetic acid beads (Novagen) at 4ºC for 3hrs. The beads are then washed with 10ml of wash buffer (20mM Tris- HCl, 20% Glycerol, 2mM PMSF, 20mM EDTA, 40mM Imidazole, 600mM KCl, 2mM βMe, 0.1% NP40) for 9 times. The beads are then loaded into a column and the protein was eluted out with elution buffer (20mM Tris-HCl, 20% Glycerol, 2mM PMSF, 20mM EDTA, 250mM Imidazole, 100mMKCl, 2mM βMe, 0.1% NP40). Elutions were collected in aliquots. The eluted proteins were further dialyzed against BC100 buffer (20mM Tris-HCl, 20% Glycerol, 2mM PMSF, 20mM EDTA, 20mM Imidazole,100mMKCl, 2mM βMe, 0.1% NP40) and snap frozen in liquid nitrogen and stored at -80ºC. The purification profile for His6-PC4 checked on a 12% SDS-PAGE (Figure 2.3.1)

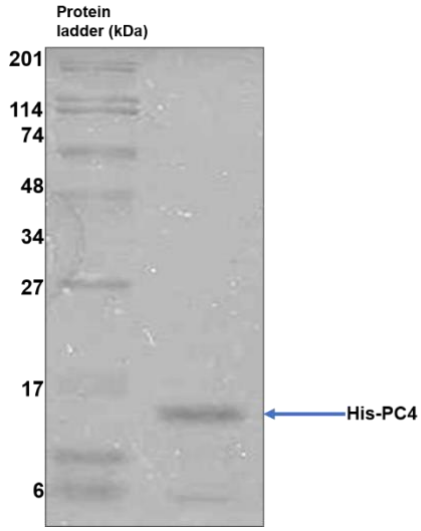

Figure 2.3.1: Purification of bacterially expressed recombinant His6-PC4 from *E. coli* BL21 cells. Representative purification profiles of His6-PC4 resolved on a 12% SDS-PAGE and stained with CBB.

2.3.2 Purification of acetylation defective PC4 mutants

Therefore, using wild type PC4-His6 as the DNA template, lysine (K) residues 26 and 28 were mutated in combination to arginine (R), lysine residues 53 and 68 were mutated in combination to arginine (R) and lysine residue(K) at position 5 mutated to arginine (R) generating PC4K26R-K28R, PC4K53R-K68R double mutant clones and PC4K5R single point mutant clone respectively by site directed mutagenesis technique (QuickChange II XL site directed mutagenesis kit, Stratagene). The clones, PC4K53R-K68R and PC4K2628R obtained in lab were screened for the desired mutations and confirmed by sequencing. Acetylation site PC4 mutants were purified till homogeneity using Ni-NTA agarose column as described in the previous section. All proteins were dialyzed against BC100 buffer and snap frozen in liquid nitrogen and stored at-80ºC. The purification profile for different His6-PC4-acetylation defective mutants checked on a 12% SDS-PAGE (Figure 2.3.2)

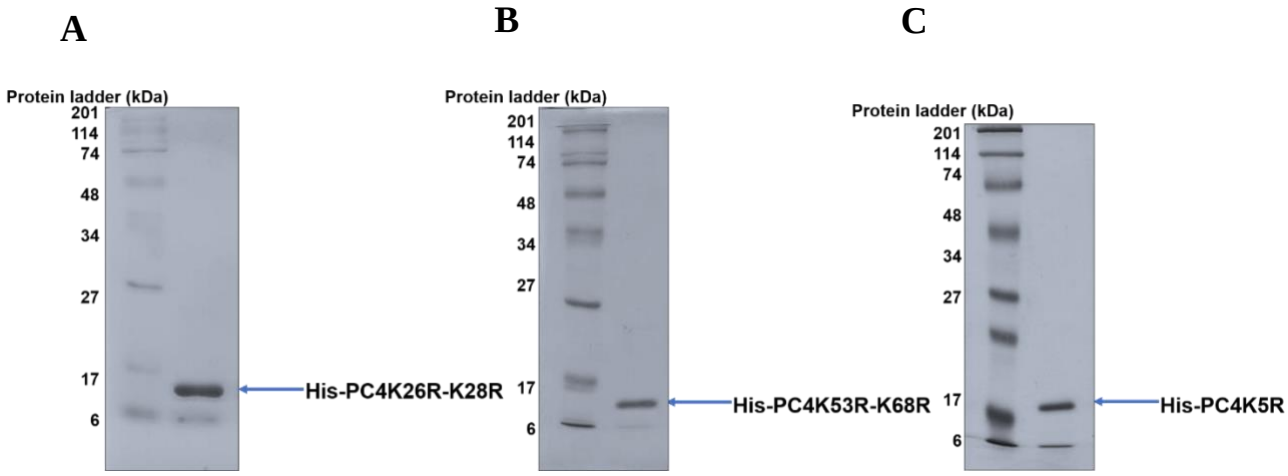

Figure 2.3.2: Purification profiles for different acetylation defective mutants; His6- PC4K26R-K28R (A), His6- PC4K53R-K68R (B) and His6- PC4K5R (right panel) (C).

2.3.3 Purification of bacterial expressed untagged PC4

Untagged PC4 purification: A two-column purification protocol was employed to purify untagged recombinant PC4 (Ge and Roeder, 1994) using heparin Sepharose followed by phosphor-cellulose P11 columns. *E. coli* BL21 cells were transformed with native PC4 expression vector in presence of 100µg/ml ampicillin. 100ml of LB medium containing 100µg/ml ampicillin was inoculated from the transformed colony and grown overnight at 37ºC. This overnight culture was further inoculated into 900ml of Luria Bertani (LB) broth containing 100µg/ml ampicillin and grown at 37ºC until the O.D. reaches 0.6 (O.D. 600). The culture was then induced with 0.5mM IPTG for 3hrs at 37ºC. The cells were harvested and resuspended in homogenization buffer BC300 (20mM Tris-HCl pH7.4, 20% glycerol, 0.2mM EDTA, 300mM KCl, 0.1% NP40, 2mM PMSF and 2mM ß Mercaptoethanol) and sonicated with 2 cycles of 5minutes each with burst of 5seconds. The cleared supernatant was obtained by centrifugation at 16000rpm for 30mins at 4ºC. The supernatant was passed through BC300 pre-equilibrated heparin sepharose column. The column was washed 2-3 times column volume by

BC300 and eluted with BC500 (20mM Tris-HCl pH7.4, 20%glycerol, 0.2mM EDTA, 500mM KCl, 0.1% NP40, 2mM PMSF and 2mM ß-Mercaptoethanol). The eluted fractions were analysed by 12% SDS-PAGE (Figure9A). Fractions majorly containing PC4 protein were pooled and was loaded onto a BC500 pre-equilibrated phosphocellulose P11 (Whatman) column. The column was washed with 25ml of BC500 and eluted with BC850 (20mM Tris-HCl pH7.4, 20%glycerol, 0.2mM EDTA, 850mM KCl, 0.1% NP40, 2mM PMSF and 2mM ß Mercaptoethanol). The PC4 protein containing fractions were pooled (Figure 2.3.3 A) and dialysed in BC100 (20mM Tris-HCl pH7.4, 20% glycerol, 0.2mM EDTA, 100mM KCl, 0.1% NP40, 2mM PMSF and 2mM ß Mercaptoethanol), aliquoted and snap frozen in liquid nitrogen and stored at -80ºC. The purification profile for untagged PC4 after dialysis was checked on a 15% SDS-PAGE (Figure 2.3.3 B).

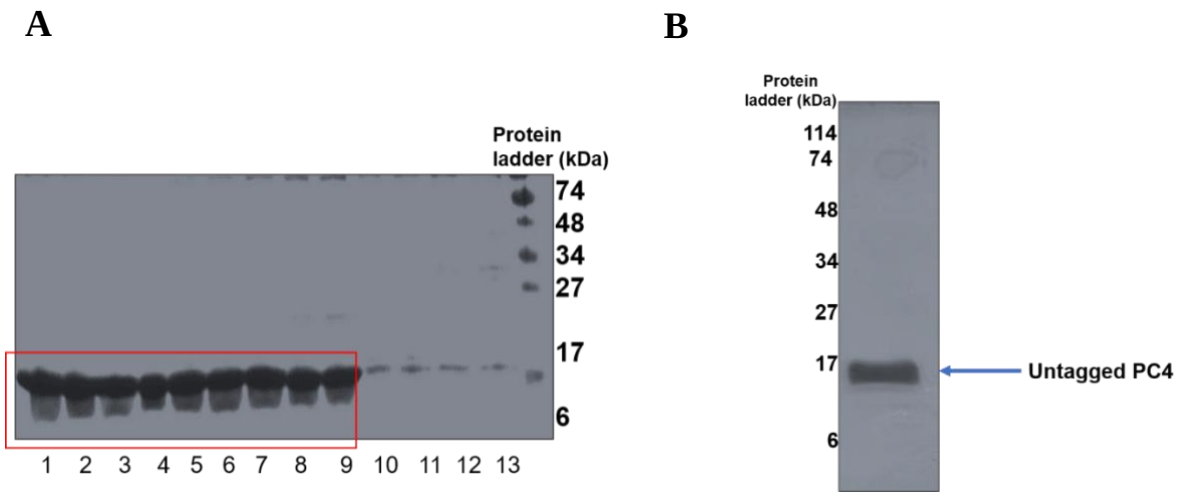

Figure 2.3.3: Purification profile of untagged PC4 after passing through two columns namely heparin Sepharose followed by phosphocellulose (A). The fractions from lane 1-9 (shown within red box) had been pooled together for dialysis. The purification profile of untagged PC4 after dialysis (B).

2.3.4 Purification of bacterial expressed untagged Phospho-defective PC4 mutants and phosphomimic PC4

Untagged phosphor-defective PC4 mutant MTP5 (PC4S13A-S15G-S17A-S19G) and MTP6 (PC4S13A-S15G-S17A) where serine residues (S) were mutated to alanine (A) and glycine (G) at four and three sites respectively and untagged phosphomimic purification (PM-PC4) where serine residues (S) at 13,15,17 and 19 position were mutated to aspartic acid (D) were generated by by site directed mutagenesis technique (QuickChange II XL site directed mutagenesis kit, Stratagene). The clones were confirmed by sanger sequencing. The untagged MTP5, MTP6 and PM-PC4 were purified in the same way as untagged PC4 by two-column purification protocol (Ge and Roeder, 1994) using heparin Sepharose followed by phosphor-cellulose P11 columns with only changes in the induction conditions. The secondary culture was induced with 0.5mM IPTG for 4 hrs at 37ºC after the O.D. reaches within the range of 0.6-0.7 (O.D. 600). The purification profile for untagged PC4 phospho-defective mutants and phosphomimic mutant after dialysis were checked on a 15% SDS-PAGE (Figure 2.3.4).

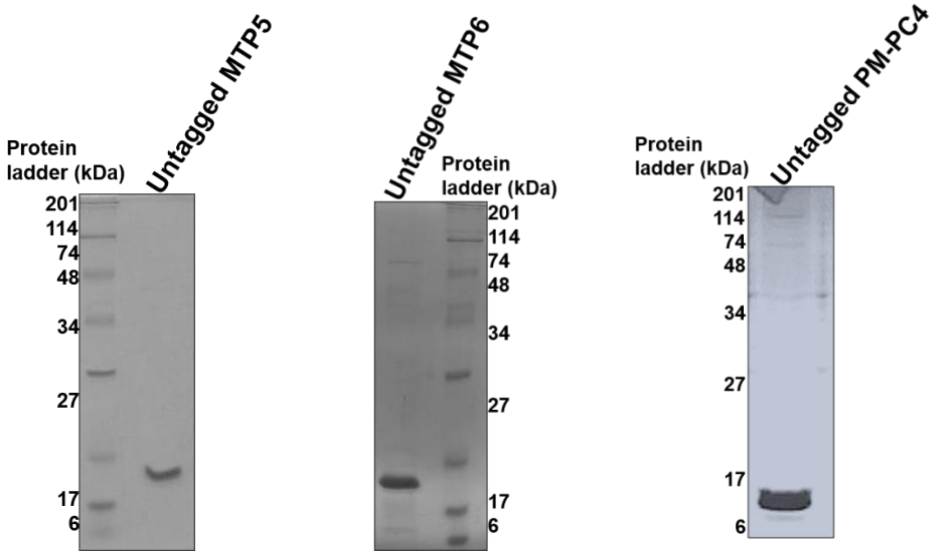

Figure 2.3.4: Purification profile of untagged phosphor-defective mutant MTP5, phosphor-defective mutant MTP6 and untagged phosphomimic mutant PM-PC4 checked on 15% SDS-PAGE and stained with CBB (from left to right respectively).

2.3.5 Purification of His-tagged human somatic linker histone H1 variants

E. coli BL21 cells were transformed with different somatic linker H1 variants that are C-terminal six histidine tagged. 100ml of LB medium containing 50µg/ml Kanamycin was inoculated from the transformed colony and grown overnight at 37ºC. This overnight culture was further inoculated into 900 ml of Luria Bertani broth containing 50µg/ml Kanamycin and grown at 37ºC until the O.D. reaches 0.8 (O.D. 600). The culture was then induced with 0.5mM IPTG for 3hrs at 37ºC. Cells were harvested by centrifugation at 6000rpm at 4ºC for 10mins. After lysis, the cell lysates were precipitated with 5%perchloric acid to remove bacterial proteins. The protein was then purified from the resulting supernatant by precipitation with 15% trichloroacetic acid, washed once with acidified acidified acetone (0.5ml of concentrated HCl/100ml) and twice with chilled acetone, and air dried, dissolved in BC100 (20mM Tris-HCl pH7.4, 20% glycerol, 0.2mM EDTA, 100mM KCl, 0.1% NP40, 2mM PMSF and 2mM ß-Mercaptoethanol). The protein fractions were analysed on 12% SDS-PAGE (Figure 2.3.5), aliquoted and snap frozen in liquid nitrogen and stored at -80ºC.

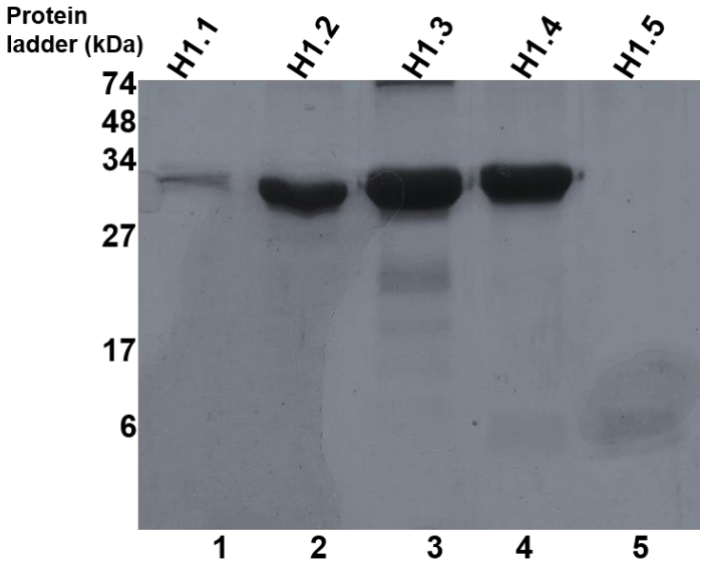

Figure 2.3.5: Purification of bacterially expressed recombinant His6-H1 variants from *E. coli* BL21 cells. Representative purification profiles of five different somatic H1 variants His6-H1.1, H1.2, H1.3, H1.4 and H1.5 (lane 1-5) resolved on a 12% SDS-PAGE and stained with CBB.

2.3.6 Purification of His-tagged human somatic linker histone H1 domains

Different deletion constructs of H1 domains were cloned into pET28b vector generating His6-tagged ΔC (C-terminal domain deleted), ΔN (N-terminal domain deleted), and ΔNC (N-terminal and C-terminal domains deleted), expressed them in bacteria, and was purified from *E.coli* BL21 cells in the same way under same induction conditions as was carried out for linker H1 variants. The schematic of different deletion constructs of linker H1 variant H1.2 has been shown indicating the residues being deleted in each of the construct (Fig.2.3.6 A). The protein fractions for each deletion construct were analysed on 12% SDS-PAGE (Figure 2.3.6 B), aliquoted and snap frozen in liquid nitrogen and stored at -80ºC.

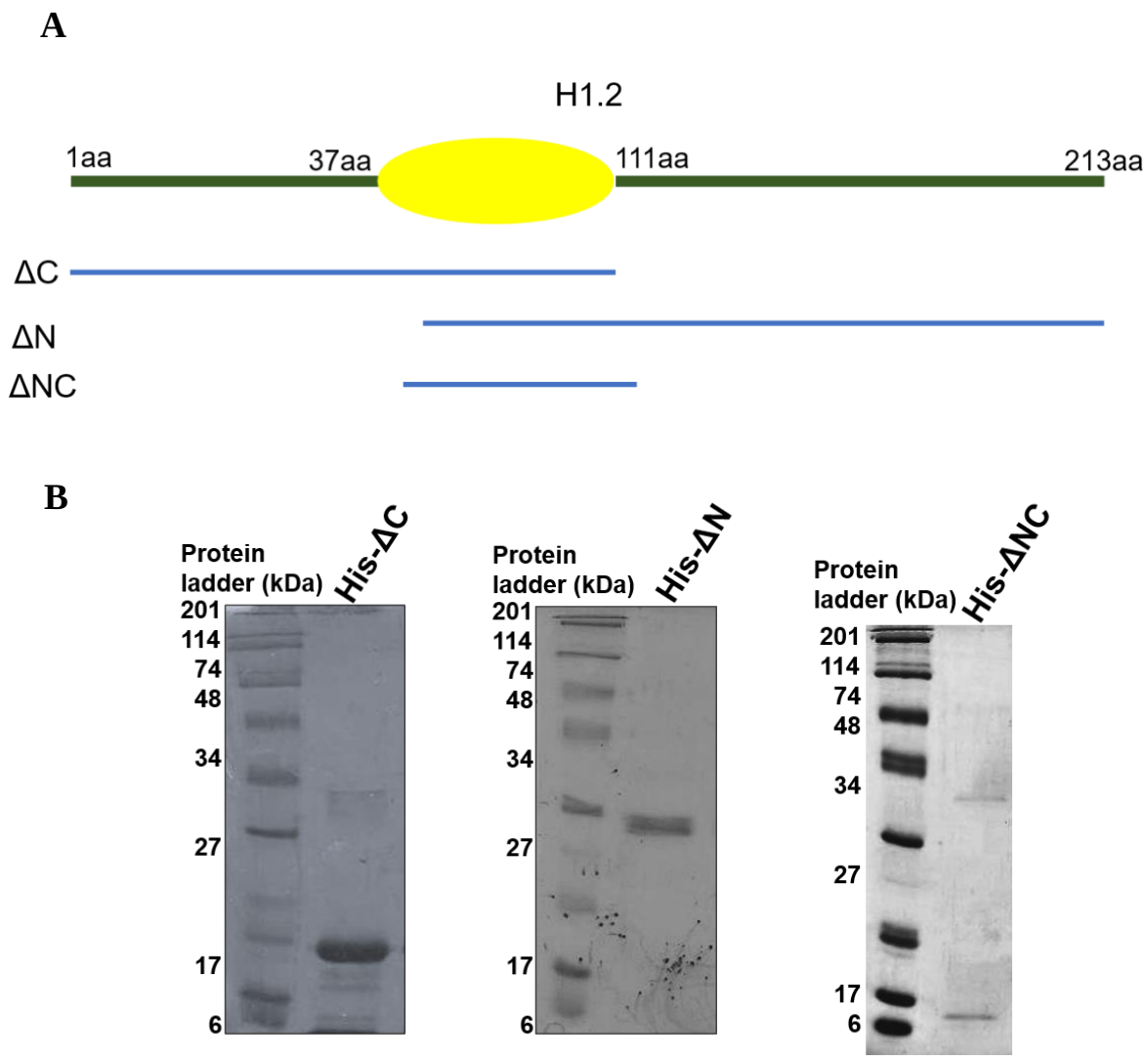

Figure 2.3.6: (A) Schematic representation of the linker H1.2 domain organisation indicating the different deletion constructs, ΔC, ΔN and ΔNC and the stretch of residues present in each construct. (B)Purification profile of bacterially expressed recombinant His6- ΔC, His6- ΔN and His6- ΔNC (from left to right respectively) resolved on a 12% SDS-PAGE and stained with CBB.

2.3.7 Purification of recombinant proteins from baculovirus-infected Sf21 cells

KAT3b or p300 enzyme was expressed as C-terminal His6-tagged proteins and purified using Ni-NTA (Novagen) affinity purification from the respective, recombinant baculovirus infected Sf21 cells. Briefly, Sf21 cells were cultured in

five 150mm dishes till 100% confluent after which fresh complete TC100 media (Himedia) with 10% FBS was added and then scrapped to detach the monolayer following which the cells were counted and 9 million cells transferred to fresh culture dishes, just before infection. The cells were kept in suspension during infection, and 200 µl of the viral particles containing culture supernatant were added drop wise over the surface of the culture dishes at room temperature. Following infection, they were further incubated at 27˚C. The infected cells are checked for the viral expression based on the change in morphology [cubical, spindle, or capsule shaped etc]. 70hrs post infection (prior to rupture and release of the viral particles into the culture supernatant cells were harvested by scrapping and pelleting at 1000 rpm for 10 min. Cell pellet was washed once with 1X PBS and then lysed in cold lysis buffer (homogenization buffer) containing 10mM tris-HCl pH 7.5, 10% Glycerol, 0.1% NP0, 2mM β Mercaptoethanol, 0.2mM PMSF, 500mM NaCl, 15mM Imidazole and 1X protease inhibitory cocktail (Sigma) using a Dounce homogenizer (5 strokes- 4 times with 3 min interval). After lysis, the lysate was centrifuged at 16,000rpm for 30 min and the supernatant was collected and 200µl of Ni-NTA beads, pre-washed and equilibrated with the homogenization buffer, were added and allowed to bind for 3hrs at 4°C on an end-to-end rotor. The beads were washed 7-8 times in wash buffer containing 10mM tris-HCl pH 7.5, 10% Glycerol, 0.2%NP40, 2mM β-Mercaptoethanol, 2mM PMSF, 300mM NaCl and 15mM Imidazole for poly-His tag proteins. After binding, the proteins were eluted using elution buffer containing 10mM tris-HCl, pH-7.5, 10% Glycerol, 0.1% NP0, 2mM β- Mercaptoethanol, 0.2mM PMSF, 200mM NaCl, 250mM Imidazole and 1X protease inhibitory cocktail. The protein was checked in 8% SDS-PAGE (Figure 2.3.7) and then stored at - 80°C after snap freezing them in small aliquots.

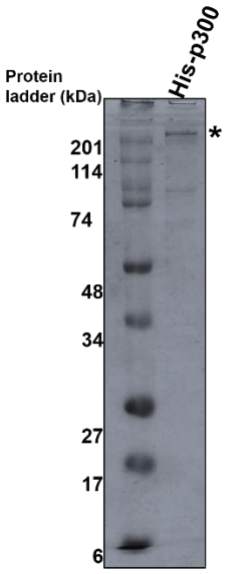

Figure 2.3.7: Purification of His6-p300 expressed in Sf21 insect cells

2.3.8 Purification of bacterially expressed Xenopus core histones

pLyS cells were transfected with the pET-histone expression plasmid and plated in LB plates containing Ampicillin (50µg/ml) and chloramphenicol 25µg/ml incubated at 37°C overnight. 5 ml of LB medium containing ampicillin and chloramphenicol was inoculated with single colonies, at 37°C overnight. About 5 different colonies were tested for induction. Next morning 5 ml of LB medium containing ampicillin and chloramphenicol was inoculated with 50µl of the overnight culture and shaken until the OD600 reaches 0.5~0.7, and then induced with 0.2mM IPTG for 4 h. The induction was checked on an 18% SDS PAGE and the best induced colony was selected to further inoculate 1lt of LB medium containing ampicillin and chloramphenicol with 1ml of the overnight culture and grown till OD600 reaches 0.5~0.7 and induced with 0.2mM IPTG for 4 h. The cells were harvested by centrifugation at room temperature, resuspended to homogeneity in 100ml wash buffer (50mMTris-HCl, pH 7.5, 100mMNaCl, 1mMNa-EDTA, 1mMbenzamidine), and flash-frozen in liquid nitrogen and stored at -80°C. The cell suspension was thawed in a warm water bath. The cell

suspension becomes extremely viscous as lysis occurs. The viscosity is reduced by shearing with an Ultraurrx homogeniser and centrifuged for 20min at 4℃ and 23000g. The pellet obtained contains the inclusion bodies of the corresponding histone protein. The pellet is washed by completely resuspending in 100ml. wash buffer plus 1% Triton-X-100 and centrifuged for 10min at 4℃ and 12000rpm. This step was repeated once with wash buffer plus Triton and twice with wash buffer. After the last wash, the drained pellet was stored at -80℃. The purification profile for bacterially expressed Xenopus core histones (H2A, H2B, H3 and H4) were checked on 15% SDS-PGAE.

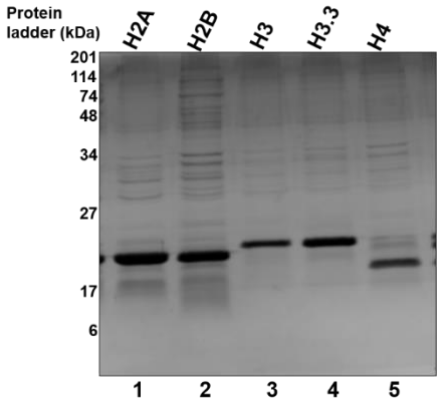

Figure 2.3.8: The pellet containing the histones resuspended in 30ml unfolding buffer (7M guanidinium HCl, 20mM Tris-HCl, pH7.5, 10mM DTT) loaded on a 15% SDS-PAGE and stained with CBB showing the profile for individual Xenopus core histones before histone octamer refolding.

2.3.9 Purification of linker histone H1 from HeLa cells

Histone H1 was purified from HeLa cells according to the method developed by Mirzabekov et al. with slight modifications (Mirzabekov AD. et al., 1990). The cells were harvested, washed with PBS, and then lysed in 140 mM NaCl, 10 mM Tris-HCl (pH 7.5), and 0.5% Triton X-100, followed by three washes with the same buffer without detergent. The nuclei were collected, washed with 0.35 M NaCl, and 10 mM Tris-HCl (pH 7.5), and then resuspended in 5% trichloro acetic

acid (CCl3COOH) and rotated at 4 °C for 80 min. After centrifugation at 4000g for 15 min, the soluble histone H1 supernatant was dialyzed against 10 mM HCl and 2 mM β-mercaptoethanol. The dialyzed sample was lyophilized and stored at -80 °C. For chromatin reconstitution, the lyophilized protein was resuspended in 10 mM Tris-HCl (pH 7.5), 1 mM EDTA, 500 mM NaCl, 0.05% NP-40, and 20% glycerol. The purification profile of linker H1 extracted from Hela cells was checked on 12% SDS-PAGE after lyophilized protein has been resuspended to be used for nucleosome folding experiments (Figure 2.3.9).

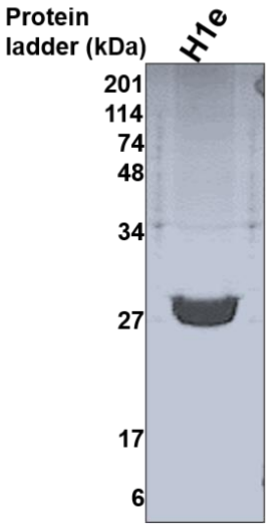

Figure 2.3.9: Purification profile of linker histone H1 extracted from HeLa cells

2.4. Protocols for different *in vitro* assays and analysis

2.4.1 *In vitro* Acetylation Assay

2.4.1.1 Filter Binding Assay

The activity of p300 was assayed by Filter binding assay. 1µg of Histone H4 or Histone H3 was incubated with 1µl of p300 enzyme (1:10 diluted) at 30ºC for 30 mins in 2X HAT buffer (1X composition: 50mM Tris-HCl pH 8.0, 10% glycerol, 1mM DTT, 1mM PMSF, 0.1mM EDTA), 10mM Na-butyrate and 1µl of 2.1 Ci/mmol of [^{3}H]-acetyl CoA. The reaction mixture was then spotted on a

Phosphocellulose P-81 filter paper. The radioactive counts were recorded on a Wallac 1409 Liquid scintillation counter.

2.4.1.2. Histone Acetyltransferase (HAT) gel assay

HAT assays were performed using 500ng/1µg of recombinant PC4 500ng/1µg of recombinant mutants of PC4 incubated in HAT assay buffer at 30ºC for 30mins with or without 1µl of 3.3 Ci/mmol of [^{3}H]- acetyl CoA, baculovirus expressed recombinant p300, and 10mM Na-butyrate. To visualize the radiolabelled acetylated protein, the reaction products were resolved electrophoretically on 12% SDS-polyacrylamide gel and subjected to fluorography. The gel was stained by CBB to ascertain the presence of protein in equal amounts in each of the reaction and was later equilibrated in DMSO for 1 hr. Later the gel was incubated in scintillation fluid (22.5% w/v PPO solution in DMSO) for 30 mins and then rehydrated in water for 2hrs. The gel was dried using a gel drier and exposed in an X-ray cassette using a film for 7days in -80°C. The film was later developed to get intensity profiles for each of the reactions as shown in figure 2.4.1.2.

The HAT assay was also carried out to check the acetylation levels by western blotting using either 1µg of His-PC4 or 1ug of His-PC4K26R-K28R acetylation defective mutant, 1µl of p300 (~ 20,000 Counts/µl), 2X HAT buffer, 10mM Na-Butyrate and 40 µM of cold (non-radioactive) acetyl-CoA was incubated at 30ºC for 30 mins. Mock acetylation reaction was also set up without acetyl-CoA. The reaction mixture after 30 mins of incubation was stopped and 1X SDS-dye was added and loaded on to 15% SDS-PAGE followed by immunoblotting to be probed with PC4K26-28ac antibody.

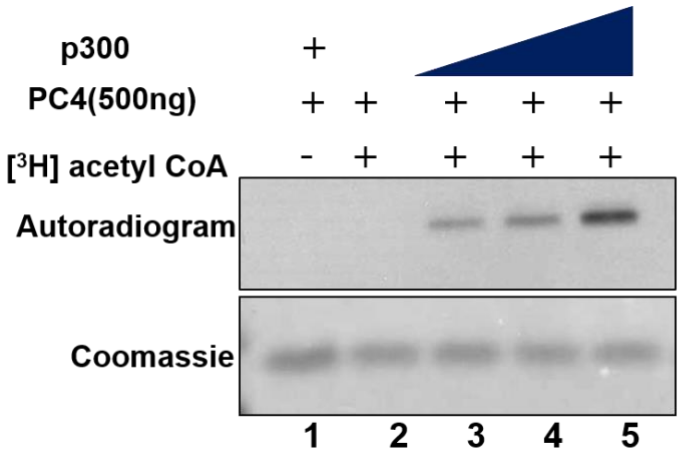

Figure 2.4.1.2: Dose dependent acetylation of PC4 by p300 enzyme: *In vitro* acetylation assay using C-terminal His tagged bacterially expressed recombinant PC4 (500ng) was carried out with increasing counts of baculovirus expressed recombinant full length p300 enzyme (5000,10,000 and 20,000 counts) (lane 3,4 and 5 respectively) for 30mins at 30ºC showed a gradual increase in the acetylation levels of PC4 from the intensity profiles (lane 3,4and 5). Acetylation was not observed either in the absence of [^{3}H]- acetyl CoA (lane 1) or in the absence of enzyme p300 (lane 2). Coomassie shows equal protein loading.

2.4.2 *In vitro* Kinase assay

Approximately 1µg of protein substrate (PC4 or phosphorylation defective mutants; MTPs) was incubated with the enzyme 1µl Casein Kinase II (20mU) at 30ºC for 30 mins in 2X Phospho buffer (1X composition:50mM Hepes-KOH, pH7.6, 125mM NaCl, 10mM MgCl2, 6% Glycerol, 5mM DTT, 0.5mM PMSF), 5mM cold ATP and [γP^{32}] ATP. To check phosphorylation the reaction mixture was then loaded onto a 12% SDS-PAGE, dried and exposed in an X-ray cassette using a film for 3days in -80°C cooler. The film was later developed to get intensity profile for the reaction as shown in figure 2.4.2.

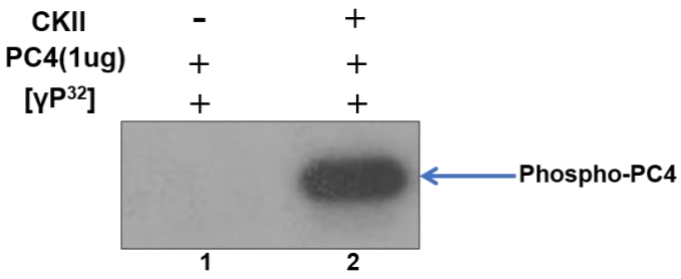

Figure 2.4.2 *In vitro* kinase assay: The intensity profile of PC4 subjected to *In vitro* kinase assay by CKII using 5mM cold ATP and [γ-P^{32}] ATP. Lane 2 indicating phosphorylation of PC4 by CKII (indicated by the blue arrow) vs lane 1 containing no enzyme control.

2.4.3 *In vitro* mass phosphorylation of PC4

For mass phosphorylation of PC4, approximately 600ng untagged PC4 or phosphorylation defective mutants MTP5 and MTP6 were incubated with 1µl Casein Kinase II enzyme (20mU) in 2X Phospho buffer, 10 mM cold ATP at 30ºC for 30 mins, followed by four replenishment with the enzyme CKII (20mU) and ATP (5mM) at 30mins interval. After last replenishment, final incubation was done overnight to ascertain completion of the reaction. Mock phosphorylation reaction was set with the same components except the enzyme CKII, and similar protocol was followed. Approximately 250ng of the protein from the reaction mix was loaded on to a 15%SDS-PAGE and stained with CBB to observe a mobility shift of phosphorylated PC4 (Figure 2.4.3). The same reaction mix was used for *in vitro* interaction assays.

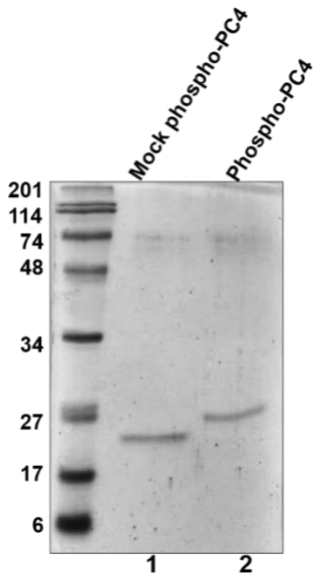

Figure 2.4.3: CBB stained gel representation of mass phosphorylated PC4 (lane 2), resolved on a 15% SDS PAGE.

2.4.4 *In vitro* interaction assays

Ni-NTA pull down assays were carried out where one of the interacting proteins is His-tagged. The linker histone interaction ability of PC4 was characterized by incubating 10µl of Ni-NTA beads with 1µg of C-terminal six histidine tagged histone variant H1.1 and 250ng of different modified forms of PC4, phosphor-defective PC4 along with phosphomimic PC4 in a final reaction volume of 300µl in BC buffer containing 150mM KCl supplemented with 30mM imidazole at 4ºC for 3hours. The beads were washed three times (1ml each time) with the incubation buffer containing 200mM KCl. The Ni-NTA pull down complex was analyzed by western blotting using anti-PC4 and anti-His antibody. Control experiments were performed with 10µl of Ni-NTA incubated with 250ng of different modified forms of PC4, phosphor-defective PC4 along with phosphomimic PC4 without His-H1 in the same buffer. 30 ul of each of the reaction mix was kept aside before adding Ni-NTA beads to be used as input.

2.4.5 *In vitro* Reconstitution of nucleosomal array

To study the nucleosomal compaction by PC4 upon phosphorylation a nucleosome array was reconstituted involving the following steps:

2.4.5.1 Refolding of histone octamer

The histones proteins are mixed in equimolar ratio and dialyzed at 4℃ against a 2L refolding buffer (2M NaCl, 10mM Tris-HCl, PH 7.5, 1 mM Na-EDTA, 5mM 2-mercaptoehanol) with at least three changes. The second or third dialysis step should be performed overnight. The proteins are then centrifuged and if precipitation occurs the sample is concentrated according to the volume necessary for the size column. The histone octamers are then purified from aggregates and dimers/tetramers on a sizing column (HiLoad Superdex 200, Pharmacia) and analysed the column fractions eluted in the refolding buffer by running it on18%SDS-PAGE (Figure 2.4.5.1). After which the fractions containing the octamer are pooled together to determine the concentration spectrophotometrically (A276=0.45 for a solution of 1mg/ml) and stored at 4℃.

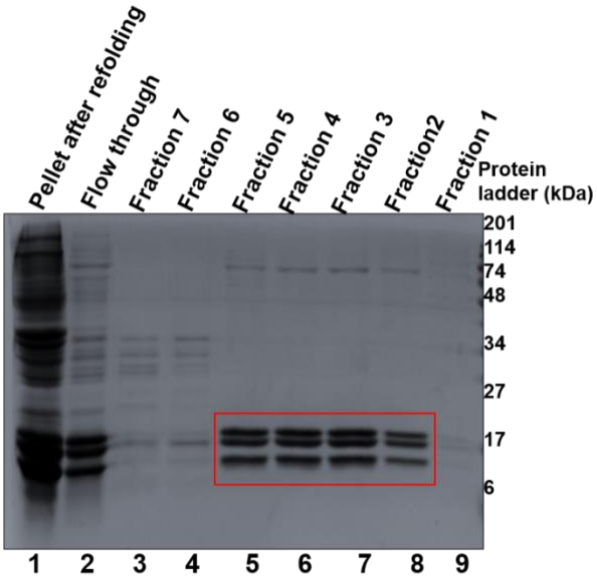

Figure 2.4.5.1: Each of the core histones purified from the pellet fraction of pLys cells subjected to dialysis in refolding buffer followed by purification. The CBB

stained 15% SDS-PAGE showing the different fractions loaded after purification of the histone octamer through a sizing column and only the fractions containing pure histone octamer (lane 5-8) indicated within the red box were pooled together for nucleosomal reconstitution.

2.4.5.2Purification of DNA template 12×177bp fragment

The DNA used for the assembly is 177×12bp tandem repeat of the 601sequence is cloned in pWM530-177-12. The pWM530 vector map is shown in Figure 2.4.5.2A. A Single colony of DH5α transformed with this vector is inoculated in 50ml LB for overnight culture from a freshly transformed plate. 50ml of the primary culture is then transferred into the 750ml of 675ml of SOB (108g of tryptone, 216g yeast extract and 36ml of glycerol for 9lts of SOB), 75ml of phosphate buffer (20.79g of KH_2PO4 147.8g of and $K_2HPO4.3H_20$ (1:10), amp concentration 100ug/ml, incubated at 37℃ for 4-5h, and then incubated the culture at 42 ℃, for about 12-13h. The bacterial culture is pelleted in falcons by centrifugation at 4000 rpm for 30mins at 4°C. The pellet was resuspended in 30ml of cold S1 (25mM Tris pH 8.0, 50mM Glucose and 10mM EDTA pH 8.0) added to each bottle and transferred to large bottles and vortexed to form a uniform suspension. 120ml of fresh S2 (0.2M NaOH and 1% SDS) is then added, mixed gently at room temperature for 5-10mins, to obtain the clarified transparent highly viscous the solution. 210ml of cold S3 (potassium acetate solution pH 5.2) is then added and mixed to make a homogeneous suspension, and incubated on ice for 10mins. The suspension is then centrifuged at 4℃ at 4000rpm for 30min. The supernatant is carefully discarded following 4 layers of gauze filtration to remove suspended impurities and then transferred to 4L Beaker (about 2.4L). The Plasmid DNA is then recovered by adding 0.52 times the volume of isopropyl alcohol (about 1.2L), mixed evenly, and kept at room temperature for 15min. For precipitating the DNA, it is then centrifuged at 15000gx15min followed by 70% ethanol wash at 15000gx10min at 4 ℃. The DNA is then subjected to overnight

restriction enzyme digestion by EcoRV in 100ml of TE (10mM/50mM of TE with 100ug/ml of RNase) at 37°C followed by PEG precipitation (added 1/5 volume of 4M NaCl,2/5 volume of 40% PEG 6000) to remove RNA at 37 ℃ for 5min, and then kept on ice for 30min. It is then centrifuged at 4℃ at 20000gx15min, the supernatant (containing RNA) is discarded followed by 70% ethanol wash and dissolving the precipitate in the 50ml TE. The protein contamination and peg were removed by phenol: Chloroform (1/5 volume) (1:1) extraction at 20℃ at 20000gx10min twice collecting the aqueous phase. DNA extraction was carried out by Chloroform: isoamyl alcohol (1/5 volume) at 20 ℃ at 20000gx10min, collecting the upper aqueous phase. The DNA was obtained after overnight precipitation by 1/10 volumes of 3M NaAc pH5.2 and 2.5 times volume of ethanol followed by 70% ethanol wash and dissolved in TE. The EcoRV digested plasmid DNA was then checked on 1% agarose gel showing several fragments (Figure 2.4.5.2C). The 177-12 fragment can be easily purified from digested vector through different percentages of PEG (5.5%, 6%, 6.5%, 7% and 7.5% of PEG were used) solutions containing 100mM NaCl were used for precipitation or gel extraction. The samples were mixed at 37°C for 5mins and then for 30mins on ice and spun at 4°C at 20000g for 25mins, following which the PEG contamination was removed and DNA was collected by ethanol precipitation. The quality of the DNA for each of the PEG% was checked in 1% agarose gel and the % of PEG which contains only the larger fragment of 177×12bp was then used to precipitate DNA from a larger culture volume (Figure 2.4.5.2D). The sequence of the larger fragment containing the 177×12bp is shown in Figure 2.4.5.2B.

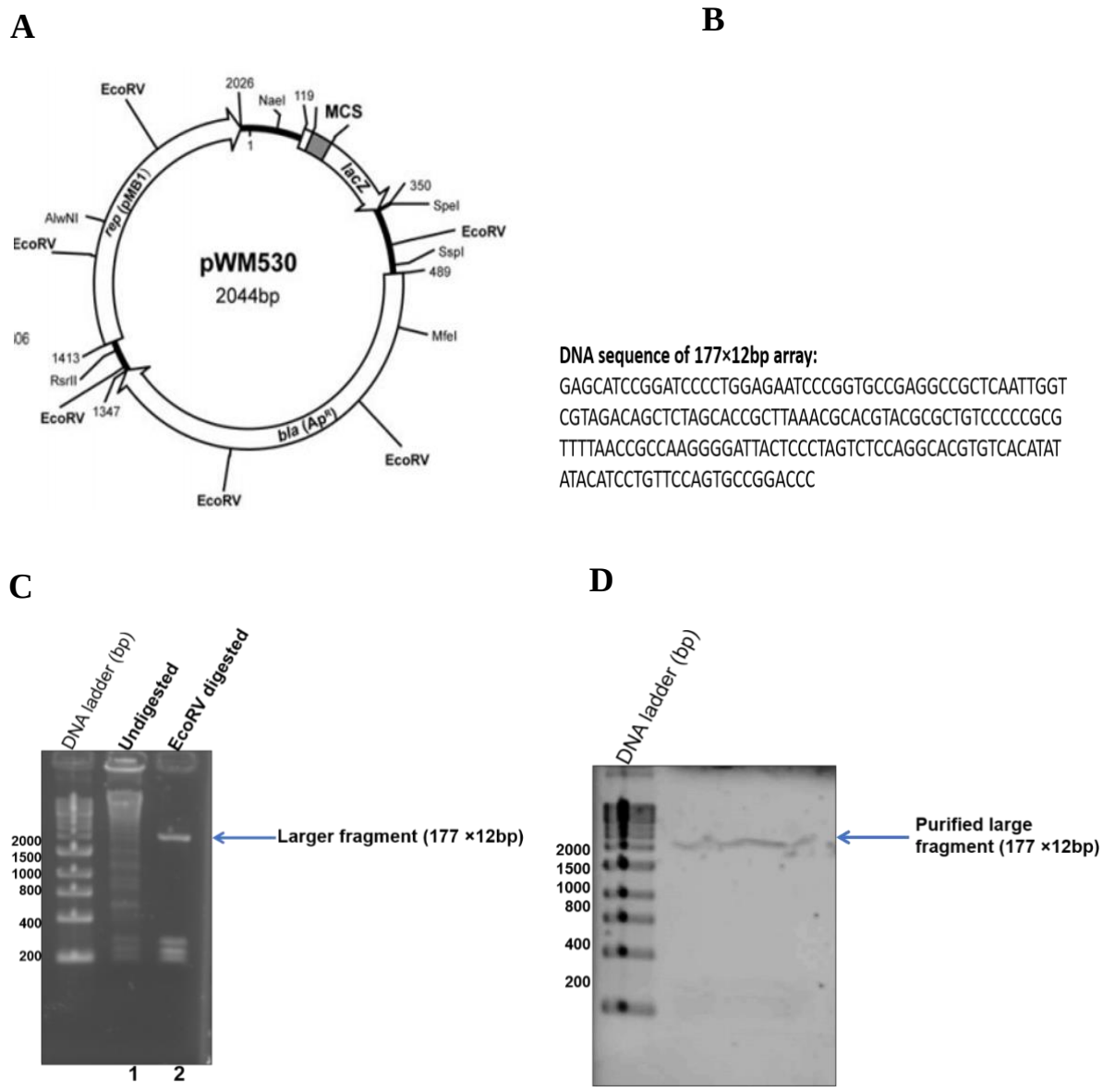

Figure 2.4.5.2: (A) The vector map of pWM530 plasmid. (B) The sequence of 177×12bp array used for nucleosome reconstitution. (c) EcoRV digested pWM530 plasmid where the large fragment corresponding to 177×12bp array has been indicated by the blue arrow. (D) The profile of EcoRV digested pWM530 plasmid after precipitation in the desired % of PEG containing only the purified large fragment of 177×12bp DNA array (indicated by the blue arrow).

2.4.5.3Nucleosome assembly

The Nucleosome array reconstitution is achieved by mixing histone octamers and array DNA in the ratio of 1:2 (which can be modified depending on the volume

of the assembly being set up) in high salt buffer (2M NaCl) and slowly lowering the concentration of NaCl to 0.6M by pump dialysis (Figure 2.4.5.3A). The histone octamers are mixed with the DNA in TE buffer with final salt concentration of 2M NaCl which is then added into dialysis tube (Novagen, D-TubeTM-MWCO 6-8KDa) and the dialysed the mix in 1xTE with 2M NaCl buffer at 4℃. Then add the TE buffer using peristaltic pump into the dialysis buffer to decrease the salt concentration to 0.6M NaCl for 17hours. Following this, the dialysis tubes containing the nucleosome is kept in HEPES EDTA (HE) buffer pH 8.0 for 3hours at 4℃. Following this, the concentration of the nucleosome is measured at A260nm in the nanodrop and A260/280 ratio should be ˜ 1.8. The nucleosome is stored at 4℃ for further processing by EM imaging or compaction experiments. The schematic for nucleosome array reconstitution has been shown in the figure 2.4.5.3B. The nucleosome array is visualized by EM after reconstitution (Fig.2.4.5.3 C).

A

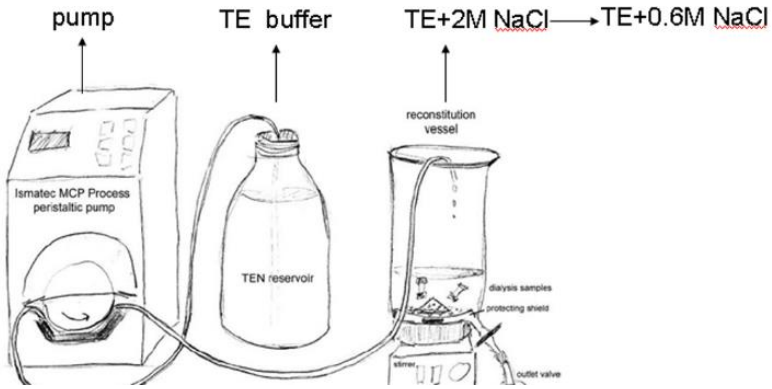
pump
TE buffer
TE+2M NaCl
TE+0.6M NaCl
reconstitution vessel
Ismatec MCP Process peristaltic pump
TEN reservoir
dialysis samples
protecting shield
stirrer
outlet valve

B

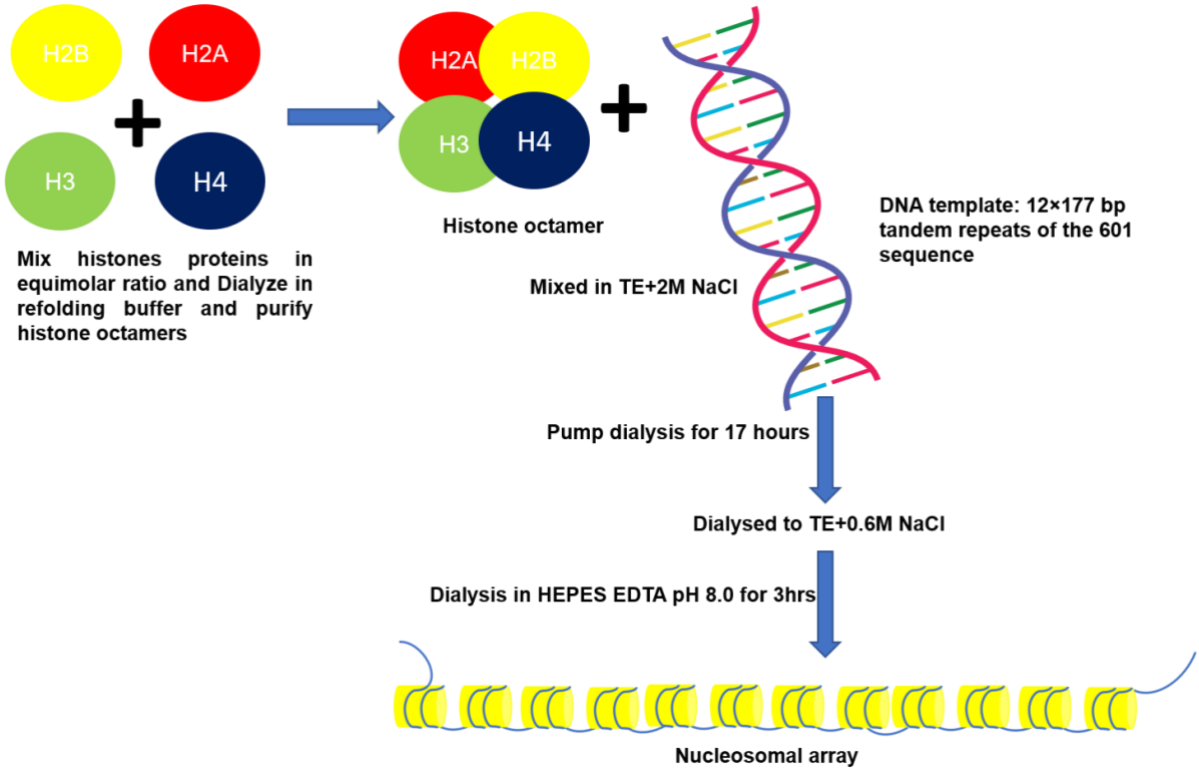
H2B
H2A
H3
H4
Mix histones proteins in equimolar ratio and Dialyze in refolding buffer and purify histone octamers
H2A
H2B
H3
H4
Histone octamer
Mixed in TE+2M NaCl
DNA template: 12×177 bp tandem repeats of the 601 sequence
Pump dialysis for 17 hours
Dialysed to TE+0.6M NaCl
Dialysis in HEPES EDTA pH 8.0 for 3hrs
Nucleosomal array

C

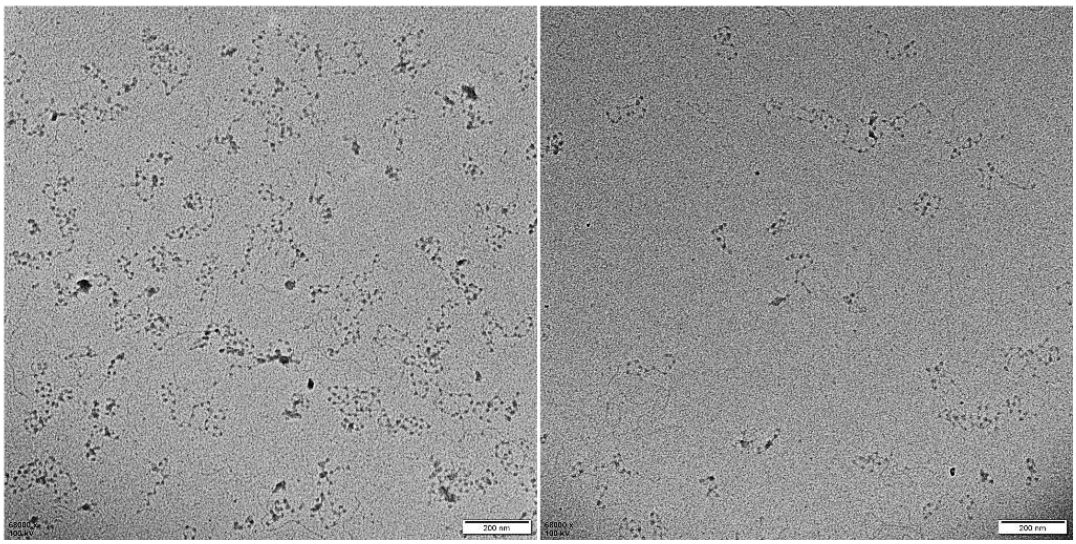

Figure 2.4.5.3: (A)The setup for the nucleosome assembly showing the gradual dialysis of the DNA-octamer mix inside the dialysis tubes from the 2M NaCl salt to 0.6M NaCl in 1X TE with the help of the peristaltic pump for 17hours. (B) The schematic showing *in vitro* reconstitution of nucleosomal array. (C) The EM image of nucleosomal array after metal shadowing of nucleosomal DNA. Scale bar represents 200nm.

2.4.6 Compaction of *in vitro* reconstituted nucleosome by protein

The *in vitro* reconstituted nucleosome was incubated with different concentration of PC4 and Phosphomimic PC4 on ice after dialysis in HE buffer, pH 8.0 but for H1 mediated compaction, linker H1 was added in 0.6M NaCl in 1XTE buffer for 3hrs (since H1 could not compact efficiently in HE buffer) then followed by dialysis in HE buffer. The sub optimal stoichiometric ratios of linker H1 to nucleosome core particle (NCP) was chosen for complementation experiments with PC4 and Phosphomimic-PC4. The schematic showing Compaction of *in vitro* reconstituted nucleosome by protein which is then subjected to sedimentation velocity analysis and EM imaging.

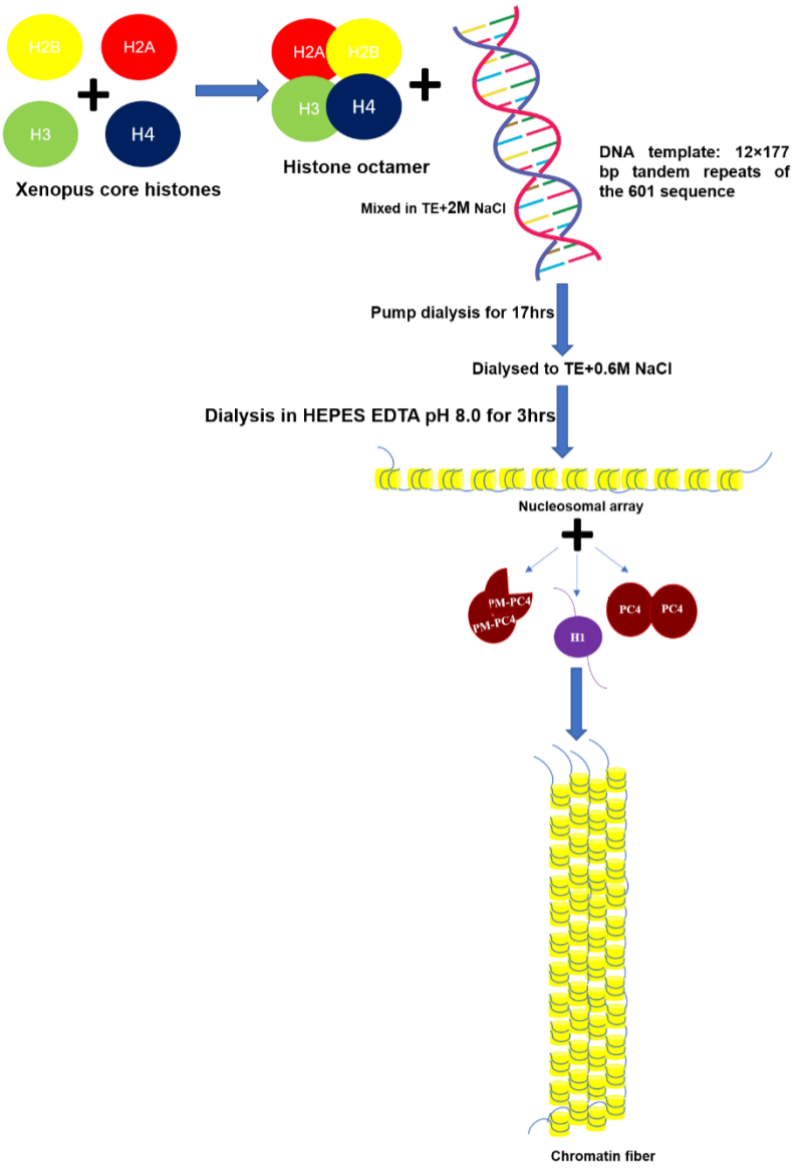

Figure 2.4.6: The schematic showing Compaction of *in vitro* reconstituted nucleosome by protein.

2.4.6.1 Sedimentation velocity analysis by Analytical ultracentrifugation

To study the compaction of the nucleosome by proteins the most accurate way to calculate the sedimentation coefficient values of the samples in an analytical ultracentrifuge where the sample being spun was monitored in real time through an optical detection system, using ultraviolet light absorption and/or interference optical refractive index sensitive system. This allowed us to observe the evolution

of the sample concentration versus the axis of rotation profile as a result of the applied centrifugal field. To study and compare the compaction ability of wild type and phosphomimic PC4, the nucleosome (20ug of DNA for each sample) was incubated with equal amount (in uM) of each of the protein keeping the salt concentration same with BC100 and making up the volume up to 400ul by adding HE buffer for the AUC for 3-4hours. Before the AUC the absorbance of the samples was checked in the nanodrop; the absorbance of the samples should optimally be in the range of 0.3-0.9 OD measured against the HE buffer being used as blank which is also used in AUC for each sample so that the absorbance of detector is not "wasted" on background absorbance from the buffer or do not contribute to the absorbance at the wavelength selected for measurement. Because of the imprecision of the monochromator, the wavelength cannot be changed during the experiment in the XLA/XLI instruments and if several samples are to be measured at different concentrations, they still must be measured at the same wavelength. This may require that samples to be sorted by absorbance and to be run separately, each set at a different wavelength. The samples are added into the left cabinet of the cell and the volume is always taken little lesser than the buffer which is added in the right cabinet of the cell. The cells are tightly sealed using copper screws and place in the rotor along with a balance that determines the radius r of the rotor. Initially a wavelength scan was run on the sample and buffer from 220-300 nm at 3000rpm to ensure that the absorbance is appropriate for all the samples and there is no leakage to assure optimal data collection. Sedimentation experiments were performed on a Beckman Coulter Proteome Lab XL-I using a 4-hole An-60Ti rotor. Samples with an initial absorbance at 260 nm of approximately 0.3-0.9 were equilibrated for 2 h at 20ºC under a vacuum in a centrifuge prior to sedimentation. The absorbance at 260 nm was measured using a continuous scan mode during sedimentation at 32,000×g in 12 mm double-sector cells. The data was analysed using enhanced van Holde-Weischet analysis and Ultrascan II 9.9 revision 1504. The S_w20 values

(sedimentation coefficient corrected for water at 20ºC) were calculated with a partial specific volume of 0.622 ml/g for chromatin, and the buffer density and viscosity were adjusted. The average sedimentation Save coefficients were determined at the boundary midpoint (S50).

2.4.6.2 Electron Microscopy

2.4.6.2.1 Metal shadowing

For Electron microscopy (EM) imaging visualising nucleosomal array the nucleosomal array is prepared for metal shadowing for which the sample is fixed in 0.4% glutaraldehyde for 30 min on ice and 1x spermidine is added before loading the sample on to Copper grids and incubated for 2mins blotted and washed in water and alcohol gradient and dried. The copper grid is then placed on a glass slide for metal shadowing using a tungsten filament under a vacuum with 0.2×10-5 torr pressure at low voltage and 15-18amp current for 15mins in rotating condition. This allows spraying of a coat of a heavy metal (such as tungsten) at an oblique angle making the surface of a specimen visible. This technique creates a three-dimensional view of the nucleosomal DNA with the DNA itself appearing darker during EM imaging. The grids were transferred into a FEI Titan Krios electron microscope (FEI, Eindhoven).

2.4.6.2.2 Negative staining

The reconstituted chromatin samples were negatively stained for which they are chemically fixed in 0.2% glutaraldehyde for 30 min on ice. After fixation, the chromatin sample was absorbed onto the glow-discharged 300 mesh R2/1 Quantifoil (Quantifoil Micro Tools GmbH, Jena, Germany) holey grids for 1 to 1.5 min, blotted using 4 s blotting time at 100% humidity and stained with uranyl sulfate to stain the protein white against a black background for 45seconds, blotted and dried for 1minute before imaging.

2.4.7 Dot Blot assay

The specificity of the PC4K26,28ac antibody was checked by dot blot where increasing doses of the unconjugated acetylated peptide was spotted at equally spaced circles on a nitrocelluose membrane along with the umodified protein at the highest concentration. The blot is allowed dry for 10mins on an aluminium foil after spotting of the peptides followed by blocking in 2.5% skimmed milk solution for 1hour and then incubated with PC4K26-28ac antibody for a period of 8-12 hrs at 4°C depending on the affinity of the antibody. Further, after subjecting to washing with 1X PBS or PBST (PBS with 0.1% Tween 20), appropriate HRP conjugated secondary antibody solution was added and incubated for 1hr at room temperature, after which the blots were washed once again as mentioned earlier. The signal from expected protein of interest was developed using the Biorad Clarity chemiluminescence kit, as per the manufacturer's protocol. The blots were exposed in TMS (Kodak X-Ray films), for different time points and developed using GBX-Developer-Fixer Kit (Premiere Kodak reagents) or by using Biorad Chemidoc system.

2.4.8 Isothermal calorimetry

Isothermal titration calorimetry(ITC) measurements were taken using a MicroCal ITC200 instrument (MicroCal, Inc.). Aliquots (2 μL) of Linker H1.1 at a concentration of 21 μM were injected from the syringe into the cell of 240 μL filled with 2 μM of phosphoPC4 or mock-phospho PC4. Titrations were conducted in 20 mM Tris-HCl (pH 7.5), 0.2 mM EDTA, and 100 mM KCl buffer. To minimize the contribution of dilution to binding heat, the protein solutions were dialyzed against the same buffer prior to the ITC experiments. Injections weremade at intervals of 120s, and the duration of each injection was 0.4 s. To ensure proper mixing after each injection, a constant stirring speed of 1000 rpmwas maintained during the experiment. The control experiment was

performed via injection of buffer in the ITC cell containing H1.1. All molarity calculations of PC4 were conducted according to its reported molecular mass 14.395 kDa while H1 was taken as a monomer. The heat change versus the molar ratio of the titrated products was plotted and analyzed using the origin7 software, which yielded the stoichiometry (n, in terms of the number of molecules of H1 per phospho-PC4 or mock phospho-PC4) and the dissociation constant (Kd).

2.5 Protocols for different *in vivo* assays

2.5.1 Active chromatin and heterochromatin isolation

40×10^6 Hela cells harvested washed in PBS collected by centrifugation at 400*g* for 5 min at 4°C. The cells were resuspended in Buffer A with 0.1% (v/v) NP-40, 1mM DTT and PIC (proteinase inhibitor cocktail), and sit the tube on ice for 10min. The nuclei are centrifuged at 500xg for 3min at 4°C. The supernatant is discarded and nuclei is washed by Buffer A with 1mM DTT at 1x10^7 nuclei/ml for once. The nuclei are resuspended at 1x10^7 nuclei/ml in Buffer A with 0.01 U/ml MNase*, 1 mM DTT and PIC;). The digestion is stopped by 0.01M EDTA, and then NaCl is added to 0.2M. 50μg/ml RNase A is added and incubated at 37°C for 1 hr. 100μg/ml Proteinase K and 1%SDS is then added and incubated at 55°C for 2 hrs. Extract twice with equal volume of phenol/chloroform/isoamylalcohol (25:24:1) and once with chloroform/isoamylalcohol (24:1). 50μg Glycogen or LPA (linear polyacrylamide, from 5 mg/ml stock), 10%V/V 3M Na-acetate (PH5.2) and 2.5V pre-cooled EtOH is added to precipitate the DNA, placed at -80°C for 20min; Centrifuge tubes for 10min at maximum speed in a microcentrifuge to pellet the DNA. Decant the supernatant and resuspend the pellet in 1ml 75% Ethanol. Centrifuge tubes for 5 min at maximum speed in a microcentrifuge to pellet the DNA. Repeat the wash once. Decant supernatant and air-dry the DNA pellet for 2min. Resuspend the DNA pellet in 50μl of TE. Place at 37°C for 1 hr to dissolve the DNA completely. 1ug of each sample is run on a 1% Agarose. The remaining

nuclei resuspended in TEEP20 buffer (10 mM Tris-HCl [pH 8.0],1 mM EDTA, 1 mM EGTA, 250 M PMSF, 20 mM NaCl), incubated at 4degrees overnight. Nuclear debris was removed by centrifugation leaving soluble chromatin in the supernatant. Soluble chromatin layered on 5-40% discontinuous sucrose gradient in 13.2ml ultracentrifuge tube and spin at 34000 rpm for 5hrs (the rotor could not reach 41000 rpm so set at lower rpm for longer time). 500ul fractions were collected from the gradient by upward displacement and the DNA was purified from part of those fractions by SDS/proteinase K digestion, phenol-chloroform extraction, and ethanol precipitation. The DNA from each of the fractions were loaded onto 1% agarose gel and the remaining part of the corresponding fractions were used for western.

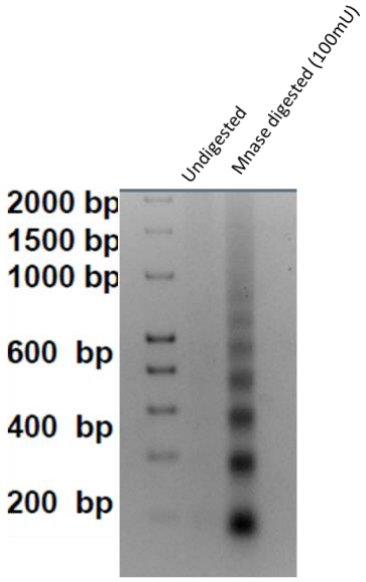

Figure 2.5.1: MNase digestion pattern of the chromatin from HEK293 cells using 100mU of MNase enzyme before sucrose gradient fractionation.

2.5.2 Nuclear fractionation

293 cells were collected from two100-mm plates at two different stages mitotic phase (G2/M arrest) and in the interphase stage and washed with 2 ml of cold 1x PBS (plus PI). Mitotic block was performed by addition of 2mM thymidine for

24 hrs, followed by washing twice with 1X PBS and releasing in DMEM containing 10%FBS for 3hrs. 100ng/ml of nocodazole was finally added for 12 hrs to block the cells in prometaphase following which they were harvested. The cell pellet (0.4 ml) was resuspended in 1 ml buffer A (0.3 M sucrose, 60 mM KCl, 60 mM Tris-HCl, pH 8.0, 2 mM EDTA, and 0.4% NP-40 plus PI) and incubated on ice for 5 min, followed by a five minutes spin at 2,000 rcf at 4°C. 0.8 ml of the cytosolic fraction was collected. After one wash with buffer A, the nuclei (0.2 ml) were resuspended in 0.5 ml of 100 mM NaCl-containing mRIPA (6 strokes in a 7-ml Dounce homogenizer) and spun at 6,000 rcf for 5 min. The supernatant was designated as nuclear extract (100 mM). The pellet was similarly resuspended in 2x pellet volume of mRIPA with 1M NaCl concentrations and separated the pellet and supernatant fraction for Western blotting analysis. Both supernatant and the pellet fraction for mitotic and interphase stage were loaded along with cytosolic phase probing with cytosolic markers like tubulin, nuclear markers like histones. The acetylation levels of PC4 was studied by probing with PC4K26-28ac antibody.

2.5.3 Micrococcal Nuclease (MNase) assay

Respective Flag-PC4, Flag-PM-PC4 and Flag-MTP5 cells were grown in DMEM medium supplemented with 10% fetal Bovine serum (FBS). The nuclei were prepared from packed cells suspended in hypotonic buffer (10mM Tris HCL, 10mM KCL and 15mM $MgCl_2$) followed by 10 min incubation at 4C. The nuclei were digested with MNase (0.2U/µL) for different time points at room temperature in nuclei digestion buffer (10% glycerol, 10mM Tris-HCLpH-8, 3mM $CaCl_2$, 150mM NaCl, 0.2mM PMSF). MNase digestion was stopped by the addition of 10mM EDTA and proteinase K at 37degrees for 30mins followed by RNase A treatment for 1hr at 37degress. The DNA is then extracted by phenol chloroform extraction and ethanol precipitation. 1ug of each of the samples were loaded on 1% agarose gel and ran for 4-5 hours in an EtBr free agarose gel

electrophoresis system at 50volts for better resolution of the MNase bands. Figure 2.5.3 shows the standardisation of MNase assay at different time points of MNase digestion and using different concentrations of MNase enzyme for digestion (# M0247S, NEB).

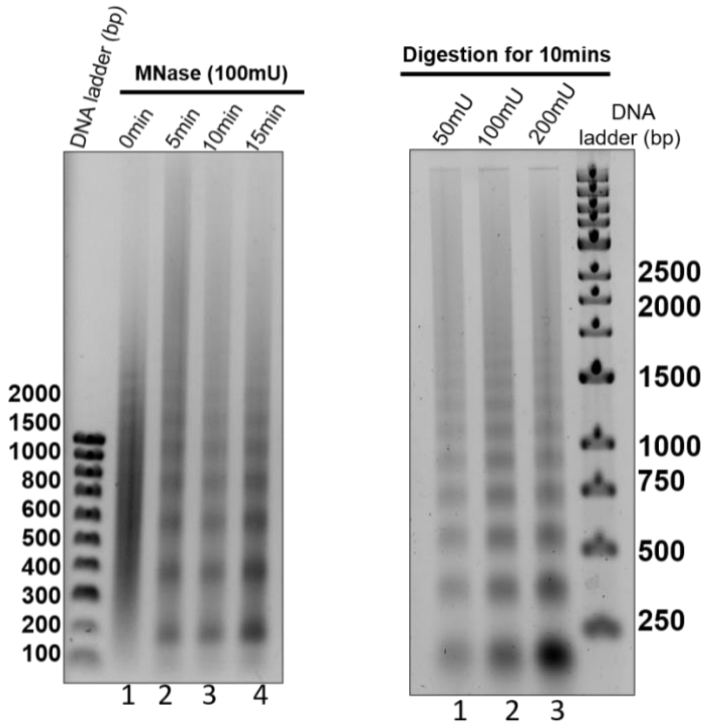

Figure 2.5.3: MNase digestion pattern of the chromatin from HEK293 cells using 100mU of MNase enzyme for different time points (0,5,10 and 15mins; Lane 1-4 respectively) in the left panel. MNase digestion pattern of chromatin from HEK293 cells upon digestion with different units of MNase enyme (50mU,100mU and 200mU from lane 1-3 respectively) for 10 mins in the right panel.

2.5.4 Chromatin immunoprecipitation assay (ChIP)

HeLaS3 cancer cells were grown in Dulbecco modified Eagle medium and 10% foetal bovine serum up to 90% confluency. Cells were cross-linked using 1% formaldehyde followed by cell lysis in SDS lysis buffer (1% SDS, 10mM EDTA, 50mM Tris–HCl, pH 8.0). Chromatin was sonicated six times for 10 s at 91%

power setting. Following sonication, the pulldowns for ChIP assays were performed with anti-AcPC4 antibody (lab raised and purified) diluted in cold dilution buffer (0.01% SDS, 1.1% Triton X-100,1.2mMEDTA, 16.7mMTris–HCl, pH 8.0, 167mM NaCl) at 4 °C overnight. Furthermore, pre-blocked protein G-Sepharose (Amersham Pharmacia) was added for binding for 2-3 hours at 4 °C. Beads were washed thrice with low-salt buffer (0.1% SDS, 1% TritonX-100, 2 mM EDTA, 20mM Tris–HCl, pH 8.0, 150mM NaCl) followed by three times high salt buffer (0.1% SDS, 1% Triton X-100, 2 mM EDTA, 20mM Tris–HCl, pH 8.0, 500mM NaCl), LiCl buffer (250mM LiCl, 1% NP40, 1% NaDOC, 1mM EDTA, 10 mM Tris–HCl, pH 8.0) and TE (10 mM Tris–HCl, pH 8.0, 1 mM EDTA) wash. Elution buffer (0.2%SDS, 100 mM NaHCO3) along with 200 mM NaCl was added to the washed beads, and the bead solution was kept for 6-8hours at 65 °C. Pulldowns were deproteinized using 0.1 mg/ml of proteinase K (Sigma) and 0.04 mg/ml of RNase A (Sigma) were added to the bead solution and the mixture was incubated for 2 h at 37°C. The immunoprecipitated samples were ethanol precipitated and used for ChIP-PCR analysis using primers for some the selected PC4 target gene promoters and non-specific region of the genome as negative controls to check for the AcPC4 binding to these genomic regions.

The details of the ChIP primers used are stated in the table below:

Gene Name	**Primer Name**	**Forward Primer (5'-3')**	**Reverse Primer (5'-3)**
PLK1	Site 1	GGAGAAACCCCGAAGGAAT	GGGAAAACCTGATTGACACG
PLK1	Site 2	GCCTTTGCGGTTCTAACAAG	AAGCTCCTGCGGTTCACTT
C-MYC	Site 1	CCAACAAATGCAATGGGAGT	GGAGGAAAACGATGCCTAGA
C-MYC	Site 2	CAGGAGGGGCGGTATCTG	TGTATTATGCATTATGTATGCACAGC
BUB1B	Site 1	GCCATTGAATCCCAAAAACT	CTCCGTGCTCTCGCGTCT
BUB1B	Site 2	CCCAACACTCAAAACAGCAA	AGCAGGCTTAGGCAAAACA
NEGATIVE CONTROL	Site 1	ACAGGAGTAGGCTACCTCAAA	ACTCAGAGCAAGGAGAGTACTAA
NEGATIVE CONTROL	Site 2	GGGAGTGGTATGATCTCGATTT	CAAATTGGTGATATATCCACAGAGA

Table 2.5.24: List of primer sequences used for ChIP.

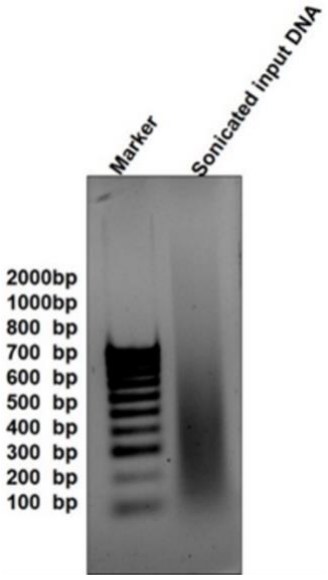

Figure 2.5.4: The sonication condition generated the ChIP DNA in the region of 200-500bp which is a standard size of the DNA fragment required for the ChIP analysis.

2.5.5 Indirect Immunocytochemistry

Mammalian cells were cultured on 0.1% poly-L-lysine coated coverslips in sterilized culture dishes and transfected with the various mammalian expression constructs (as mentioned earlier) and allowed to grow further till the point of collection as per the experimental requirements. At the end point, cells on the coverslips were rinsed with 1X PBS and fixed in 2-4% paraformaldehyde for 15 minutes. Subsequently the monolayer was washed thrice with 1X PBS and permeabilized with 0.1% Triton X-100 for 5 minutes. Once permeabilized, cells were blocked with 5% FBS at 37ºC for 30 mins, after which the cells were incubated with the primary antibody for 1hr under constant mixing conditions on a gel rocker. The cells were then washed thrice with 1X PBS and appropriate Alexa Fluor conjugated secondary antibodies were added in 1% FBS solution in 1:500-1:1000 dilution and incubated for 30 min in dark. The cells were then washed thrice with 1X PBS and stained with Hoechst dye (4µg/ml in 1X PBS) for 20 minutes to visualize the DNA. The coverslips were then mounted over grease free glass slides using 70% glycerol. Confocal microscopic images of immuno-stained cells were captured using Zeiss LSM Meta 510.

2.5.6 Fluorescence activated cell sorting (FACS)

2.5.6.1 Cell cycle analysis by FACS

HEK 293 cells were synchronized at different cell cycle stages (the details of treatment for cell synchronization are given later) which are given later and Propidium Iodide (PI) staining was done. Briefly, cells were harvested by mild

trypsinization (0.25%) followed by centrifugation at 2000 rpm for 10 mins at 4°C. Cells were washed with cold PBS by centrifugation at 2000 rpm for 10 mins at 4°C. Cells were fixed in cold 70% Ethanol which was added dropwise along with mild vortexing. Samples were left for 12 hours or more at -20°C, after which Ethanol was removed followed by two washes in cold PBS. RNase (100 µg/ml) treatment was subsequently given at 37°C for 30 mins to ensure only DNA staining. 50µg/ml propidium iodide was added for staining. For cell cycle analysis singlet population of cells were gated from the scatter plot and the peak intensity was measured depending on the DNA content and taking asynchronous cells as control the scatter plot was plotted for each cell cycle stage.

2.5.6.2 Cell sorting by FACS

For generation of PC4 knockdown stable cell line, HEK293 were transduced with pGIPZ vector containing the sh8 clone. The infected cells were sorted using FACS Aria III on the basis of GFP expression (Figure 2.6.3.3.1 A). For proper gating of the samples atleast 10000 events are needed. HEK293 without any GFP vector was taken as a control for proper gating (P1) of GFP+ve cells from the GFP-ve cells. Among the GFP+ve cells further gating was done to sort out only the high GFP+ve cells (P2 population in figure 2.6.3.3.1 A).

2.5.7 Hematoxylin and Eosin (H&E) staining

Paraffin blocks containing the samples were sectioned with each section measuring a thickness of 5µm. The sections were placed on hot water to stretch adequately and collected over clean glass slides coated with silane. They were fixed to the slide by incubating overnight at 40°C and for 2 hours at 60°C prior staining. The slides were serially processed in xylene, 100% ethanol and distilled water for two changes of five minutes each. They were stained with hematoxylin diluted in water at a ratio of 1:1 for seven minutes. Excess stain was washed off under running water and then stained with eosin for five minutes. Excess eosin

was removed by dipping the slides in water and serially treated with 70% ethanol, 100% ethanol and Xylene for 1-2 minutes each. The slides were dried and mounted with cover slip. Images of normal and tumor regions were taken to mark the region containing cells.

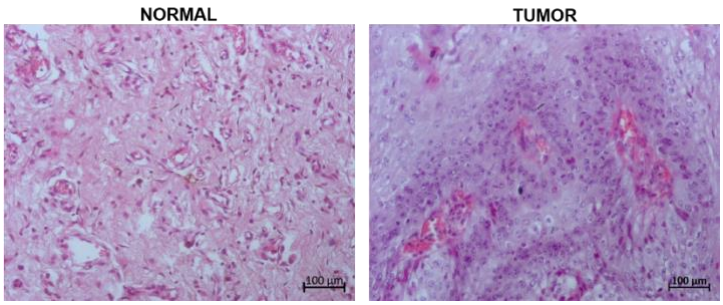

Figure 2.5.7: Hematoxylin and Eosin staining of a pair of tumor and adjacent normal tissue from an oral cancer patient.

2.5.8 Immunohistochemistry

The oral cancer patient samples used in the study were collected from Sri Devaraj Urs Academy of Higher Education and Research (SDUAHER) after obtaining Bioethics clearances from both institutes (SDUAHER and JNCASR). The samples were collected with prior consent from the patients. The tumor and adjacent normal tissue (2 cm away from the resected tumor margin) samples were fixed in 10% formalin for 24–48 h. The tissue samples were dehydrated and embedded in paraffin blocks. 5µm sections of the samples were made using a microtome (Leica, Germany). The tissue samples were stained with hematoxylin and counterstained with eosin. The regions with a higher density of cells were marked and those regions where punctured from the tissue blocks with a 1mm puncturing tool. The 1mm sections were placed onto a tissue microarray precast block. 5µm sections were placed on silane-coated slides. The paraffin was then removed in xylene, followed by dehydration of the samples in 100% alcohol and rehydration in water. Epitope retrieval was done in sodium citrate buffer by boiling for 10 min followed by incubation in 0.9% H2O2 in methanol for 15 min.

The samples were blocked in 5% skimmed milk for 45 min and probed with primary antibody of interest. The Strept-Avidin Biotin (biotinylated secondary antibodies (anti-rabbit+anti-mouse) and HRP-conjugated streptavidin) kit from Abcam, was used. The immuno-reactivity of the antigen was measured by the intensity of the brown precipitate formed in the presence of the chromogen diaminobenzidine tetrahydrochloride (Sigma Aldrich, USA) followed by counterstaining with hematoxylin. The staining was examined and imaged. Semi-quantitative analysis of the staining (H-scoring) was performed by assigning values between 0 and 3 (0=no stain to 3=strong stain) per cell in a field (3 fields per sample) using the ImageJ add-on IHC profiler (Varghese F., et al., 2014). H-score is calculated by the following formula: H-score= 0x% cells with no stain+1x% cells (low stain) +2x% cells (moderate stain) +3x% cells (strong stain), which can range from 0 to 300. Therefore, higher the H-score corresponds to higher levels of protein. Mann-Whitney Test was used for statistical analysis.

2.5.9 Immuno-pulldown

2.5.9.1 M2 agarose pull down to study interacting partners

To study the association of Flag-PC4, Flag-Phosphomimic PC4 (Flag-PM-PC4) and Flag-phospho-defective mutant (Flag-MTP5) with chromatin protein linker H1 in HEK293 PC4 knockdown cells, or Flag-PC4K26-28R, Flag-PC4 and Flag-PC4 acetylation mimic with RNA pol II or GTFs or p53, the individual Flag fusion constructs were stably transfected; cells were harvested and washed once with 1X PBS and lysed by adding 1ml of chilled lysis buffer (50 mM Tris-HCl, pH 7.4; 150 mM NaCl; 5 mM EDTA; 1% triton X-100; 1X-Complete protease inhibitor). Cells were incubated at 4ºC for 1hr with constant mixing. Lysate was clarified by centrifuging at 13,000 rpm at 4°C for 10 mins and incubated with 30µl of anti-Flag M2 agarose beads (pre-washed and equilibrated in lysis buffer; Sigma # F2426) for 3hrs at 4ºC with uniform mixing. The beads were collected by centrifugation for 3mins at 2,000 rpm at 4ºC and the supernatants were

removed by aspiration. The pellets were washed once with 1 ml of cold lysis buffer, twice with tris buffered saline (TBS; 50 mM tris-HCl, pH 7.4; 150 mM NaCl) and eluted in 30µl of 500ng/µl of 3X-FLAG peptide (Sigma#F4799) in TBS buffer. The immunoprecipitated samples were then resolved in a 12% SDS-PAGE and immunoblot analysis was done for verifying the pulldown protein and their interacting partners.

2.5.9.2 M2 agarose pull down from chromatin fraction

To study the association of Flag-PC4, Flag-Phosphomimic PC4 (Flag-PM-PC4) and Flag-phospho-defective mutant (Flag-MTP5) with core histones in HEK293 PC4 knockdown cells. Cells were collected from two 100-mm plates and washed with 2 ml of cold 1x PBS (plus PI). The cell pellet (0.4 ml) was resuspended in 1 ml buffer A (0.3 M sucrose, 60 mM KCl, 60 mM Tris-HCl, pH 8.0, 2 mM EDTA, and 0.5% NP-40 plus PI) and incubated on ice for 5 min, followed by a 5 minutes spin at 2,000 rcf at 4°C. 0.8 ml of the cytosolic fraction was collected. After one wash with buffer A, the nuclei (0.2 ml) were resuspended in 0.5 ml of 100 mM NaCl-containing mRIPA (6 strokes in a 7-ml Dounce homogenizer) and spun at 6,000 rcf for 5 min. The supernatant was designated as nuclear extract (100 mM). The pellet was similarly resuspended in 2x pellet volume of mRIPA with sequentially increased NaCl concentrations (200, 300, 400 and 600 mM) and a ten-minute incubation on ice. The high salt fraction was incubated with 30µl of anti-Flag M2 agarose beads (pre-washed and equilibrated in lysis buffer; Sigma # F2426) for 3hrs at 4ºC with uniform mixing. The beads were collected by centrifugation for 3mins at 2,000 rpm at 4ºC and the supernatants were removed by aspiration. The pellets were washed once with 1 ml of cold lysis buffer, twice with tris buffered saline (TBS; 50 mM tris-HCl, pH 7.4; 150 mM NaCl) and eluted in 30µl of 500ng/µl of 3X-FLAG peptide (Sigma#F4799) in TBS buffer. The immunoprecipitated samples were then resolved in a 15% SDS-PAGE and

immunoblot analysis was done for verifying the pulldown protein and their interacting partners.

2.5.9.3 Pull down using purified PC4K26-28ac and purified PC4 antibody to study interacting partners

Hela cells or oral cancer cells transfected with different constructs were seeded in three 100mm dishes were harvested and lysed in RIPA lysis buffer and the supernatant collected as RIPA lysate was then incubated with IgG purified PC4K26-28ac and PC4 antibody (5ug and 10ug of each antibody) and IgG purified from pre-immune sera for the control pulldown for few minutes before adding protein G sepharose that is pre-equilibrated in RIPA lysis buffer for pulldown in end to end rotor at 4° for 6hours before collecting the beads after washing in 500ul of lysis buffer 3times at 2000 rpm for 3mins and adding 1X SDS-Dye and denaturing at 90degrees before loading onto a SDS-PAGE gel for western blotting.

2.5.10. Cell Synchronization for studying PC4 acetylation across cell cycle

2.5.10.1 G0/G1 block

HEK293 cells or oral cancer cells maintained in DMEM containing 10% FBS, were synchronized at the G0/G1 boundary by serum deprivation for 72hrs at a confluence of 60-70%.

2.5.10.2 G1/S block

Double thymidine block was carried out for synchronization of cells at the G1/S boundary. Briefly, 30-40% confluent HEK293 cells were treated with 2mM Thymidine for 18 hrs (first block). The cells were then released from the block by washing twice with warm 1X PBS and then by addition of DMEM containing

10% FBS. 9hrs post release in complete media, 2mM thymidine was again added to the cells and harvested 17hrs later.

2.5.10.3 G2/M block

Mitotic block was performed by addition of 2mM thymidine for 24 hrs, followed by washing twice with warm 1X PBS and releasing in DMEM containing 10%FBS for 3hrs. 100ng/ml of nocodazole was finally added for 12 hrs to block the cells in prometaphase following which they were harvested.

The cells at each stage were harvested and processed for either FACS analysis (mentioned before) or western blotting to study the levels of PC4 acetylation across different cell cycle stages.

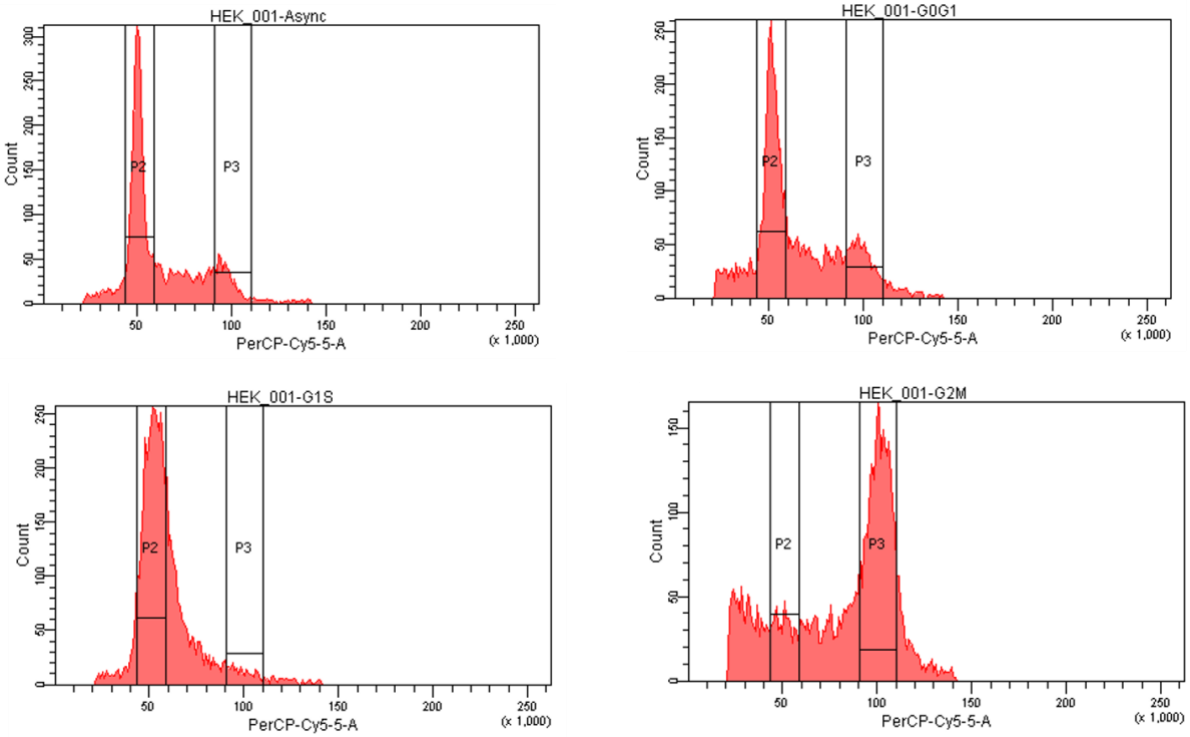

Figure 2.5.10: FACS analysis showing singlet population of cells gated from the scatter plot and the peak intensity measured depending on the DNA content. The peak value of each graph shows that the cells are synchronized at different stages corresponds to the DNA content the respective stage

2.6 Cell Culture

2.6.1 Mammalian cell culture

All mammalian cell lines (Figure 2.6.1), mentioned in the subsequent chapters, were procured from ATCC collection and grown as per the recommendations provided by ATCC guidelines. Briefly, the adherent cells were rinsed once with Dulbecco's phosphate buffered saline (Himedia) and then trypsinized with the prescribed amount of trypsin (Himedia) until the cells detach from the monolayer. Harvested cells were then resuspended in fresh media containing foetal bovine serum (FBS) and then dispensed into the cell culture dishes. These cell lines were grown at 37◦C with 5% CO2 till appropriate confluency is reached. Cells were then treated with various small molecule modulators mentioned in the appropriate text according to the nature of experiment done before harvesting them for further analysis. The culture conditions for each of the cell lines is mentioned in Table 2.6.1.

Serial Number	**Cell line**	**Media+ selection pressure + growth factor requirements**
1	HEK293	DMEM (High glucose) + 10% FBS
2	pGIPZ non silencing vector transduced HEK293 (shNS)	DMEM (High glucose) + 10% FBS
3	pGIPZ PC4 sh8 transduced HEK293 (PC4 KD)	DMEM (High glucose) + 10% FBS+0.02mg/ml Puromycin
4	Flag-constructs transfected HEK293 PC4 KD cells	DMEM (High glucose) + 10% FBS+0.02mg/ml Puromycin + 1mg/ml neomycin
5	HeLa S3	DMEM (High glucose) + 10% FBS
6	HeLa	DMEM (High glucose) + 10% FBS
7	AW13516	DMEM (High glucose) + 10% FBS
8	UMSCC	DMEM (High glucose) + 10% FBS
9	NT8e	DMEM (High glucose) + 10% FBS
10	AW8507	DMEM (High glucose) + 10% FBS
11	Het1a	Bronchial Epithelial Cell Growth Medium

Table 2.6.1: Base media with selection pressure and supplement requirements for various cell lines.

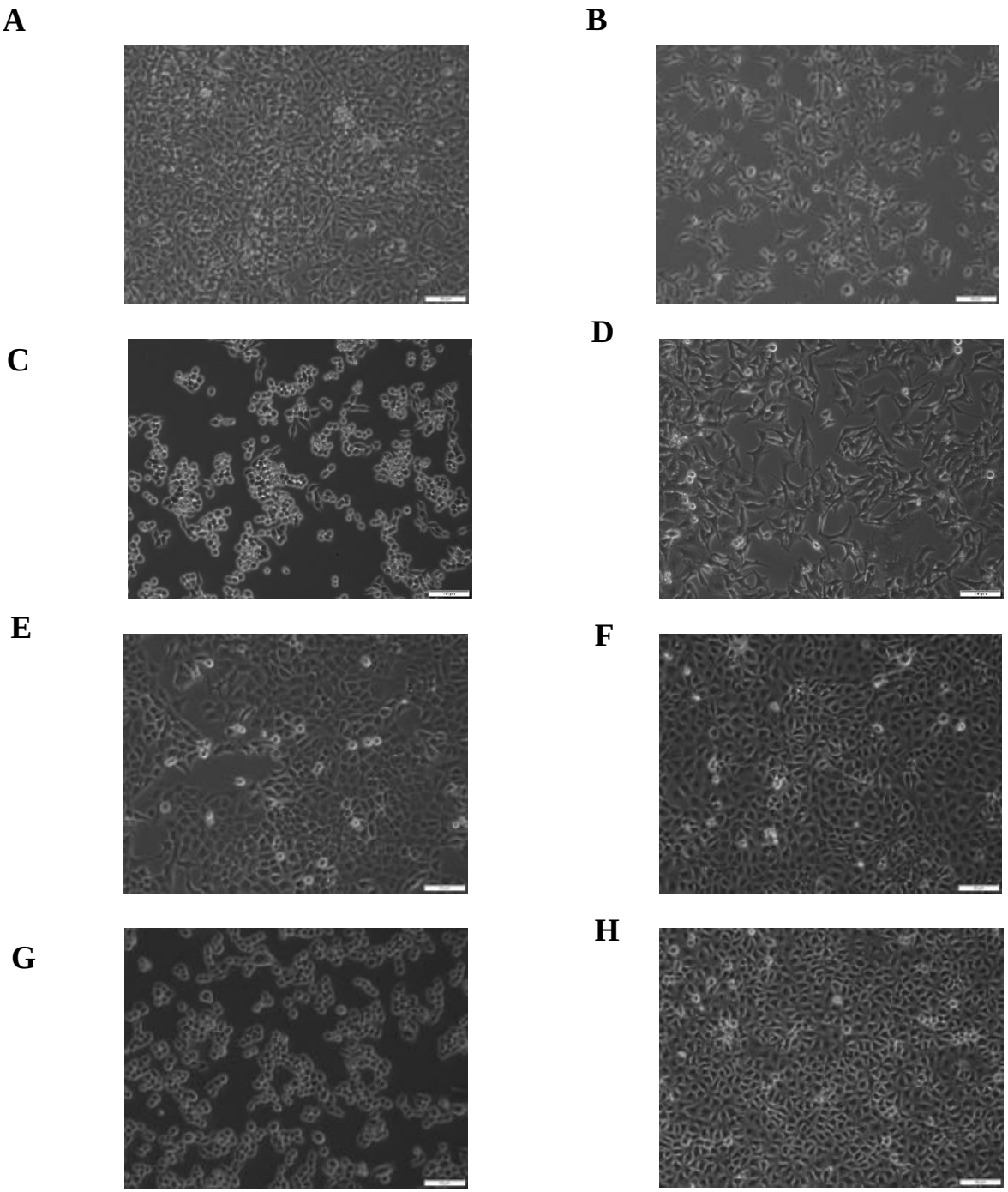

Figure 2.6.1: Morphological features of the mammalian cells, grown in a monolayer- A. shNS HEK293; B. PC4 KDHEK293; C. HelaS3; D. Hela; E. AW8507; F. AW13516; G. UMSCC; H. NT8e; Scale bar represents 50μm.

2.6.2 Insect Cell Culture

The insect ovarian cell line Sf21 from Spodoptera frugiperda (Figure 2.3.2) was procured from Invitrogen. The frozen stock vial was thawed on 37ºC water bath and was diluted ten times with pre-warmed Grace's insect medium (Gibco) supplemented with 0.1% Pluronic acid solution (Invitrogen # F-68), 0.1% yeastolate (Invitrogen), 10µg/ml gentamycin (Invitrogen), 10%FBS and antibiotic (penicillin, streptomycin and amphotericin B) mixture. The cells were seeded in a T25 flask and allowed to adhere to the flask for 45minutes, following which the media was changed to completely remove the DMSO from the cryo-preservation media. The cell further allowed to grow at 27ºC BOD incubator till 70-80% confluence. The spent media was then discarded and 5ml of fresh Grace's complete media, with all the supplements, was added to the flask. The adhered cells were scraped and sub-cultured at 1:3 ratio. The cells were counted using a haemocytometer (Neubauer's Chamber) and seeded in appropriate numbers for infection, as required. For cryopreservation, the cells were harvested after scraping, pelleted down upon centrifuging at 1000 rpm for 3mins, resuspended in freezing mixture (40% Grace's medium, 50% FBS and 10% DMSO) and transferred to cryo-vials (Corning), which were finally frozen slowly inside a cryo-cooler containing isopropanol, at -80ºC for 24hrs, following which the vials were transferred to liquid nitrogen cylinders.

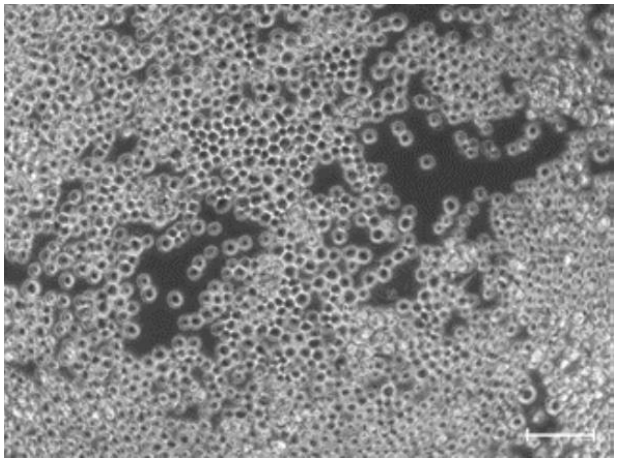

Figure 2.6.2: Morphological features of Sf21 cells, grown in a monolayer. Scale bar represents 100μm.

2.6.3 Mammalian cell Transfection

2.6.3.1 Transfection of Plasmid DNA

Plasmid vectors, competent for expression of various Flag-tagged proteins in mammalian cells, were transfected by using lipofectamine 2000 Plus (Invitrogen). Briefly, the cells were seeded in culture dishes as per the manufacturer's recommendations and allowed to grow till 50-60% confluence. Recommended amount of DNA and the prescribed volume of Lipofectamine 2000 was added to individual microfuge tubes and incubated at room temperature in appropriate volume of the media without serum and antibiotic. After the end of the initial mixture, DNA and Lipofectamine containing media were mixed and allowed to form complexes at room temperature for 15 mins, following which the mixture was added over the monolayer and mixed uniformly by gentle shaking of the culture dishes. 6-8hrs post transfection, the transfected media was discarded and fresh complete media was supplemented to the cells. Cells were harvested at appropriate times post transfection and analysed for various assays by means of western blot analysis or indirect immunofluorescence. Standard amount of DNA for the corresponding cell culture dishes are mentioned in Table

2.6.3.1 and the transfection reagents used for the different cell lines are detailed in Table 2.6.3.2.

Diameter of the Culture Dish	**Amount of DNA transfected**
35mm dish/ 6-well plate	2µg
60mm dish	4ug
100mm dish	10ug

Table 2.6.3.1: Standard DNA amounts transfected for different culture dishes.

The following conditions were maintained for transfection of different cell lines:

Cell Line	**DNA: Transfection Reagent (µg: µl)**
HEK293	1:2 (DNA: Lipofectamine)
HeLa	1:3 (DNA: Lipofectamine)

Table 2.6.3.2: Standard DNA: transfection reagents used for different cell lines.

2.6.3.2. Transfection of siRNA

MDA-MB-231 cells were transfected with either control siRNA (Silencer™ Negative Control No. 1 siRNA; Invitrogen # AM4611) or a heterogeneous mixture of siRNAs that all target the same mRNA sequence of human p300 (EHU155151, MISSION® esiRNA human EP300; esiRNA1, Sigma). Briefly, HEK293 cells were seeded in a 60mm dish format as per the manufacturer's recommendations and allowed to grow till 30% confluence. 10nM of either the control siRNA or the siRNA pool targeting p300 were added to individual microfuge tubes and incubated at room temperature in 250µl of DMEM without serum and antibiotic. 5µl of Lipofectamine RNAiMAX Reagent (Invitrogen) was incubated at room temperature in 250µl of DMEM without

serum and antibiotic. After the end of the initial mixture of 5mins, siRNAs and transfection reagent containing media were mixed and allowed to form complexes at room temperature for 20mins, following which the 500µl mixture was added over the monolayer and mixed uniformly by gentle shaking of the culture dishes. 1.5-2ml of DMEM containing 10%FBS was also added to each dish. 6hrs post transfection, the transfected media was discarded and fresh complete media was supplemented to the cells. Cells were harvested after 48hrs post transfection and analysed for various assays.

2.6.3.3Generation of stable cell lines

2.6.3.3.1 Stable knockdown of PC4 in HEK293

10ug of pGIPZ-sh8 vector was transfected in HEK293T cells along with appropriate amounts of viral gene containing plasmids psPAX2 (5ug), pRS-Rev (1.5ug) and pCMV-VSV-G (3.5ug) to package the mammalian clone into the viral particles. 48hours post transfection, the viral particles in the culture supernatant are collected and used to infect HEK293 cells for 8hours with 50ug/ml of DEAE-dextran. The infected cells were sorted using FACS Aria III on the basis of GFP expression and characterized on the basis of downregulation of endogenous PC4 expression.

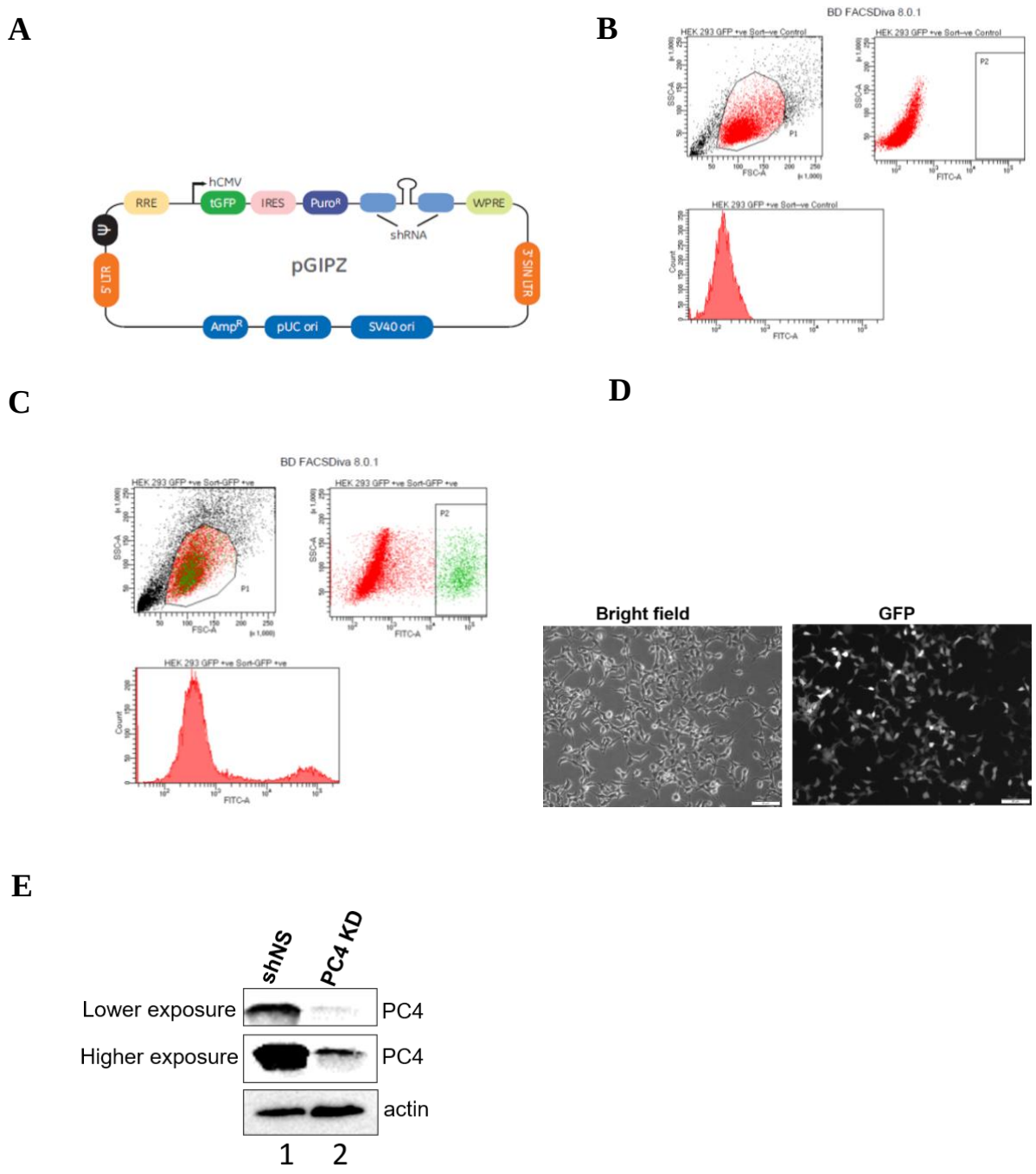

Figure 2.6.3.3.1: Generation of PC4 stable knockdown cell line in HEK293 cells. A. Vector map of pGIPZ vector obtained from Dharmacon. B. FACS analysis showing sorting of GFP+ve HEK293 (P1) cells from GFP-ve HEK293 cells. C. Morphology of HEK293 PC4 knockdown cells (bright field panel on the left) expressing GFP (right panel) has been shown after sorting (bottom panel). D. FACS analysis showing sorting of high GFP+ve HEK293 cells from low

GFP+ve HEK293 cells (P2). Scale bar represents 100µm. E. Western blot representation for the characterization of PC4 stable knockdown HEK293 cells.

2.6.3.3.2 Generation of Flag expressing cell lines

Plasmid vectors, competent for expression of Flag-tagged proteins (pCMV10) in mammalian cells, were transfected by using lipofectamine 2000 Plus (Invitrogen) following which the cells were seeded in culture dishes as per the manufacturer's recommendations and allowed to grow till 50-60% confluence. Recommended amount of DNA and the prescribed volume of Lipofectamine 2000 Transfection Reagent was added to individual microfuge tubes and incubated at room temperature in appropriate volume of the media without serum and antibiotic. After the end of the initial mixture, DNA and Lipofectamine containing media were mixed and allowed to form complexes at room temperature for 5-10mins, following which the mixture was added over the monolayer and mixed uniformly by gentle shaking of the culture dishes. 4-6hrs post transfection, the transfected media was discarded and fresh complete media was supplemented to the cells with neomycin selection. Cells were harvested at appropriate times post transfection and analyzed for various assays by means of western blot analysis or indirect immunofluorescence.

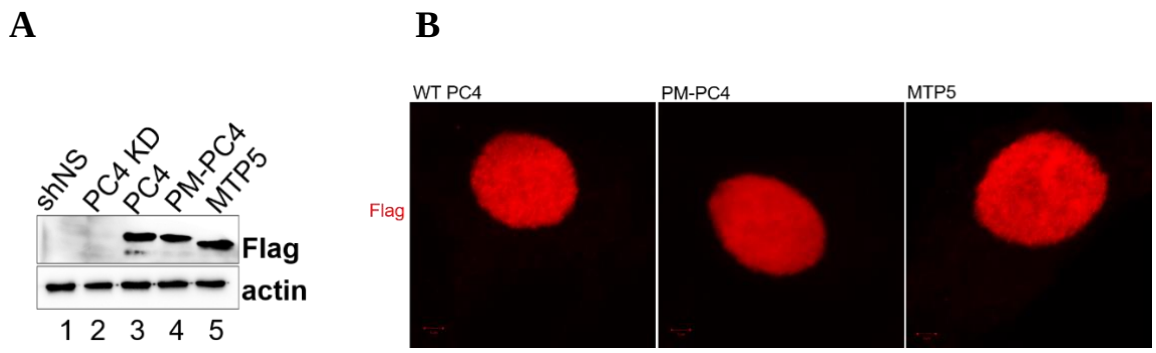

Figure 2.6.3.3.2: (A) Flag expression check by western blotting in PC4 knockdown HEK293 cells expressing Flag-tagged PC4, phosphomimic PC4 (PM-PC4) and phosphomutant PC4 (MTP5). (B) HEK 293 cells transfected with Flag-tagged PC4, phosphomimic PC4 (PM-PC4) and phosphomutant PC4 (MTP5) in PC4 knockdown background was analysed for their subcellular localisation by fluorescent microscopy.

2.6.3.3.3 Stable knockdown of PC4 in AW13516 and UMSCC

10ug of pGIPZ-sh8 vector was transfected in HEK293T cells along with appropriate amounts of viral gene containing plasmids psPAX2 (5ug), pRS-Rev (1.5ug) and pCMV-VSV-G (3.5ug) to package the mammalian clone into the viral particles. 48hours post transfection, the viral particles in the culture supernatant are collected and used to infect AW13516 and UMSCC cells for 12hours with 25ug/ml of DEAE-dextran. The infected cells were sorted using FACS Aria III on the basis of GFP expression and characterized on the basis of downregulation of endogenous PC4 expression.

A **B**

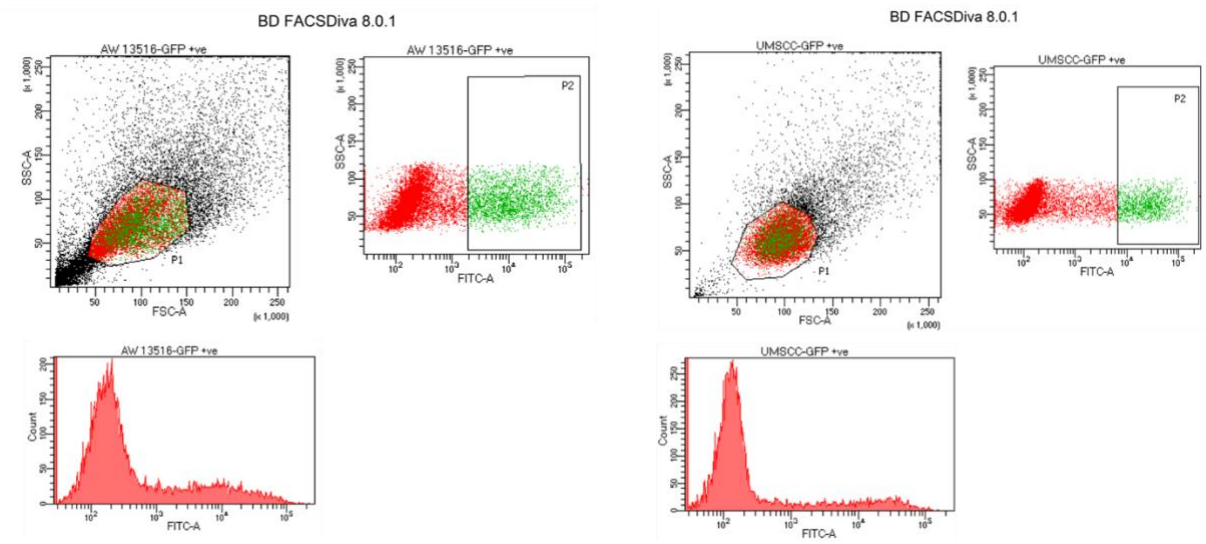

Figure 2.6.3.3.3.1: Generation of PC4 stable knockdown cell line in oral cancer cells. (A-B) FACS analysis showing sorting of high GFP+ve AW13516

(A) and UMSCC (B) (P1) cells from low GFP+ve AW13516 (A) and UMSCC (B) cells respectively.

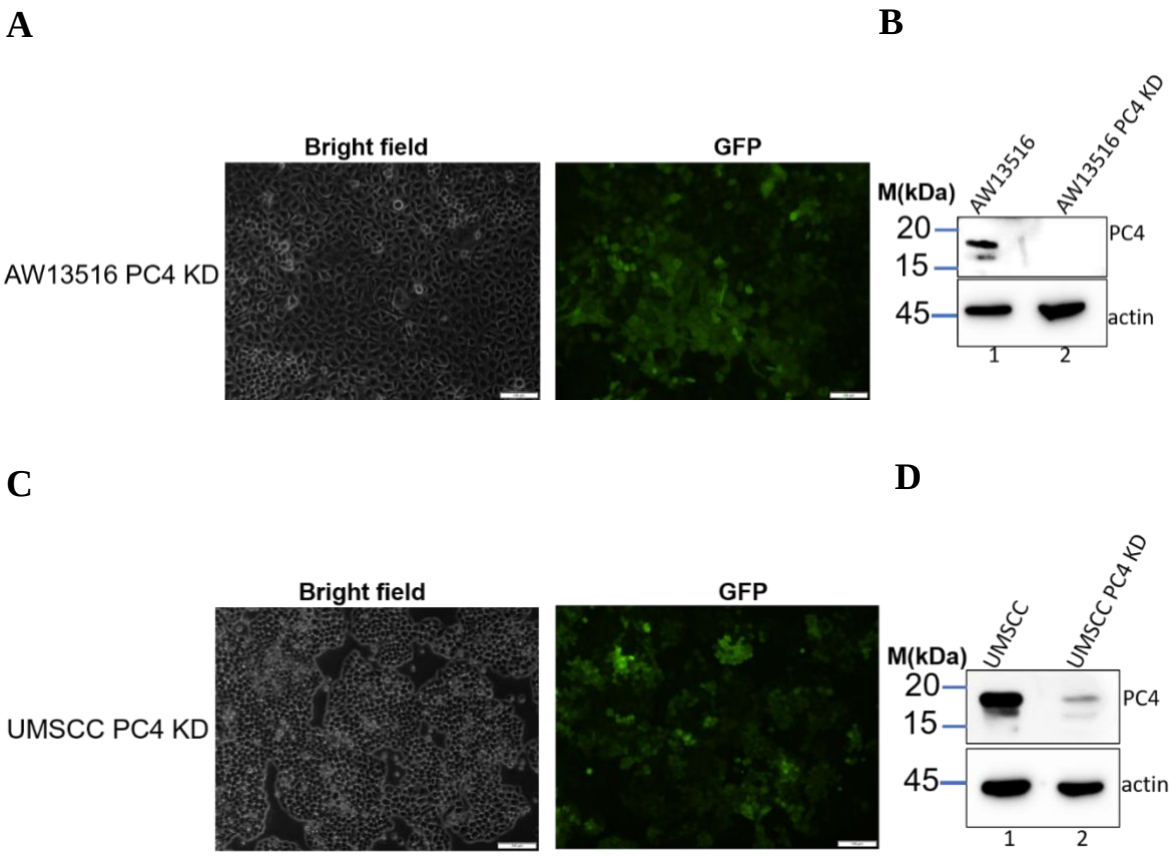

Figure 2.6.3.3.3.2: Generation of PC4 stable knockdown cell line in oral cancer cells. A. Morphology of AW13516 PC4 knockdown cells (bright field panel on the left) expressing GFP (right panel) has been shown after sorting. Scale bar represents 100µm. B. Western blot representation for the characterization of PC4 stable knockdown AW13516 cells. C. Morphology of UMSCC PC4 knockdown cells (bright field panel on the left) expressing GFP (right panel) has been shown after sorting. Scale bar represents 100µm. D. Western blot representation for the characterization of PC4 stable knockdown UMSCC cells.

2.7 Generation of polyclonal antisera

2.7.1 Generation of polyclonal antisera against K26-K28 acetylated peptide of PC4 in rabbit

A peptide containing two acetylated lysine residues corresponding to acetylated lysines26 and 28 of PC4 protein was designed based on the best predicted antigenicity value (Immunomedicine Tools: online antigenicity prediction site) and hydrophobicity value (PEPTIDE 2.0/ ExPASy Bioinformatics Resource Portal site) and conjugated with Keyhole Limpet Hemocyanin (Genemed Synthesis Inc.). KLH-C-EVDKKLK(ac)RK(ac)KQVAPE (residues 20 to 34). Regular immunization schedules were followed as shown in Figure2.7.1 to raise the antibody against acetylated PC4 in rabbit. Briefly, 500µl of conjugated peptide was emulsified with equal volume of Freund's Complete Adjuvant and injected subcutaneously into two rabbits. This was followed by first booster doses after 2 weeks when 250µl of conjugated peptide was emulsified with equal volume of Freund's Incomplete Adjuvant and similarly injected subcutaneously. After 2weeks, the second booster was given same as the first. After 2 weeks of second booster major bleeding was done to obtain immunized blood from one rabbit and serum was extracted whereas a third booster was given to the other rabbit and 2 weeks later major bleed was collected. The specificity of this major bleed was confirmed by western blot analysis and used further characterizations.

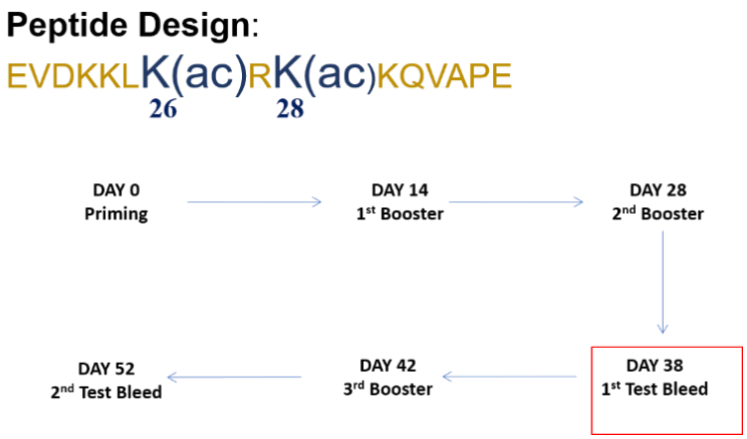

Figure 2.7.1: Schematic for raising polyclonal antisera against PC4 K26-28 acetylated (PC4K26-28ac) indicating the sequence of peptide antigen and the red box indicating the bleed that is used as PC4K26-28ac antibody for further experiments.

2.7.2 Generation of polyclonal antisera against PC4 peptide in rabbit and mouse

A peptide containing a region of PC4 protein which is conserved across human and mouse (Figure 2.7.2. left panel) was designed based on the best predicted antigenicity value (Immunomedicine Tools: online antigenicity prediction site) and hydrophobicity value (PEPTIDE 2.0/ ExPASy Bioinformatics Resource Portal site) and conjugated with Keyhole Limpet Hemocyanin (Genemed Synthesis Inc.). KLH-C- DNMFQIGKMRYVSVRDFKGK (residues 61 to 80). Regular immunization schedules were followed to raise the antibody against acetylated PC4 in rabbit as well as in mouse. Briefly, 500µl and 70ul of conjugated peptide was emulsified with equal volume of Freund's Complete Adjuvant and injected subcutaneously into two rabbits and two mice respectively. This was followed by first booster doses after 2 weeks when 250µl of conjugated peptide was emulsified with equal volume of Freund's Incomplete Adjuvant and similarly injected subcutaneously for rabbits and first booster for mouse was done

using 50ul of peptide was emulsified with equal volume of Freund's Incomplete Adjuvant after 21days. After 2weeks, the second booster was given same as the first for rabbit and after 3weeks for mice followed by third booster in the same way and major bleed was collected after each booster both for rabbit and mice. The specificity of this major bleed was characterized by western blot analysis (Figure 2.7.2 right panel).

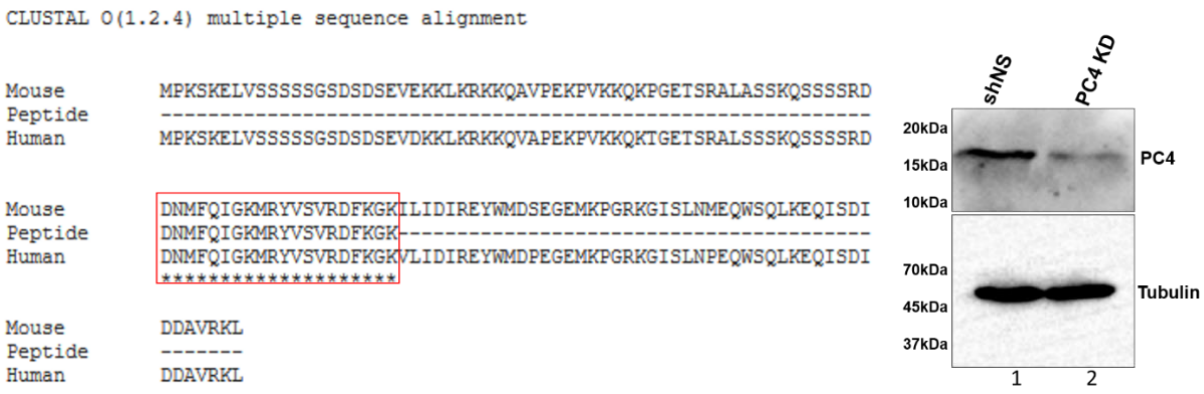

Figure 2.7.2: The conserved region of PC4 protein sequence that was used to generate the polyclonal antisera against PC4 (both in human and in mouse) shown within the red box (left panel). Western blot representation of anti-DNMFQIGKMRYVSVRDFKGK peptide antibody against PC4 in cell lysates on the right panel. PC4 KD HEK293 cells (lane 2 of western blot image) been used to check the specificity of the peptide antibody for PC4 protein in cells.

2.7.3 Generation of polyclonal antisera against PC4 protein in rabbit and mouse

The same immunization schedule was followed as was done for generating antisera against PC4 peptide mentioned in 2.7.2 except for the fact that full length recombinant PC4 protein was purified bacterially expressed cells and was dialyzed in 1X PBS and lyophilized. The lyophilized protein was then dissolved in water and emulsified with Freund's Complete Adjuvant upon priming and with

Freund's Incomplete Adjuvant for booster doses respectively. The major bleed was collected after second and third boosters which was then characterized by Western blotting.

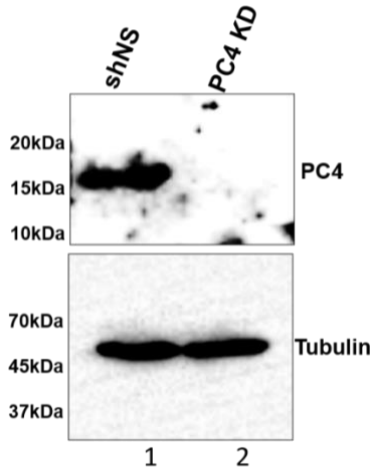

Figure 2.7.3: Western blot representation of PC4 antibody raised against the full length PC4 protein injected for immunization in in cell lysates. PC4 KD HEK293 cells (lane 2) been used to check the specificity of the antibody for PC4 protein in cells.

2.7.4 IgG purification of Antibody

Both the PC4K26-28acetylation specific antibody as well as PC4 antibody generated in lab was purified from 500ul of crude serum that was mixed with 20ul of Protein G-sepharose (Invitrogen) equilibrated with 1mM Tris pH8.0 and allowed to mix for 1hour in the end to end rotor at 4°C and then passed through a column after allowing the beads to settle for 15mins. The beads were washed with 100mM Tris pH 8.0 followed by washes with 10mMTris pH 8.0 and finally eluted in glycine pH 3.0. The eluted antibody is dialyzed in 50% glycerol in 1XPBS before being stored at -20°C for use. IgG was also purified from pre-immune sera to be used for control immuno-pull down. The integrity of IgG purified PC4K26-28ac and PC4 antibody was checked by loading the purified antibody onto a 12% SDS-PAGE with and without denaturation (Figure 2.7.4).

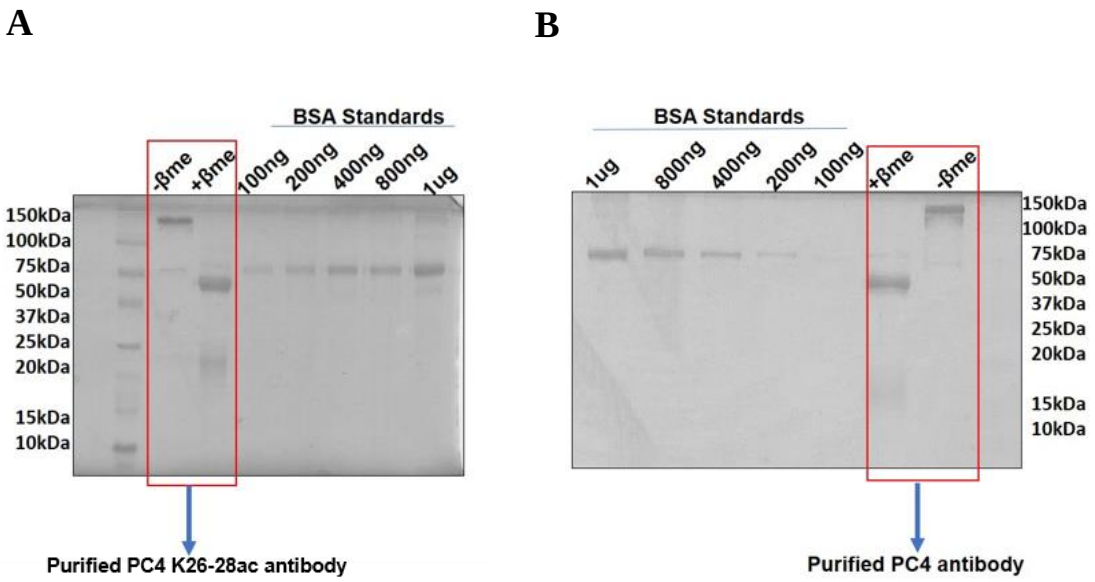

Figure 2.7.4: The integrity of the purified antibodies was checked by running the antibody with and without denaturation (without βme and heating) in a 12% SDS-PAGE to check both the heavy and the light chains. The purification profile for the acetylation specific PC4 (PC4K26-28ac) antibody and for PC4 specific antibody is shown in Panel A and B respectively.

Chapter 3: Results

Chapter outline

3.1. Understanding the implications of CKII-mediated phosphorylation of PC4 on its genome organisation function and thereby the regulation of gene expression

3.2. Understanding the Implications of p300 mediated acetylation of PC4 on its coactivator function and probable role in cancer manifestation

3.1. Understanding the implications of CKII-mediated phosphorylation of PC4 on its genome organisation function and thereby the regulation of gene expression

3.1.1 General Introduction

Human Positive coactivator 4 (PC4) is a highly abundant nuclear protein, discovered as a bona fide non-histone chromatin associated protein (Das C., et al., 2006) involved in multiple cellular processes ranging from genomic organisation, transcription regulation (Garavís M and Calvo C,2017), neurogenesis (Swaminathan A., et al.,2016), regulation of autophagy (Sikder S., et al., 2019), DNA replication (Pan et al., 1996), to DNA damage repair (Mortusewicz O, Evers B, and Helleday T., 2015) (Figure 3.1.1.1). However, the molecular mechanism behind these roles of PC4 in these processes are yet to be elucidated. Post-translational modifications (PTMs) often contribute to multifunctionality of proteins. Post-translational modifications of chromatin proteins have been a major modulator of chromatin structure and thereby regulating chromatin template dependent functions.

PC4 undergoes two major post-translational modifications phosphorylation and acetylation. PC4 Phosphorylation negatively regulates its double strand DNA binding and unwinding ability, co-activator function (Ge and Roeder.,1994, Kretzschmar et al., 1994 and Jonker H.R.A et.al., 2006). CKII is a well-characterized Ser/Thr-specific protein kinase that is responsible for hyperphosphorylation of PC4 N-terminus inside the cells (Ge and Roeder.,1994). Phosphorylation by CKII abolishes its interaction with an activation domain as well as its ability to mediate activator-dependent transcription (Ge and Roeder.,1994). PC4 phosphorylation is likely to alter the conformation of PC4 and, in turn, its ability to interact with VP16 (Ge and Roeder.,1994 and Jonker H.R.A et.al., 2006). PC4 has also recently been shown to be a substrate of mitotic

kinases Aurora A and Aurora B and has implications in cytokinesis and mitosis (Dhanasekaran et al., 2016).

Knockdown of PC4 has shown drastic alteration in the nuclear architecture and chromosomal defects (Dhanasekaran K., et al., 2016 and Sikder S., et al., 2019) which indicates that PC4 is critical for maintaining genome integrity and has a role beyond its involvement in transcriptional activation. Majority of PC4 in cells is present in phosphorylated state and Casein Kinase II (CKII) is the dominant kinase responsible for its hyperphosphorylation at the N-terminal serine-rich region. Despite the inhibitory effects of phosphorylation, the abundance of phosphorylated PC4 in cells intrigued us to find the implications of this modification on its chromatin associated functions.

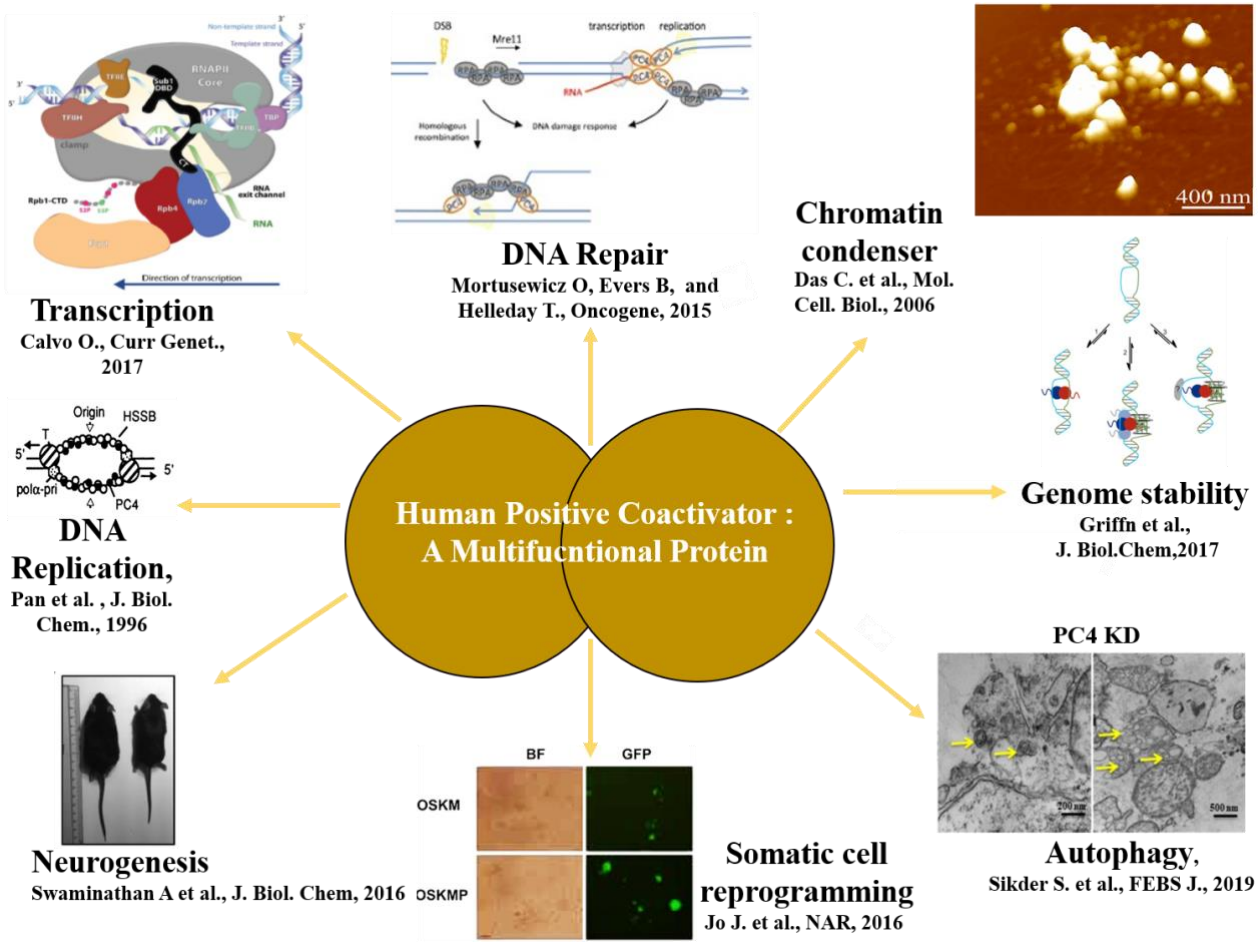

Figure 3.1.1.1: Pictorial depiction of various molecular and cellular activities associated with Human Positive Co-activator 4.

Human Positive co-activator 4 is evolutionarily conserved and is present in other eukaryotes and in prokaryotes (Akimoto et al. 2014; Ge and Roeder 1994; Henry et al. 1996; Huang et al. 2012; Knaus et al. 1996; Steigemann et al. 2013; Werten et al. 2016). PC4 is a DNA-binding protein of 127 amino acids long. It possesses two serine and acidic residue-rich (SEAC) regions separated by a lysine-rich (K-rich) region in the N-terminal half where the post-translational modifications occur (Figure 3.1.1.2A). Initial studies have indicated the CKII phosphorylation mainly occurs within the first serine-rich acidic tract (Ge and Roeder 1994). Therefore, we started with identification of serine residues that are critical for CKII phosphorylation. Prediction of phosphorylation sites using netphos 3.1server indicated that a stretch of the first SEAC domain of PC4 containing Serine residues 13, 15, 17 and 19 predicted to be important for phosphorylation (Figure 3.1.1.2). These serine residues were also highly conserved across species (Figure .3.1.1.3). Several mutants were generated to assay their phosphorylation ability by CKII. The implication of CKII phosphorylation in terms of its chromatin compaction ability was thus further explored by mutating and mimicking these critical serine residues in an *in vitro* reconstituted nucleosomal array as well as in cellular studies with ectopic overexpression of Flag tagged wild type, phospho-mimic and phospho-defective PC4 mutants in an endogenous PC4 knockdown background. The following section elaborates how these approaches that were undertaken to address a possible implication of CKII mediated phosphorylation in determining the chromatin compaction and epigenetic state and thereby the transcriptional outcome of PC4 dependent target genes in cells.

A

```
>Sequence       127 amino acids
#
# netphos-3.1b prediction results
#
# Sequence                 # x   Context     Score   Kinase    Answer
# ----------------------------------------------------------------------
# Sequence                 9 S   KELVSSSSS   0.910   unsp       YES
# Sequence                10 S   ELVSSSSSG   0.879   unsp       YES
# Sequence                11 S   LVSSSSSGS   0.953   unsp       YES
# Sequence                12 S   VSSSSSGSD   0.771   unsp       YES
# Sequence                13 S   SSSSSGSDS   0.997   unsp       YES
# Sequence                15 S   SSSGSDSDS   0.997   unsp       YES
# Sequence                17 S   SGSDSDSEV   0.995   unsp       YES
# Sequence                19 S   SDSDSEVDK   0.997   unsp       YES
# Sequence                50 S   SRALSSSKQ   0.996   unsp       YES
# Sequence                51 S   RALSSSKQS   0.973   unsp       YES
# Sequence                52 S   ALSSSKQSS   0.661   unsp       YES
# Sequence                55 S   SSKQSSSSR   0.970   unsp       YES
# Sequence                56 S   SKQSSSSRD   0.996   unsp       YES
# Sequence                57 S   KQSSSSRDD   0.996   unsp       YES
# Sequence                58 S   QSSSSRDDN   0.997   unsp       YES
# Sequence                73 S   MRYVSVRDF   0.998   unsp       YES
# Sequence               104 S   RKGISLNPE   0.608   PKA        YES
# Sequence               111 S   PEQWSQLKE   0.528   cdc2       YES
# Sequence               118 S   KEQISDIDD   0.986   unsp       YES
```

B

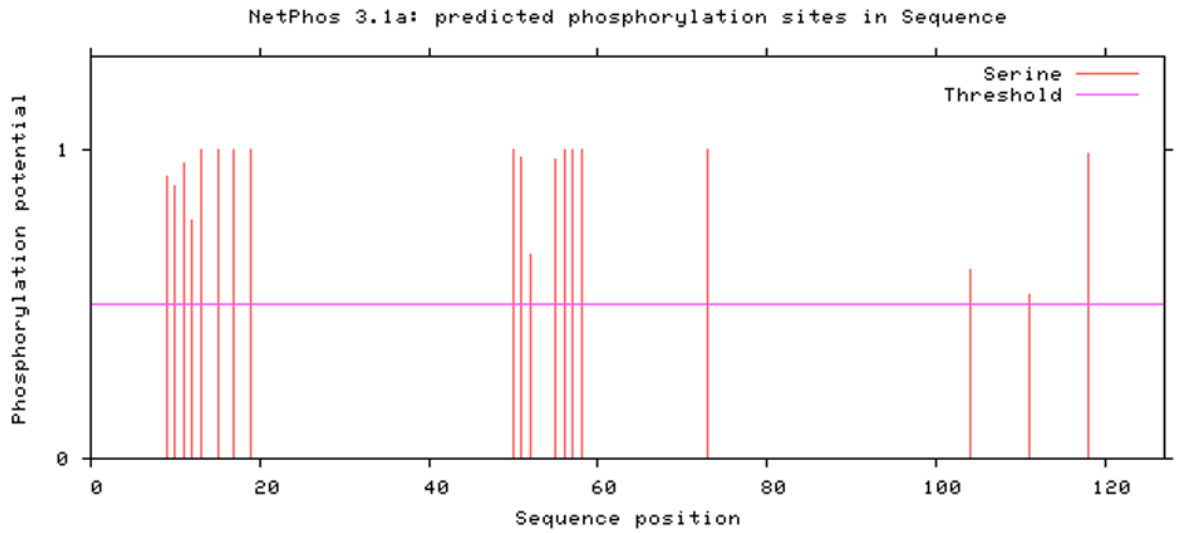

Figure 3.1.1.2: (A) Prediction score of the serine residues in PC4 getting phosphorylated within the indicated stretch (B) The plot showing the phosphorylation potential plotted against the sequence position using Net Phos 3.1.

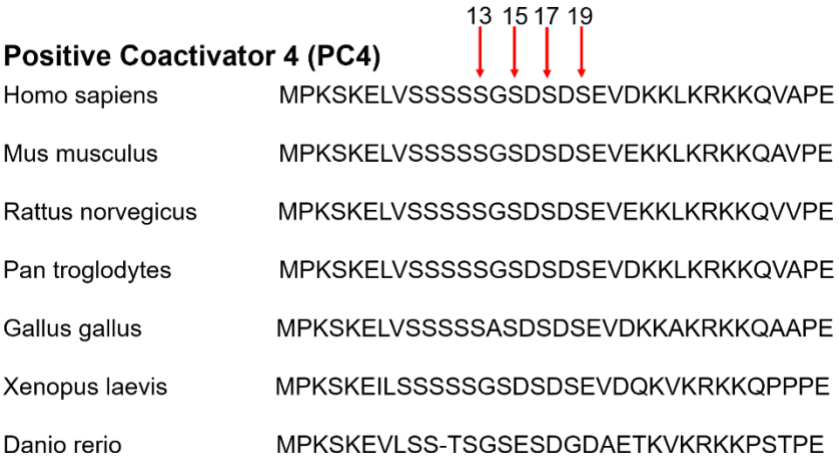

Figure 3.1.1.3: Alignment of PC4 sequence (Homo sapiens) surrounding the four serine residues 13,15,17 and 19 in different species.

3.1.2 CKII phosphorylates PC4 *in vitro*

Full length recombinant untagged PC4 purified from *E. coli* was subjected to *in vitro* kinase assay with Casein Kinase II (CKII), commercially procured from NEB. The kinase assay was carried out at 30ºC for 30 mins, followed by three replenishments with the enzyme and ATP at 30mins interval. After last replenishment, final incubation was done overnight to ascertain completion of the reaction. The mock reaction was set up in the same way containing all the components except enzyme. The phosphorylation of PC4 was confirmed both by the shift in the mobility of the PC4 protein upon phosphorylation in 12% SDS-PAGE gel and from the intensity profile on the X-ray film by radioactive assay (Figure 3.1.2A, lane 3 and 4; Figure 3.1.2B, lane 2).

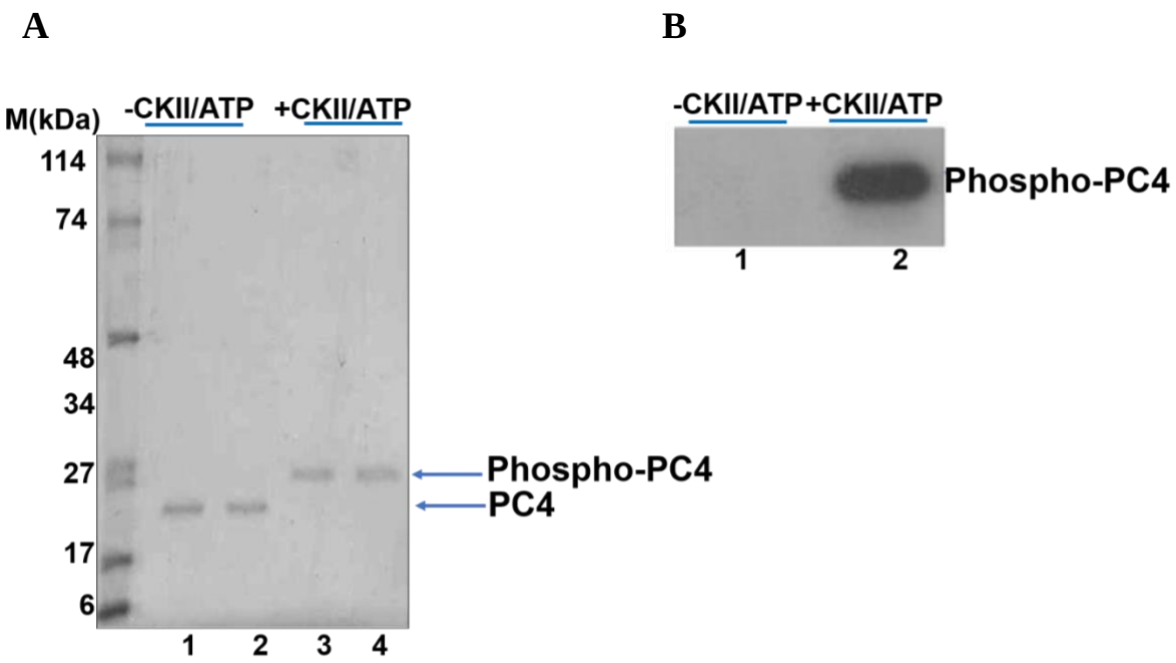

Figure 3.1.2: (A) CKII phosphorylate Max. *In vitro* kinase assay of 600ng of recombinant His6-PC4 (lanes 1-4) was performed using 1ul of CKII (20mU) in 2X Phospho-buffer, 5mM cold ATP and [γ32P] ATP was carried out 30ºC for 30 mins. The phosphorylated PC4 migrates slower than the mock phosphorylated PC4 in a 12% SDSPAGE gel. (B) The phosphorylation of PC4 was also confirmed from the intensity profile on the X-ray film by radioactive assay.

3.1.3 Determination and validation of CKII phosphorylation sites of PC4

The two serine-rich acidic domains in the N-terminal region of PC4 contain several serine residues which are potential sites for phosphorylation. Since earlier mass spectrometric studies (Ge and Roeder 1994) as well as prediction of highly probable phosphorylation sites reveal a stretch within the first serine-rich acidic tract, several point mutations were generated. *In vitro* kinase assay with these point mutants, indicate that a combination of three serine residues 13,15 and 17 (MTP6) and or four serine residues 13,15,17 and 19 (MTP5) completely lost their ability to get phosphorylated by CKII (Figure 3.1.3A). The phosphorylation ability of different mutants has been shown in the tabular form (Figure 3.1.3B)

A

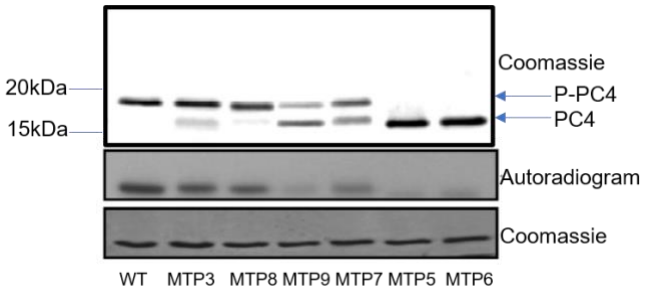

B

Name	*Residues Mutated*	*Phosphorylation Ability*
MTP3	17	+
MTP6	13, 15, 17	-
MTP5	13, 15, 17, 19	-
MTP7	13, 15	+++
MTP8	13, 17	++
MTP9	15, 17	+/-
WT		++++

Figure 3.1.3 (A)*In vitro* kinase assay performed using 600ng of wild type and different phospho-defective mutants using [Υ^{32}P] ATP and CKII enzyme. (B) Table illustrating the extent of phosphorylation ability of different serine mutants of PC4.

3.1.4 Casein Kinase II mediated phosphorylation of PC4 is critical for its interaction with linker histone H1

Although PC4 has been found to be predominantly phosphorylated *in vivo*, its physiological relevance has not been elucidated properly. The association of PC4 with chromatin was speculated to be through its preferential interaction with different core histones except the centromeric variant of histone H3, CENPA (Das C. et al 2006). Interestingly, unmodified, bacterially expressed recombinant PC4 was found to be not interacting with linker histone H1 *in vitro*. The linker histone H1 being an important chromatin component has been reported to regulate functions of other nonhistone chromatin proteins like HP1α and HMG through direct interactions (Daujat S 2005; Yinglu Li, 2018 and Zlatanova J., 1998), we tested whether PC4 interacts with linker H1 upon phosphorylation using bacterially expressed His-tagged linker H1.1 and untagged PC4. We observed that PC4 interacts with linker H1 only when it is phosphorylated as the phospho-defective mutants (MTP5 and MTP6) failed to do so (Figure 3.1.4A, lane 3 vs lanes 6 and 9). The higher migration of PC4 upon phosphorylation (Figure 3.1.4A, lane 1) is also seen in IP upon pulling down His-tagged H1(Figure 3.1.4 B, lane 3). The mock phosphorylated PC4 without CKII doesn't show any

change in the migration pattern (Figure 3.1.4A, lane 4) nor does it interact with linker H1 (Figure 3.1.4C, lane 3).

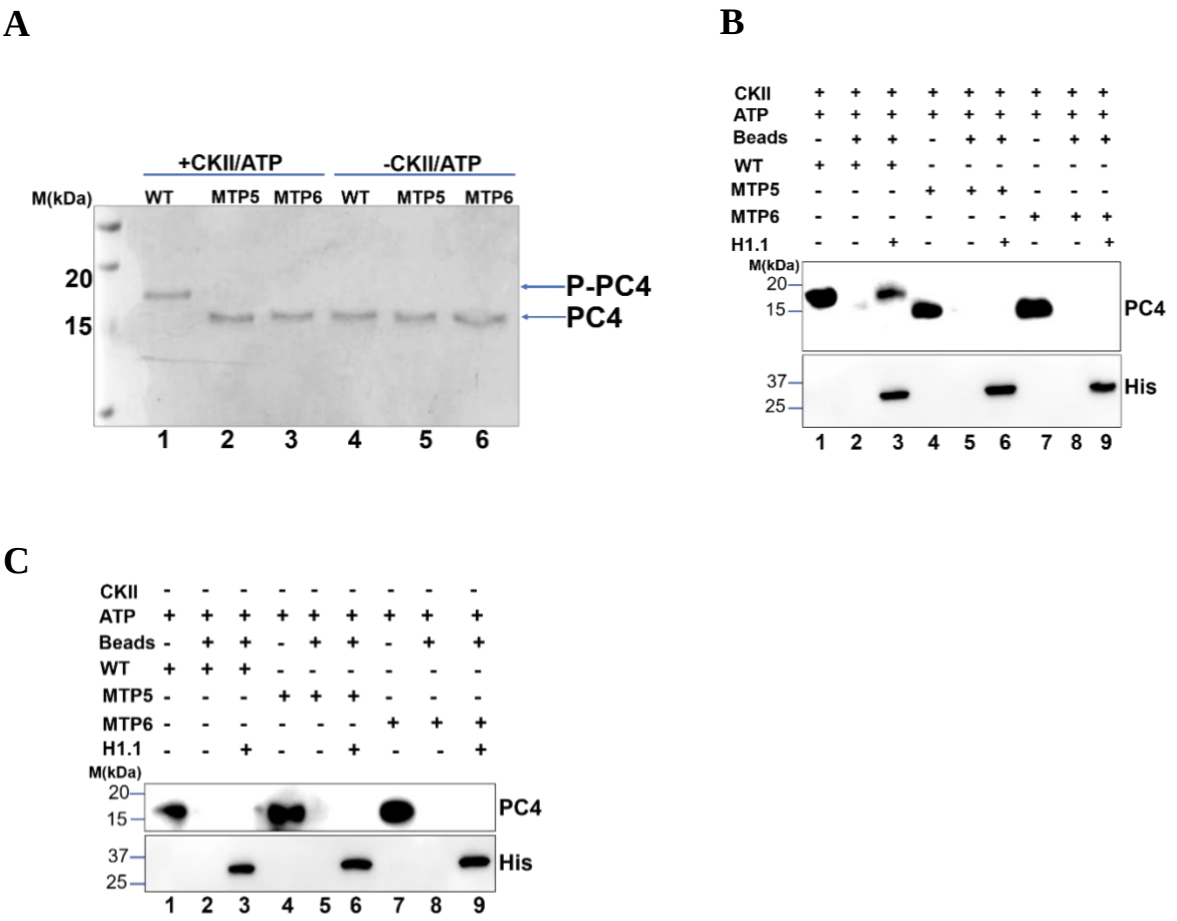

Figure 3.1.4: (A) *In vitro* kinase assay performed using 600ng of wild type and phospho-defective mutants (MTP5 and MTP6) using ATP and CKII enzyme (lanes 1-3) and only ATP for mock reactions (lanes 4-6). (B) An *in vitro* interaction assay with 250ng of each of the phosphorylated wild type PC4, phospho-mutant PC4; MTP5 and MTP6, with 1ug of His tagged linker histone H1.1 was carried out by Ni-NTA pulldown. (C) The *in vitro* interaction with his-tagged linker H1.1 using the mock controls (no CKII) of wild type PC4 and phospho-defective serine mutants (MTP5 and MTP6).

3.1.5 Quantitative Estimation of interaction of Phosphorylated PC4 with linker H1

Interaction of PC4 with linker H1 in phosphorylation dependent manner was quantified by isothermal titration calorimetry. The assay was carried out in the presence of phosphorylated and mock phosphorylated PC4 with linker H1.1 in the ratio of 6:1. Unlike, unmodified PC4 which did not show any significant enthalpy change in the presence of linker histone H1.1 (Figure 3.1.5A) phosphorylated PC4 showed a robust association leading to significant enthalpy change, with a dissociation constant of 5nM (Figure 3.1.5B) exhibiting a one-site binding model of the isotherm.

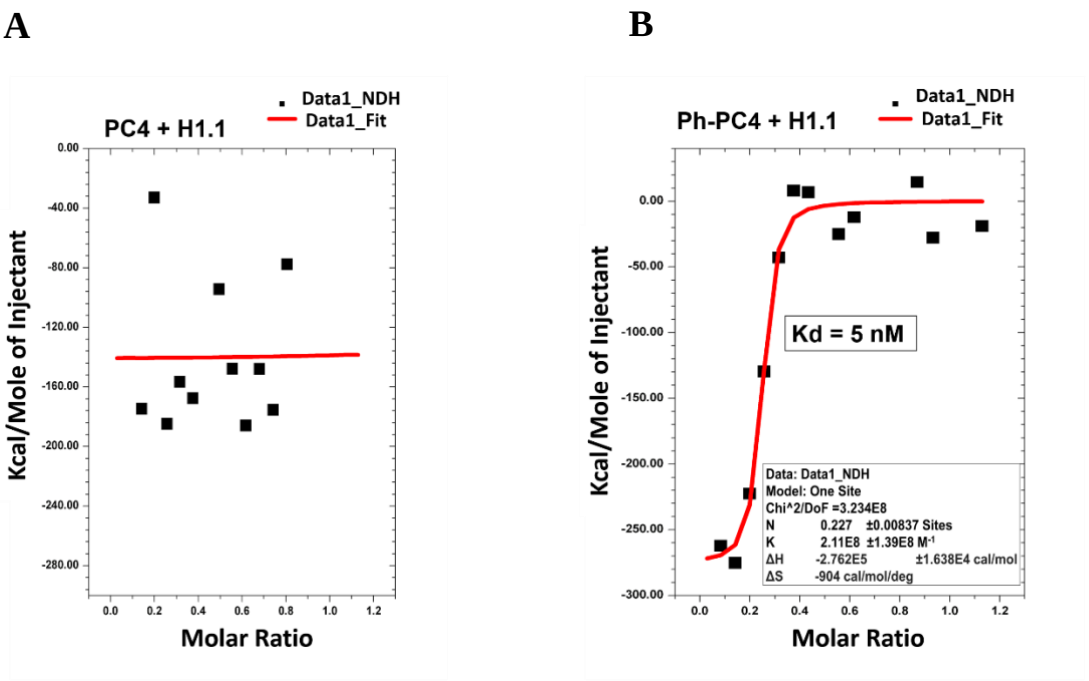

Figure 3.1.5: (A) Isothermal calorimetric titration of unmodified PC4 with linker H1.1 and (B) Isothermal calorimetric titration of phosphorylated PC4 with linker H1.1 were carried out to determine the enthalpy change and stoichiometry of interaction.

3.1.6 Phosphorylation of PC4 mediates its interaction with somatic linker H1 variants

Linker histone H1 is an important chromatin component and consist of total 11 subtypes including five canonical, replication-dependent somatic histone H1 subtypes (H1.1, H1.2, H1.3, H1.4, and H1.5) with general as well as specific functions besides 6 non-canonical histone variants. The genomic distribution and their role in chromatin processes determines both local chromatin state as well as the 3D genome architecture.

In vitro interaction studies were carried out with other somatic linker H1 variants besides H1.1 that are majorly expressed during S phase in a replication dependent manner. These histone variants despite having some specific functions do share a considerable amount of functional redundancy. PC4 interacts with the H1 variants; H1.2, H1.3, and H1.4 (Figure 3.1.6 A, B and C respectively) only upon phosphorylation since only phosphorylated PC4 is present in the IP upon pulling down His-tagged H1 variants but not mock phosphorylated PC4 (Figure 3.1.6., A, B and C, lane 2 vs lane 4 for IP panel).

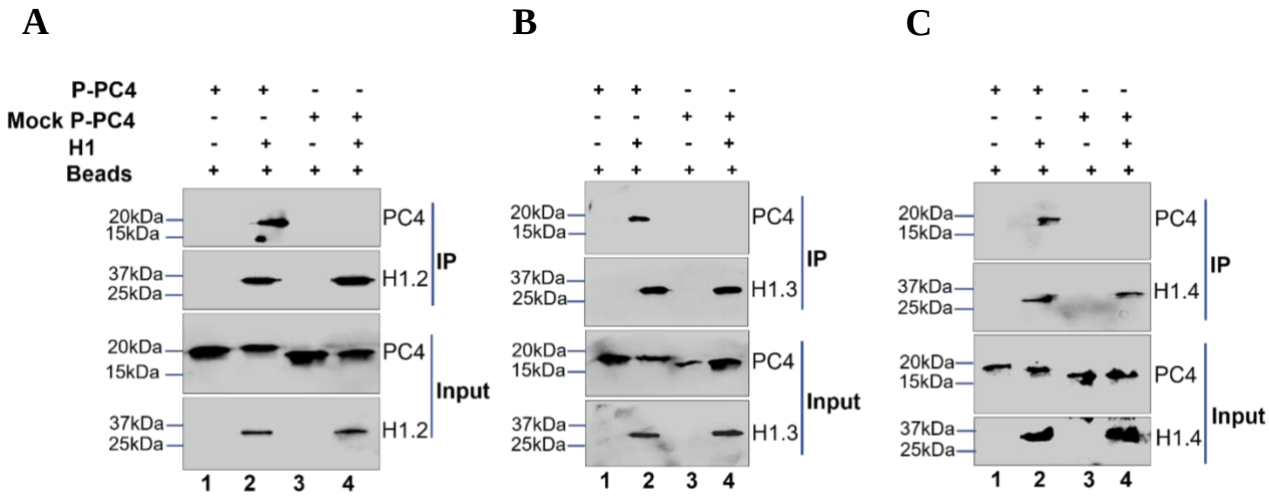

Figure 3.1.6: (A-C) *In vitro* interaction assay with phosphorylated WT-PC4 and mock phosphorylated WT PC4 (P-PC4) with different His tagged linker histone

H1 variants H1.2, H1.3, H1.4 respectively was carried out by Ni-NTA pulldown following an *in vitro* kinase assay by CKII (compare lane 2 vs lane 4 for IP panel).

3.1.7. Interactions of Phosphomimic PC4 (PM-PC4) with linker histone H1 *in vitro*

As the *in vitro* biochemical data suggest that phosphorylation of PC4 is essential to interact with linker histone H1, in order to understand the significance of this interaction in the physiological context a phosphomimic clone was generated by two sequential site directed mutagenesis, where the four critical serine residues 13,15,17 and 19 was replaced by aspartic acid (PC4S13DS15DS17DS19D). Concurring with previous studies these four serine residues which were predicted to be potential CKII sites by mass spectrometric analysis lies within the first serine rich tract and is highly conserved as shown by sequence alignment of PC4/Sub1 across different species (Figure 3.1.3). The mobility of the phosphomimic PC4 (PM-PC4) was found to be comparable to phosphorylated PC4 (P-PC4) as shown in 15% SDS-PAGE (Figure 3.1.7A, compare lane 3 vs lane 4). In contrast, the mobility of unmodified native PC4 (N-PC4) and mock phosphorylated PC4 (Mock P-PC4) was found to be faster as compared to P-PC4 or PM-PC4 (Figure 3.1.7A, compare lane 1 and lane 2 vs lane 3 and lane 4) .

In vitro interaction assay was set up to study the interaction of phosphomimic PC4 along with phosphorylated wild type PC4 and phospho-defective mutant MTP5 with His-tagged linker histone H1.1. We find that indeed the phosphomimic PC4(PM-PC4) interacts with linker histone H1.1 similar to the phosphorylated wild type PC4 upon Ni-NTA pull down (Figure 3.1.7B, lane 2 vs lane 3). The phospho-defective mutant and the mock controls for both wild type PC4 and phospho-defective mutant of PC4 did not interact with His-H1.1 upon Ni-NTA pull down (Figure 3.1.7B, lanes 4-6). There was no phosphomimic-PC4 being pulled down in the bead control indicting no non-specific interaction of phosphomimic PC4 with Ni-NTA beads (Figure 3.1.7 B, lane 1).

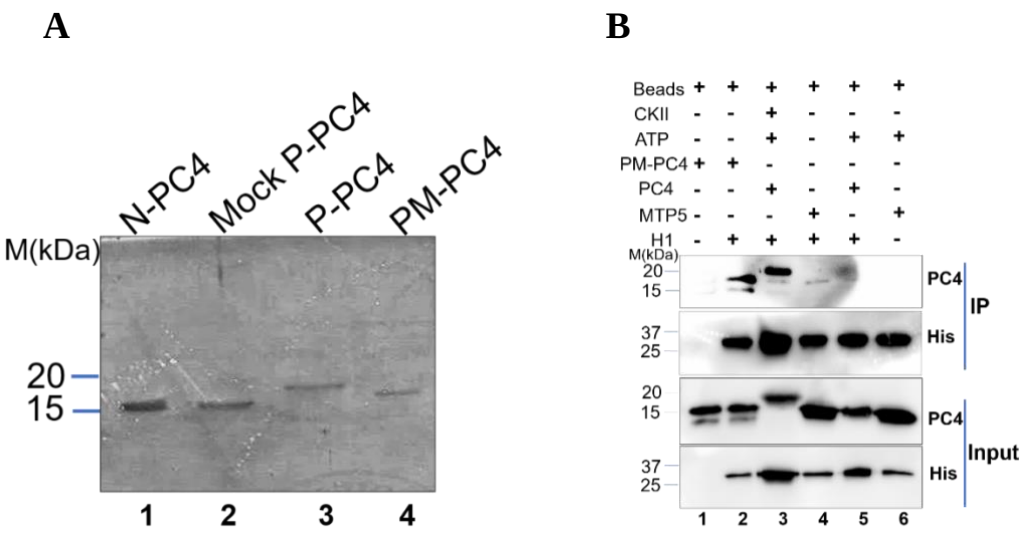

Figure 3.1.7: (A) The mobility pattern of PM-PC4 as compared to phosphorylated PC4 and unmodified PC4 in 15% SDS-PAGE stained with coomassie (B) *In vitro* interaction was performed using 250ng of phosphorylated wild type PC4 and PM-PC4 and phospho-defective mutant (MTP5) with 1ug of His tagged linker histone H1.1 was carried out by Ni-NTA pulldown.

3.1.8 Phosphomimic PC4 and Phosphorylation of PC4 interacts with C-terminal domain of linker histone H1

To further understand which domain of linker H1 could be critical for this interaction, an *in vitro* interaction assay was carried out using His-tagged N-terminal-globular domain (ΔC) of linker H1.2, C-terminal-globular domain (ΔN) constructs of linker histone H1.2, and full length H1.2 (Figure 3.1.8A) with phosphomimic-PC4 (PM-PC4), phospho-PC4 (P-PC4) and mockphospho-PC4 (Mock P-PC4) by Ni-NTA pull down. The results indicate that PM-PC4 exhibits more potent interaction with linker histone H1 harbouring globular domain along with the C-terminal domain (ΔN) instead of the N-terminal (ΔC) (Figure 3.1.8B, lane 7 vs lanes 4 and 10). The strength of interaction between PM-PC4 with full length linker histone H1 (FL) was found to be lesser when compared to the C-terminal globular domain ΔN (Figure 3.18B, lane 9 vs lanes 5 and 11). These

results indicate the C-terminal domain of linker H1 could be responsible for mediating interaction with PC4.

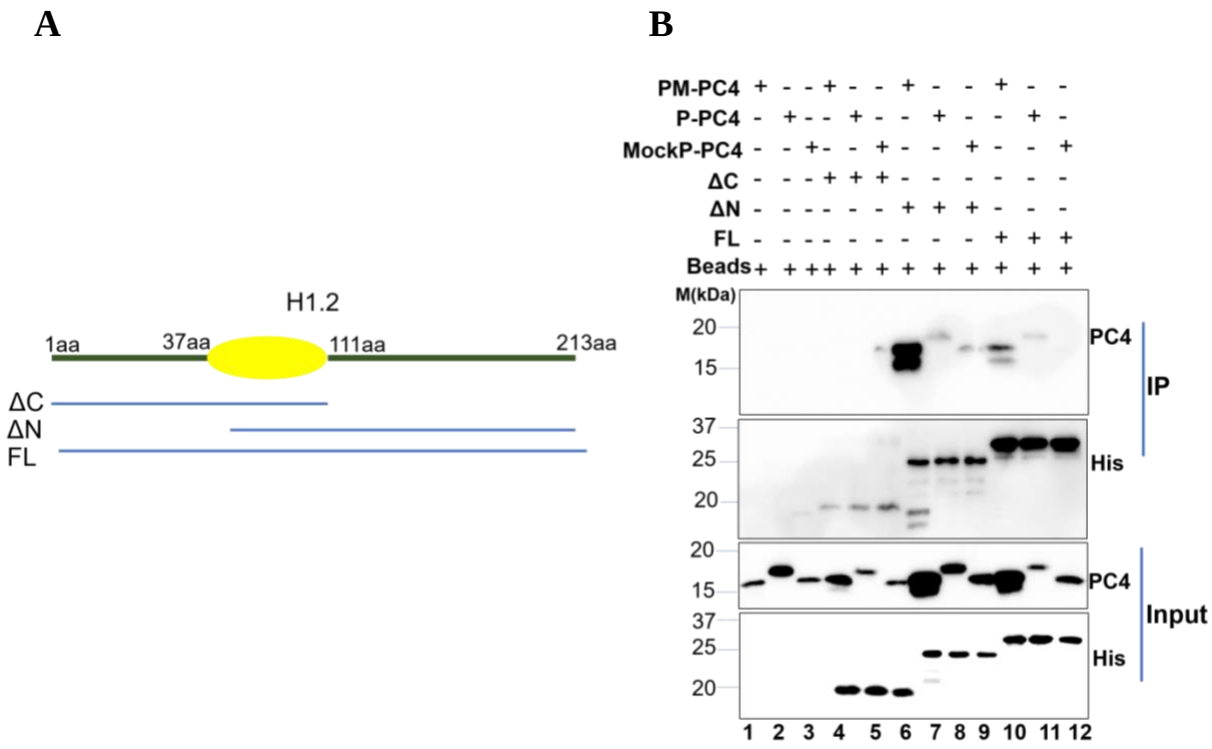

Figure 3.1.8: (A) A diagrammatic representation of the different domains of linker histone H1.2 used for the interaction studies. (B) *In vitro* interactions were carried out with different domains of His tagged H1: N-terminal globular domain (ΔC), C-terminal globular domain (ΔN) and full length (FL) with PM-PC4, P-PC4 and MockP-PC4 by similar Ni-NTA pull down and probed with anti-His and anti-PC4 antibody.

3.1.9 Phosphorylation of PC4 mediates its interaction with linker histone H1 in cells

Whether phosphorylation of PC4 mediates its interaction with liker histone H1 in cells as well we created 3X-flag tagged mammalian constructs of wild type PC4 (PC4), phosphomimic PC4 (PM-PC4) and phospho-defective PC4 (MTP5) expressing constructs in PC4 knockdown stable cell line background under neomycin selection (PC4 KD). Upon flag immuno-pull down, it was observed

that both wild type Flag tagged PC4 and Flag-PM-PC4 could efficiently interact with linker histone H1 as shown in the IP upon probing both with H1.2 variant specific as well as with pan H1 antibody (Figure 3.1.9 A and B respectively). The phospho-defective mutant MTP5 however could not pull down H1 in IP (Figure 3.1.9 A-B). Thus, phosphorylation of PC4 is critical for its interaction with linker H1 in cells as well.

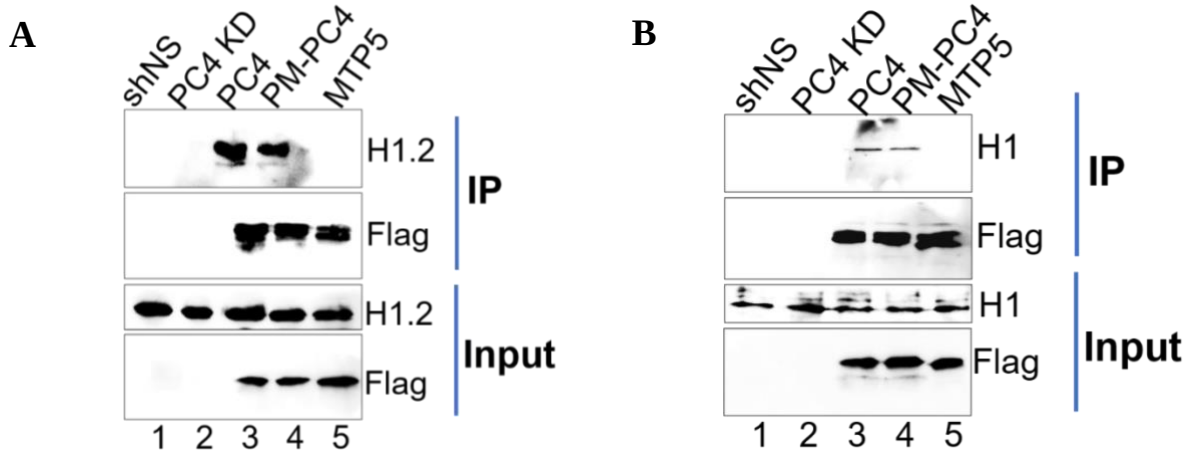

Figure 3.1.9: (A and B) Immuno-pulldown using Flag antibody carried out in Flag-PC4, Flag-PM-PC4 and Flag-MTP5 expressing 293cells in PC4 knockdown background and probed with both H1.2 specific (A) as well as pan H1 (B) antibody to detect H1 in the IP.

3.1.10 Phosphomimic PC4 promotes condensation of a reconstituted nucleosomal array

3.1.10.1 Determining concentration of Phosphomimic-PC4 (PM-PC4) mediating nucleosomal compaction

Upon establishing that phosphorylation of PC4 is essential for its interactions with the linker histone H1, both *in vitro* and *in vivo*, we wanted to address the implications of PC4 phosphorylation in terms of its chromatin compaction

functions; for which we reconstituted a nucleosomal array using 12×177bp of 601 DNA and recombinant Xenopus core histones. In order to study the effect of PC4 vs PM-PC4 protein upon nucleosomal compaction, the recombinant PC4 and Phosphomimic PC4 (PM-PC4) was mixed with the nucleosomal array and subjected to sedimentation velocity analysis by analytical ultra-centrifugation and EM imaging to visualise the incubated array. A range of concentration of PM-PC4 was tested for nucleosomal compaction (Figure 3.1.10.1) and we observed that PM-PC4 begins to induce compaction at as low as 1uM concentration and mediates significant compaction from 1.65uM unlike the unmodified PC4 (Table 3.1.10.1.C)

A

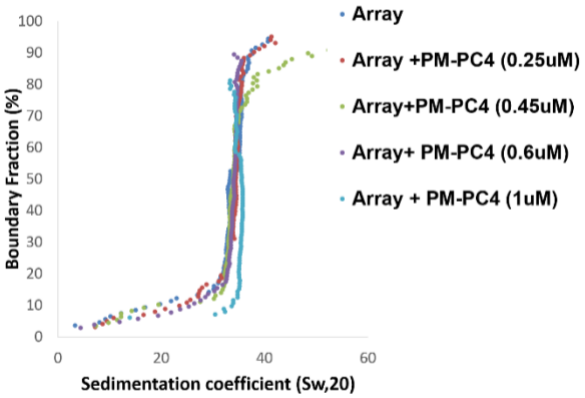

B

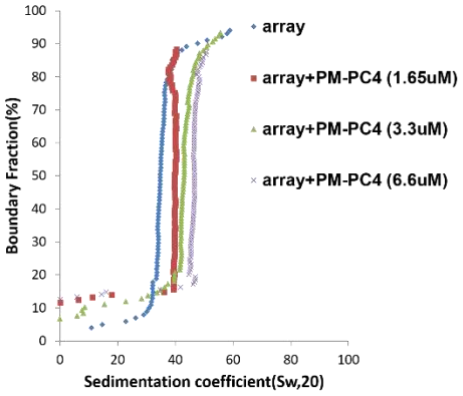

C

SAMPLE NAME	IC value at 50% boundary fraction
Array	34.77352
Array+ PM-PC4 0.25uM	34.44757
Array + PM-PC4 0.5uM	33.95616
Array + PM-PC4 0.75uM	34.09686
Array+ PM-PC4 1uM	35.60671
Array+ PM-PC4 1.65uM	39.77043
Array + PM-PC4 3.3uM	43.09998
Array + PM-PC4 6.6uM	46.66723
Array+ PC4 1.65uM	33.7177
Array + PC4 3.3uM	36.3594
Array + PC4 6.6uM	43.7535

Figure 3.1.10.1: Phosphomimic PC4 promotes chromatin condensation in a reconstituted nucleosomal system: (A-B) Sedimentation velocity analysis by analytical ultracentrifugation of PM-PC4 containing nucleosome array across a wide concentration range. (C) The sedimentation coefficient value at 50% boundary fraction ($S_{w,20}$) for different concentrations of PM-PC4 and PC4 shown in tabular form.

3.1.10.2 PM-PC4 begins to induce compaction at a lower concentration than unmodified PC4

After titrating a range of concentration of Phosphomimic PC4 upon incubating with nucleosome array and assessing the compaction from S50%(S) value , we observe that PM-PC4 begins to induce compaction at 1uM (Figure 3.1.10.2 A vs B ; C vs D). This is reflected in the diameter of the PM-PC4 bound array vs unmodified PC4 bound array (Figure 3.1.10.2E).

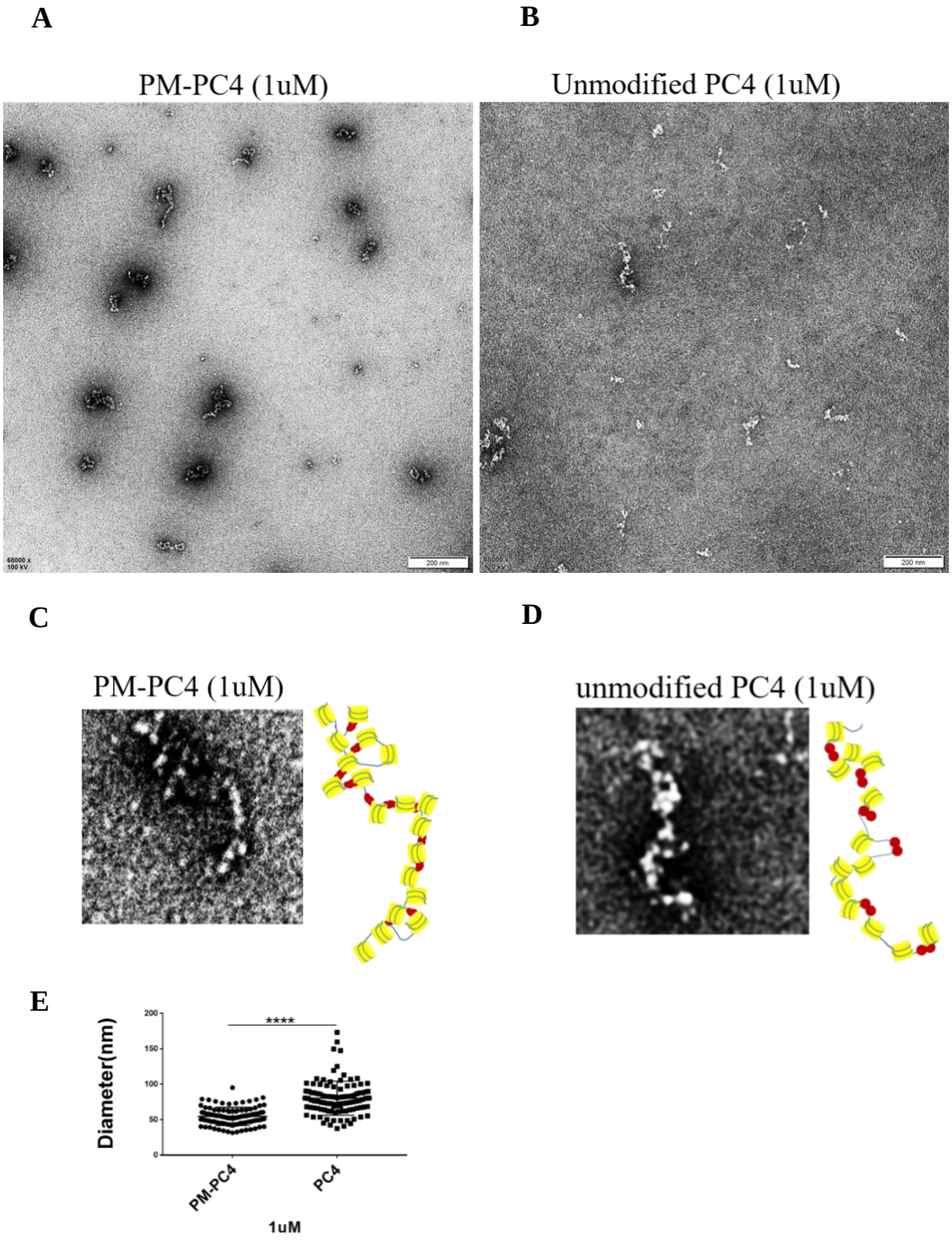

Figure 3.1.10.2: (A-B) EM images of PM-PC4 and PC4 incubated nucleosome array respectively at 1uM. (C-D) EM images of a single PM-PC4 and PC4 incubated nucleosome array respectively at 1uM. Models of representative array

shown alognside. (E) Distributions of diameters of PM-PC4 and PC4 bound compacted array particles with diameter measured in um. No. of particles measured = 102. The diameter of particles was statistically analyzed by Student's unpaired t-test (*p<0.05,**p<0.01,***p<0.001,ns-non-significant). Data represent the means ± SD.

3.1.10.3 Phosphomimic PC4 bound nucleosomal array achieves higher sedimentation coefficient value indicating greater compaction

The compaction of the nucleosomal array analysed by sedimentation velocity analytical ultracentrifugation showed that the PM-PC4 incubated nucleosomal array reaches higher sedimentation coefficient value as compared to the array incubated with unmodified wild type PC4 (by ~7S) (Figure 3.1.10.3A). The sedimentation coefficient value at a 50% boundary fraction is plotted against the stoichiometric ratio of PC4 and PM-PC4 used with respect to nucleosome core particle (NCP) indicated in X axis in Figure 3.1.10.3B. The data clearly indicates that PM-PC4 significantly increases the compaction of nucleosomal array *in vitro* than the unmodified PC4. Upon visualizing the PM-PC4 and PC4 incubated nucleosome array by EM imaging, we observed that in agreement with the sedimentation velocity analysis, the EM images also shows highly condensed nucleosome array formation *in vitro* by PM-PC4 as compared to wild type unmodified PC4 (Figure 3.1.10.3C vs D). To quantify the effects of PM-PC4 compaction on chromatin, we measured one more parameter of the arrays: the diameter of the smallest circle completely encompassing the array. The diameter distribution of the PM-PC4 bound arrays is much lower than unmodified PC4 bound array with diameter ranging from 0.06-0.16um indicating that more compacted arrays were formed by PM-PC4 (Figure 3.1.10.3E). Models of representative 12×177 oligo-nucleosomes at 0.6M monovalent salt with PM-PC4 and PC4 has been depicted alongside their respective EM images (Figure 3.1.10.3C-D). One of the condensed nucleosome arrays has been zoomed in

showing the highly compacted ordered arrays formed by PM-PC4 versus those by unmodified PC4 (Figure 3.1.10.3A).

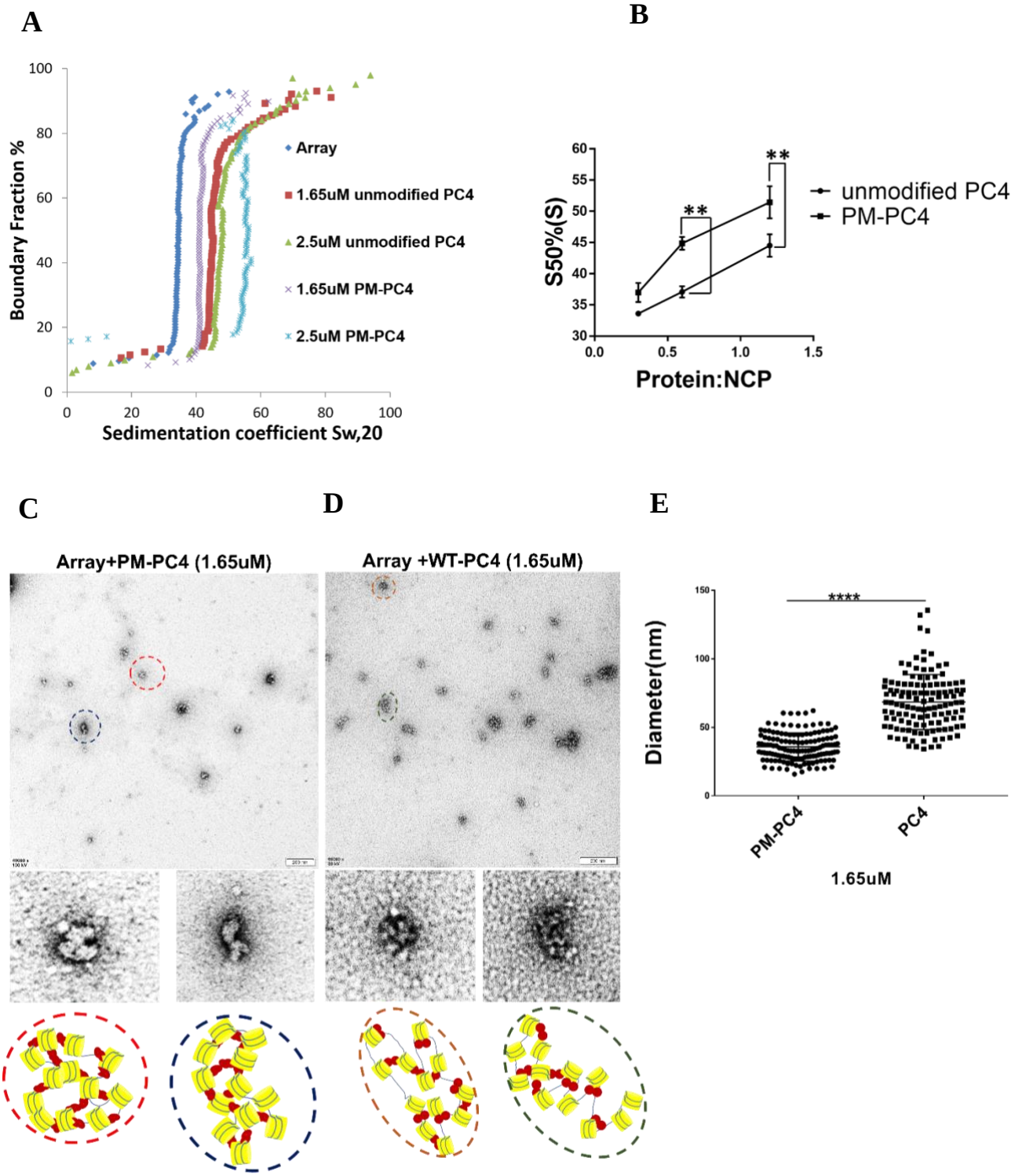

Figure 3.1.10.3: (A)Sedimentation velocity analysis by analytical ultracentrifugation of PM-PC4 and wild type PC4 containing chromatin samples. A nucleosome array without any protein is used as a control. (B) Sedimentation

coefficient values from (A) represented for the nucleosome core particle (NCP) containing increasing concentrations of PM-PC4 and WT PC4 at a 50% boundary fraction(n=3). Data represent the means ± SEM. The S50%(S) were statistically analyzed by Student's paired t-test (*p<0.05,**p<0.01,***p<0.001,ns-non-significant). (C-D) EM images of PM-PC4 and PC4 incubated nucleosome array respectively. Models of the representative condensed arrays shown in dotted circles below. (E) Distribution of diameters (in um) of PM-PC4 and PC4 bound compacted array particles. No. of particles measured = 142. Data represent the means ± SD. The S50%(S) were statistically analyzed by Student's unpaired t-test (*p<0.05,**p<0.01,***p<0.001,ns-non-significant).

3.1.10.4 Phosphomimic PC4 bound nucleosome array forms ordered structures at higher concentration

PM-PC4 reaches optimal compaction at 1.65uM concentration even though it starts compacting at 1uM (Figure 3.1.10.4 F) showing formation of PM-PC4 bound array of smaller diameter range than unmodified PC4 bound array which continues till 2.5uM concentration (Figure 3.1.10.4A-C). Upon increasing the concentration to 2.5uM PC4 starts forming disordered aggregates whereas PM-PC4 bound array still forms ordered compacted structures (Figure 3.1.10.4 B vs A). Upon adding protein at 3.3uM concentration, PM-PC4 starts forming aggregated structures (Figure 3.1.10.4D and E). Thus, these data collectively show that PM-PC4 has a better compaction ability forming highly compacted arrays as compared to WT unmodified PC4.

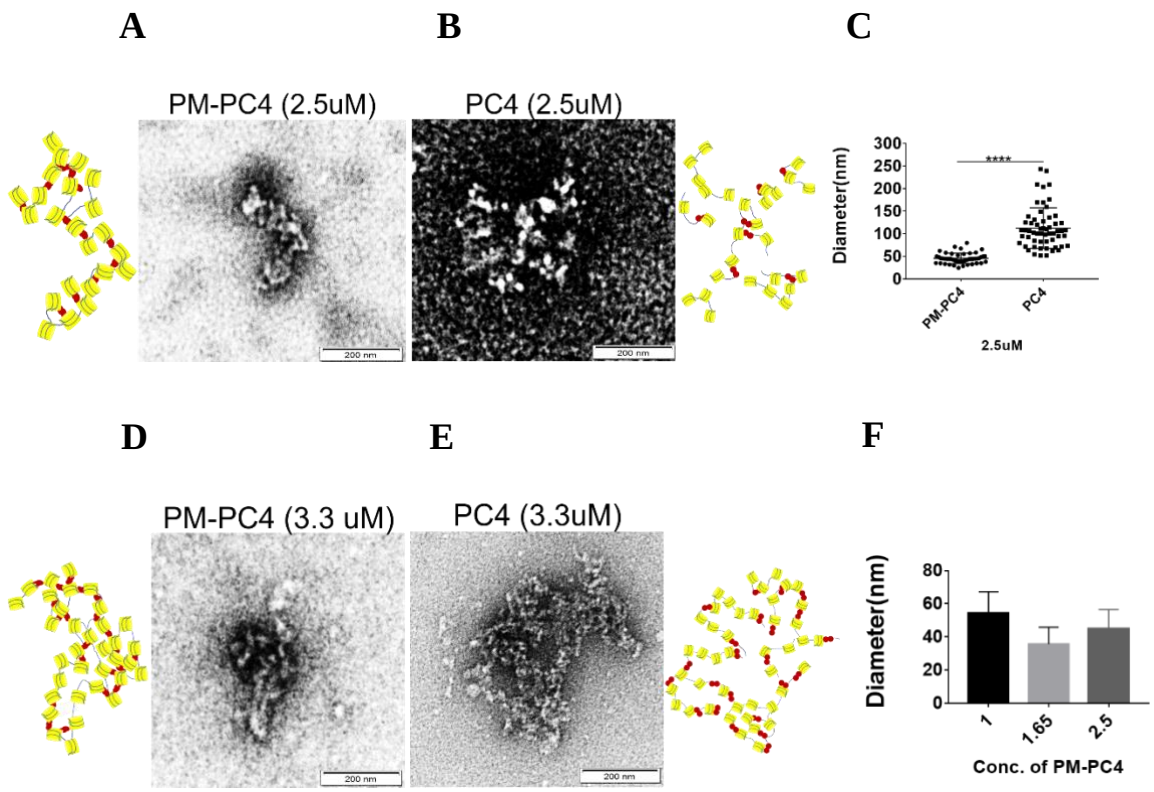

Figure 3.1.10.5: (A-B) EM images of PM-PC4 and PC4 incubated nucleosome array respectively at 2.5uM with models of representative array shown alognside. (C) Distributions of diameters (in um) of PM-PC4 and PC4 bound compacted array particles. No. of particles measured = 60. Data represent the means ± SD. The S50%(S) were statistically analysed by Student's unpaired *t*-test (*p<0.05,**p<0.01,***p<0.001,ns-non-significant).(D-E) EM images of PM-PC4 and PC4 incubated nucleosome array respectively at 3.3uM. Models of representative array structure showing aggregation.(F) The diameter distribution of PM-PC4 bound condensed array across different concentration of PM-PC4.

3.1.11 Phosphorylation enhances PC4 mediated condensation of H1 bound array forming higher order structures

Linker H1 is an important component of the chromatin that stabilises the nucleosomal structure and spacing (Woodcock L., 2006 and Robinson PJ., 2006) but it also functions through intercation with other proteins which in turn brings about chromatin modification and regulates heterchromatin formation. Since we observed that linker histone H1 interacts with PC4 only when it is phosphorylated, we wanted to study whether phosphomimic PC4 and PC4 could complement linker H1 in mediating compaction of array into highly compacted fibers. Previous studies have already shown that H1 could condense nucleosome array into compact fibers when ratio of H1 to nucleosomal core particle (H1:NCP) is 1 (Song F et al., 2014). Therefore we selected H1 bound to nucleosome array at a sub-optimal ratio where it doesnot show complete compaction (Figure 3.1.11.1 A and B). Using this H1 bound nucleosome array we incubated PM-PC4 and PC4 at concentration lower than that used for earlier compaction studies to avoid precipitation of the nulceosomal DNA. The sedimentation velocity analysis shows that PM-PC4 complements H1 acquiring higher sedimentation coefficient value as compared to wild type(by ~6S) (Figure 3.1.11.2A and C). Thus, PM-PC4 could condense H1 containing array to form highly compacted chromatin fibers unlike the wild type unmodified PC4 at the concentration used (Figure 3.1.11.2A-C). EM imaging suggest that at the indicated concentrations the proteins H1 (Figure 3.1.11.1A), PM-PC4 and unmodified PC4 (Figure 3.1.11.1C and D respectively) could not form compacted fibers alone but in presence of PM-PC4, H1 is able to form highly compacted fibers (Figure 3.1.11.3A and C) unlike with wild type unmodified PC4 (Figure 3.1.11.3B and D). PM-PC4 further compacts the H1-bound array into highly compacted ordered strcutures (Figure 3.1.11.3A and C) resembling chromatin fibers indicating that PM-PC4 might be involved in higher order chromatin

organisation (as depicted in the models of representative array alongside in Figure 3.1.11.3A and C). On the otherhand PC4 is unable to further compact H1-bound array which still exhibits unfolded nucleosome array (Figure 3.1.11.3B and D). The diameter of PM-PC4 bound H1-array are significantly smaller than the unmodified PC4 bound H1-array (Figure 3.1.11.3E). PM-PC4 starts precipitating H1-bound chromatin at a concentration where WT PC4 starts compacting H1-bound array (Figure 3.1.11.2D). These results thus indicate that the ability of PM-PC4 to further compact and assist linker H1 to form higher order structures suggesting that phosphorylation could assist PC4-mediated compaction function and thereby complementing another chromatin protein as linker H1 to form higher order nucleosomal structures.

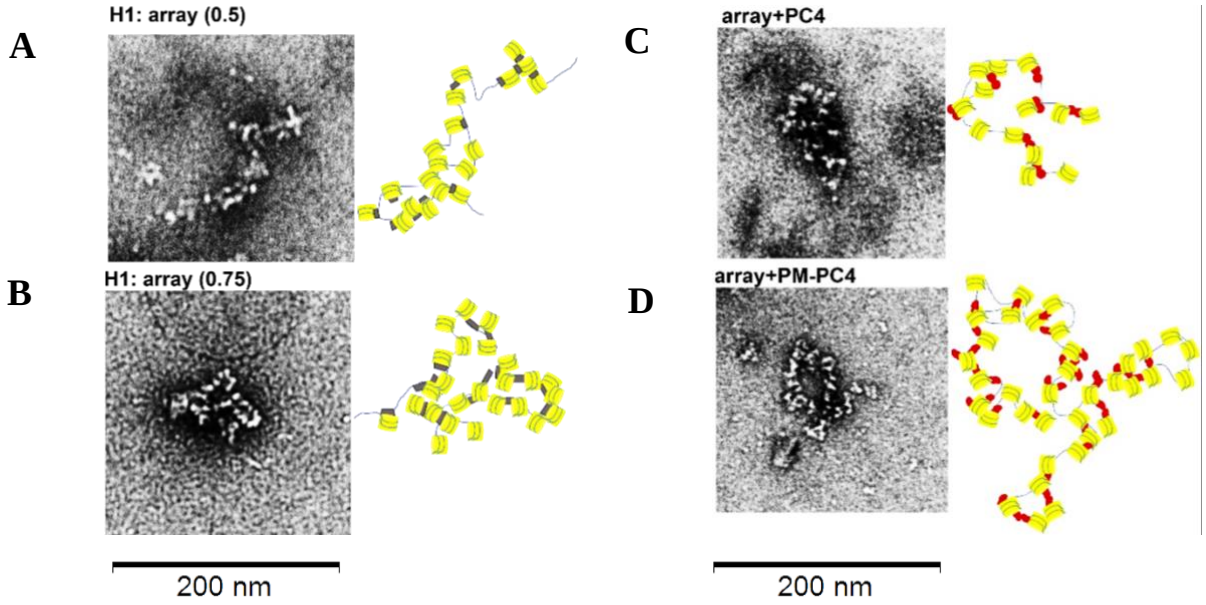

Figure 3.1.11.1: Phosphorylation enhances PC4 mediated condensation of H1 bound array forming higher order structures. (A-B) EM images of H1-array in the ratio of H1: NCP of 0.5 and 0.75 respectively, (C-D) WT PC4 and PM-PC4 containing array at 1uM respectively.

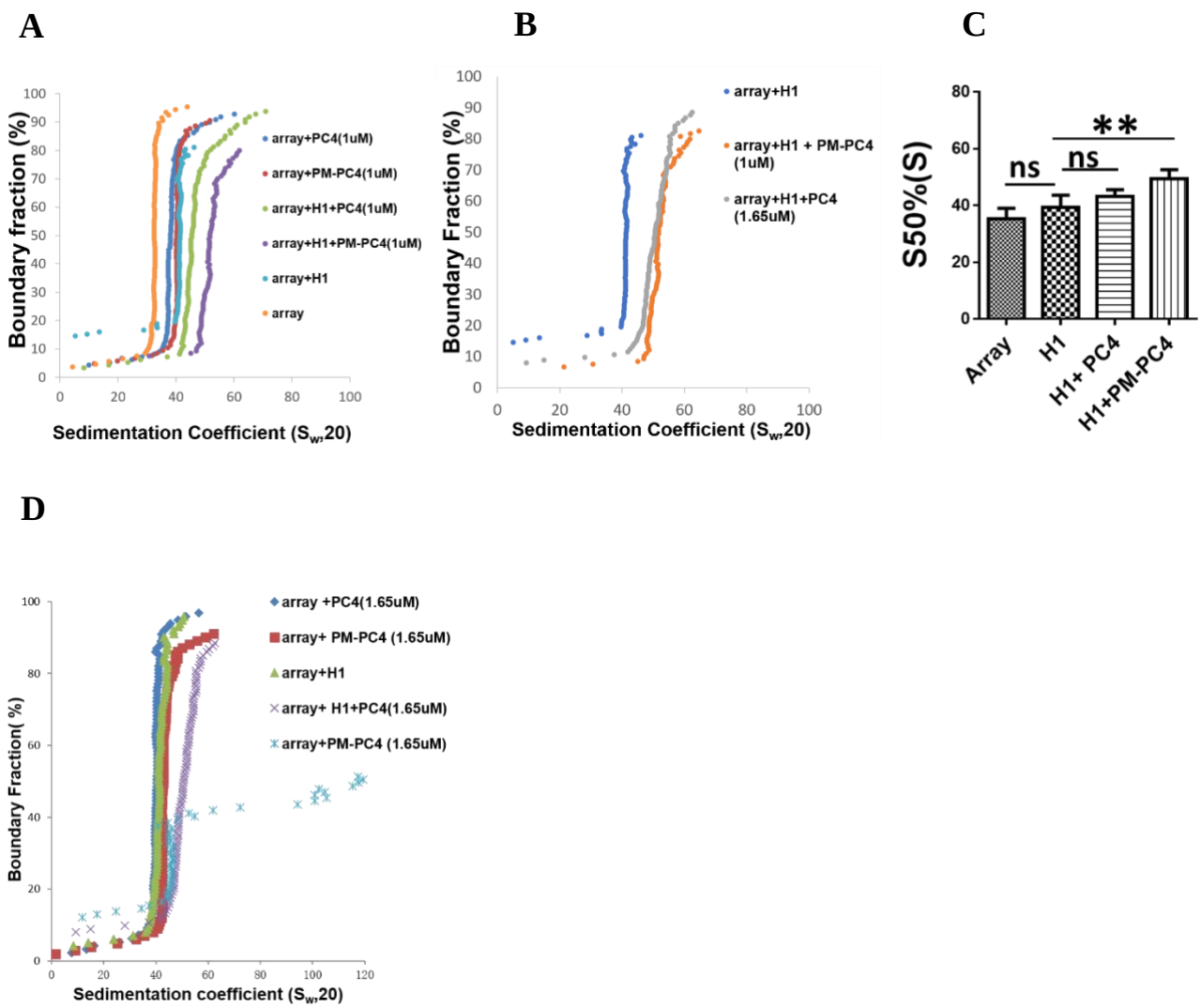

Figure 3.1.11.2: Phosphorylation enhances PC4 mediated condensation of H1 bound array forming higher order structures. (A)Sedimentation velocity analysis by analytical ultracentrifugation of H1 bound nucleosome array with PM-PC4 and WT-PC4. A nucleosome array without any protein is used as a control. (B) Sedimentation velocity analysis by analytical ultracentrifugation of H1 containing chromatin with PM-PC4 and WT-PC4. H1 containing nucleosome array is used as a control. (C) Sedimentation coefficient values from (A) at a boundary fraction of 50% (n=3). Data represent the means ± SD. The S50%(S) were statistically analysed by ordinary one-way ANOVA, Sidak's multiple comparisons test as well as Student's paired t-test (*p<0.05,**p<0.01,***p<0.001,ns-non-significant. (D) Sedimentation velocity analysis of H1 containing chromatin with 1.65uM of PM-PC4 and WT PC4

showing PM-PC4 starts aggregating the H1 chromatin sample. A nucleosome array without any protein is used as a control indicating that PM-PC4 bound array at 1.65uM starts precipitating the DNA.

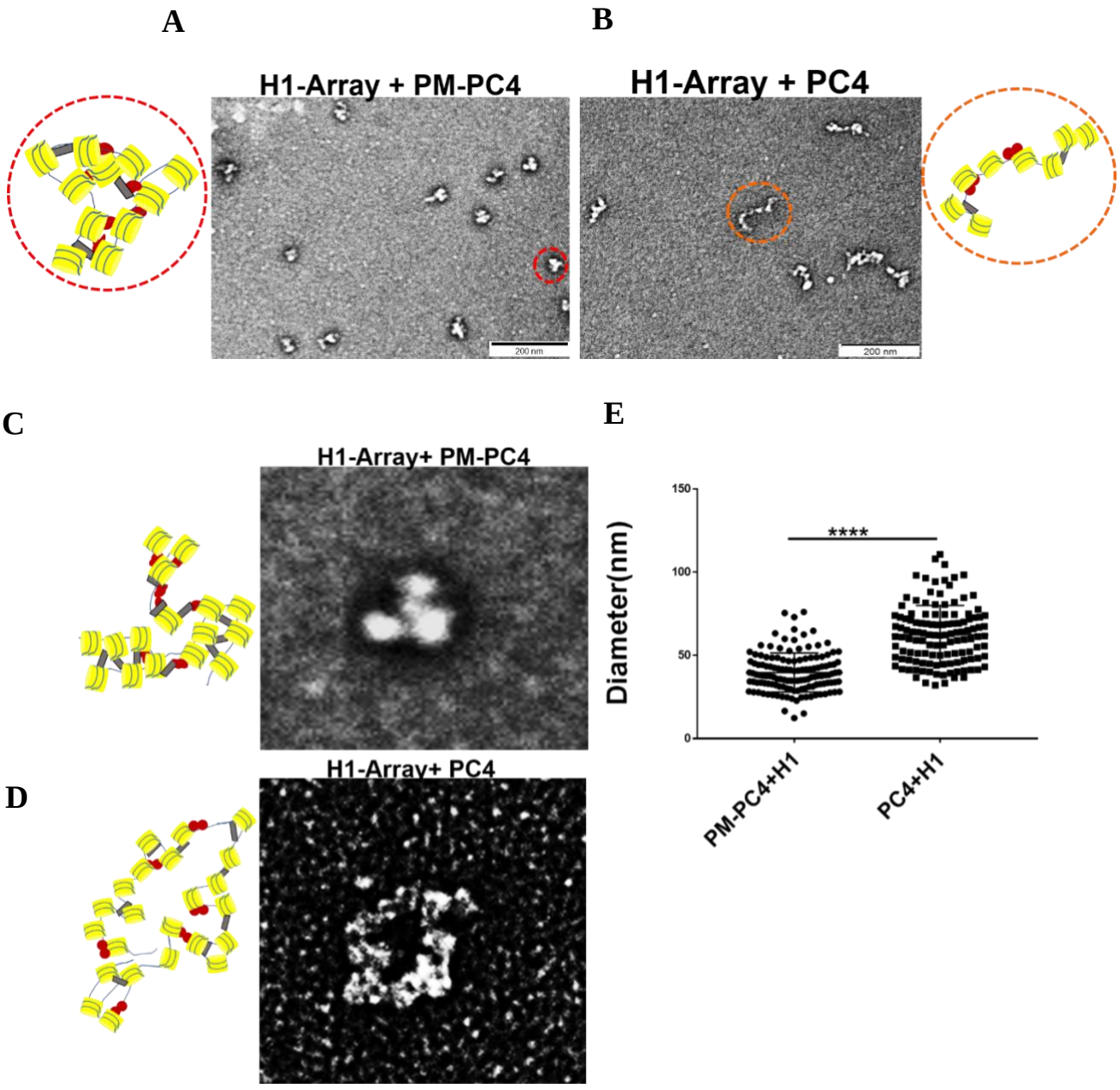

Figure 3.1.11.3: Phosphorylation enhances PC4 mediated condensation of H1 bound array forming higher order structures. (A-B) EM images of PM-PC4 and PC4 bound H1 containing array respectively showing the structure formed upon PM-PC4 and PC4 mediated compaction of H1-array respectively.

(C-D) EM image of a single PM-PC4 and PC4 bound H1 containing array respectively showing the compaction induced upon adding PM-PC4 and PC4 to H1-array respectively. Models of a representative condensed array shown in a dotted circle alongside. (E) Distributions of diameters (in um) of PM-PC4 and PC4 bound compacted array particles. No. of particles measured = 132. Data represent the means ± SD. The S50%(S) were statistically analysed by Student's unpaired t-test (*p<0.05,**p<0.01,***p<0.001,ns-non-significant).

3.1.12 Phosphorylation modulates interaction of PC4 with core histones

Earlier studies suggested that PC4 interacting preferentially with histone H3 and H2B and this interaction might contribute to PC4 mediated chromatin condensation (Das C. et al., 2006). Since PC4 being a highly abundant nuclear protein that is present majorly in the phosphorylated state, we wanted to investigate whether phosphorylation alters the strength of interaction of PC4 that is bound to the chromatin. To study this, we carried out Flag immuno-pull down from the chromatin fraction after sequential salt extraction from the nuclear extract, that is enriched in histones. The results upon probing the IP and input by western blotting, indicates that Flag tagged PC4 (PC4) and phosphomimic PC4 (PM-PC4) exhibits greater interaction with histone H3 and H2B (Figure 3.1.12A and B, lane 1 and lane 2) whereas Flag-phospho-mutant shows weaker interaction with H3 (Figure 3.1.12 A and B, lane 3) and no interaction with H2B is observed upon pull down (Figure 3.1.12 A and B, lane 3). Thus, phosphorylation modulating interaction of PC4 with H3 and H2B in the chromatin fraction inside cells (Figure 3.1.12) might account for the phosphorylation mediated chromatin compaction observed along with its interaction with linker histone H1.

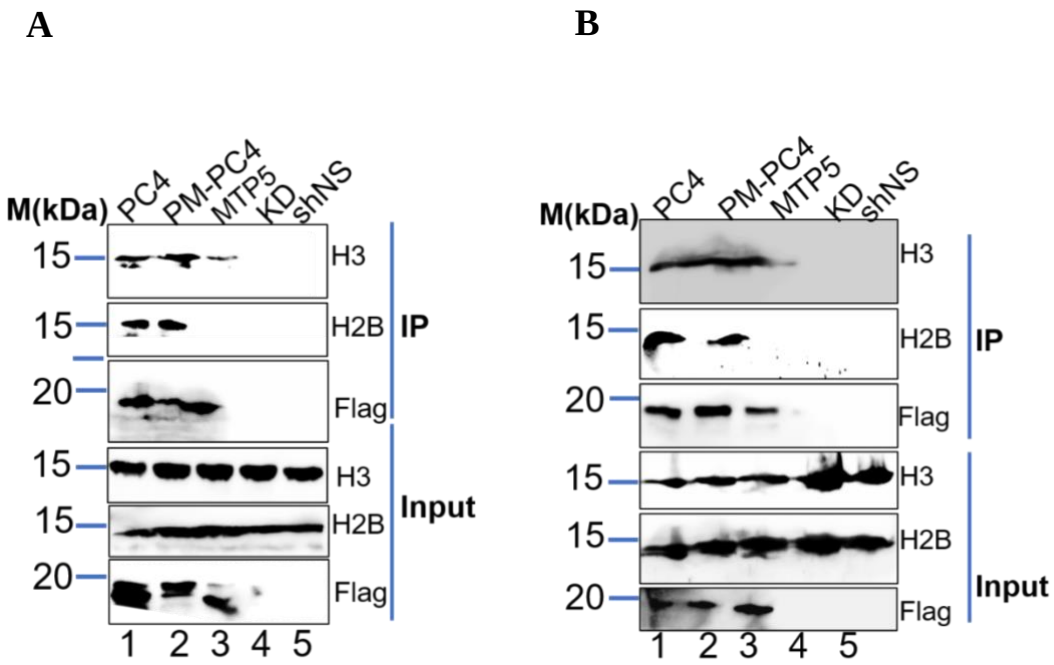

Figure 3.1.12: Phosphorylation modulates interaction of PC4 with core histones: (A and B) Immuno-pulldown using Flag antibody carried out in Flag-PC4, Flag-PM-PC4 and Flag-MTP5 expressing 293cells in PC4 knockdown background from the chromatin fraction and probed with H3 and H2B antibody in IP in two independent biological replicates shown in A and B.

3.1.13 Phosphorylation of PC4 regulates PC4 mediated chromatin compaction in cells

In order to understand how phosphorylation of PC4 mediates chromatin condensation *in vivo*, we studied chromatin compaction in cells by stably transfecting 3X-flag tagged mammalian constructs Flag-PC4 (F-PC4), Flag-Phosphomimic PC4 (F-PM-PC4) and Flag-phospho-defective mutant (F-MTP5) in PC4 knockdown HEK293 (as mentioned earlier) and analysing the sensitivity of the cellular chromatin towards Micrococcal nuclease (MNase) (Figure 3.1.13B). In agreement to previous results showing that knocking down of PC4 results in chromatin decompaction (Sikder S. et al., 2019 and Das C. et al., 2006), indeed we observe that in PC4 KD lane the chromatin is more accessible to

MNase digestion as reflected in higher intensity of mono-nucleosome and relative lane intensity being lower than vector control (shNS) (Figure 3.1.13B, lane 1 vs lane 3 and lane 2 vs lane 4 and Figure 3.1.13 C-D) indicating more open chromatin. F-PC4 and F-PM-PC4 transfection in PC4 knockdown cells significantly rescued the highly de-compacted chromatin state in PC4 Knockdown cells almost to the level of vector control cells as revealed by higher relative lane intensity and lower mono-nucleosome intensity (Figure 3.1.13C and D), which is indicative of a more condensed chromatin state. However, F-MTP5 expressing knockdown cells were still susceptible to MNase digestion like PC4 KD showing greater mono-nucleosome accumulation as compared to vector control cells (Figure 3.1.13B) reflected both in lesser lane intensity and higher mono-nucleosome intensity (Figure 3.1.13C and D). F-MTP5 transfected cells could be more susceptible to MNase digestion than knockdown cells as they show even greater mono-nucleosome accumulation than knockdown cells upon MNase digestion at 3min time point (Figure 3.1.13B). These results thus indicate that phosphorylation of PC4 induces chromatin compaction and could be involved in maintaining higher order chromatin structure *in vivo*.

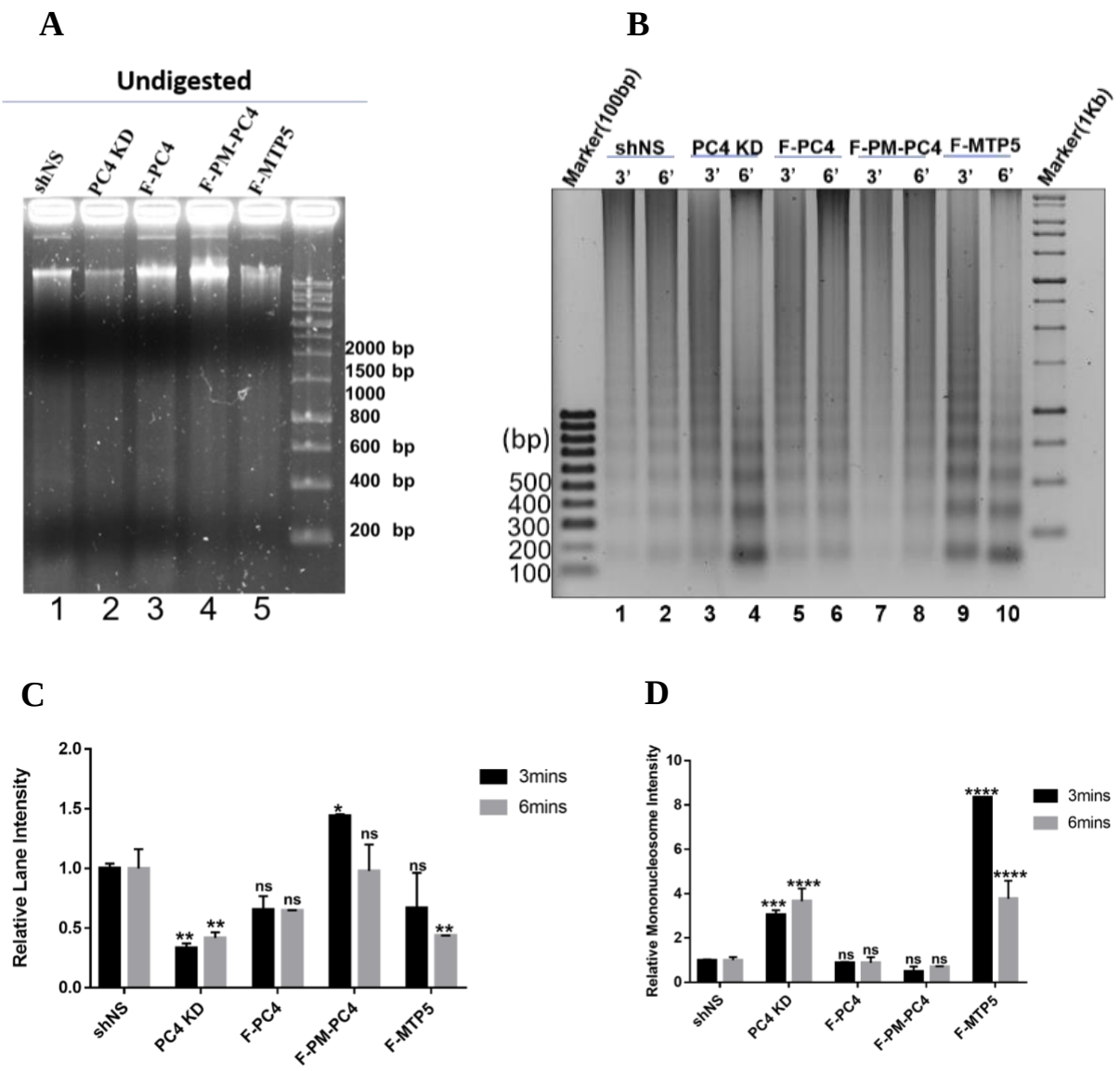

Figure 3.1.13: Phosphorylation of PC4 regulates PC4 mediated chromatin compaction in cells. (A) The undigested chromatin from all the cell lines (B) PC4 knockdown 293 cells were transfected with the indicated plasmids and chromatin fractions were extracted and analyzed by micrococcal nuclease (MNase) sensitivity assay. (C) Quantifications of lane signal intensities in (B) (n=2). Data represent the means ± SD. (D) Quantifications of band signal intensities corresponding to mono-nucleosome in every lane in (B) (n=2). Data represent the means ± SD. The data is statistically analysed by two-way ANOVA, Dunnett's multiple comparisons test (*p<0.05,**p<0.01,***p<0.001,ns-non-significant).

3.1.14 Phosphorylation of PC4 regulates epigenetic state of the cell

Since, analytical ultracentrifugation, electron microscopy and MNase sensitivity assays showed that phosphorylation of PC4 is critical for maintaining the condensed state of chromatin both *in vitro* and in cells, we were interested to find out whether phospho-PC4, is also needed in maintaining the epigenetic state of the cell. Knocking down of PC4 exhibited alteration in the epigenetic state of the cell showing enhanced levels of activation marks like histone H3 lysine9 acetylation (H3K9ac) (Figure 3.1.14 A and B), histone H3 lysine 4 trimethylation (H3K4me3) (Figure 3.1.14 A and C) and concurring with greater chromatin decompaction observed in PC4 knockdown cells, they also exhibited significant reduction in heterochromatin mark, histone H3 lysine di-methylation (H3K9me2) (Figure 3.1.14 A and D). Since H3K9ac and H3K4me3 are the active marks present at the gene promoters, we were also intrigued to see the status of some enhancer marker like histone H2B lysine 5,12,15 and 20 tetra-acetylation (H2Btetraacetylation) which however decreases significantly upon PC4 knockdown (Figure 3.1.14 A and E). However, transfecting F-PC4 and F-PM-PC4 in PC4 KD cells, significantly restored the histone modification state of shNS cells (Figure 3.1.14A-E) whereas F-MTP5 cells still showed significant change (Figure 3.1.14A-E). The activation marks H3K9ac and H3K4me3 remarkably reduced upon transfection of F-PC4 and F-PM-PC4 as compared to PC4 KD cells (Figure 3.1.14 A-C) but not upon F-MTP5 transfection (Figure 3.1.14 A-C). The heterochromatin mark H3K9me2 significantly increases in the F-PC4 and F-PM-PC4 transfected cells compared to PC4 knockdown cells but not in F-MTP5 transfected cells which is indicative of more condensed chromatin state (Figure 3.1.14 A and D). The enhancer mark H2Btetracetylation seems to increase upon F-PM-PC4 transfected cells compared to PC4 knockdown cells (Figure 3.1.14 A and E). Thus, these results clearly indicate the role of PC4

phosphorylation in maintaining chromatin compaction and thereby mediating an epigenetically repressive chromatin state inside the cells.

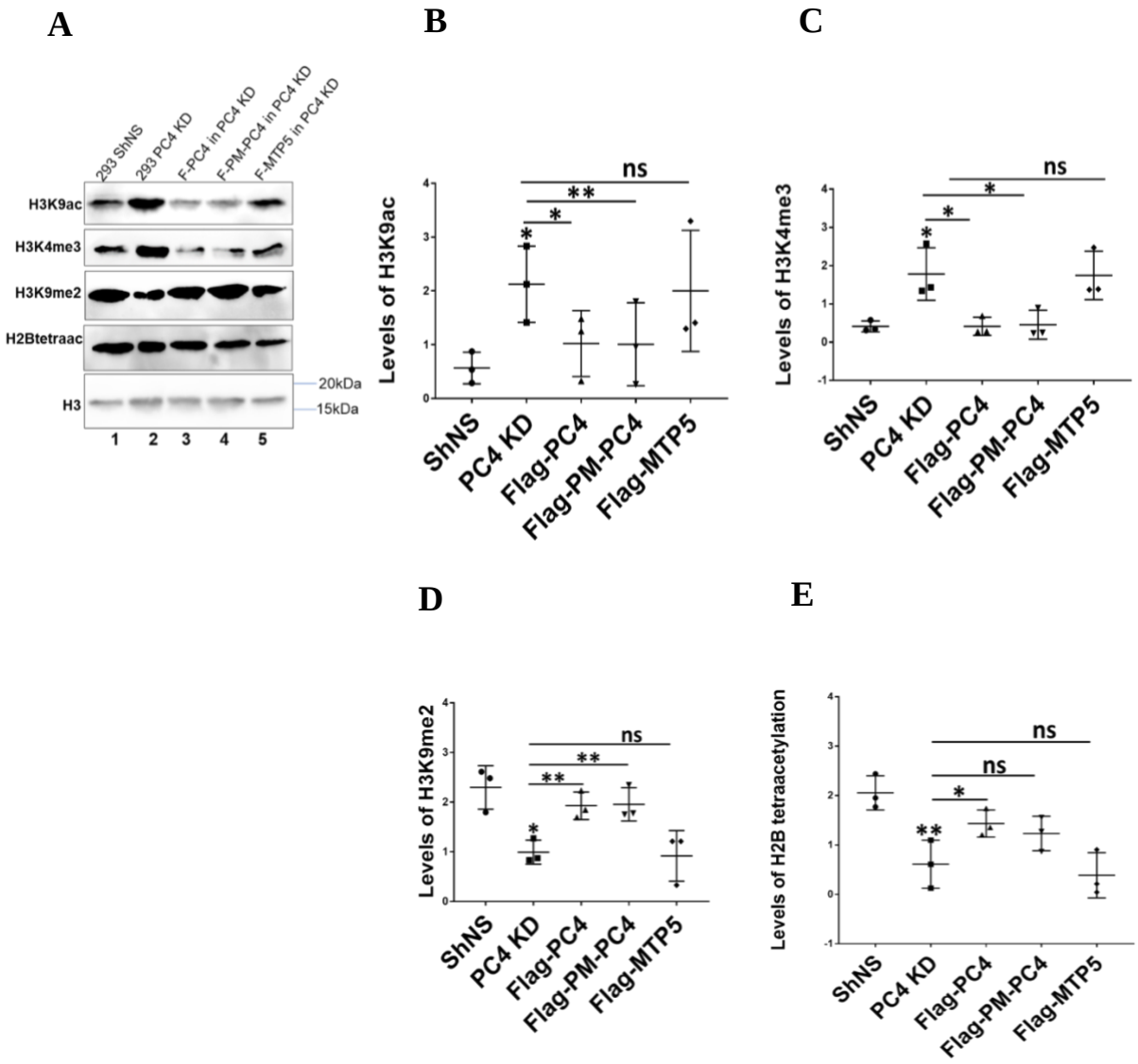

Figure 3.1.14 Phosphorylation of PC4 regulates epigenetic state of the cell: (A) Levels of different epigenetic marks checked by western blotting after transfecting F-PC4, F-PM-PC4 and F-MTP5 plasmids in PC4 knockdown cells. (B), (C), (D) and (E) Quantification of levels of epigenetic marks (n=3). Data represent the means ± SD.The data is statistically analysed by ordinary one-way ANOVA, Sidak's multiple comparisons test (*p<0.05,**p<0.01,***p<0.001,ns-non-significant).

3.1.15: Phosphorylation of PC4 represses genes that are transcriptionally induced upon PC4 knockdown

Earlier studies have shown the involvement of PC4 in REST–CoREST-mediated repression of neuronal gene expression in non-neuronal cells. Silencing of PC4 has been shown to induce histone acetylation at the promoter of neural gene sodium channel 2 (SCN2) and has shown reduced REST-CoREST occupancy at the SCN2 promoter (Das C et al.,2006). A recent study has attributed the role of PC4 in negatively regulating autophagy and maintaining genome integrity (Sikder S. et al., 2019). Earlier results have shown that phosphorylation of PC4 is involved in chromatin compaction thereby maintaining a repressive chromatin state and knocking down of this protein induces histone H3 acetylation at lysine residue 9 (H3K9ac) (Figure 3.1.14A and B). Thus, we investigated whether phosphorylation of PC4 regulates the expression of the core autophagy genes which have H3K9ac enriched at their promoters upon PC4 knockdown. Thus, we investigated whether phosphorylation of PC4 regulates the expression these core autophagy genes. We also tested the expression of three neural genes SCN2, glutamic acid decarboxylase 1 (GAD1), and muscarinic acid receptor 4 (M4) that has been shown to be downregulated upon PC4 silencing (Das C et al.,2006). SCN2, M4 gene expression that is upregulated upon stably knocking down PC4 in 293 cells is repressed back upon transfecting back Flag-PC4 (F-PC4), Flag-Phosphomimic PC4 (F-PM-PC4) but not in Flag-phosphomutant PC4 (F-MTP5) expressing cells (Figure 3.1.15.1A and B). However, such significant differences were not observed for GAD1 expression (Figure 3.1.15.1C). SCN2 and M4 is significantly downregulated in F-PC4 and F-PM-PC4 expressing knockdown cells as compared to PC4 knockdown cells but shows non-significant difference with that of the vector control (shNS) cells whereas in F-MTP5 expressing PC4 knockdown cells SCN2 and M4 expression is significantly upregulated than vector control cells and is similar to PC4 knockdown cells indicating that the

rescue of gene expression is phosphorylation dependent (Figure 3.1.15.1A-B). The core autophagy genes; DRAM1, AMPKα1, AMPKα2, ULK1, and ULK2 were significantly upregulated upon knocking down of PC4 (Figure 3.1.15.2) corroborating to the global hyperacetylation at H3 lysine residue 9 seen upon PC4 knockdown. The expression of these pro-autophagy genes; DRAM1, AMPKα1, AMPKα2, ULK1, and ULK2 seemed to be regulated by phosphorylated PC4 since their expression were significantly decreased comparable to the levels of vector control cells (shNS) upon transfecting back Flag-PC4 (F-PC4), Flag-Phosphomimic PC4 (F-PM-PC4) but not by Flag-phosphomutant PC4 (F-MTP5) (Figure 3.1.15.2 A-E).

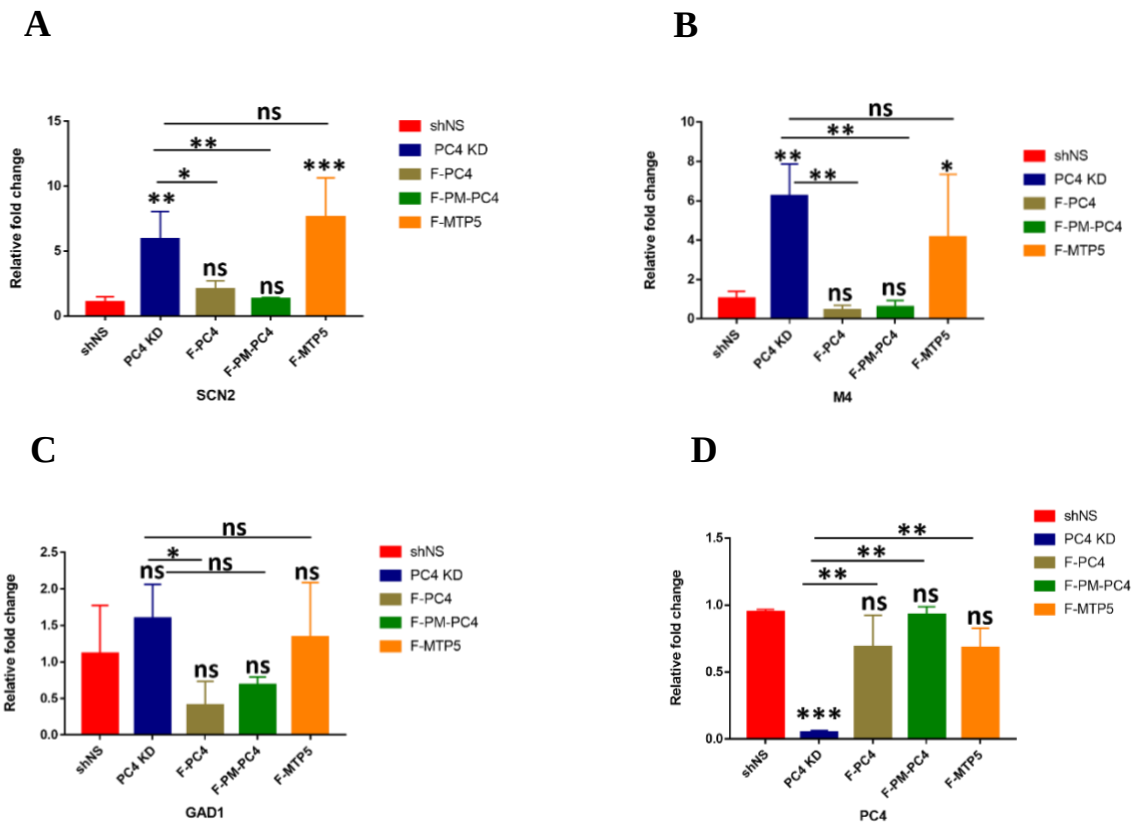

Figure 3.1.15.1: Phosphorylation of PC4 represses neuronal genes that are transcriptionally induced upon PC4 knockdown. Relative expression of (A)SCN2, (B) M4, (C)GAD1 and (D)PC4 in PC4 knockdown cells stably-transfected with WT Flag-PC4 (F-PC4), Flag-phosphomimic PC4 (F-PM-PC4) or Flag-phospho-mutant PC4 (F-MTP5) along with vector control cells (shNS)

determined by real-time PCR. All data represent the means ± SD for n=3. The data is statistically analysed by ordinary one-way ANOVA, Sidak's multiple comparisons test (*p<0.05,**p<0.01,***p<0.001,ns-non-significant).

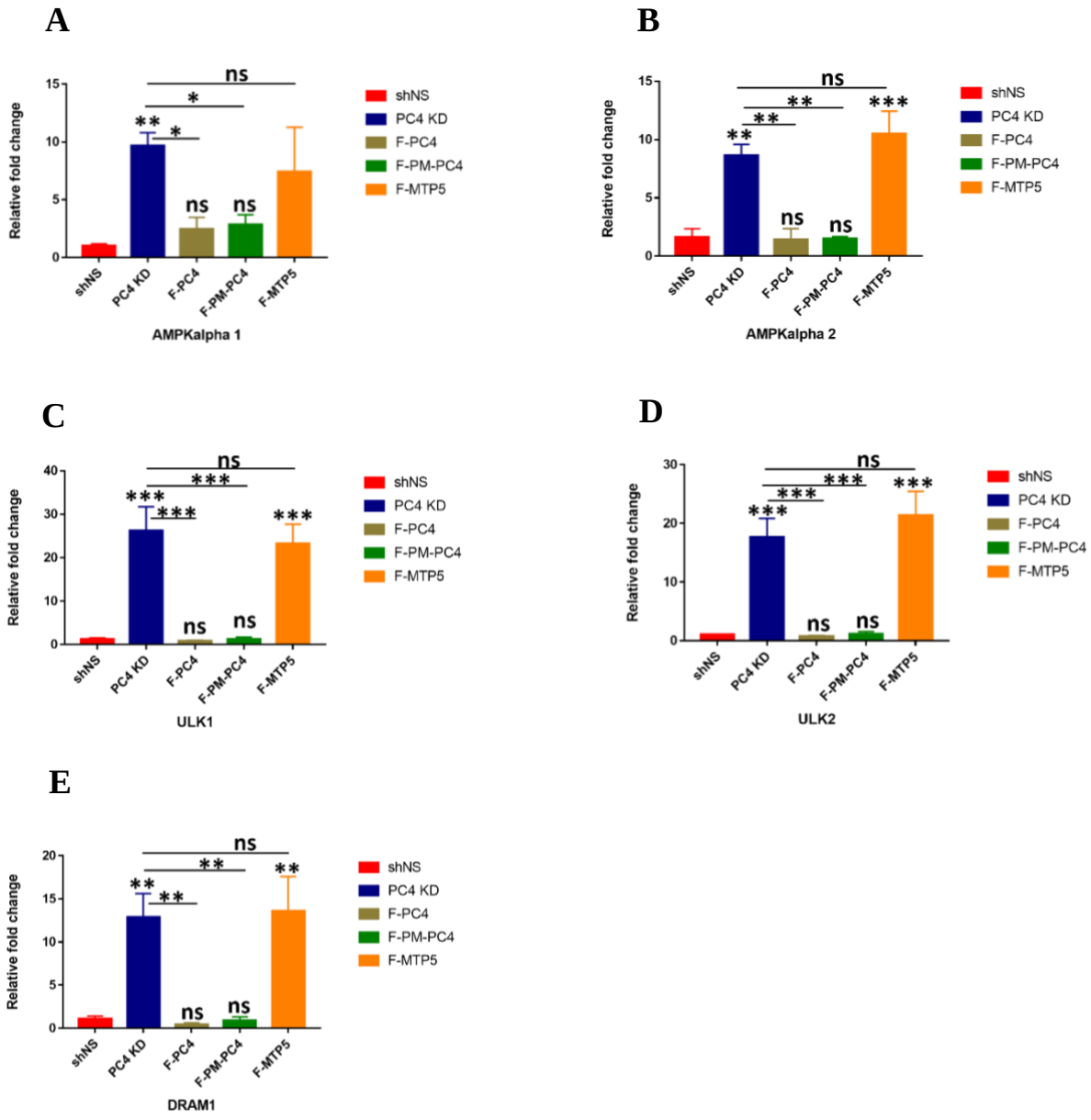

Figure 3.1.15.2: Phosphorylation of PC4 represses autophagy genes that are transcriptionally induced upon PC4 knockdown. Relative expression of (A)AMPKα1, (B)AMPKα2, (C)ULK1, (D)ULK2 and (E)DRAM1 in PC4 knockdown cells stably-transfected with WT Flag-PC4 (F-PC4), Flag-phosphomimic PC4 (F-PM-PC4) or Flag-phospho-mutant PC4 (F-MTP5) along with vector control cells (shNS) determined by real-time PCR. All data represent

the means ± SD for n=3. The data is statistically analysed by ordinary one-way ANOVA, Sidak's multiple comparisons test (*p<0.05,**p<0.01,***p<0.001,ns-non-significant).

3.1.16 Phosphorylation of PC4 negatively regulating the autophagic process

Since we observed that PC4 represses some of the autophagy regulating genes in a phosphorylation dependent manner and to establish the functional link of these gene expression results with cellular autophagy status, we looked into the Microtubule-associated proteins 1A/1B light chain 3B (LC3) and Sequestosome-1 (p62) levels both at basal conditions as well as upon treatment with Bafilomycin A (Baf), a known small molecule inhibitor autophagy (Figure 3.1.16).

LC3 exist in two forms LC3I and LC3II, LC3I gets cleaved and lipidated to generate LC3II, which goes and binds to inner and autophagosomal membrane and migrates faster on the SDS-PAGE. The conversion of LC3I to lipidated LC3II form reflects the induction of autophagy process, which is upregulated in PC4 knockdown cells but decreases upon expressing Flag-PC4 (PC4), Flag-Phosphomimic PC4 (PM-PC4) (Figure 3.1.16.1, lane 2 vs lane 3and lane 4) but not by Flag-phospho-mutant PC4 (MTP5) which shows higher LC3II levels (Figure 3.1.16.1, lane 2 vs lane 5). On the other hand, degradation of p62 which is an autophagosomal cargo indicates completion of autophagy process. p62 levels are significantly higher in Flag-PC4 (PC4), Flag-Phosphomimic PC4 (PM-PC4) expressing PC4 knockdown cells comparable to vector control cells but not in Flag-phosphomutant PC4 (MTP5) expressing cells which shows lower levels of p62 similar to PC4 knockdown 293 cells (Figure 3.1.16.1, lane 2 vs lanes 3 and 4). PC4 expression in the mutants was similar to that of vector control cells but was significantly higher as compared to PC4 knockdown cells thus accounting for the rescue effects that we observe (Figure 3.1.16.1).

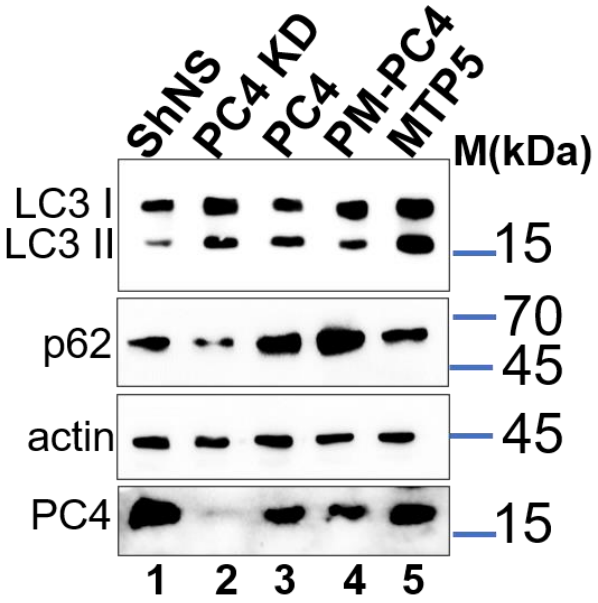

Figure 3.1.16.1: Phosphorylation of PC4 negatively regulating the autophagic process: Studying the levels of autophagy upon transfecting Flag-PC4 (F-PC4), Flag-Phosphomimic PC4 (F-PM-PC4) and Flag-phospho-defective mutant PC4 (F-MTP5) in PC4 knockdown HEK293 by probing with LC3 and p62 antibody while actin was used as loading control.

To fortify the role of PC4 phosphorylation in regulating autophagy we pre-treated the cells with a known small molecule autophagy inhibitor, Bafilomycin A (Baf) which is known to inhibit autophagy by disrupting the autophagic flux by inhibiting the lysosomal proton pump V-ATPase, resulting in a defect in autophagosome-lysosome fusion (Gozuacik D & Kimchi A, 2004). Treatment with Bafilomycin A delineates that both autophagic induction, revealed by the increase in LC3II levels (Figure 3.1.16.2, LC3II panel, lanes 3 and 4 vs lanes 1 and 2), and autophagic flux, indicated by the degradation of p62 (Figure 3.1.16.2, p62 panel, lanes 3 and 4 vs lanes 1 and 2), are induced in PC4 KD cells as compared to shNS.

Wild type PC4 and phosphomimic-PC4 expressing PC4 knockdown cells have reduced LCII levels in untreated conditions compared to the PC4 knockdown cells (Figure 3.1.16.2 lane 3 vs lanes 5 and 7) and is induced upon Baf treatment

(Figure 3.1.16.2 lane 5 vs lane 6 and lane 7 vs lane 8). On the other hand, phospho-mutant PC4 (MTP5) expressing knockdown cells have higher levels of LC3II in untreated conditions as the PC4 knockdown cells (Figure 3.1.16.2 lane 3 vs lane 9) which is induced further upon Baf treatment indicating higher levels of autophagy in cells (Figure 3.1.16.2 lane 9 vs lane 10). Degradation of p62 was observed in PC4 knockdown and MTP5 cells in untreated conditions (Figure 3.1.16.2 lane 3 and lane 9 vs lane 1, p62 panel) and it accumulates upon Baf treatment (Figure 3.1.16.2 lane 3 vs lane 4 and lane 9 vs lane 10, p62 panel) whereas p62 levels are higher in PC4 and PM-PC4 expressing knockdown cells compared to the PC4 knockdown cells in untreated conditions indicating autophagic levels being reduced (Figure 3.1.16.2 lane 3 vs lanes 5 and 7, p62 panel). Interestingly we also observed LC3I levels to be reduced in PC4 and PM-PC4 expressing knockdown cells that could reflect the transcriptional repression effect mediated by Phospho-PC4 on MAP1LC3B gene (Figure 3.1.16.2 lane 5 and lane 7, LC3I panel). Thus, these results indicate that both induction of autophagy (LC3II) as well as autophagic flux (p62) is enhanced upon PC4 knockdown and the levels are reduced back in a PC4 phosphorylation dependent manner.

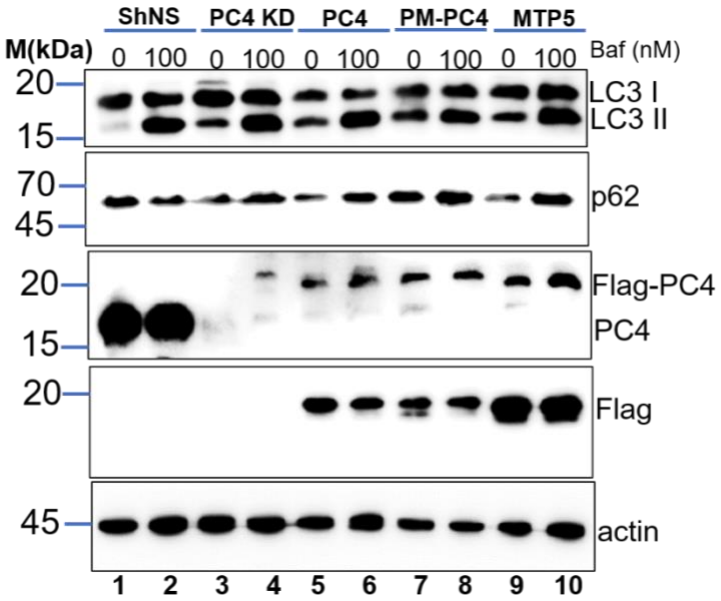

Figure 3.1.16.2: Phosphorylation of PC4 negatively regulating the autophagic process: Studying the levels of autophagy upon transfecting Flag-PC4 (F-PC4), Flag-Phosphomimic PC4 (F-PM-PC4) and Flag-phospho-defective mutant PC4 (F-MTP5) in PC4 knockdown HEK293 followed by Bafilomycin A (Baf) treatment at 100nM for 2 hours by probing with LC3 and p62 antibody while actin was used as loading control.

3.1.17 Summary

Earlier studies have shown PC4 to be a component of the chromatin (Das C et al.,2006) but the exact mechanism of PC4 mediated chromatin compaction was not known. This study however reveals a more physiological relevance of this protein modification on PC4 chromatin functions. It was therefore quite interestingly obvious for us to look deeper into significance of this modification in cells where it is abundantly present. We initially identified the critical serine residues important for CKII mediated phosphorylation by generating several mutants and conducting *in vitro* kinase assay using them. To address the relevance of phsophorylation on PC4 function, we generated both phosphomimic as well phospho-defective mutants after identifying the critical serine residues. A

novel finding in this study is the ability of PC4 to interact with chromatin protein linker H1 only upon phosphorylation. This finding provides a hint as to why PC4 is majorly present in the phosphorylation state inside cells since this post-translational modification determines the interaction of PC4 with chromatin components; linker H1, histone H3 and H2B.

The phosphorylation dependent interaction of PC4 with the H1, encouraged us to investigate the role of PC4 phosphorylation in chromatin organization in a linker histone H1 containing nucleosomal system which showed that phosphomimic PC4 enhances the compaction of H1 bound array. This indicates the possibility that phospho-PC4 interaction with linker H1, might be involved in maintaining higher order chromatin structure. Nucleosomal compaction studies show that Phosphomimic PC4 which mimicked the negative charge of a phosphorylated PC4 achieved higher sedimentation coefficient value (S50) compare to unmodified PC4. Thus, phosphorylation enhances the efficiency of PC4's chromatin condensation ability. Our study shows that phosphorylation not only regulates PC4 mediated chromatin compaction in a nucleosomal system but also *in vivo*. PC4 being a chromatin protein; upon knockdown of PC4, cells exhibit chromatin decompaction that is rescued by expressing back wild type PC4 which gets phosphorylated inside cells and phosphomimic PC4 but not by phospho-defective mutants as indicated by MNase assay. This study also addresses the effect of PC4 phosphorylation onto the epigenetic state of the cell. PC4 has been shown to be critical for genome integrity and knocking down of PC4 leads to alteration in the epigenetic state (Sikder S. et al., 2019). Interestingly we found that this alteration in the epigenetic state that is observed upon PC4 knockdown is rescued upon transfecting F-PM-PC4 and F-PC4 but not upon transfecting F-MTP5 which clearly tells that phosphorylation of PC4 regulates the epigenetic state of the cell. PC4 phosphorylation mediated chromatin condensation may lead to a repressed epigenetic state as indicated by the levels of activation marks like

H3K9ac and H3K4me3 and the level of heterochromatin mark H3K9me2. The repressed epigenetic state mediated by PC4 phosphorylation may lead to gene repression in cells. Therefore, we next addressed the effect of PC4 phosphorylation on gene expression. The repression of the neural genes; SCN2 and M4, that has been shown earlier to be repressed in non-neuronal cells by PC4 mediated repressor complex indicate that phosphorylated PC4 and phosphomimic PC4 could repress back these gene expression levels to that of the vector control cells but phospho-defective mutant failed to do so. Some of the autophagy regulating genes that earlier has been shown to upregulated upon PC4 silencing due to induction of H3K9ac levels at their promoters (Sikder S. et al., 2019) have also been shown to be repressed in a PC4 phosphorylation dependent manner. Here we see that indeed the negative regulation of autophagy genes mediated by PC4 phosphorylation has also been reflected at the level of autophagic process. These Flag-expressing PC4 knockdown cells however expressed PC4 at the same level. Neither the expression of wild type PC4, phosphomimic PC4 and phospho-defective mutants were different nor did they alter PC4 localization which indicates that PC4 mediated chromatin condensation leading to gene repression is a phosphorylation dependent phenomenon.

3.2. Understanding the Implications of p300 mediated acetylation of PC4 on its coactivator function and probable role in cancer manifestation

3.2.1 General Introduction

PC4 was initially discovered to be a transcriptional co-activator and PC4 facilitates activator dependent transcription by RNA pol II through direct interactions with the general transcription factors as well as other transcriptional activators like p53, Tat, BRCA1, AP2 (Banerjee S, 2004, Haile D1999, Kannan P, 1999 and Holloway., 2000). PC4 being majorly present in the phosphorylated state inside the nucleus and phosphorylation of PC4 being inhibitory to its co-activator function suggest that a different form of PC4 being involved in transcriptional activation. Since earlier evidence suggested the induction of its double strand DNA binding ability, which is required for its co-activation function (Kaiser K., Steizer G., and Meisterernst M., 1995), upon acetylation by p300 (Batta K and Kundu T.K.,2007); we hypothesized whether acetylation of PC4 mediates its co-activator function. Acetylation mediated by KAT3B or p300 imparts enhanced dsDNA binding ability, a unique DNA bending property, enhanced interaction with activator p53 which in turn enhances DNA binding and transactivation function of p53 (Batta K. and Kundu T.K., 2007) are indicative of involvement of acetylated PC4 with transcription. In order to study the physiological relevance of acetylated PC4, we need to first detect the presence of acetylated form of PC4. Therefore, we generated an acetylation-specific antibody. We first characterised the specificity of the antibody both in *in vitro* by HAT assays using acetylation defective mutants as well in cellular assays by targeting p300 using both siRNA and small molecule approach.

For further understanding of the physiological role of acetylated PC4 and its implications, we employed oral cancer model system because it provides a p300

mediated hyperacetylated environment as shown in earlier reports (Arif M. et al., 2010 and Shandilya J., et al., 2009). An important implication of non-histone protein acetylation has been observed in oral cancer where upon acetylation of NPM1, a non-histone substrate of p300, the localisation of the protein changes from the nucleolus to the nucleoplasm leading to RNA Polymerase II-mediated transcription co-activation and gene expression promoting oral carcinogenesis (Shandilya et al., 2009). Often non-histone protein acetylation like p53 can fine tune the enzymatic activity of p300 through the enhancement of p300 autoacetylation which then accumulates near the transcription start sites. The Gain-of function mutant p53, known to impart aggressive proliferative properties in tumor cells, also activates p300 autoacetylation (Kaypee S. et al., 2018). The histone chaperone NPM1 which gets acetylated by p300 is hyperacetylated in oral cancer patients, also seems to be a specific inducer of p300 autoacetylation through a reversible binding between NPM1 and p300 which can modulate p300 acetyltransferase activity and this induction of p300 autoacetylation could be the cause of NPM1-mediated tumorigenicity (Kaypee S et al., 2018). PC4 being a substrate of p300 and a global regulator of p53 (Banerjee S et al., 2004, Batta K and Kundu T.K.,2007 and Mondal P. et al., 2019), oral cancer provides a physiological context of understanding the implications of acetylated PC4 in transcriptional activation.

A

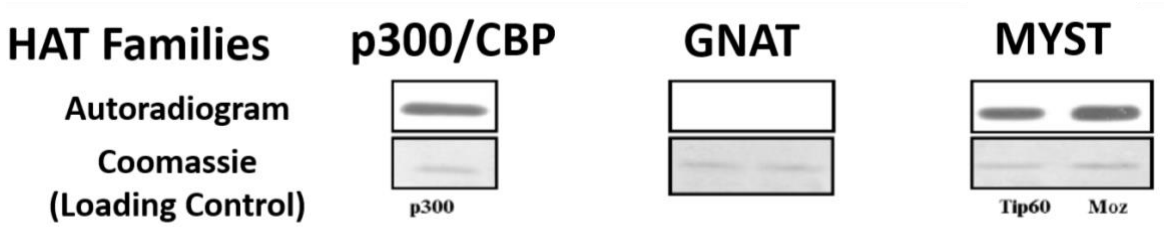

B

MPKSKELVSSSSSGSDSDSEVDKKL**K**R**K**KQVAPEKPVKKQKTGETSRALSSS

KQSSSSRDDNMFQIG**K**MRYVSVRDFKGKVLIDIREYWMDPEGEMKPGRKGI

SLNPEQWSQLKEQISDIDDAVRKL

Figure 3.2.1: (A) *In vitro* HAT assay with recombinant PC4 with full length enzymes from different KAT families indicating PC4 being acetylated by KAT3B or p300 (Figure adapted from Kumari S, and Kundu TK unpublished). (B) PC4 protein sequence indicating the high scoring acetylation sites in green. Flag tagged PC4 transfected in Hela cells were immuno-pulled down for mass spectrometric analysis.

3.2.2 Identification of residues critical for p300 mediated acetylation *in vitro*

To assess the existence of PC4 acetylation *in vivo*, it is essential to find out the lysine residues getting acetylated in the cell. Therefore, FLAG tagged PC4 mammalian construct was transfected transiently into Hela cells and FLAG-PC4 was pulled down using M2-agarose beads. Bead bound proteins were resolved in SDS-PAGE and the band corresponding to PC4 (Batta K and Kundu TK, unpublished) was subjected to in gel tryptic digestion followed by MALDI-TOF analysis. Peptide mass fingerprinting data suggested that at least four lysine residues (K26, K28, K53, K68) (Figure 3.2.1B) in PC4 gets acetylated (Batta K and Kundu TK, unpublished). C-terminal six histidine tagged PC4 acetylation

defective mutant clones were transformed and expressed in *E. coli* BL21 to purify the acetylation defective proteins.

Since these four lysine residues (K26, K28, K53, K68) were high scoring sites to get acetylated in PC4 (Figure 3.2.1B), we wanted to study whether these sites were important for p300 mediated acetylation of PC4. Therefore, an *in vitro* acetylation assay was carried out using wild type PC4-His6 along with other acetylation defective mutants PC4K26 28R, PC4K53 68R and PC4K5R (another mutant where lysine at 5th residue is mutated to arginine, this site was not a high scoring acetylation site according to mass spec analysis was also checked for its effect on p300 mediated acetylation). 500ng of each of the protein substrate was incubated with 20,000 counts of baculovirus expressed recombinant full length p300 enzyme (enzyme activity determined by filter binding assay) and [^{3}H]-acetyl CoA at 30ºC for 30mins in 1X HAT buffer for the HAT reaction to occur followed by gel assay to finally get the intensity profiles for the levels of acetylation on X-ray films. Acetylation of PC4 K53 68R and PC4K26 28R are highly compromised as compared to PC4 wild type indicating that Lysine 53 ,68, 26 and 28 might be critical for p300 mediated acetylation of PC4 (Figure 3.2.2 A, compare lane 5 vs lane 8 and lane 5 vs lane 7) with PC4 K53 68R showing the least acetylation (Figure 3.2.2A, compare lane 6 vs lane 8 and lane 7 vs lane 8) among the other mutants and PC4K5R did not show much change in the acetylation levels compared to wild type (Figure 3.2.2A, compare lane 5 vs lane 6). The fold change in the acetylation level compared to wild type PC4 is plotted (Figure 3.2.2B).

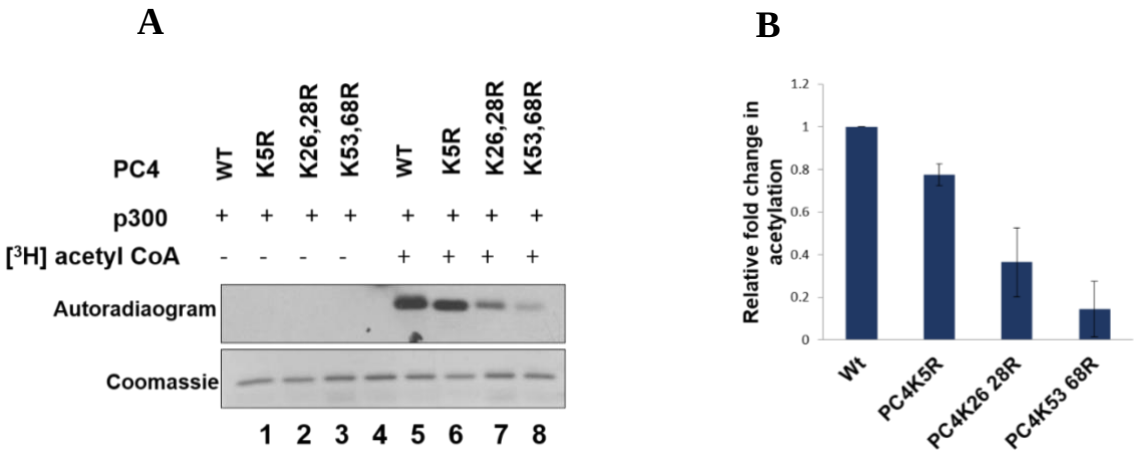

Figure 3.2.2: Identification of residues critical for p300 mediated acetylation *in vitro*: (A) *In vitro* acetylation assay using C-terminal his tagged bacterial expressed recombinant PC4 (wild type) and acetylation defective PC4 mutants was carried out with baculovirus expressed recombinant full length p300 enzyme for 30mins at 30ºC. (B) The fold change in the acetylation level compared to wild type PC4 is plotted showing that lysine residues 53, 68, 26 and 28 might be critical for p300 mediated acetylation of PC4. Coomassie shows equal protein loading.

3.2.3 Characterisation of PC4 acetylation specific antibody

As stated earlier in order to understand the physiological relevance of acetylated PC4 we generated a polyclonal antibody against two acetylated lysine residues corresponding to acetylated lysines26 and 28 of PC4 protein. The PC4K26 28ac antibody was then studied for its specificity for acetylated PC4 and whether these sited were indeed specific for p300 mediated acetylation.

3.2.3.1 Acetylated Lysine 26 and 28 residues selected for antibody generation

We observed by in vitro HAT assay that when lysine 26, 28 and lysine 53, 68 were mutated in combination, p300 mediated acetylation of PC4 was highly compromised. A peptide containing two acetylated lysine residues corresponding to acetylated lysines26 and 28 of PC4 protein was designed based on the best predicted antigenicity value (Immunomedicine Tools: online antigenicity

prediction site) and hydrophobicity value (PEPTIDE 2.0/ ExPASy Bioinformatics Resource Portal site). The antigenicity index of the peptide against acetylated lysines26 and 28 of PC4 were higher than that of the peptides generated against acetylated lysines53 and 68 of PC4 (Figure 3.2.3.1A) since the two lysine 26 and 28 residues were closer to each other than the lysine residues 53 and 68. Therefore we generated acetylation specific antibody using the former peptide against acetylated lysine 26 and 28, the two highly conserved residues across species (Figure 3.2.3.1B).

A

Peptides generated against K26 and K28

	Antigenecity index
KLKRKKQVAP	1.0369
KLKRKKQVA	1.0339
VDKKLKRKKQV	1.0382
KKLKRKKQVAP	1.0272
KKLKRKKQVA	1.0235
EVDKKLKRKKQVAP	1.0285
EVDKKLKRKKQVA	1.0258

Peptides generated against K53 and K68

	Antigenecity index
SSKQSSSSRDDNMFQIGKMR	0.9492
SKQSSSSRDDNMFQIGKMR	0.9459
SKQSSSSRDDNMFQIGKM	0.9500
ALSSKQSSSSRDDNMFQIGKMR	0.9681
LSSKQSSSSRDDNMFQIGKMR	0.9636

B

Positive Coactivator 4 (PC4)

26 28

Homo sapiens	MPKSKELVSSSSSGSDSDSEVDKKLKRKKQVAPE
Mus musculus	MPKSKELVSSSSSGSDSDSEVEKKLKRKKQAVPE
Rattus norvegicus	MPKSKELVSSSSSGSDSDSEVEKKLKRKKQVVPE
Pan troglodytes	MPKSKELVSSSSSGSDSDSEVDKKLKRKKQVAPE
Gallus gallus	MPKSKELVSSSSSASDSDSEVDKKAKRKKQAAPE
Xenopus laevis	MPKSKEILSSSSSGSDSDSEVDQKVKRKKQPPPE
Danio rerio	MPKSKEVLSS-TSGSESDGDAETKVKRKKPSTPE

Figure 3.2.3.1: (A) Antigenicity index calculated for peptides against acetylated lysine 26 ,28 and acetylated lysine 53, 68 of PC4 with the highest ones being marked within red box (B)Alignment of PC4 sequence (Homo sapiens) surrounding the two lysine residues 26 and 28 in different species.

3.2.3.2 PC4 K26 28ac antibody specifically probes the acetylated PC4 *in vitro*

An *in vitro* acetylation assay was carried out using wild type PC4-His6 along with the acetylation defective mutant PC4K26 28R with 20,000 counts of baculovirus expressed recombinant full length p300 enzyme (enzyme activity determined by filter binding assay) and cold-acetyl CoA at 30ºC for 30mins followed by western blotting and probed with PC4K26 28ac antibody. The PC4K26 28 ac antibody specifically probed with wild type PC4 which undergoes acetylation and not the acetylation defective mutant (Figure 3.2.3.2, compare lane 5 vs lane 8 and lane 5 vs lane 7).

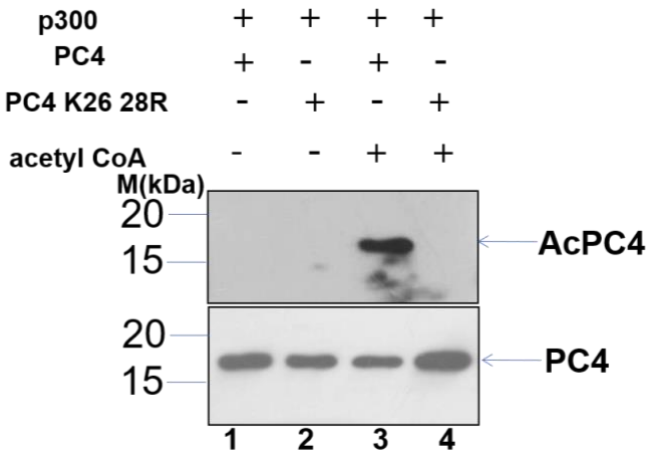

Figure 3.2.3.2 PC4 K26 28ac antibody specifically probes the acetylated PC4 *in vitro*: Polyclonal antibodies were generated in rabbit using this peptide and were checked for their affinity and specificity for acetylated PC4 *in vitro*. Wilde type PC4 and acetylation defective mutant were acetylated by p300 in an *in vitro* acetylation assay along with no acetyl CoA controls. The blot is re-probed with PC4 antibody to show equal protein loading.

3.2.3.2 PC4 K26 28ac antibody specifically probes the acetylated PC4 in cells

PC4K26 28ac antibody doesn't shown any non-specific antigenicity as it specifically probes PC4 in HEK293 cells and does not show any band in HEK293 PC4 knockdown cells (Figure 3.2.3.2A). HEK293 cells were treated with deacetylase inhibitor, sodium butyrate (NaBu),1mM for 24 hours. The cells were then processed for both western blotting and immunofluorescence and tested with PC4K2628ac antibody. The PC4 K26 28ac antibody specifically probed acetylated form of PC4 in cells which is enriched upon NaBu treatment (Figure 3.2.3.2.1B, lane 2 vs lane 1 and Figure 3.2.3.2.2A) along with the acetylated recombinant PC4 protein in western blotting (Figure 3.2.3.2.1B, lane 3). A histone acetylation mark was also checked to verify that the NaBu treatment has worked both for western (Figure 3.2.2.1C, lane 2 vs lane 1) and IF (Figure 3.2.3.2.2 C). PC4 levels however remains unchanged upon NaBu treatment as shown by IF which further validates the specificity of the antibody for the acetylated form of PC4 (Figure 3.2.3.2.2B).

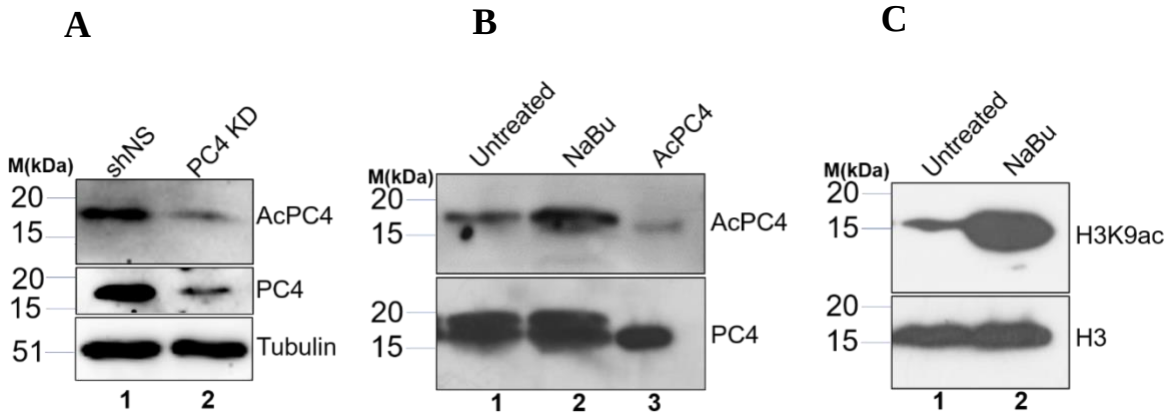

Figure 3.2.3.2.1: PC4 K26 28ac antibody specifically probes the acetylated PC4 in cells. (A) HEK293 and HEK293 PC4 knockdown cells immuno-blotted with AcPC4 and PC4 antibody (B) Immunoblotting of HEK293 cells upon NaBu treatment for 24hours with AcPC4 antibody. PC4 antibody used as loading

control (C) Immunoblotting of HEK293 cells upon NaBu treatment to check H3K9 acetylation levels. H3 were used for protein loading.

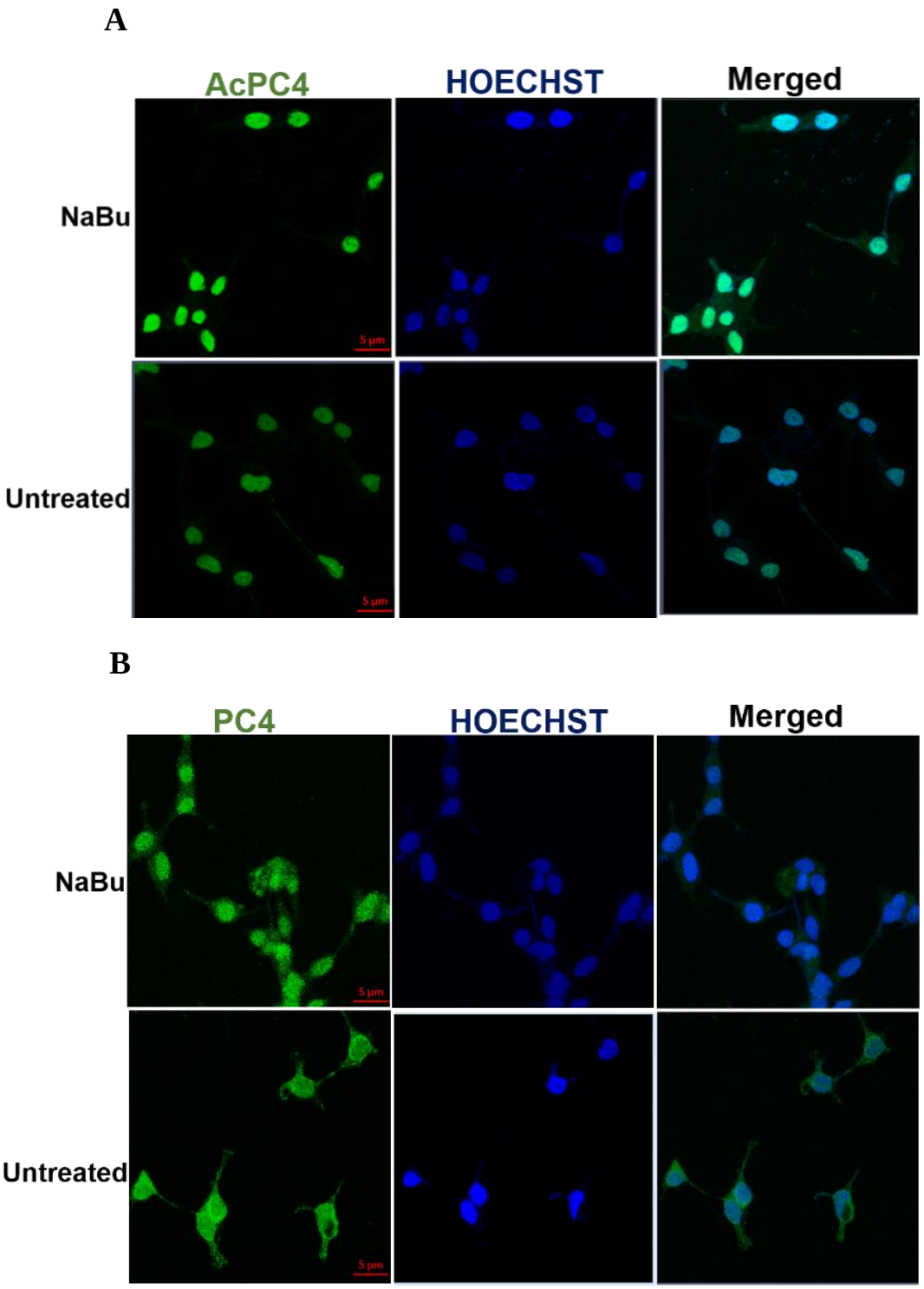

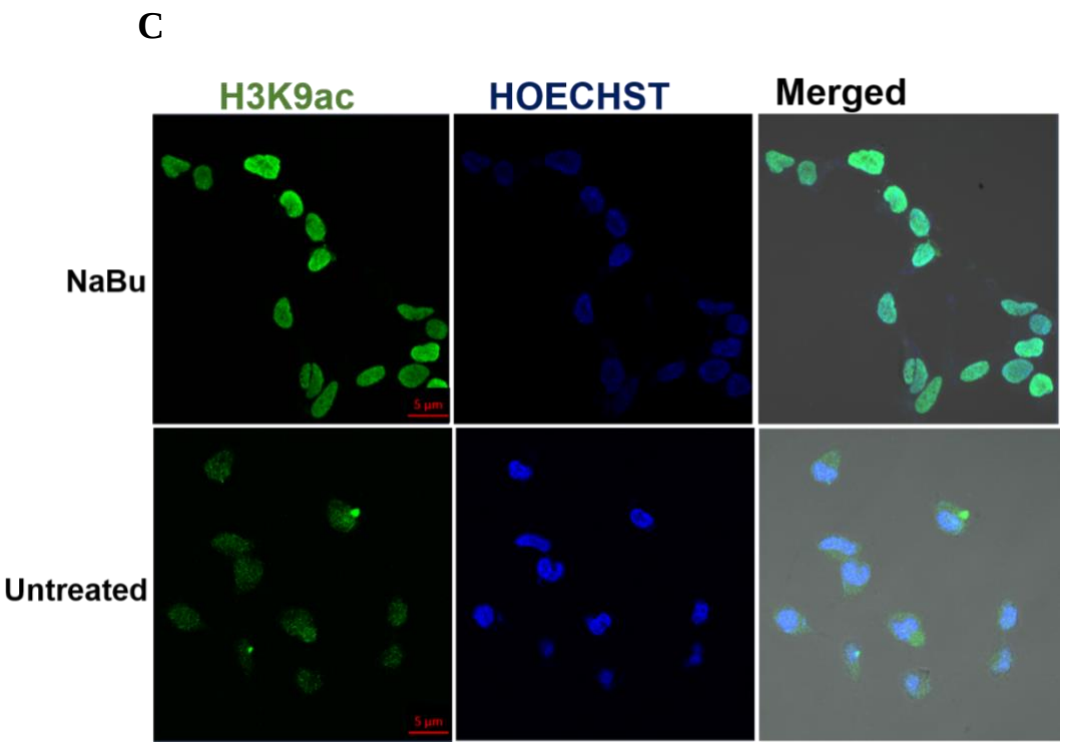

Figure 3.2.3.2.2: PC4 K26 28ac antibody specifically probes the acetylated PC4 in cells. HEK 293 cells treated with NaBu was analysed for the subcellular localisation and levels of (A) AcPC4, (B) PC4 and (C) H3K9acetylation by fluorescent microscopy.

3.2.4 Acetylation of PC4 across cell cycle

3.2.4.1 Localisation of acetylated PC4 during cell cycle

PC4 is a nuclear protein that has been shown to be associated with the chromatin throughout different stages of cell cycle (Das C et al., 2006) . We wanted to study the localisation of acetylated PC4 across cell cycle stages for which cells were grown to 50-60% confluency on polyl-lysine coated coverslips and processed for immunofluorescence by staining with both PC4 and acetylated PC4 antibody. The cells were then visualised by LSM880 microscope from Zeiss under 63xmagnification. Acetylated PC4 is highly present in the interpahse stage of cell cycle and it reduces upon mitosis since the levels gradually decreases during prometaphase and is completely absent from the metaphase cells (Figure

3.2.4.1A). Acetylation of PC4 again reappears during telophase stage (Figure 3.2.4.1A). PC4 levels however doesnot change during different stages of cell cycle (Figure 3.2.4.1 B).

A

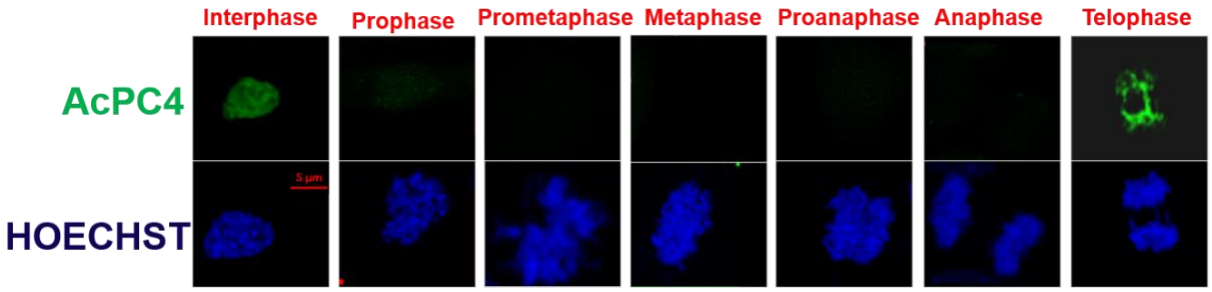

B

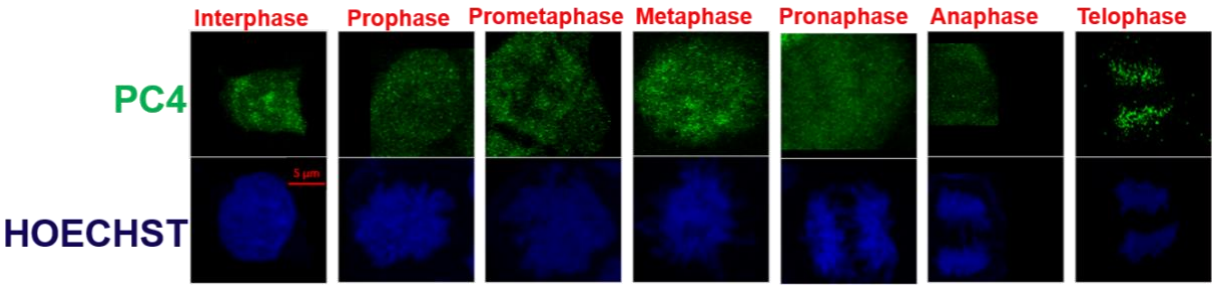

Figure 3.2.4.1: Localisation of acetylated PC4 during cell cycle: Asynchronous HEK293 cells grown on coated coverslips and immuno stained with (A) AcPC4 and (B) PC4 antibody and visualised at 63X magnification.

3.2.4.2 Acetylation of PC4 reduces upon mitosis

The acetylation levels of PC4 were further studied by western blotting by arresting cells at different stages of the cell cycle. For arresting the cells at different stages of the cell cycle the cell synchronization was done as mentioned before (Materials and Methods) and for the FACS analysis singlet population of cells were gated from the scatter plot and the peak intensity was measured depending on the DNA content and taking asynchronous cells as control the scatter plot was plotted for each stage. The cell synchronization at different stages was also verified by specific cell cycle stage markers (Figure 3.2.4.2.1C-D).

Acetylated PC4 level is significantly decreased in G2/M stage (Figure 3.2.4.2.1A-B) as shown by western blotting of lysates prepared from cells arrested at different cell cycle stages.

Co-immunofluorescence studies in Flag-PC4 cells were carried out using anti-Flag and anti-AcPC4 antibody which indicates compact metaphase chromosomes are devoid of acetylated PC4 whereas it is present with interphase chromatin (Figure 3.2.4.2.2). This observation along with western blotting results suggest that acetylation may not be present in the compact and transcriptionally inactive chromatin present in the metaphase cells but is associated with open and transcriptionally active chromatin in the interphase stage.

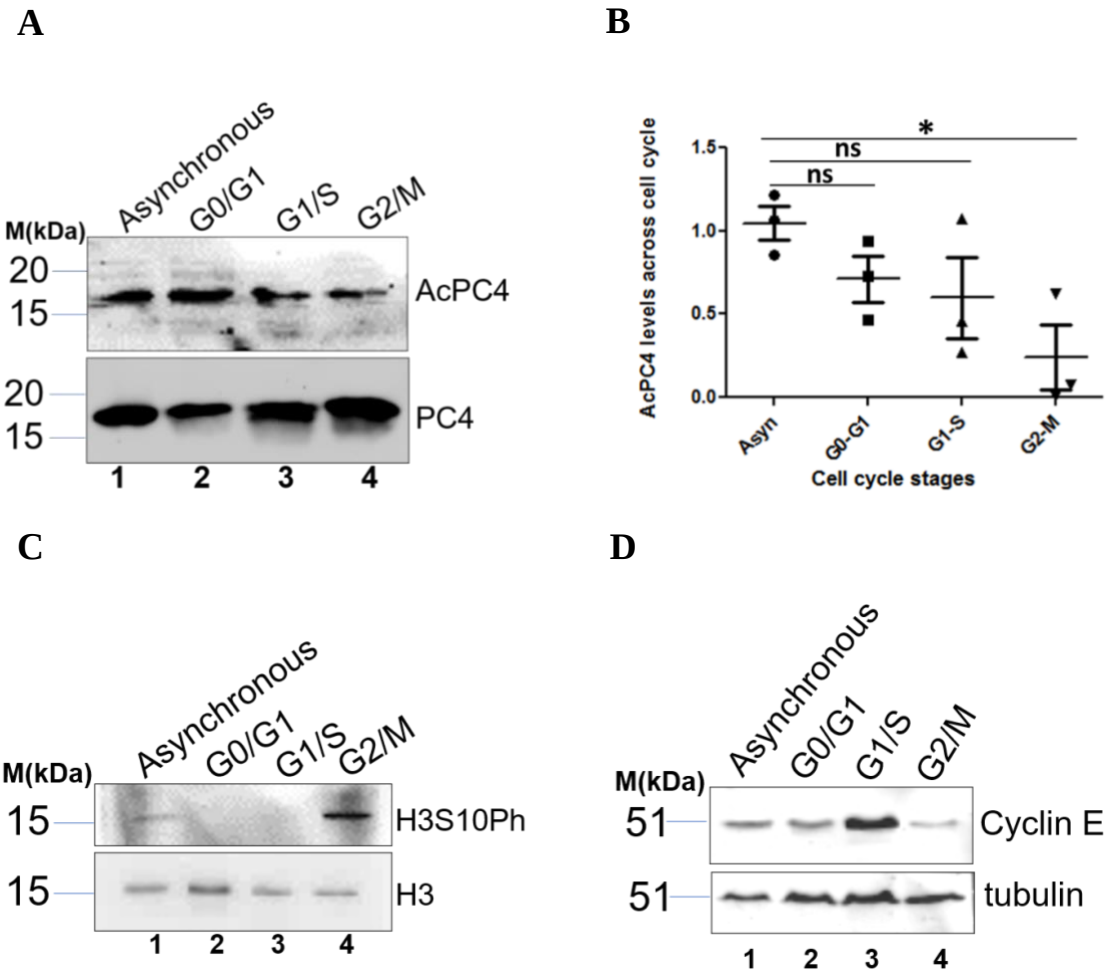

Figure 3.2.4.2.1: Acetylation of PC4 reduces upon mitosis. (A)Western blotting showing Acetylation levels of PC4 in HEK293 arrested at different stages of the cell cycle. (B) Quantification of levels of AcPC4 (n=3). Data represent the

means ± SD.The data is statistically analysed by ordinary one-way ANOVA, Sidak's multiple comparisons test (*p<0.05,**p<0.01,***p<0.001,ns-non-significant). (C) Western blotting of H3S10phosphorylation (H3S10ph) levels as a mitotic marker across different stages of cell cycle. (D) Western blotting of cyclin E levels, a G1/S marker, across different stages of cell cycle.

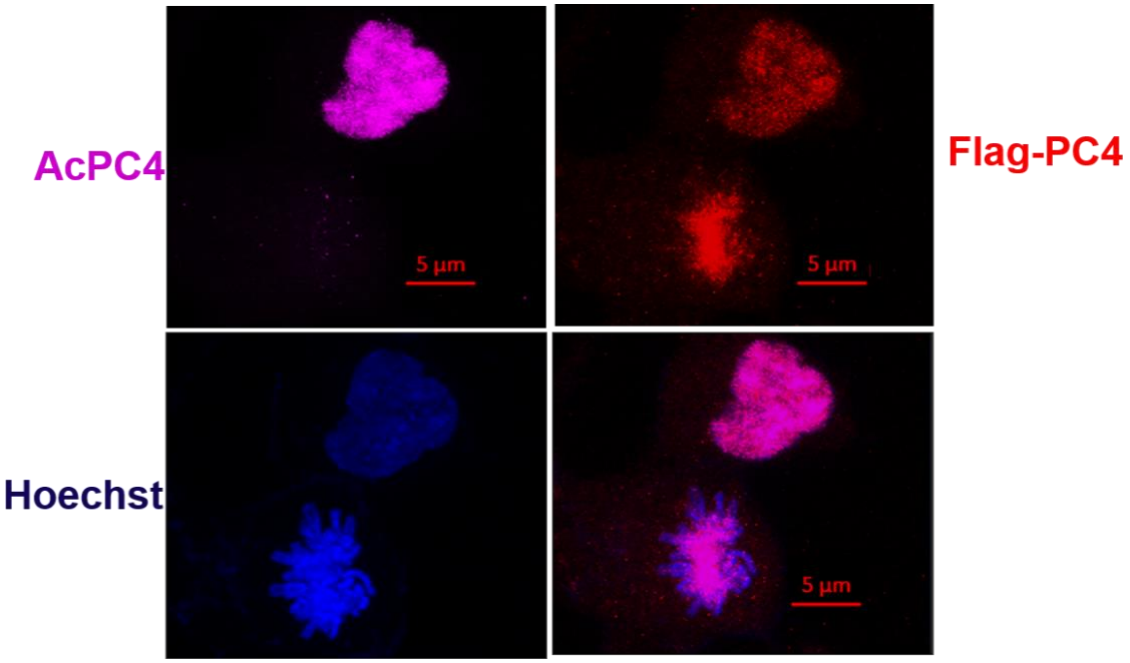

Figure 3.2.4.2.2: Acetylation of PC4 reduces upon mitosis. Co-immunofluorescence of asynchronous HEK293 cells grown on coated coverslips and immuno stained with both AcPC4 and Flag antibody (to probe PC4) and visualised at 63X magnification.

3.2.4.3 Acetylated PC4 is not associated with chromatin upon mitotic arrest

293 cells were collected from two100-mm plates and washed with cold PBS. The cell pellet (0.4 ml) was resuspended in 1 ml buffer A (0.3 M sucrose, 60 mM KCl, 60mM Tris-HCl, pH 8.0, 2 mM EDTA, and 0.4% NP-40 plus PI) and incubated on ice for 5 min, followed by a 5 minutes spin at 2,000 rcf at 4°C. 0.8 ml of the cytosolic fraction was collected. After one wash with buffer A, the nuclei (0.2 ml) was resuspended in 0.5 ml of 100 mM NaClcontaining mRIPA (6 strokes in

a 7-ml Dounce homogenizer) and spun at 6,000 rcf for 5 min. The supernatant was designated as nuclear extract (100 mM). The pellet was similarly resuspended in 2x pellet volume of mRIPA with 1M NaCl concentrations and separated the pellet and supernatant fraction for Western blotting analysis. The chromatin fraction of the interphase stage shows higher levels of acetylated PC4 without a change in the PC4 levels across the two stages but is not present in the chromatin fraction of mitotic cells (Figure 3.2.4.3A, lane 2 vs lane 1). Histone H3 is present in the chromatin fraction of both mitotic and interphase cells which is taken as the positive control. On the other hand, tubulin is taken as a control for cytosolic fraction and is not present in the nuclear fraction indicating the fractionation process has occurred properly without any cross contamination from other fractions (Figure 3.2.4.3B, lanes 1-2 vs lanes 3-4). Thus, further reiterating the observation that mitotic chromatin which is highly compacted is devoid of the acetylated form of PC4.

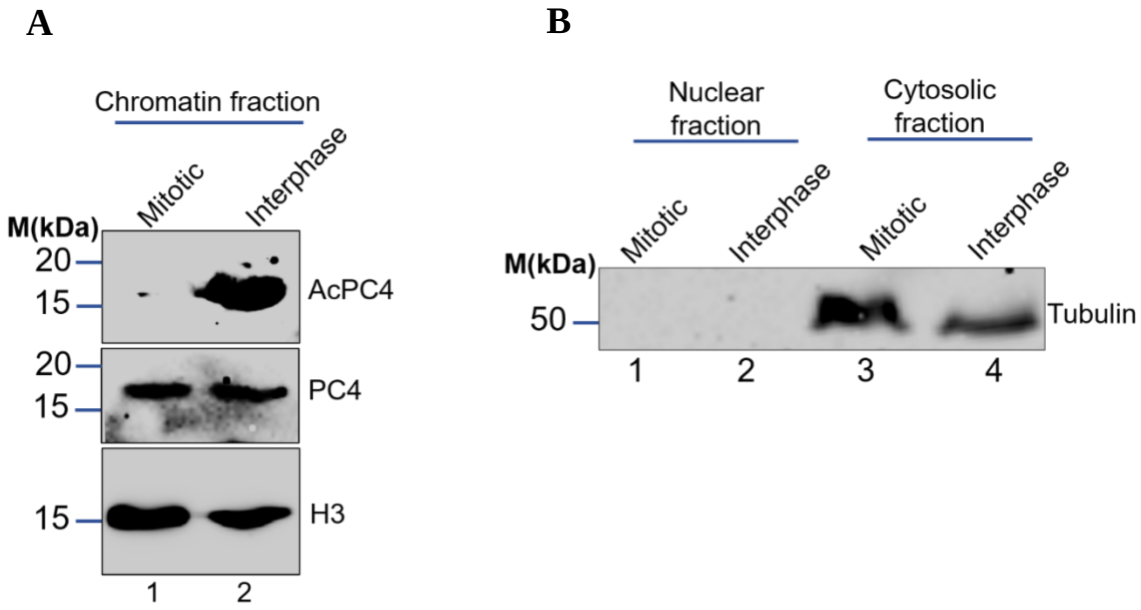

3.2.4.3 Acetylated PC4 is not associated with chromatin upon mitotic arrest: (A) Nuclear extraction followed by high salt extraction to isolate the chromatin fraction was carried out from HEK293 cells that has been arrested at mitotic stage and interphase stage probed with histone H3 as positive control, PC4 and AcPC4.

(B) The nuclear and cytosolic fraction from both mitotic and interphase cells were probed with tubulin as control to check the fractionation.

3.2.5 Lysine 26 and 28 residues in PC4 gets acetylated by p300 *in vivo*

3.2.5.1 Acetylation of PC4 reduces upon treatment with p300 specific inhibitor

HEK293 cells were seeded and treated with different doses of the inhibitors for 24 hours before harvesting for making cell lysates in RIPA lysis buffer and loaded onto 12% SDS-PAGE and probed with PC4 acetylation antibody and with PC4 to check for loading. The cells were seeded in a 6well plate and treated with 25μM and 50μM of embelin which is a known PCAF-specific inhibitor (Modak R. et al, 2013), 50μM and 100μM of LTK-14(Arif M. et al, 2009), a p300-specific inhibitor and 10μM and 20μM of C646 (Cole PA et al, 2010) at around 70% confluency and treated for 24 hours before harvesting. Histone acetylation marks like H2AK5 acetylation and H3K9acetylation were also checked as further validation that treatment is specific for the KATs tested (Figure 3.2.5.1C). A decrease in acetylation levels of PC4 upon treating with increasing dose of LTK-14 and C646 was observed as compared to DMSO control (Figure 3.2.5.1, lanes 4-6 vs lane 1) but no decrease is seen upon treatment with Embelin, which is a PCAF inhibitor (Figure 3.2.5.1, lane 2-3 vs lane 1). The reduction in the levels of acetylation of PC4 upon different inhibitor has been plotted showing statistically significant decrease in AcPC4 levels upon LTK-14 and C646 treatment (Figure 3.2.5.1B)

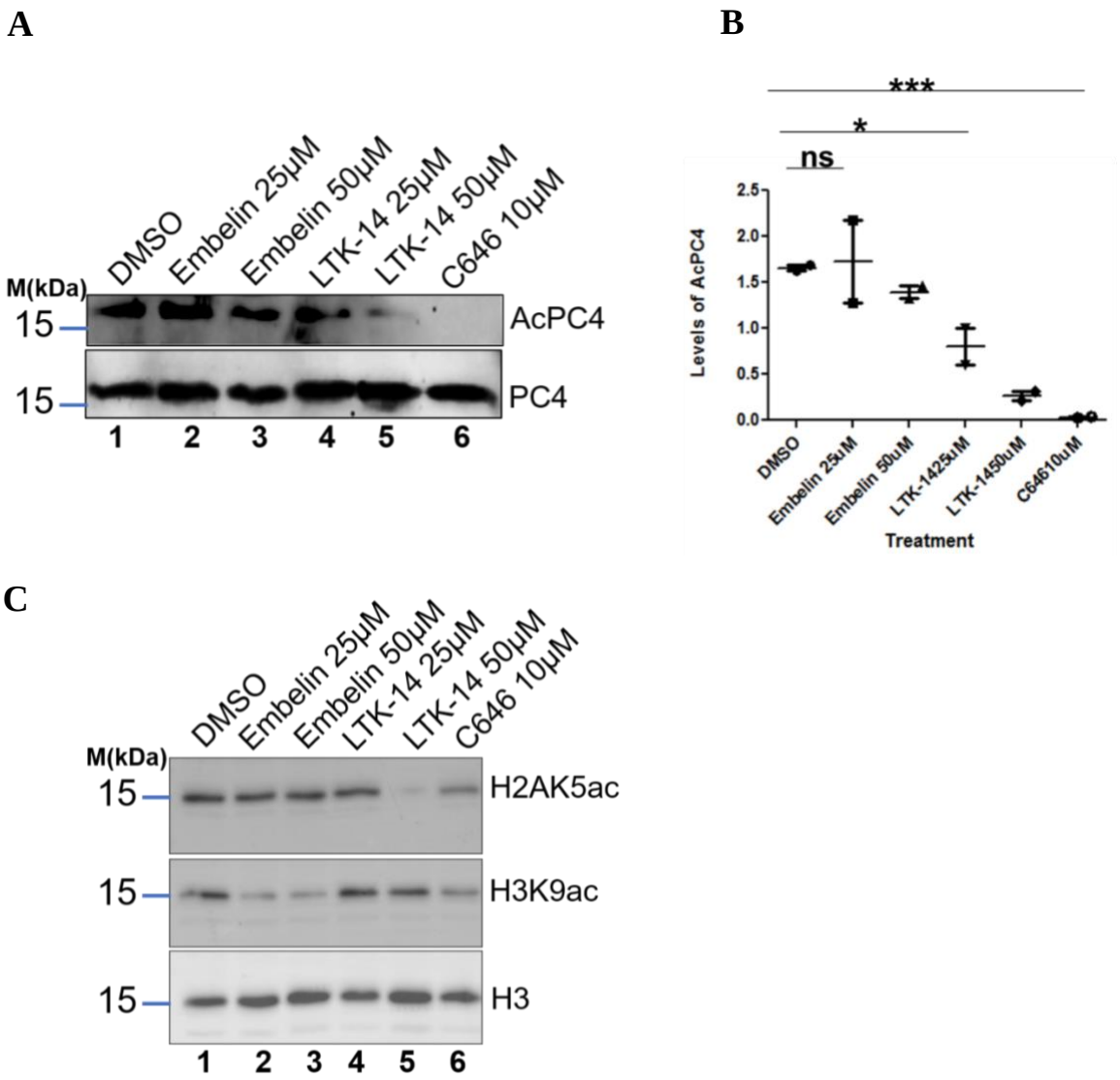

3.2.5.1 Acetylation of PC4 reduces upon treatment with p300 specific inhibitor: (A) Western blotting showing levels of PC4 acetylation upon probing with PC4 K26 28ac antibody and with PC4 antibody for equal protein loading upon treatment with different doses of Embelin (25μM and 50 μM), LTK-14(25μM and 50 μM), and a single dose of C646 (10 μM) in HEK293 cells. (B) Quantification of levels of PC4 acetylation upon inhibitor treatment (n=3). Data represent the means ± SD.The data is statistically analysed by ordinary one-way ANOVA, Sidak's multiple comparisons test (*p<0.05,**p<0.01,***p<0.001,ns-non-significant). (C) Western blotting showing levels of H2AK5 acetylation and H3K9 acetylation along with H3 antibody for equal protein loading upon the same treatment.

3.2.5.2 Acetylation of PC4 reduces upon silencing p300

Cells were seeded in a 6 well plate and transfected at 50-60% confluency with two selected concentrations of p300 siRNA (10 and 20nM from sigma) in complete media followed by media change at 24 hours and seeding in a 60mm dish and grown for another 24hours before harvesting for western blotting. The levels of p300 was studied followed by p300 specific histone acetylation marks and acetylation of PC4 with the specific antibody was analysed. There is gradual decrease in the p300 levels upon treatment with increasing doses of the specific siRNA targeting p300 (Figure 3.2.5.2C, lane 2 vs 4) which also corresponds to the decrease in the levels of p300 specific histone acetylation mark H3K18ac from 10-20nM as compared to control siRNA in lane 1 and 2 (Figure 3.2.5.2D, lane 2 vs lane 4). There is decrease in the acetylation levels of PC4 upon p300 siRNA treatment as compared to the control siRNA (Figure 3.2.5.2A, lane 2 vs lane 4) which has also been represented quantitatively for two biological repeats in the graph in Figure 3.2.5.2B indicating a statistically significant decrease in the PC4 acetylation levels upon treatment with p300 specific siRNA at 20nM.

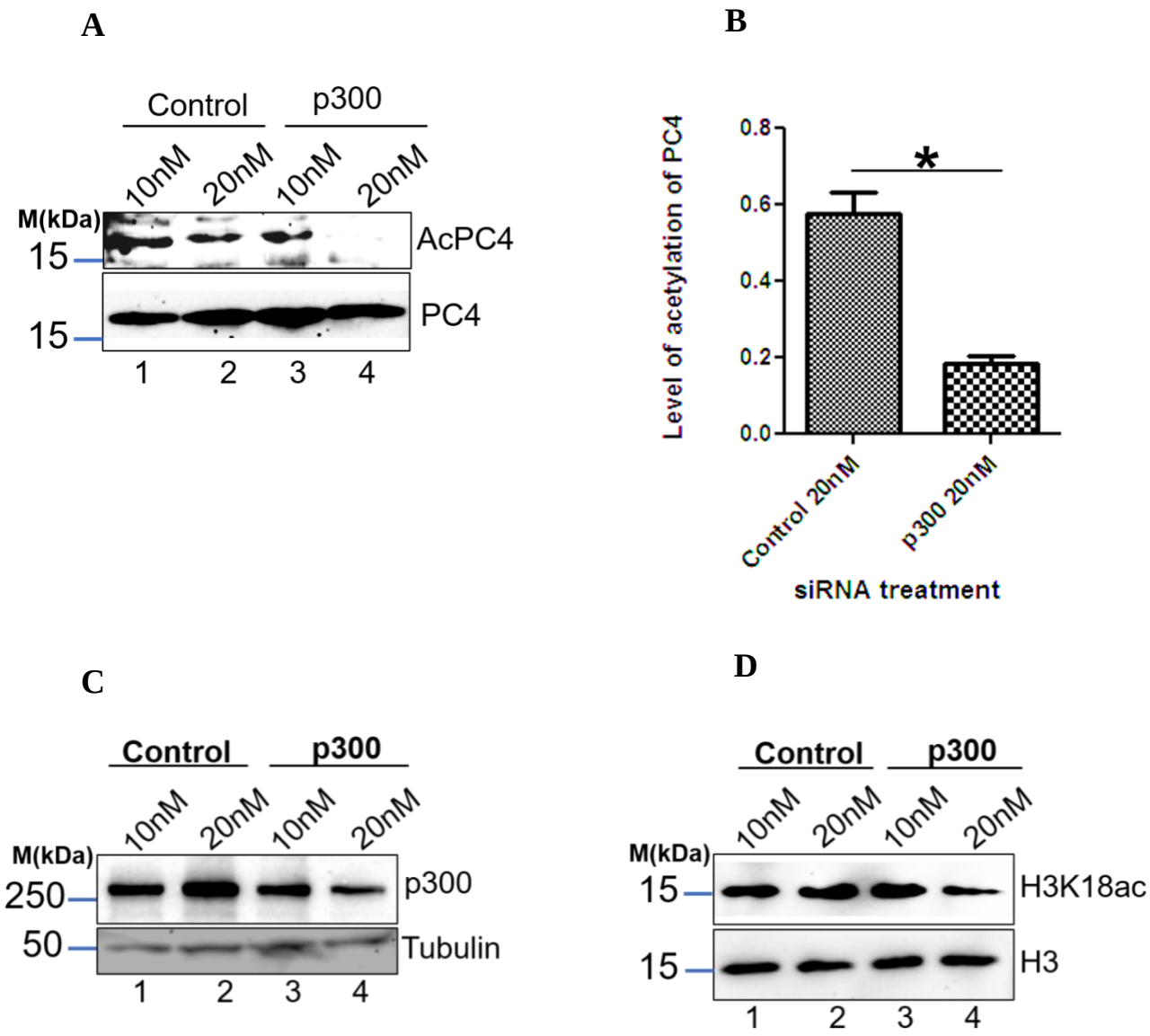

3.2.5.2 Acetylation of PC4 reduces upon silencing p300: (A) Western blotting showing levels of PC4 acetylation upon probing with PC4 K26 28ac antibody and with PC4 antibody for equal protein loading upon treatment with different doses of siRNA against p300. (B) Quantification of levels of PC4 acetylation upon inhibitor treatment (n=2). Data represent the means ± SD.The data is statistically analysed by students unpaired t-test (*p<0.05,**p<0.01,***p<0.001,ns-non-significant).(C) Western blotting showing levels of p300 along with tubulin antibody for equal protein loading upon p300 silencing with siRNA.(D) Western blotting showing levels of H3K18 acetylation along with H3 antibody for equal protein loading upon p300 silencing with siRNA.

3.2.5.3 Acetylation of PC4 increases upon treatment with a p300 specific activator

HeLaS3 cells were treated with two doses of CSP-TTK21 50 and 100ug/ml along with 100ug/ml of CSP as control in 60mm dishes for 24hours before harvesting the cells for western blot analyisis. The activator treatment was initially verified for the levels of p300 specific histone acetylation mark H3K14ac which shows that there is gradual increase in the H3K14ac levels upon treatment with increasing doses of CSP-TTK21 as compared to CSP control (Figure 3.2.5.3D, compare lane 3 vs lane 1 and lane 2 vs lane 1). The levels of acetylated p300, the catalytically active form of the enzyme, was also checked since CSP-TTK21 specifically targets the enzymatic activity of p300, which is seen to gradually increase upon treatment with increasing dosed of CSP-TTK21 as compared to CSP control (Figure 3.2.5.3C, compare lane 3 vs lane 1 and lane 2 vs lane 1). The acetylation levels of PC4 seems to follow the same trend thus indicating a specificity for p300 mediated acetylation at these two lysine residues (Figure 3.2.5.3A, compare lane 3 vs lane 1 and lane 2 vs lane 1 and Figure 3.2.5.3B). Another histone acetylation mark, H4K16ac , which is not a p300 specific mark, remains unchanged upon CSP-TTK21 treatment (Figure 3.2.5.3E, lane 2 and 3 vs lane 1).

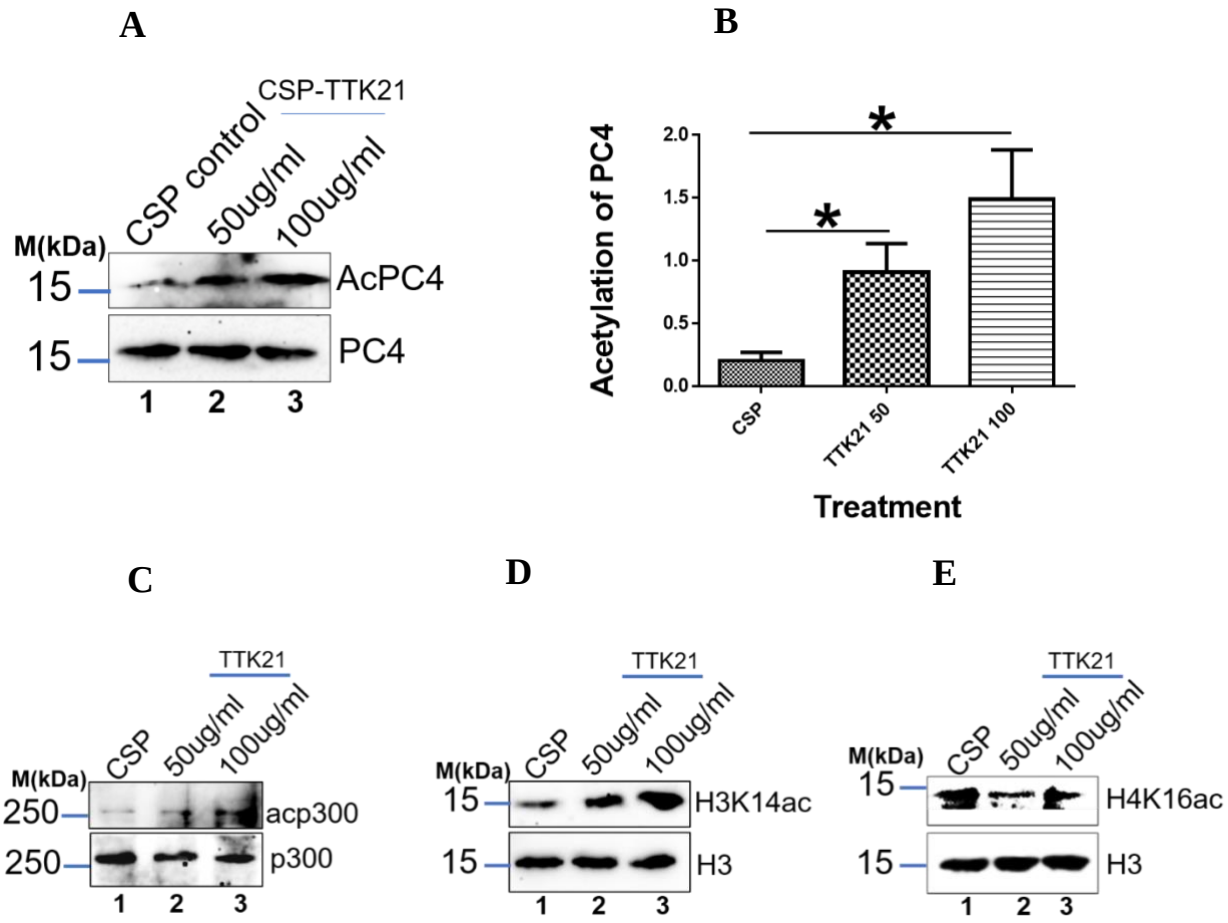

3.2.5.3 Acetylation of PC4 increases upon treatment with a p300 speific activator: (A) Western blotting showing levels of PC4 acetylation upon probing with PC4 K26 28ac antibody and with PC4 antibody for equal protein loading upon treatment with different doses of p300 activator CSP-TTK21. (B) Quantification of levels of PC4 acetylation upon CSP-TTK21 treatment (n=3). Data represent the means ± SD.The data is statistically analysed by students unpaired t-test (*p<0.05,**p<0.01,***p<0.001,ns-non-significant). (C) Western blotting showing levels of acetylatedp300 along with p300 antibody for equal protein loading upon CSP-TTK21 treatment. (D) Western blotting showing levels of H3K14 acetylation along with H3 antibody for equal protein loading upon CSP-TTK21 treatment. (E) Western blotting showing levels of H4K16 acetylation along with H3 antibody for equal protein loading upon CSP-TTK21 treatment.

3.2.6 PC4K26,28ac antibody specifically pulls down PC4 from cells

The affinity purified PC4K26 28 acetylation specific antibody against PC4 was characterised for its specificity for PC4 in cells. The acetylation antibody is detected in the whole cell lysates of different cell lines but not in the PC4 Knockdown HEK293 (PC4 KD) cells validating the specifity of the antibody in the cells as well (Figure 3.2.6A, lane 1 and lane 2 vs lane 3). The specificity of the AcPC4 antibody was initially investigated by dot blot where the increaseing doses of the unconjugated acetylated peptide was spotted at equally spaced circles on a nitrocelluose membrane along with the umodified protein at the highest concentration. Affinity purified PC4K26,28ac antibody is specifically detected by acetylated peptide at as low as 20ng of the peptide showing increase in dose dependent manner till 250ng of the peptide and it does not bind to recombinant PC4 protein even at 250ng concentration as shown by dot blot (Figure 3.2.6B, lane 3-6 vs lane 1). The antibody was then used for pulling down the endogenous acetylated PC4 using two different concentrations, 5ug and 10ug. 10ug of acetylation specific PC4 antibody could immunoprecipitate PC4 but not the IgG which is taken as the negative control indicating that affinity purified PC4K26 28ac antibody specifically immunoprecipitates PC4 and does not pull down any non-specific protein (Figure 3.2.6C, lane 5 vs lane 4).

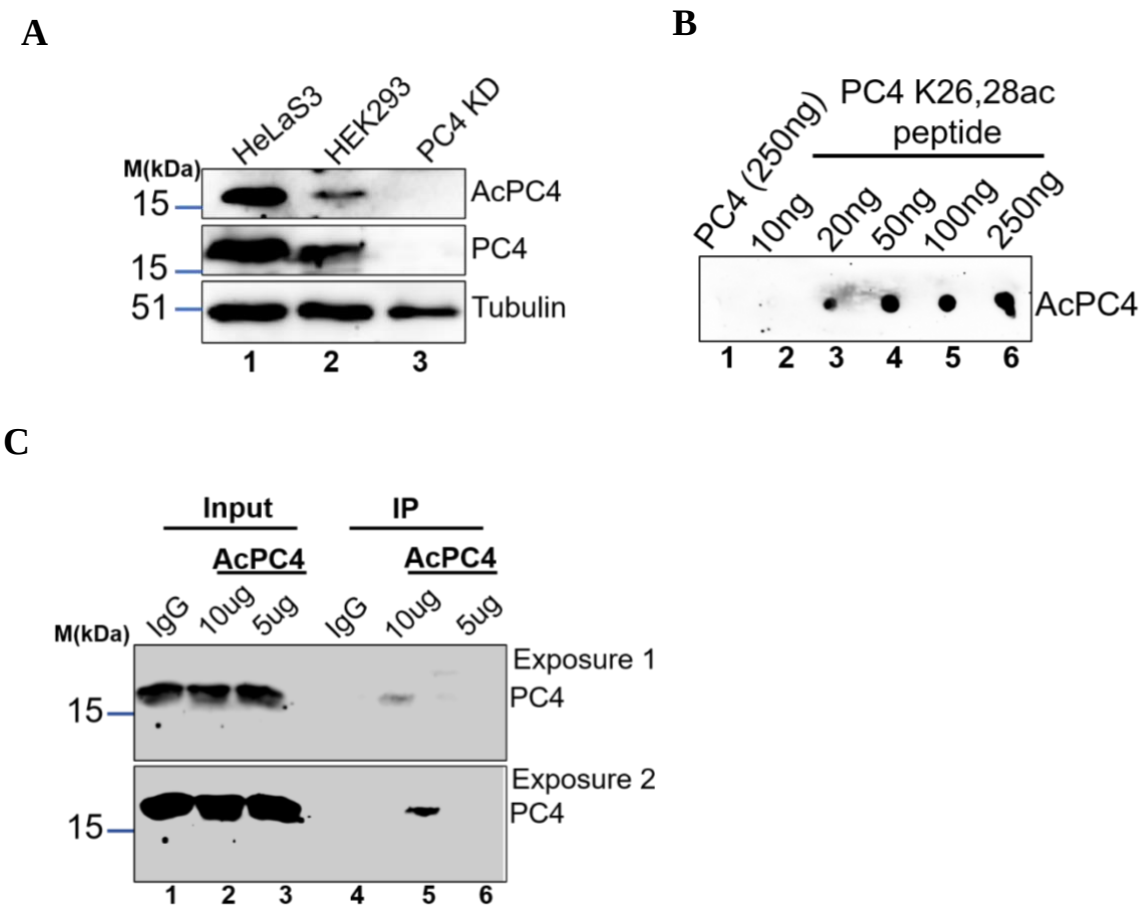

Figure 3.2.6:PC4K26,28ac antibody specifically pulls down PC4 from cells: (A) Western blotting in whole cell lysates probed with AcPC4 antibody along with PC4 and tubulin antibody for protein loading. (B) Dot blot assay with increasing amounts of PC4K26 28ac peptide and 250ng of recombinant PC4 protein probed with AcPC4 antibody. (C) Immunoprecipitation with AcPC4 antibody from HelaS3 cells probed with PC4 antibody.

3.2.7 Studying the occupancy of Acetylated PC4 at PC4 target gene promoters

Since we wanted to study the implications of acetylation of PC4 in its transcriptional coactivation function. Therefor a preliminary attempt was made to study the oocupancy of acetylated PC4 onto the promoters of some of the PC4 target genes inside the cells. For this, we carried out chromatin immunoprecipitaion (ChIP) in HeLaS3 cell line to see the enrichment of

acetylated PC4 at the basal level without any stimulation. 10ug of AcPC4 antibody was used for ChIP using 20million cells of HeLaS3. All the ChIP primers of the target as well as control non-specific regions were checked before the ChIP for the melt curve to see if any non-specific amplification occurs or not. The sonication condition was standardized and checked by running the ChIP DNA sample in 1% agarose gel (Figure 2.5.4). The ChIP analysis was performed on promoters having PC4 binding sites and the acetylated PC4 occupancy was studied by pulling down the complex using the site specific anti Ac-PC4 antibodies from HeLaS3 cells which shows that at the basal level there is 1.5-1.8 fold more enrichment of the acetylation specific PC4 antibody as compared to upon IgG pull down at two different sites on the c-Myc promoter (Myc site 1 and site 2) and on one site of PLK1 promoter (PLK1 site 2) , and not much change in the enrichment is observed for the negative control which is a non-specific region taken from the c-Myc gene (Figure 3.2.7).

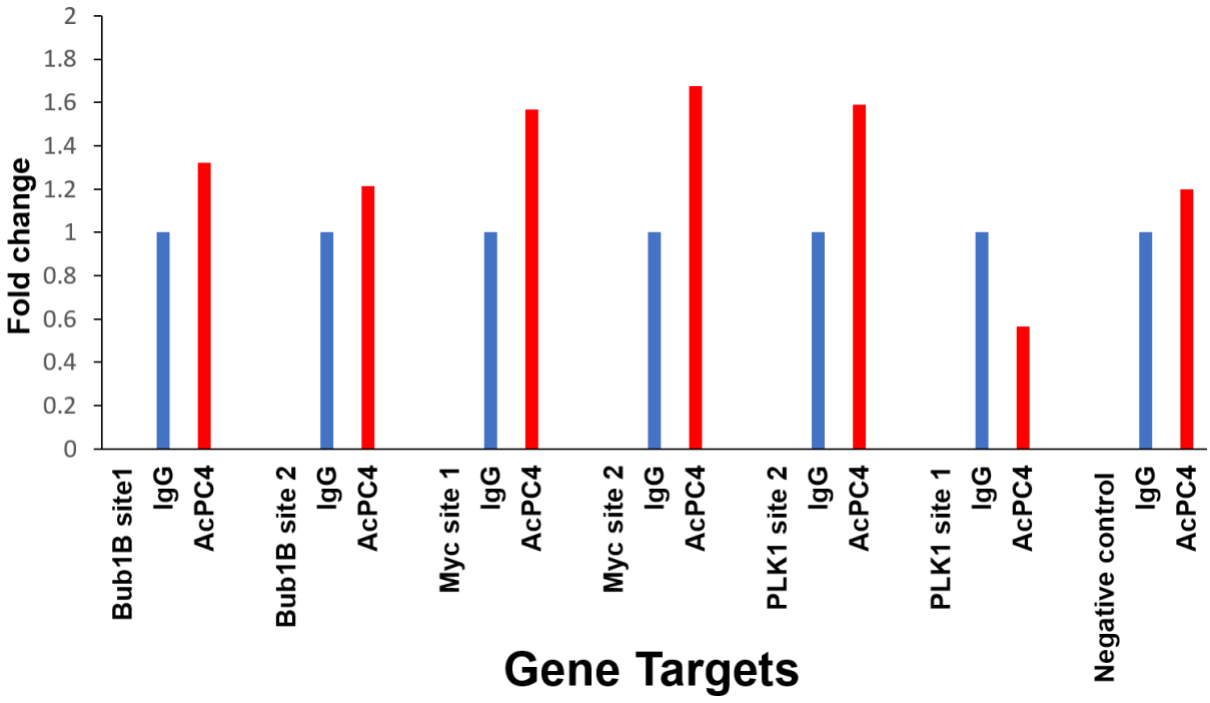

Figure 3.2.7 Studying the occupancy of Acetylated PC4 at PC4 target gene promoters: ChIP-qPCR to determine the occupancy of Acetylated PC4 (AcPC4) at PC4-responsive gene promoters.

3.2.8 Acetylation of PC4 in oral cancer cells

The PC4K26 28acetylation specific (AcPC4) antibody generated was studied for its specificity for acetylated PC4 and was used to investigate the p300 mediated acetylation of PC4. The results indicate that lysine residues 26 and 28 are specific for p300 mediated acetylation and therefore to further characterise the implications of acetylated PC4 we wanted to explore a model system where PC4 acetylation could be highly enriched. This would help us to both probe for the acetylated form of PC4 and then further investigate its functions in cells. Since we stated earlier that oral cancer provides a hyperacetylated environment showing both hyper levels of acetylate p300 and p300 specific histone acetylation (Aeif et al., 2010), we investogated the levels of acetylated PC4 in oral cancer cells. Four oral cancer cell line AW13516 , derived from poorly differentiated squamous cell carcinoma, AW8507, epidermoid carcinoma of the tongue, NT8e, derived from upper aero-digestive tract , UMSCC, a unique head and neck squamous carcinoma cell line isolated from the tumor located on the floor of the mouth of a male patient , alog with Het1a, esophagus epithelial normal cells were harvested for western blotting and probed for both PC4 and acetylated PC4 levels. PC4 levels are higher in oral cancer cells (AW13516, AW8507,NT8e,UMSCC) as compared to Het1a, normal epithelial cells (Figure 3.2.8A and B). Therefore the acetylation levels of PC4 is also higher thus providing a physiological scenario to study the implications of acetylated PC4 (Figure 3.2.8A and C).

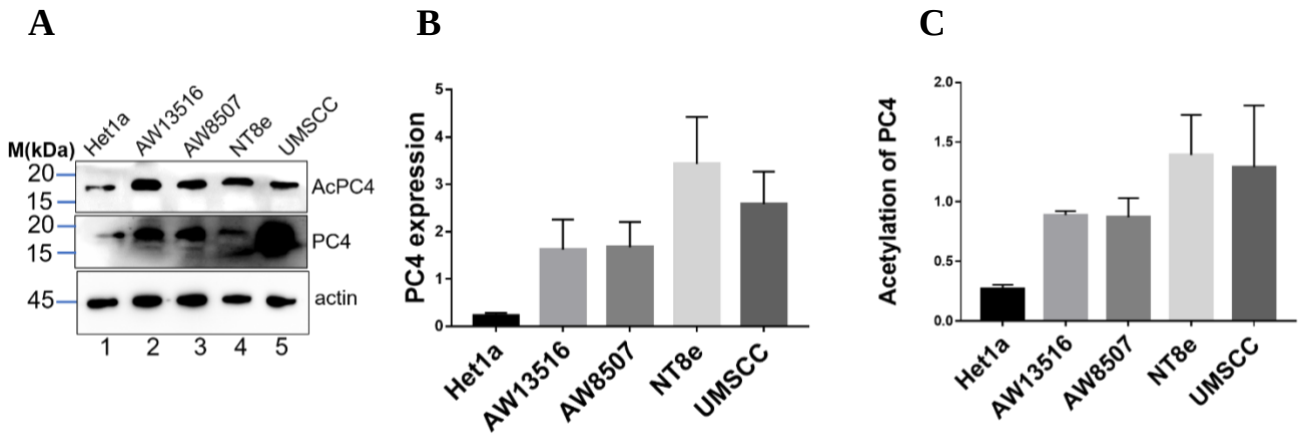

3.2.8 Acetylation of PC4 in oral cancer cells: (A) PC4 and AcPC4 levels in oral cancer cells shown by western along with actin as loading control. (B-C) Quantitation of PC4 and AcPC4 levels respectively in oral cancer cells as compared to Het1a normal esophageal epithelial cells from two independent biological replicates.

3.2.9 Acetylated PC4 interacts with elongating RNA polymerase II

In order to investigate that acetylated PC4 is involved in the transcription regulation, we attempted to carry out immunoprecipitation of acetylated PC4 from cells and probed for some of its interacting partners. The largest subunit of RNA polymerase II contains a unique C-terminal domain important for coupling of transcription and mRNA processing. This domain consists of a repeated heptameric sequence (YSPTSPS) that is phosphorylated at serines 2 and 5. Serine 2 is phosphorylated during elongation by the Ctk1 kinase (Ahn S A, Kim M, Buratowski S, 2004). Interestingly we observed that upon pulling down acetylated PC4 from AW13516 cells (Figure 3.2.9A, lane 2 vs lane 1)as well as from UMSCC cells (Figure 3.2.9B, lane 2 vs lane 1, we oberved serine 2 phosphorylated RNA pol II (polIIS2-P) which is the actively transcribing polymerase, interacting with acetylated PC4 but not with IgG immunoprecipitated samples (Figure 3.2.9A and B, lane 2 vs lane 1). We also oberved acetylated PC4 interacting with mutant p53 in AW13516 (p53 R273H)

(Figure 3.2.9A, lane 2 vs lane 1). We also studied its interaction with a heterochromatin partner linker histone H1 and acetylated PC4 did not show any interaction with linker H1 (Figure 3.2.9A). These results suggest that acetylated PC4 interacts with active trancription machinery and is not associated with heterochromatin.

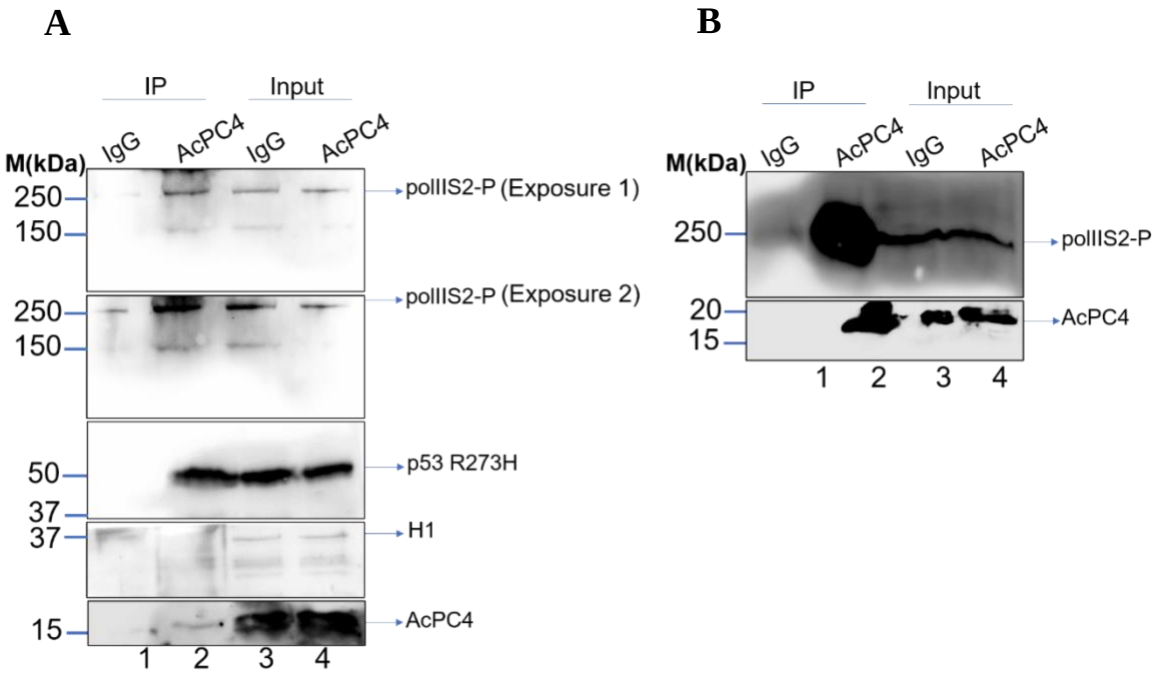

Figure 3.2.9.Acetylated PC4 interacts with elongating RNA polymerase II: Immuno-pulldown using AcPC4 antibody along with IgG from pre-immune sera was carried out in (A) Aw13516 and (B) UMSCC cells and probed with serine 2 phosphorylated RNA pol II (polIIS2-P), linker H1,p53 and AcPC4 antibody in (A) and with serine 2 phosphorylated RNA pol II (polIIS2-P), linker H1, and AcPC4 antibodies in (B).

3.2.10 Studying the levels of PC4 acetylation in oral cancer patient samples

Since earlier studies have shown a hyperacetylated environment in oral cancer patient samples correlating with higher histone acetylation levels and hyperacetylated p300 (Arif et al., 2010), PC4 being a non-hsitone substrate of p300, we were curious to study the acetylation status of PC4 in oral cancer patient

samples. We did a preliminary analysis of the TCGA datasets from cBioportal that PC4 expression across 30 cancer types which indicates PC4 to have a moderate to high expression at the mRNA level in head and neck cancer which falls under oral cancer (Figure 3.2.10.1 denoted with black bordered box). In this plot each dot represents a patient data and the dots are colored differently denoting the kind of perturbations that occurs for SUB1 gene that encodes for PC4 in these pateints. We see that most patients falling under the category of head and neck cancer possess amplification of the PC4 gene (Figure 3.2.10.1, red colored dots within head and neck cancer) which might indicate a possibility of perturbed expression level of PC4 in this cancer.

As mentioned earlier we wanted to study the status of PC4 acetylation in oral cancer patient samples for which we conducted immunohistochemistry with PC4 and acetylated PC4 (AcPC4) antibodies in 21 pair of tumor and adjacent normal tissues from oral cancer patient samples which were collected from Sri Devaraj Urs Academy of Higher Education and Research, Kolar. We have currently analysed data from 21 patients for PC4 and AcPC4 staining (Figure 3.2.10.2 A and C respectively) which have been quantified by plotting the H-score for tumor and normal tissues for each patient sample (Figure 3.2.10.2 B and D respectively). The data indicates significantly higher levels of PC4 and acetylated PC4 in tumor compared to normal tissues. We have also studied levels of acetylated p300 (Acp300) for 5 pairs of tumor and adjacent normal tissues(Figure 3.2.10.2E-F) and we are currently looking studying the levels of acp300 in more patient samples. The IHC data from oral cancer patients suggest hyperacetylation of PC4 in the tumor region (Figure 3.2.10.2C-D) that might provide us a window to explore its effect on gene expression thereby contributing to tumor manifestation. This data is a first report of the transcription co-activator PC4 to be highly acetylated in tumor and therefore we would further like to delve into the implications of this modified PC4 being altred in a pathophysiological conditions.

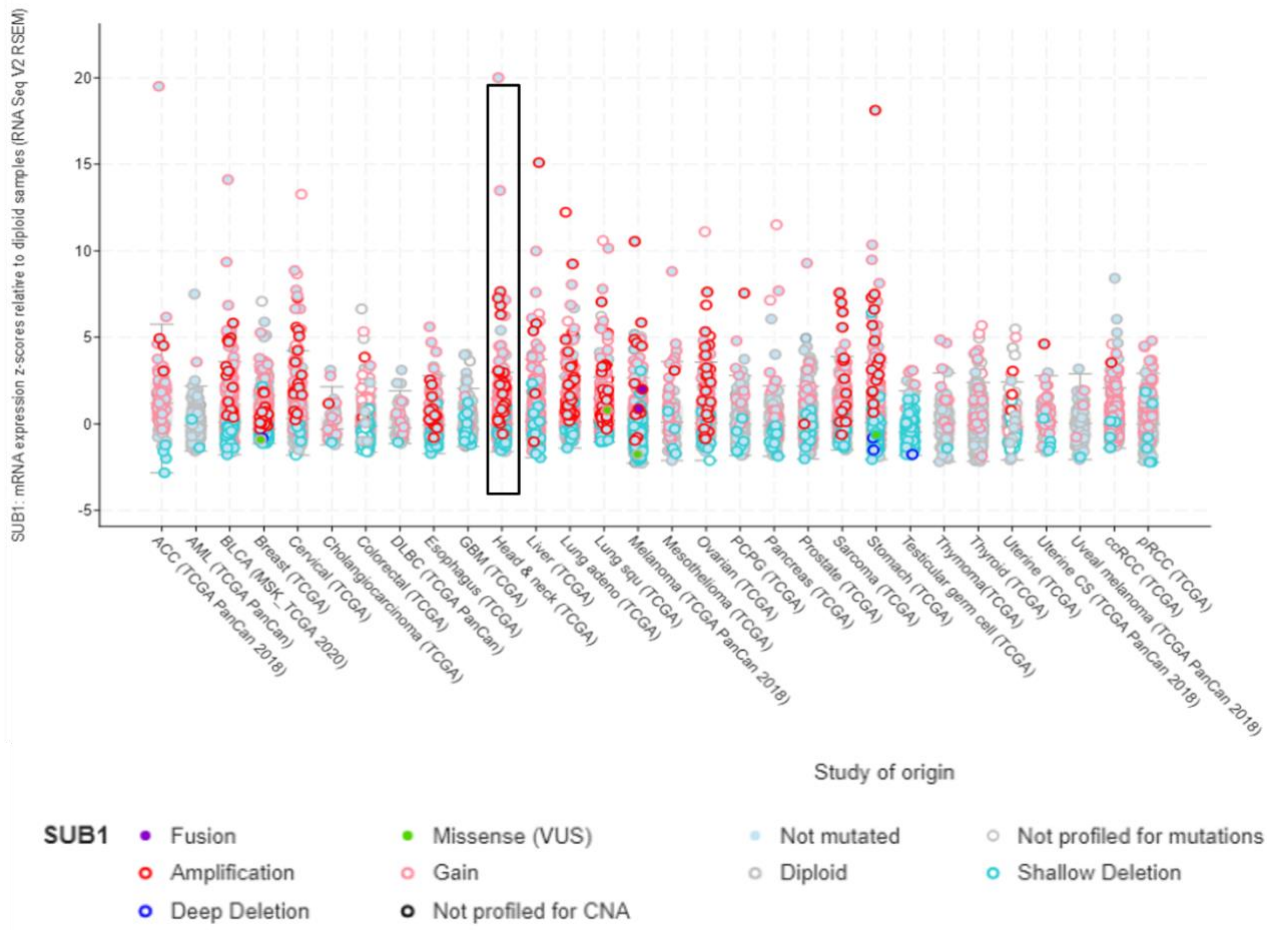

Figure 3.2.10.1.Studying the levels of PC4 acetylation in oral cancer patient samples: PC4 mRNA expression expressed as Z-scores from RNA sequencing data of patient data from TCGA database shown for 30 cancer types.

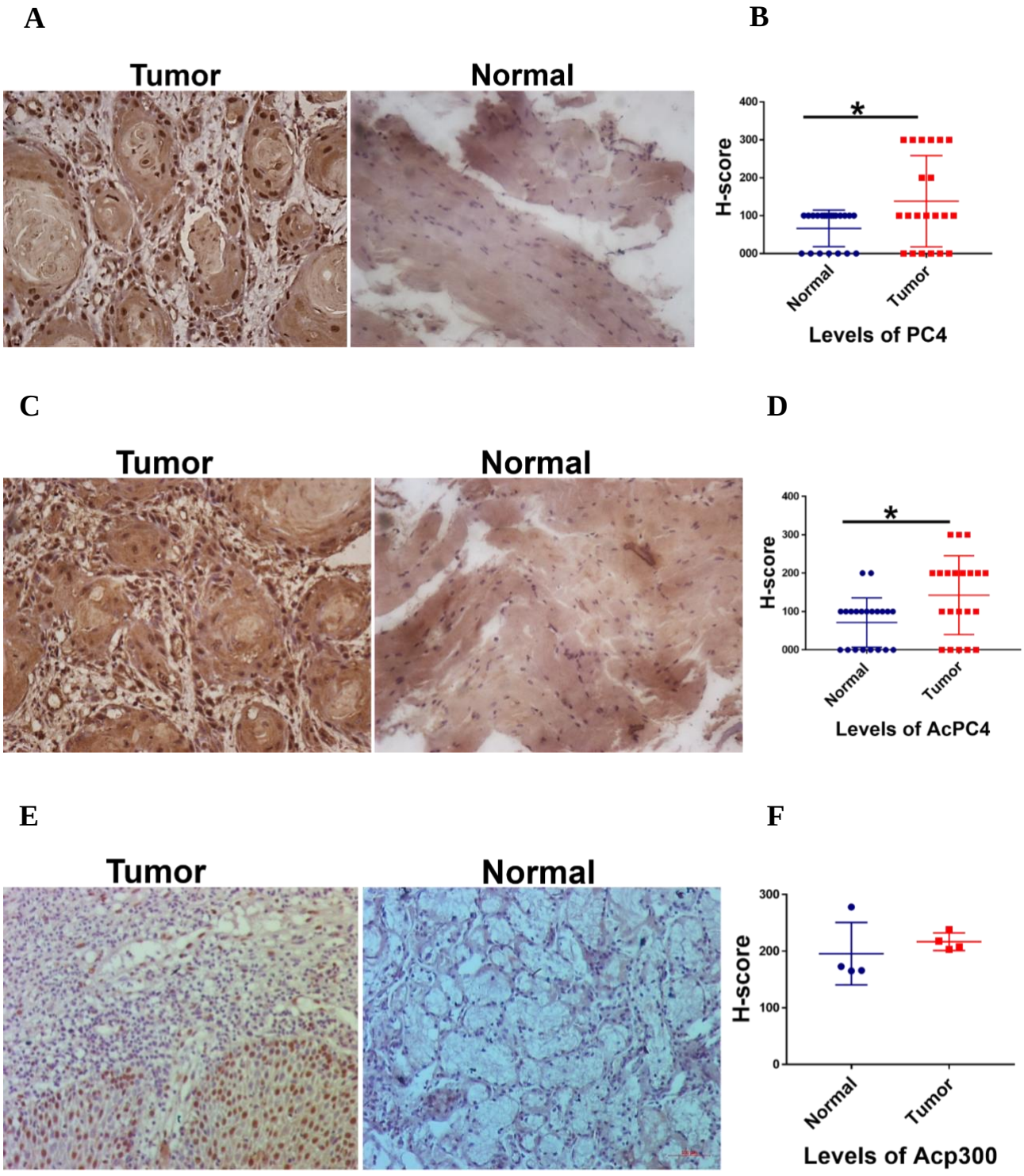

Figure 3.2.10.2. Studying the levels of PC4 acetylation in oral cancer patient samples: (A, C and E) Immunostaining of tissues from oral cancer patient samples from the site of tumor and adjacent norml region with PC4, AcPC4 and Acp300 antibodies respectively to study its expression levels. (B and D) Quantification of PC4 and AcPC4 levels respectively by plotting the H-scores of

the immunostined tissue samples in tumor and in adjacent normal tissue for n=21 (number of patients). Data represent the means ± SD.The data is statistically analysed by students unpaired t-test (*p<0.05,**p<0.01,***p<0.001,ns-non-significant).(F) Quantification of Acp300 levels respectively by plotting the H-scores of the immunostined tissue samples in tumor and in adjacent normal tissue for n=5 (number of patients).

3.2.11 Summary

In this part of the study we attempt to understand the role of acetylated PC4 in cells. We initially identified the lysine residues that are important for p300 mediated acetylation by *in vitro* HAT assay using acetylation defective mutants. In order to study the role of acetylated PC4 it was imperative to be able to identify the acetylated form of the protein in cells and for that we generated an acetylation specific antibody using a peptide was designed against the specific sites in rabbit. The antibody was characterised to be specific for acetylated PC4 and PC4 is acetylated at lysine residues 26 and 28 specifically by KAT p300 in cells. Compact metaphase chromosomes were found to be devoid of acetylated PC4 and there was no association of acetylated PC4 with mitotic chromatin that suggests that acetylation of PC4 is asscoicated with interphase chromatin which is more open and trancriptionally active and not with transcriptionally silent compact metaphase chromosome. These observation correlated with reduction in PC4 acetylation levels observed upon mitosis both by western and immunofluorescence studies unlike the PC4 levels that remains unchanged during cell cycle. The acetylation specific antiboy has also been shown to specifically immunoprecipitates PC4 from cells and has also been shwon to occupy the promoters of some of the PC4 responsive genes a shown by ChIP in HelaS3 cells.

Studies have shown that p300 mediated acetylation of non-histone substrates like NPM1 and p53 play a role in tumour manifestation (Shandilya J., et al., 2009 and Kaypee S., et al., 2018). PC4 being a substrate of p300, we therefore studied the

levels of acetylated PC4 along with acetylated p300 which is the catalytically active form of the enzyme in oral cancer patient samples. PC4 expression was higher in oral cancer cells thus enriching the acetylated levels of PC4 making oral cancer an ideal system to study the implications of Acetylated PC4. We indeed observe Acetylated PC4 levels to be highly enriched in tumor tissues compared to normal in oral cancer patient samples. Thus PC4 acetylation seem to be triggered in tumors like the other substrates of p300 shown in earlier studies. This study thus shows for the first time that the acetylated form of the transcription coactivator PC4 is elevated in tumor, providing another important example of aberrant acetylation of non-histone proteins in cancer. Thus to explore further the implications of the acetylated PC4 , we carried out immuno-precipitation studies with acetylated PC4 antibody from oral cancer cells, AW13516 and UMSCC and we interestingly observe that acetylated PC4 interacts with elongating RNA polII. This association of acetylated PC4 with actively transcribing polymerase thus validates our hypothesis that acetylation of PC4 might be regulating its co-activator function. We also observe PC4 to interact with mutant p53 expressed in AW13516 cells but it does not exhibit interaction with heterchromatin protein linker H1. These observations thus hint at the association of acetylated PC4 with transcription , therefore to further validate the role of acetylated PC4 in regulating the co-activator function, we plan to generate Flag tagged wild type PC4, Flag tagged PC4 acetylation defective mutant and Flag tagged PC4 acetylation mimic transfected in PC4 KD cells to investigate the effect of acetylation on the expression of PC4 target genes.

Thus in this study we attempted to understand the role of acetylated PC4 in cells. Since eralier reports hinted at p300 mediated acetylated PC4 to have better dsDNA binding ability, we began our study with the identification of the lysine residues that are critical for p300 mediated acetylation. We generated a polyclonal acetylation specific antibody against a combination of critical lysine

residues 26 and 28. We found that indeed this antibody is specific for probing the acetylation form of PC4 and these two lysine rediues are important for p300 mediated acetylation in cells. Using this antibdy as tool we find that acetylated PC4 is associated with actively transcribing polII and is associated with interphase chromatin and is not present in the compact mitotic chromatin. Acetylated PC4 is also present at some of the known PC4 target genes at basal level in Hela S3 cells. Since PC4 is involved in activator -dependent transcription, to probe the PC4 that is involved in transcriptional activation , we explored the role of acetylated PC4 in oral cancer system. Earlier studies have shown oral cancer to have hyperacetylated environment where p300 is hyperacetylated and p300 specific histone acetylation marks are elevated (Shandilya J et al., 2009, Kaypee S. et al., 2018). Our observation also corroborates with this finding since we observe acetylated PC4 to be enriched in oral cancer cells and tumor tissues from oral cancer patients collected from Sri Devaraj Urs Academy of Higher Education and Research, Kolar. We are currently carrying out further studies on understanding the effect of hyperacetylated PC4 upon its transcriptional co-activation function and how this might affect the gene expression contributing to tumourigenesis.

Chapter 4: DISCUSSION AND FUTURE PERSPECTIVE

Chapter outline

4.1. Discussion

4.2. Implications of the role of PC4 phosphorylation in maintaining chromatin compaction in DNA damage repair and maintenance of genome integrity

4.3 Implications of p300 mediated acetylation of PC4 on its coactivator function and probable role in cancer manifestation

4.4 Role of post-translational modifications as a functional switch for a multifunctional nuclear protein, PC4.

4.1 Discussion

Non-histone chromatin proteins are an integral part of the regulation process of the highly dynamic eukaryotic genome possessing a hierarchical order of chromatin organisation. Human positive co-activator 4 is one such crucial nonhistone chromatin protein. PC4 is bona fide component of the chromatin that is abundantly present in the nucleus. PC4 as the name suggest is also an important transcriptional co-activator that interacts both with the general transcription factors as well as with transcription factors.

Post-translational modifications of chromatin proteins have been a major modulator of chromatin structure and thereby of chromatin template dependent functions. PC4 is highly enriched in the phosphorylated form inside the nucleus despite its inhibitory effects on its DNA binding ability and co-activator function whereas KAT3B mediated acetylation enhances these functions.

This study therefore sets to decipher the implications of two major modifications of PC4 on its two distinct functions. Our results suggest that phosphorylated PC4 mediates its chromatin compaction function and acetylated PC4 might be important for its co-activator functions. These findings not only show the importance of post-translational modifications of a single protein that might be regulating its two distinct chromatin-associated distinct functions but also the different gene regulatory pathways that might be controlled by a single protein. Understanding the relevance of a modification provides a target to tweak with the specific functions of a multifunctional protein like PC4 and also providing scope for designing strategies to target specifically the modifications of a protein that could be the functional form helping in regulation of certain pathways.

nuclear protein, discovered as a bona fide non-histone chromatin associated protein (Das C., et al., 2006) involved in multiple cellular processes ranging from genomic organisation, transcription regulation (Garavís M and Calvo C,2017), neurogenesis (Swaminathan A., et al.,2016), regulation of autophagy (Sikder S., et al., 2019), DNA replication (Pan et al., 1996), to DNA damage repair (Mortusewicz O, Evers B, and Helleday T., 2015). However, the molecular mechanism behind these roles of PC4 in these processes are yet to be elucidated. Post-translational modifications (PTMs) often contribute to multifunctionality of proteins. Post-translational modifications of chromatin proteins have been a major modulator of chromatin structure and thereby regulating chromatin template dependent functions. PC4 undergoes two major post-translational modifications phosphorylation and acetylation. Phosphorylation negatively regulates its double strand DNA binding and unwinding ability, co-activator function (Ge and Roeder.,1994 and Jonker H.R.A et.al., 2006) and its acetylation by KAT3B/p300 (Kumar, B. R., V. Swaminathan, S. Banerjee, and T. K. Kundu. 2001). On the contrary p300 mediated acetylation of PC4 has been reported to enhance its double strand DNA binding ability, DNA bending ability and also enhances DNA binding of transcription factors like p53 (Batta K and Kundu T.K., 2007).

Knockdown of PC4 has shown drastic alteration in the nuclear architecture and chromosomal defects (Dhanasekaran K., et al., 2016 and Sikder S., et al., 2019) which indicates that PC4 is critical for maintaining genome integrity and has a role beyond its involvement in transcriptional activation. The two modifications of PC4; phosphorylation mediated by CKII and acetylation mediated by KAT3B/ p300, exhibiting such opposing effects on PC4 might be a playing a role in switching its two distinct functions inside the cells. In this study we attempted to understand the role of these two important post-translational modifications and their implications on the cellular functions of PC4.

4.2. Implications of the role of PC4 phosphorylation in maintaining chromatin compaction in DNA damage repair and maintenance of genome integrity

Earlier studies have shown PC4 to be a component of the chromatin (Das C et al.,2006) but the exact mechanism of PC4 mediated chromatin compaction was not known. Till now, the functional consequence of phosphorylation of PC4 has been shown in the light of its cofactor binding properties where the positive charge of its lysine-rich region gets progressively masked by phosphoserines (Jonker H.R.A et.al., 2006). The results discussed in this chapter however reveals a more physiological relevance of this protein modification on PC4 chromatin functions. A novel finding in this study is the ability of PC4 to interact with chromatin protein linker H1 only upon phosphorylation. This finding provides a hint as to why PC4 is majorly present in the phosphorylation state inside cells. Phosphorylation might be mediating its genome organising function by modulating its interaction with chromatin partners linker H1 and core histone H3 and H2B as indicated by the results discussed in this study. This study shows that phosphorylation enhances the efficiency of PC4's chromatin condensation ability thus explaining the presence of phosphor-PC4 in the nucleus. Compaction studies using H1-bound array shows how two non-histone chromatin proteins, PC4 and linker H1, might be involved in maintain higher order chromatin structure. This probably answers the question why PC4 needs to be present mostly in the phosphorylated state cells so that, it remains tightly associated with the chromatin to maintain chromatin architecture in cells. We also observe the effect of PC4 phosphorylation onto the epigenetic state of the cell maintaining a repressed chromatin state leading to gene repression in cells.

Till date studies have shown PC4 to regulate gene expression by directly binding to the promoter of the genes (Sikder S. et al., 2019; Chakravarthi BVSK. et al., 2013; Luo P. et al., 2019) and interacting with transcription machinery throughout

the transcription cycle (Calvo O, 2017) but this study shows for the first time that phosphorylated PC4 regulates gene expression by modulating chromatin state. This study shows an alternate mechanism of PC4 mediated gene expression, not as a transcriptional co-activator but as a chromatin condenser. The chromatin state has been shown to determine the accessibility of different epigenetic modifiers on to the chromatin thus regulating the epigenetic state of the cell. Studies have shown earlier how chromatin architectural proteins could regulated epigenetic modifications of both histone as well as non-histone proteins (Lin JH, et al.,2005, Lu X, et al., 2013, Yang SM, et al., 2013). Our results led us to propose a model that phosphorylation of PC4 is crucial for its chromatin condensation function that leads to an epigenetically repressed chromatin and thereby controlling gene expression (Figure 4.2).

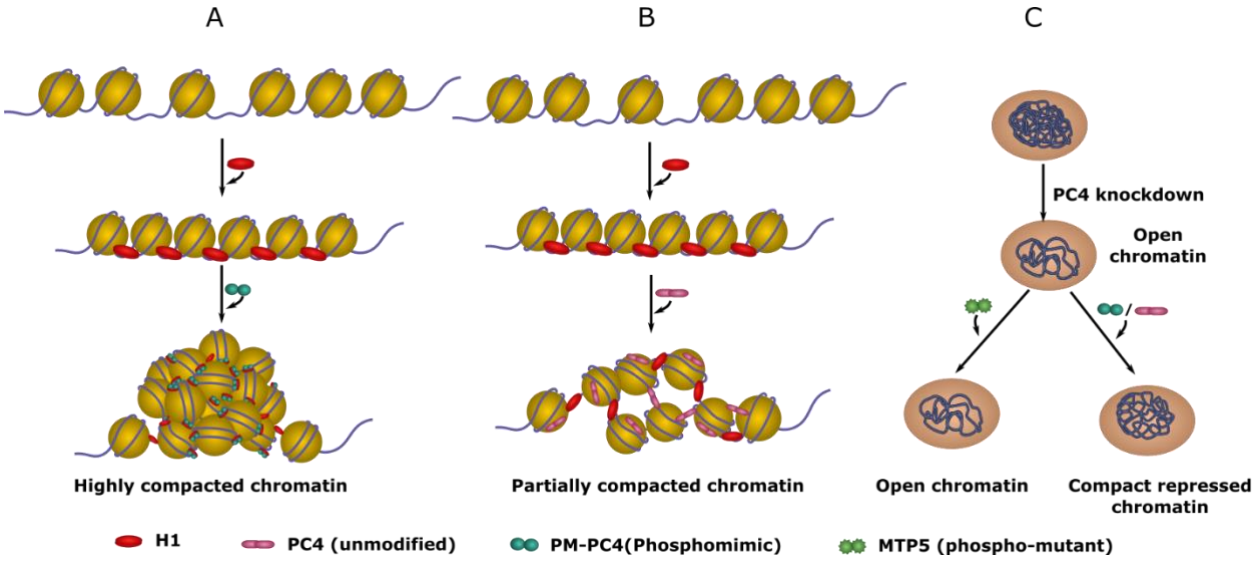

Figure 4.2: Model depicting PC4 mediated chromatin organisation upon phosphorylation. (A) Nucleosome array bound by linker H1 folds into highly compacted chromatin in the presence of Phosphomimic-PC4 (PM-PC4) (B) Nucleosome array bound by H1 forms partially folded array in the presence of unmodified PC4. (C) Silencing of PC4 leads to opening of the chromatin and subsequent gene activation in cells. This phenomenon is rescued upon expressing

PC4, that is phosphorylated inside cells, and PM-PC4, as they mediate chromatin compaction and reinstate the repressed chromatin state. On the other hand, expression of Phospho-mutant PC4 (MTP5) fails to compact the chromatin and repress the genome, activated upon PC4 knockdown.

Studying post-translational modification of chromatin proteins such as PC4, often gives a lot of scope to our understanding of how modulation of chromatin structure might occur in different biological contexts like disease or differentiation. Phosphorylation of histones has been a nodal regulator of chromatin compaction during important cellular processes as mitosis, meiosis and apoptosis. Implications of phosphorylation of non-histone chromatin proteins adds another layer of regulation to the complex chromatin dynamics.

However, there are some unresolved questions that arises and could be explored further. The detailed structural mechanism of Phospho-PC4 interacting with linker H1 or Phospho-PC4 binding to nucleosome contributes to its chromatin compaction functions needs to be answered. *In vitro* studies show that phosphorylated PC4 interacts with all linker H1 variants and Phosphomimic PC4 interacts strongly with C-terminus compared to N-terminus and full length. Studying the effect of phospho-PC4 mediated chromatin compaction and thereby gene expression upon disruption of PC4-H1 interaction could give us further mechanistic insights into the interplay of these two architectural proteins in maintaining higher order chromatin structure. One of the possible ways to study the detailed structural mechanism of PC4 mediated chromatin compaction would be solving the Cryo-EM structure of PC4 with nucleosome and PC4 with chromatosome. Since phosphorylation of PC4 has been shown to rescue the drastic chromatin de-compaction observed upon PC4 knockdown, analysing the changes in chromatin accessibility in Flag wild type, phosphomimic and phospho-mutant expressing cells by assays like ATAC-seq would show us the specific chromatin regions that are compacted by phospho-PC4. Chromatin wide

occupancy of linker H1 by ChIP sequencing along with chromatin accessibility changes could show us which chromatin regions are modulated by these two chromatin proteins. The neural genes that were repressed by PC4 in phosphorylation dependent manner have been shown to have REST-CoREST and HP1α containing repressor complex recruited to their promoters (Das C et al., 2010) and on the other hand important autophagy regulating genes which have enriched H3K9ac levels at their promoters are also repressed by phosphor-PC4. Thus, there could be different modes of regulating chromatin condensation by phosphor-PC4 at different genes in different contexts. Thus, it would be interesting to study what determines the specificity of gene repression by phosphor-PC4 in different physiological conditions.

This study shows that phosphorylation of PC4 is critical for its chromatin compaction function and maintenance of epigenetic state its effect could be explored in the area of DNA damage regulated by PC4. The role of PC4 has been studied in various aspects of DNA damage starting from preventing mutagenesis and oxidative DNA damage through its involvement in transcription coupled repair by binding to multifunctional DNA repair protein XPG (Pan, Z. et al., 1996) or being an activator of Non-homologous end joining (NHEJ) and double stranded DNA repair activity (Batta, K., et al., 2009). Since PC4 has been shown to accumulate rapidly at the DNA damage sites in the mammalian cells enhancing joining of the noncomplementary DNA ends stimulating double strand break rejoining *in vivo,* whether modulating its phosphorylation status have any effect on this would be interesting. This would open up more arena of how signalling pathways regulating DNA repair might cross talk with kinases that phosphorylated proteins like PC4.

PC4 has emerged as an important protein that is required for the maintenance of the nuclear shape and integrity and PC4 phosphorylation by mitotic kinase Aurora B has been a contributing factor to it (Dhanasekaran et al., 2016). PC4 attributes

to genome integrity by regulating several processes such as autophagy (Sikder S. et al., 2019) and chromosome segregation during mitosis, spindle assembly (Dhanasekaran K. et al., 2016) as well as suppressing G4 DNA mediated structures (Lopez C R. et al., 2017). Therefore, delineating different signalling cues mediating PC4 phosphorylation and identifying the specific residues getting phosphorylated and identifying different interacting partners in different contexts would further enhance our knowledge about how phosphorylation of PC4 contributes to various processes regulated by PC4 in maintaining the genome integrity.

4.3 Implications of p300 mediated acetylation of PC4 on its coactivator function and probable role in cancer manifestation

In our attempt to understand that why PC4 is enriched in phosphor form inside the nucleus despite negatively regulating its co-activator function, we delved into investigating another important modification that occurs in PC4, acetylation mediated by KAT3B or p300. Our findings in this study shows that acetylated PC4 might regulating its co-activator function and is associated with active chromatin quite opposite to the phosphorylated form. One probable explanation could be that post-translational modifications often act as fine tuner of protein functions restricting their localization, interaction and stability. Since PC4 is a transcriptional co-activator that has been involved in activating transcription of several transcription factors like p53, NFκB, VP16, there could signal dependent cues that might acetylate a certain population of PC4 that is not associated with chromatin compaction. Therefore, studying the implication of acetylated PC4 in such scenario would be more relevant. Thus, oral cancer provides a perfect system since acetylated PC4 has been shown to be enriched in oral cancer cells. To address this mechanistically we are currently generating wild type, acetylation defective and acetylation mimic mutants of PC4 in PC4 knockdown background

in oral cancer cells and look into the PC4 target gene expression levels as well as probing for some of the tumorigenic properties that would indicate that indeed the acetylation of PC4 is important for regulating transcription co-activation function that also translates into carcinogenesis. This will also explain the hyperacetylation of PC4 that is observed in oral cancer cells and patient samples. Aberrant acetylation of a non-histone proteins like PC4 may provide understanding of the specific gene pathways getting perturbed in oral cancer and how these pathways facilitate tumorigenesis. Studying the functional implications of this modification would also provide scope for designing strategies to target specifically the modifications of a protein that could be the functional form helping in disease progression. Genome-wide distribution of acetylated PC4 will enlighten our understanding of what regulatory regions of the chromatin are occupied by acetylated PC4 and how that might contribute to its functionality.

4.4 Role of post-translational modifications as a functional switch for a multifunctional nuclear protein, PC4

The experiments conducted in an attempt to understand the two objectives laid down in this study has provided the foundation of a possible switch mechanism between the two major modifications of PC4 that could be mediated via the cross-talk between the two different modified forms of PC4 or via cross-talk between upstream signaling pathways modulating the two modified forms of PC4. We already know from earlier evidences that Phosphorylated PC4 inhibits its ability to undergo acetylation. Given that CKII mediated phosphorylated form PC4 being so enriched within the nucleus, questions the possibility of it being acetylated at the same time. Therefore, further understanding of the upstream players that are responsible for PC4 acetylation-deacetylation or PC4 phosphorylation-dephosphorylation dynamics would help as to spatially dissect the two forms of PC4 within the nucleus. Further probing deeper into the

interacting partners of different modified forms of PC4 as well as studying the genome wide occupancy of the two modified forms would lead us in understanding the underlying molecular switch regulating the multifunctionality of PC4. Based on the results of our study we propose a model of how the two modifications of PC4 might be regulating its functions inside a cell (Figure 4.3).

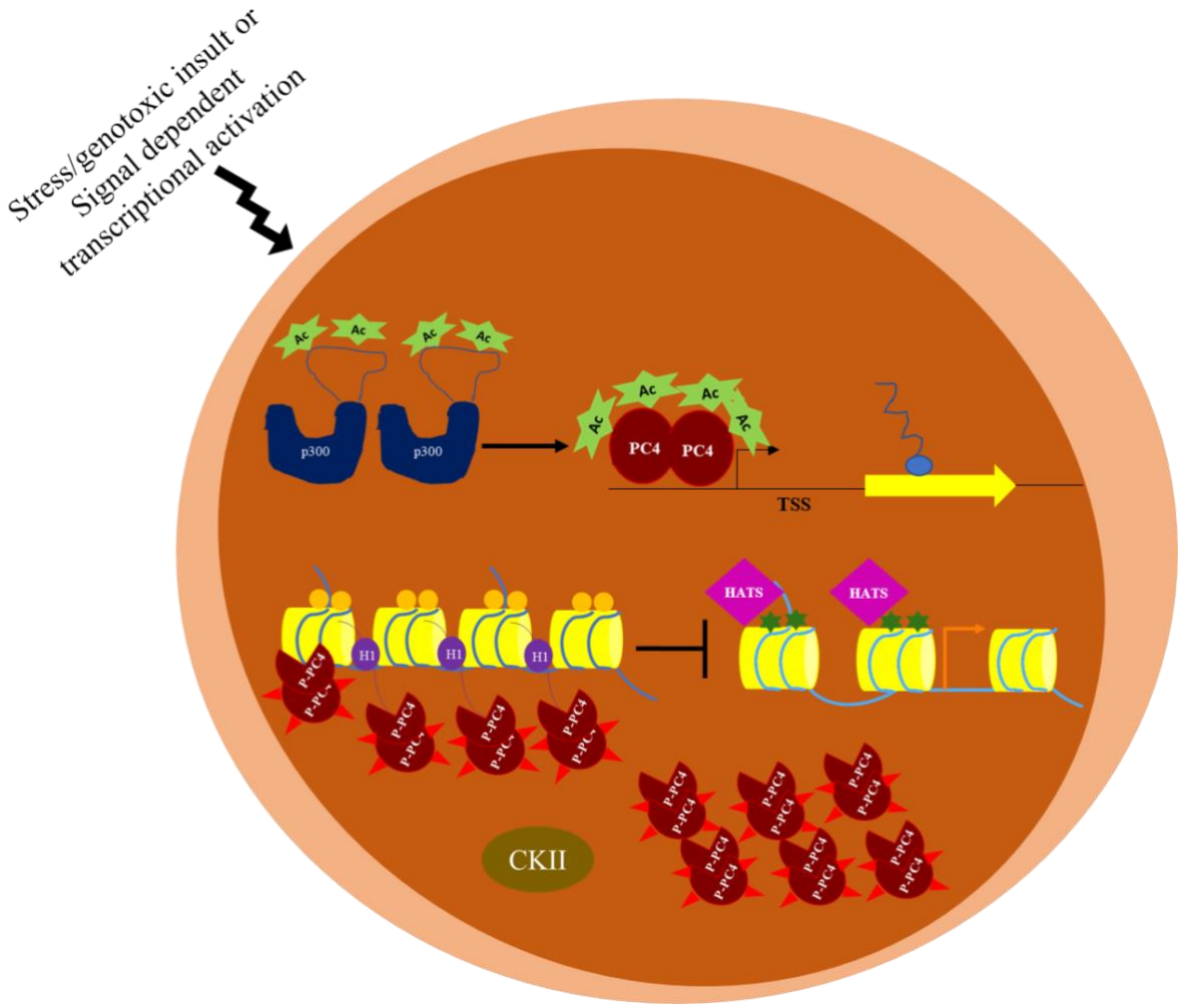

Figure 4.3: Post-translational modifications of PC4 regulating its function as genome organizer and as transcriptional co-activator in cells. PC4 is enriched in the phosphorylated form mediated by CKII in cells and this mediates chromatin compaction thereby maintaining a condensed repressive chromatin state inhibiting gene expression. Upon signal dependent transcriptional activation PC4 get acetylated by KAT3B/p300 and the acetylated PC4 acts as the transcriptional co-activator mediating gene expression.

LIST OF PUBLICATIONS

1.**Mustafi P.**, Hu M., Kumari S., Das C., Li Gu., Kundu T.K. Phosphorylation-dependent association of human chromatin protein PC4 to linker histone H1 regulates genome organization and transcription (Manuscript under review).

2. **Mustafi P.,** Joshi I., Washimkar K R., Mohiyuddin A., Mugale M N. and Kundu T.K. p300 mediated acetylation of PC4 regulates transcriptional activation of genes implicated in oral cancer manifestation. (Manuscript under preparation).

3.Sikder S., Kumari S., **Mustafi P.**, Ramdas N., Padhi S., Saha A., Bhadhuri U., Banerjee B., Manjithaya R. and Kundu T.K. Nonhistone human chromatin protein PC4 is critical for genomic integrity and negatively regulates autophagy. FEBS J. 2019 Nov;286(22):4422-4442. doi:10.1111/febs.14952. Epub 2019 Jun 6.

REFERENCES

Aagaard L., Schmid M., Warburton P., Jenuwein T. (2000). Mitotic phosphorylation of SUV39H1, a novel component of active centromeres, coincides with transient accumulation at mammalian centromeres. J Cell Sci.113,817-29.

Acker J., Nguyen NT., Vandamme M., Tavenet A., Briand-Suleau A., Conesa C. (2014). Sub1 and Maf1, two effectors of RNA polymerase III, are involved in the yeast quiescence cycle. PLoS One 9,e114587.

Adair JE., Kwon Y., Dement GA., Smerdon MJ., Reeves R. (2005). Inhibition of nucleotide excision repair by high mobility group protein HMGA1. J Biol Chem.280(37):32184-92.

Agarwal N., Hardt T., Brero A., Nowak D., Rothbauer U., Becker A., Leonhardt H., Cardoso MC. (2007). MeCP2 interacts with HP1 and modulates its heterochromatin association during myogenic differentiation. Nucleic Acids Res.35(16),5402-8.

Agresti A., Bianchi ME. (2003). HMGB proteins and gene expression. Curr Opin Genet Dev.13,170.

Ahel D., Horejsí Z., Wiechens N., Polo SE., Garcia-Wilson E., Ahel I., Flynn H., Skehel M., West SC., Jackson SP., Owen-Hughes T., Boulton SJ. (2009). Poly(ADP-ribose)-dependent regulation of DNA repair by the chromatin remodeling enzyme ALC1. Science. 325(5945),1240-3.

Ahn SH., Henderson KA., Keeney S., Allis CD. (2005). H2B (Ser10) phosphorylation is induced during apoptosis and meiosis in S. cerevisiae. Cell Cycle.4,780-3.

Akimoto Y., Yamamoto S., Iida S., Hirose Y., Tanaka A., Hanaoka F., Ohkuma Y. (2014). Transcription cofactor PC4 plays essential roles in collaboration with the small subunit of general transcription factor TFIIE. Genes Cells. 19(12),879-90.C

Akoulitchev S., Chuikov S., Reinberg D. (2000). TFIIH is negatively regulated by cdk8-containing mediator complexes. Nature.407(6800),102-6.

Alexiadis V., Waldmann T., Andersen J., Mann M., Knippers R., and Gruss C. (2000). The protein encoded by the proto-oncogene DEK changes the topology of chromatin and reduces the efficiency of DNA replication in a chromatin-specific manner. Genes Dev. 14,1308–1312.

Allepuz-Fuster P., Martínez-Fernández V., Garrido-Godino AI., Alonso-Aguado S., Hanes SD., Navarro F., Calvo O. (2014). Rpb4/7 facilitates RNA polymerase II CTD dephosphorylation. Nucleic Acids Res.42(22),13674-88.

Andrews AJ., Chen X., Zevin A., Stargell LA., Luger K. (2010). The histone chaperone Nap1 promotes nucleosome assembly by eliminating nonnucleosomal histone DNA Interactions. Mol Cell.37,834–842.

Andrews AJ., Luger K. (2011). Nucleosome structure(s) and stability: variations on a theme. Annu Rev Biophys. 40,99–117.

Angelov D., Molla A., Perche PY., Hans F., Côté J., Khochbin S., Bouvet P., Dimitrov S. (2003). The histone variant macroH2A interferes with transcription factor binding and SWI/SNF nucleosome remodeling. Mol Cell.11,1033–1041.

Arif M., Vedamurthy BM., Choudhari R., Ostwal YB., Mantelingu K., Kodaganur GS. and Kundu TK. (2010). Nitric oxide-mediated histone hyperacetylation in oral cancer: target for a water-soluble HAT inhibitor, CTK7A. Chem Biol.17,903-913.

Aucott R., Bullwinkel J., Yu Y., Shi W., Billur M., Brown JP., Menzel U., Kioussis D., Wang G., Reisert I., Weimer J., Pandita RK., Sharma GG., Pandita TK., Fundele R., Singh PB. (2008). HP1-beta is required for development of the cerebral neocortex and neuromuscular junctions. J Cell Biol.183(4),597-606.

Baarends WM., Hoogerbrugge JW., Roest HP., Ooms M., Vreeburg J., Hoeijmakers JH., Grootegoed JA. (1999). Histone ubiquitination and chromatin remodeling in mouse spermatogenesis. Dev Biol.207(2),322-33.

Baldassarre G., Fedele M., Battista S., Vecchione A., Klein-Szanto AJ., Santoro M., Waldmann TA., Azimi N., Croce CM., Fusco A. (2001). Onset of natural killer cell lymphomas in transgenic mice carrying a truncated HMGI-C gene by the chronic stimulation of the IL-2 and IL-15 pathway. Proc Natl Acad Sci U S A.98(14):7970-5.

Baker SA., Chen L., Wilkins AD., Yu P., Lichtarge O., Zoghbi HY. (2013). An AT-hook domain in MeCP2 determines the clinical course of Rett syndrome and related disorders. Cell.152(5),984-96.

Banerjee S., Kumar B. R., and Kundu T. K. (2004). General transcriptional coactivator PC4 activates p53 function. Mol. Cell. Biol. 24, 2052-2062.

Barbieri M., Chotalia M., Fraser J., Lavitas LM., Dostie J., Pombo A., Nicodemi M. (2012). Complexity of chromatin folding is captured by the strings and binders switch model. Proc Natl Acad Sci U S A.109,16173–16178.

Barlesi F., Giaccone G., Gallegos-Ruiz MI., Loundou A., Span SW., Lefesvre P., Kruyt FA. and Rodriguez JA. (2007). Global histone modifications predict prognosis of resected non small-cell lung cancer. Journal of clinical oncology : official journal of the American Society of Clinical Oncology.25,4358-4364.

Barski A., Cuddapah S., Cui K., Roh TY., Schones DE., Wang Z., Wei G., Chepelev I., Zhao K. (2007). High-resolution profiling of histone methylations in the human genome. Cell.129, 823–37.

Bartlett J., Blagojevic J., Carter D., Eskiw C., Fromaget M., Job C., Shamsher M., Trindade IF., Xu M., Cook PR. (2006). Specialized transcription factories. Biochem Soc Symp 73,67–75.

Bates D.L., Thomas J.O. (1981). Histones H1 and H5: One or two molecules per nucleosome? Nucleic Acids Res. 9,5883–5894.

Batta K., and Kundu TK. (2007). Activation of p53 function by human transcriptional coactivator PC4: role of proteinprotein interaction, DNA bending, and posttranslational modifications. Mol Cell Biol 27, 7603–7614.

Batta K., Yokokawa M., Takeyasu K., and Kundu T. K. (2009). Human transcriptional coactivator PC4 stimulates DNA end joining and activates DSB repair activity. J Mol Biol.385,788-799.

Bednar J., Garcia-Saez I., Boopathi R., Cutter A.R., Papai G., Reymer A., Syed S.H., Lone I.N., Tonchev O., Crucifix C., Menoni H., Papin C., Skoufias DA., Kurumizaka H., Lavery R., Hamiche A., Hayes JJ., Schultz P., Angelov D., Petosa C., Dimitrov S. (2017). Structure and dynamics of a 197 bp nucleosome in complex with linker histone H1. Mol. Cell.66, 384–397.

Belova GI., Postnikov YV., Furusawa T., Birger Y., Bustin M. (2008). Chromosomal protein HMGN1 enhances the heat shock-induced remodeling of Hsp70 chromatin. J Biol Chem.283,8080.

Beneke S. (2012). Regulation of chromatin structure by poly(ADP-ribosyl)ation. Front Genet.3,169.

Bertulat B., De Bonis ML., Della Ragione F., Lehmkuhl A., Milden M., Storm C., Jost KL., Scala S., Hendrich B., D'Esposito M., Cardoso MC. (2012). MeCP2 dependent heterochromatin reorganization during neural differentiation of a novel Mecp2-deficient embryonic stem cell reporter line. PLoS One.7(10),e47848.

Brero A., Easwaran HP., Nowak D., Grunewald I., Cremer T., Leonhardt H., Cardoso MC. (2005). Methyl CpG-binding proteins induce large-scale chromatin reorganization during terminal differentiation. J Cell Biol.169(5),733-43.

Brock MV., Herman JG., Baylin SB. (2007). Cancer as a manifestation of aberrant chromatin structure. Cancer J.13(1),3-8.

Broxmeyer H.E., Kappes F., Mor-Vaknin N., Legendre M., Kinzfogl J., Cooper S., Hangoc G., and Markovitz D.M. (2012). DEK regulates hematopoietic stem engraftment and progenitor cell proliferation. Stem Cells Dev.21,1449–1454.

Bianchi ME., Manfredi A. (2004). Chromatin and cell death. Biochim Biophys Acta.1677,181.
Bianchi ME., Agresti A. (2005). HMG proteins: dynamic players in gene regulation and differentiation. Curr Opin Genet Dev.15,496.

Bienvenu T., Chelly J. (2006). Molecular genetics of Rett syndrome: when DNA methylation goes unrecognized. Nat Rev Genet7(6),415-26.

Birger Y., West KL., Postnikov YV., Lim JH., Furusawa T., Wagner JP., Laufer CS., Kraemer KH., Bustin M. (2003). Chromosomal protein HMGN1 enhances the rate of DNA repair in chromatin. EMBO J.22(7),1665-75.

Birger Y., Catez F., Furusawa T., Lim JH., Prymakowska-Bosak M., West KL., Postnikov YV., Haines DC., Bustin M. (2005). Increased tumorigenicity and sensitivity to ionizing radiation upon loss of chromosomal protein HMGN1. Cancer Res.65(15),6711-8.

Birger Y., Davis J., Furusawa T., Rand E., Piatigorsky J., Bustin M. (2006). A role for chromosomal protein HMGN1 in corneal maturation. Differentiation.74(1),19-29.

Böhm V., Hieb AR., Andrews AJ., Gansen A., Rocker A., Tóth K., Luger K., Langowski J. (2011). Nucleosome accessibility governed by the dimer/tetramer interface. Nucleic Acids Res.39(8),3093-102.

Bonaldi T., Langst G., Strohner R., Becker PB., Bianchi ME. (2002). The DNA chaperone HMGB1 facilitates ACF/CHRAC-dependent nucleosome sliding. EMBO J.21,6865.

Bonev B., Cavalli G. (2016). Organization and function of the 3D genome. Nat. Rev. Genet. 17,661–678.

Boyes J., Byfield P., Nakatani Y., and Ogryzko V. (1998). Regulation of activity of the transcription factor GATA-1 by acetylation. Nature.396, 594-598.

Braberg H., Jin H., Moehle EA., Chan YA., Wang S., Shales M., Benschop JJ., Morris JH., Qiu C., Hu F., Tang LK., Fraser JS., Holstege FC., Hieter P., Guthrie C., Kaplan CD., Krogan NJ. (2013). From structure to systems: high-resolution, quantitative genetic analysis of RNA polymerase II. Cell.154(4),775-88.

Brandsen J., Werten S., van der Vliet P. C., Meisterernst M., Kroon J., and Gros P. (1997). C-terminal domain of transcription cofactor PC4 reveals dimeric ssDNA binding site. Nat. Struct.Biol. 4,900-903.

Briggs SD., Xiao T., Sun ZW., Caldwell JA., Shabanowitz J., Hunt DF., Allis CD., Strahl BD. (2002). Gene silencing: trans-histone regulatory pathway in chromatin. Nature.418(6897),498.

Brown DT., Izard T., Misteli T. (2006). Mapping the interaction surface of linker histone H10 with the nucleosome of native chromatin *in vivo*. Nat Struct Mol Biol.13,250 – 255.

Buganim Y., Faddah DA., Jaenisch R. (2013). Mechanisms and models of somatic cell reprogramming. Nat Rev Genet.14(6),427-39.

Bustin M., Reeves R. (1996). High-mobility-group chromosomal proteins: architectural components that facilitate chromatin function. Prog. Nucleic Acid Res. Mol. Biol.54,35–100.

Bustin M.(2001). Revised nomenclature for high mobility group (HMG) chromosomal proteins. Trends Biochem. Sci.26 ,152-153.

Bustin M., Catez F., Lim JH. (2005). The dynamics of histone H1 function in chromatin. Mol Cell.17,617.

Caldwell RB., Braselmann H., Schoetz U., Heuer S., Scherthan H., Zitzelsberger H. (2016). Positive Cofactor 4 (PC4) is critical for DNA repair pathway re-routing in DT40 cells. Sci Rep.6,28890.

Calnan DR. and Brunet A. (2008) The FoxO code. Oncogene 27:2276-2288.

Calvo O, and Manley J. L. (2001). Evolutionarily conserved interaction between CstF-64 and PC4 links transcription, polyadenylation, and termination. Mol. Cell. 7,1013-1023.

Calvo O., Manley JL. (2005). The transcriptional coactivator PC4/Sub1 has multiple functions in RNA polymerase II transcription. EMBO J.24(5),1009-20.

Calvo O. (2018). Sub1 and RNAPII, until termination does them part. Transcription.9(1),52-60.

Cantó C., Sauve AA., Bai P. (2013). Crosstalk between poly(ADP-ribose) polymerase and sirtuin enzymes. Mol Aspects Med. 34(6),1168-201.

Canzio D., Chang EY., Shankar S., Kuchenbecker KM., Simon MD., Madhani HD., Narlikar GJ., Al-Sady B. (2011). Chromodomain-mediated oligomerization of HP1 suggests a nucleosome-bridging mechanism for heterochromatin assembly. Mol Cell. 41(1),67-81.

Canzio D., Liao M., Naber N., Pate E., Larson A., Wu S., Marina DB., Garcia JF., Madhani HD., Cooke R., Schuck P., Cheng Y., Narlikar GJ. (2013). A conformational switch in HP1 releases auto-inhibition to drive heterochromatin assembly. Nature.496(7445),377-81.

Cao K., Lailler N., Zhang Y., Kumar A., Uppal K., Liu Z., Lee EK., Wu H., Medrzycki M., Pan C., Ho PY., Cooper GP Jr., Dong X., Bock C., Bouhassira EE., Fan Y. (2013). High-resolution mapping of H1 linker histone variants in embryonic stem cells. PLoS Genet 9,e1003417.

Cao R., Wang L., Wang H, Xia L., Erdjument-Bromage H., Tempst P., Jones RS., Zhang Y. (2002). Role of histone H3 lysine 27 methylation in Polycomb-group silencing. Science.298,1039-1043.

Catez F., Brown DT., Misteli T., Bustin M. (2002). Competition between histone H1 and HMGN proteins for chromatin binding sites. EMBO Rep.3,760.

Catez F., Ueda T., and Bustin M. (2006). Determinants of histone H1 mobility and chromatin binding in living cells. Nat Struct Mol Biol.13, 305-310.

Chakravarthi BV., Goswami MT., Pathi SS., Robinson AD., Cieślik M., Chandrashekar DS., Agarwal S., Siddiqui J., Daignault S., Carskadon SL., Jing X., Chinnaiyan AM., Kunju LP., Palanisamy N., Varambally S. (2016). MicroRNA-101 regulated transcriptional modulator SUB1 plays a role in prostate cancer. Oncogene.35(49),6330-6340.

Chandrasekharan MB., Huang F., Sun ZW. (2009). Ubiquitination of histone H2B regulates chromatin dynamics by enhancing nucleosome stability. Proc Natl Acad Sci U S A.106(39),16686-91.

Chang SC., Lai YC., Chen YC., Wang NK., Wang WS., Lai JI. (2018). CBX3/heterochromatin protein 1 gamma is significantly upregulated in patients with non-small cell lung cancer. Asia Pac J Clin Oncol.14(5):e283-e288.

Chan HM. and La Thangue NB. (2001). p300/CBP proteins: HATs for transcriptional bridges and scaffolds. J Cell Sci 114:2363-2373.

Chen CY., Chang CC., Yen CF., Chiu MT., Chang WH. (2009). Mapping RNA exit channel on transcribing RNA polymerase II by FRET analysis. Proc Natl Acad Sci USA.106,127–132.

Chen LF. and Greene WC .(2003) .Regulation of distinct biological activities of the NF-kappaB transcription factor complex by acetylation. J MolMed (Berl) 81:549-557.

Chen K., Chen Z., Wu D., Zhang L., Lin X., Su J., Rodriguez B., Xi Y., Xia Z., Chen X., Shi X., Wang Q., Li W. (2015). Broad H3K4me3 is associated with increased transcription elongation and enhancer activity at tumor-suppressor genes. Nat Genet. 47,1149–57.

Chen RZ., Akbarian S., Tudor M., Jaenisch R. (2003). Deficiency of methyl-CpG binding protein-2 in CNS neurons results in a Rett-like phenotype in mice. Nat Genet.27(3),327-31.

Chen Y., Sprung R., Tang Y., Ball H., Sangras B., Kim S. C., Falck JR., Peng J., Gu W., Zhao Y. (2007). Lysine propionylation and butyrylation are novel post-translational modifications in histones. Mol. Cell. Proteomics.6, 812–819.

Cherukuri S., Hock R., Ueda T., Catez F., Rochman M., Bustin M. (2008). Cell cycle-dependent binding of HMGN proteins to chromatin. Mol Biol Cell.19,1816.

Chou DM., Adamson B., Dephoure NE., Tan X., Nottke AC., Hurov KE., Gygi SP., Colaiácovo MP., Elledge SJ. (2010). A chromatin localization screen reveals poly (ADP ribose)-regulated recruitment of the repressive polycomb and NuRD complexes to sites of DNA damage. Proc Natl Acad Sci U S A.107(43),18475-80.

Ciccarone F., Zampieri M., Caiafa P. (2017). PARP1 orchestrates epigenetic events setting up chromatin domains. Semin Cell Dev Biol.63,123-134.

Clapier C R., and Cairns B R., (2009). The biology of chromatin remodeling complexes. Annu Rev Biochem 78,273-304.

Cloos PA., Christensen J., Agger K., Maiolica A., Rappsilber J., Antal T., Hansen KH., Helin K. (2006). The putative oncogene GASC1 demethylates tri- and dimethylated lysine 9 on histone H3. Nature.442(7100),307-11.

Cohen DR., Matarazzo V., Palmer AM., Tu Y., Jeon OH., Pevsner J., Ronnett GV. (2003). Expression of MeCP2 in olfactory receptor neurons is developmentally regulated and occurs before synaptogenesis. Mol Cell Neurosci.22(4),417-29.

Costanzo A., Merlo P., Pediconi N., Fulco M., Sartorelli V., Cole PA., Fontemaggi G., Fanciulli M., Schiltz L., Blandino G., Balsano C., and Levrero M. (2002). DNA damage-dependent acetylation of p73 dictates the selective activation of apoptotic target genes. Mol Cell 9:175-186.

Cremer T., Kurz, A., Zirbel R., Dietzel, S., Rinke B., Schrock E., Speicher M. R., Mathieu U., Jauch A., Emmerich P., Scherthan H., Ried T., Cremer C., and Lichter P. (1993). Role of chromosome territories in the functional compartmentalization of the cell nucleus. Cold Spring Harb Symp Quant Biol 58,777-792.

Cremer T., and Cremer C. (2001). Chromosome territories, nuclear architecture and gene regulation in mammalian cells. Nat. Rev. Genet. 2, 292-301.

Cremer T., Cremer M., Dietzel S., Müller S., Solovei I., Fakan S. (2006). Chromosome territories--a functional nuclear landscape. Curr Opin Cell Biol. 18(3),307-16.

Dai J., Higgins JM. (2005). Haspin: a mitotic histone kinase required for metaphase chromosome alignment. Cell Cycle. 4,665-8.

D'Amours D., Desnoyers S., D'Silva I., Poirier G.G., Poly(ADP-ribosyl)ation reactions in the regulation of nuclear functions, Biochem. J.342, 249–268.

Daniel JA., Torok MS., Sun ZW., Schieltz D., Allis CD., Yates JR 3rd., Grant PA. (2004). Deubiquitination of histone H2B by a yeast acetyltransferase complex regulates transcription. J Biol Chem.279(3),1867-71.

Das C., Hizume K., Batta K., Kumar B. R., Gadad S. S., Ganguly S., Lorain, S., Verreault, A., Sadhale P. P., Takeyasu K., and Kundu T. K. (2006). Transcriptional coactivator PC4, a chromatin-associated protein, induces chromatin condensation. Mol Cell Biol 26, 8303–8315.

Das C., Gadad S. S., and Kundu T. K. (2010). Human positive coactivator 4 controls heterochromatinization and silencing of neural gene expression by interacting with REST/NRSF and Co-REST. J Mol Biol.397,1-12.

Das C., Lucia MS., Hansen KC., Tyler JK. (2009). CBP/p300-mediated acetylation of histone H3 on lysine 56. Nature.459,113-117.

Das D., Scovell WM. (2001). The binding interaction of HMG-1 with the TATA-binding protein/TATA complex. J Biol Chem.276,32597.

Dasgupta A., Scovell WM. (2003). TFIIA abrogates the effects of inhibition by HMGB1 but not E1A during the early stages of assembly of the transcriptional preinitiation complex. Biochim Biophys Acta.1627,101.

Daujat S., Zeissler U., Waldmann T., Happel N., Schneider R. (2005). HP1 binds specifically to Lys26-methylated histone H1.4, whereas simultaneous Ser27 phosphorylation blocks HP1 binding. J Biol Chem.280(45),38090-5.

Davey CA., Sargent DF., Luger K., Maeder AW., Richmond TJ. (2002). Solvent mediated interactions in the structure of the nucleosome core particle at 1.9 Å resolution. J Mol Biol. 319, 1097–1113.

David L., Polo JM. (2014). Phases of reprogramming. Stem Cell Res.12(3),754-61.

Deal RB., Henikoff JG., Henikoff S. (2010). Genome-wide kinetics of nucleosome turnover determined by metabolic labeling of histones. Science. 328,1161–1164.

Dekker J. (2014). Two ways to fold the genome during the cell cycle: insights obtained with chromosome conformation capture. Epigenetics Chromatin.7,25.

Dekker J., Mirny L. (2016). The 3D Genome as Moderator of Chromosomal Communication. Cell. 164,1110–1121.

Della Ragione F., Filosa S., Scalabrì F., D'Esposito M. (2012). MeCP2 as a genome-wide modulator: the renewal of an old story. Front Genet.3,181.

Dettmann A., Jaschke Y., Triebel I., Bogs J., Schroder I., Schuller HJ. (2010). Mediator subunits and histone methyltransferase Set2 contribute to Ino2-dependent transcriptional activation of phospholipid biosynthesis in the yeast Saccharomyces cerevisiae. Mol Genet Genom.283,211–221.

Dhanasekaran K., Kumari S., Boopathi R., Shima H., Swaminathan A., Bachu M., Ranga U., Igarashi K., Kundu TK. (2016). Multifunctional human transcriptional coactivator protein PC4 is a substrate of Aurora kinases and activates the Aurora enzymes. FEBS J.283(6),968-85.

di Bari MG., Ciuffini L., Mingardi M., Testi R., Soddu S., Barilà D. (2006). c-Abl acetylation by histone acetyltransferases regulates its nuclear-cytoplasmic localization. EMBO Rep.7,727-733.

Ding HF., Rimsky S., Batson SC., Bustin M., Hansen U. (1994). Stimulation of RNA polymerase II elongation by chromosomal protein HMG-14. Science.265,796.

Dixon JR., Selvaraj S., Yue F., Kim A., Li Y., Shen Y., Hu M., Liu JS., Ren B. (2012). Topological domains in mammalian genomes identified by analysis of chromatin interactions. Nature. 485,376–380.

Dixon JR., Jung I., Selvaraj S., Shen Y., Antosiewicz-Bourget JE., Lee AY., Ye Z., Kim A., Rajagopal N., Xie W., Diao Y., Liang Ji., Zhao H., Lobanenkov Victor V., Ecker Joseph R., Thomson James A., Ren B. (2015). Chromatin architecture reorganization during stem cell differentiation. Nature. 518,331–336.

Dorigo B., Schalch T., Kulangara A., Duda S., Schroeder RR., Richmond TJ. (2004). Nucleosome arrays reveal the two-start organization of the chromatin fiber. Science 306,1571–1573.

Downs JA., Kosmidou E., Morgan A., Jackson SP. (2003). Suppression of homologous recombination by the Saccharomyces cerevisiae linker histone. Mol Cell.11(6),1685-92.

Dowen JM., Fan ZP., Hnisz D., Ren G., Abraham BJ., Zhang LN., Weintraub AS., Schuijers J., Lee TI., Zhao K., Young Richard A. (2014). Control of cell identity genes occurs in insulated neighborhoods in mammalian chromosomes. Cell.159,374–387.

Du Z., Song J, Wang Y., Zhao Y., Guda K., Yang S., Kao HY., Xu Y., Willis J., Markowitz SD., Sedwick D., Ewing RM. and Wang Z. (2010). DNMT1 stability is regulated by proteins coordinating deubiquitination and acetylation-driven ubiquitination. Sci Signal.3,ra80.

Dutta R., Tiu B., Sakamoto KM. (2016). CBP/p300 acetyltransferase activity in hematologic malignancies. Mol Genet Metab. 119(1-2),37-43.

Eissenberg JC., Elgin SC. (2000). The HP1 protein family: getting a grip on chromatin. Curr Opin Genet Dev. 10(2),204-10.

Elsheikh SE., Green AR., Rakha EA., Powe DG., Ahmed RA., Collins HM., Soria D., Garibaldi JM., Paish CE., Ammar AA., Grainge MJ., Ball GR., Abdelghany MK., Martinez-Pomares L., Heery DM. and Ellis IO. (2009). Global histone modifications in breast cancer correlate with tumor phenotypes, prognostic factors, and patient outcome. Cancer Res.69,3802-3809.

Eltsov M., Maclellan KM., Maeshima K., Frangakis AS., Dubochet J. (2008). Analysis of cryo-electron microscopy images does not support the existence of 30-nm chromatin fibers in mitotic chromosomes in situ. Proc Natl Acad Sci USA 105,19732–19737.

Ellwood KB., Yen YM., Johnson RC., Carey M. (2000). Mechanism for specificity by HMG-1 in enhanceosome assembly. Mol Cell Biol.20,4359.

Erdel F., Rademacher A., Vlijm R., Tünnermann J., Frank L., Weinmann R., Schweigert E., Yserentant K., Hummert J., Bauer C., Schumacher S., Al Alwash A., Normand C., Herten DP., Engelhardt J., Rippe K. (2020). Mouse Heterochromatin Adopts Digital Compaction States without Showing Hallmarks of HP1-Driven Liquid-Liquid Phase Separation. Mol Cell.78(2),236-249.

Erkina TY., Zou Y., Freeling S., Vorobyev VI., Erkine AM. (2010). Functional interplay between chromatin remodeling complexes RSC, SWI/SNF and ISWI in regulation of yeast heat shock genes. Nucleic Acids Res.38(5),1441-9.

Espada J., Ballestar E., Fraga MF., Villar-Garea A., Juarranz A., Stockert JC., Robertson KD., Fuks F., Esteller M. (2004). Human DNA methyltransferase 1 is required for maintenance of the histone H3 modification pattern. J Biol Chem. 279(35):37175-84.

Fan JY., Rangasamy D., Luger K., Tremethick DJ. (2004). H2A.Z alters the nucleosome surface to promote HP1alpha-mediated chromatin fiber folding. Mol Cell 16(4),655-61.

Fan Y., Nikitina T., Morin-Kensicki EM., Zhao J., Magnuson TR., Woodcock CL., Skoultchi AI. (2003). H1 linker histones are essential for mouse development and affect nucleosome spacing *in vivo.* Mol Cell Biol.23(13),4559-72.

Farrelly LA., Thompson RE., Zhao S., Lepack AE., Lyu Y., Bhanu NV., Zhang B., Loh YE., Ramakrishnan A., Vadodaria KC., Heard KJ., Erikson G., Nakadai T., Bastle RM., Lukasak BJ., Zebroski H 3rd., Alenina N., Bader M., Berton O., Roeder RG., Molina H., Gage FH., Shen L., Garcia BA., Li H., Muir TW., Maze I. (2019). Histone serotonylation is a permissive modification that enhances TFIID binding to H3K4me3. Nature.567(7749),535-539.

Fashena SJ., Reeves R., Ruddle NH. (1992). A poly(dA-dT) upstream activating sequence binds high-mobility group I protein and contributes to lymphotoxin (tumor necrosis factor-beta) gene regulation. Mol Cell Biol. 12,894.

Fedele M., Battista S., Manfioletti G., Croce CM., Giancotti V., Fusco A. (2001). Role of the high mobility group A proteins in human lipomas. Carcinogenesis. 22(10):1583-91.

Fedele M., Fidanza V., Battista S., Pentimalli F., Klein-Szanto AJ., Visone R., De Martino I., Curcio A., Morisco C., Del Vecchio L., Baldassarre G., Arra C., Viglietto G., Indolfi C., Croce CM., Fusco A. (2006). Haploinsufficiency of the Hmga1 gene causes cardiac hypertrophy and myelo-lymphoproliferative disorders in mice. Cancer Res.66(5):2536-43.

Feinberg AP., Ohlsson R., Henikoff S. (2006). The epigenetic progenitor origin of human cancer. Nat Rev Genet.7,21–33.

Festenstein R., Sharghi-Namini S., Fox M., Roderick K., Tolaini M., Norton T., Saveliev A., Kioussis D., Singh P. (1999). Heterochromatin protein 1 modifies mammalian PEV in a dose- and chromosomal-context-dependent manner. Nat Genet. 23(4),457-61.

Fichou Y., Nectoux J., Bahi-Buisson N., Rosas-Vargas H., Girard B., Chelly J., Bienvenu T. (2009). The first missense mutation causing Rett syndrome specifically affecting the MeCP2_e1 isoform. Neurogenetics. 10, 127.

Fischle W., Wang Y., Allis CD. (2003). Histone and chromatin cross-talk. Curr Opin Cell Biol.15,172–183.

Fousteri M., Vermeulen W., van Zeeland AA., Mullenders LH. (2006). Cockayne syndrome A and B proteins differentially regulate recruitment of chromatin remodeling and repair factors to stalled RNA polymerase II *in vivo*. Mol Cell.23,471.

Forlani G., Giarda E., Ala U., Di Cunto F., Salani M., Tupler R., Kilstrup-Nielsen C., Landsberger N. (2010). The MeCP2/YY1 interaction regulates ANT1 expression at 4q35: Novel hints for Rett syndrome pathogenesis.Hum. Mol. Genet.19, 3114–3123.

Fraga MF., Ballestar E., Villar-Garea A., Boix-Chornet M., Espada J., Schotta G., Bonaldi T., Haydon C., Ropero S., Petrie K., Iyer NG., Perez-Rosado A., Calvo E., Lopez JA., Cano A., Calasanz MJ., Colomer D., Piris MA., Ahn N., Imhof A., Caldas C., Jenuwein T. and Esteller M. (2005). Loss of acetylation at Lys16 and trimethylation at Lys20 of histone H4 is a common hallmark of human cancer. Nature genetics.37,391-400.

Frasca F., Rustighi A., Malaguarnera R., Altamura S., Vigneri P., Del Sal G., Giancotti V., Pezzino V., Vigneri R., Manfioletti G. (2006). HMGA1 inhibits the function of p53 family members in thyroid cancer cells. Cancer Res. 66(6):2980-9.

Freeman W.H., Benjamin P. (2005). *Genetics: A Conceptual Approach***,** 2nd ed., Nature Eduation.

Fujita N., Watanabe S., Ichimura T., Ohkuma Y., Chiba T., Saya H., Nakao M. (2003). MCAF mediates MBD1-dependent transcriptional repression. Mol Cell Biol.23(8),2834-43.

Fukuda A., Nakadai T., Shimada M., Tsukui T., Matsumoto M., Nogi Y., Meisterernst M., Hisatake K. (2004). Transcriptional coactivator PC4 stimulates promoter escape and facilitates transcriptional synergy by GAL4-VP16. Mol Cell Biol.24(14),6525-35.

Fu M., Wang C., Reutens AT., Wang J., Angeletti RH., Siconolfi-Baez L., Ogryzko V., Avantaggiati ML., Pestell RG. (2000). p300 and p300/cAMP-response element-binding protein-associated factor acetylate the androgen receptor at sites governing hormone-dependent transactivation. J Biol Chem. 275,20853-20860.

Fu M., Rao M., Wang C., Sakamaki T., Wang J., Di Vizio D., Zhang X., Albanese C., Balk S., Chang C., Fan S., Rosen E., Palvimo JJ., Jänne OA., Muratoglu S., Avantaggiati ML., Pestell RG. (2003). Acetylation of androgen receptor enhances coactivator binding and promotes prostate cancer cell growth. Mol Cell Biol 23:8563-8575.

Fusco A., Fedele M. (2007). Roles of HMGA proteins in cancer. Nat Rev Cancer. 7(12),899-910.

Fussner E., Ching RW., Bazett-Jones DP. (2011). Living without 30nm chromatin fibers. Trends Biochem Sci 36, 1–6.

Fung JC., Liu W., Deruijter WJ., Chen H., Abbey C., Sedat JW., and Agard DA. (1996). Towards fully automated high resolution electron tomography. J. Struct. Biol. 116,181-189.

Furusawa T., Lim JH., Catez F., Birger Y., Mackem S., Bustin M. (2006). Down-regulation of nucleosomal binding protein HMGN1 expression during embryogenesis modulates Sox9 expression in chondrocytes. Mol Cell Biol.26,592.

Fyodorov DV., Zhou BR., Skoultchi AI., Bai Y. (2018). Emerging roles of linker histones in regulating chromatin structure and function. Nat Rev Mol Cell Biol.19(3),192-206.

Gabellini D., Green MR., Tupler R. (2002). Inappropriate gene activation in FSHD: a repressor complex binds a chromosomal repeat deleted in dystrophic muscle. Cell.110,339.

Gabrovsky N, Georgieva M, Laleva M, Uzunov K, Miloshev G. (2013). Histone H1.0--a potential molecular marker with prognostic value for patients with malignant gliomas. Acta Neurochir (Wien).155(8),1437-42.

Gamble MJ., Fisher RP. (2007). SET and PARP1 remove DEK from chromatin to permit access by the transcription machinery. Nat Struct Mol Biol.14,548–555.

Garavís M., González-Polo N., Allepuz-Fuster P., Louro JA., Fernández-Tornero C., Calvo O. (2017). Sub1 contacts the RNA polymerase II stalk to modulate mRNA synthesis. Nucleic Acids Res.45(5),2458-2471.

Garavís M., Calvo O. (2017). Sub1/PC4, a multifaceted factor: from transcription to genome stability. Curr Genet.63(6),1023-1035.

García A., Rosonina E., Manley JL., Calvo O. (2010). Sub1 globally regulates RNA polymerase II C-terminal domain phosphorylation. Mol Cell Biol.30(21),5180-93.

García A., Collin A., Calvo O. (2012). Sub1 associates with Spt5 and influences RNA polymerase II transcription elongation rate. Mol Biol Cell.23(21),4297-312.

García-Jiménez C., García-Martínez JM., Chocarro-Calvo A. and De la Vieja A. (2014). A new link between diabetes and cancer: enhanced WNT/β-catenin signaling by high glucose. J Mol Endocrinol.52:R51-66. Wasylishen

Garcia-Saez I., Menoni H., Boopathi R., Shukla M.S., Soueidan L., Noirclerc-Savoye M., Le Roy A., Skoufias D.A., Bednar J., Hamiche A., Angelov D., Petosa C., Dimitrov S. (2018). Structure of an H1-bound 6-nucleosome array reveals an untwisted two-start chromatin fiber conformation. Mol. Cell. 72, 902–915.

Gaughan L., Logan IR., Cook S., Neal DE., Robson CN. (2002). Tip60 and histone deacetylase 1 regulate androgen receptor activity through changes to the acetylation status of the receptor. J Biol Chem. 277,25904-25913.

Ge H., Zhao Y., Chait BT., Roeder RG. (1994). Phosphorylation negatively regulates the function of coactivator PC4. Proc Natl Acad Sci USA 91, 12691–12695.

Georgel PT., Horowitz-Scherer RA., Adkins N., Woodcock CL., Wade PA., Hansen JC. (2003). Chromatin compaction by human MeCP2. Assembly of novel secondary chromatin structures in the absence of DNA methylation. J Biol Chem.278(34),32181-8.

Gerlitz G., Hock R., Ueda T., Bustin M. (2009). The dynamics of HMG protein-chromatin interactions in living cells. Biochem Cell Biol.87,127.

Ghosh R.P., Nikitina T., Horowitz-Scherer R.A., Gierasch L.M., Uversky V.N., Hite K., Hansen J.C., Woodcock C.L. (2010). Unique Physical Properties and Interactions of the Domains of Methylated DNA Binding
Protein 2. Biochemistry.49, 4395–4410.

Gibson B. A., Doolittle L.K., Schneider M.W.G., Jensen L.E., Gamarra N., Henry L., Gerlich D.W., Redding S., Rosen M.K. (2019). Organization of chromatin by intrinsic and regulated phase separation. Cell 179, 470-484.

Gilbert N., Boyle S., Fiegler H., Woodfine H., Carter N P., Bickmore W A. (2004). Chromatin Architecture of the Human Genome. Cell 118(5),555-566.

Goldman JA., Garlick JD., Kingston RE. (2010). Chromatin remodeling by imitation switch (ISWI) class ATP-dependent remodelers is stimulated by histone variant H2A.Z. J Biol Chem. 285,4645–4651.

Golipour A., David L., Liu Y., Jayakumaran G., Hirsch CL., Trcka D., Wrana JL. (2012). A late transition in somatic cell reprogramming requires regulators distinct from the pluripotency network. Cell Stem Cell.11(6),769-82.

Goto H., Tomono Y., Ajiro K., Kosako H., Fujita M., Sakurai M., Okawa K., Iwamatsu A., Okigaki T., Takahashi T., Inagaki M. (1999). Identification of a novel phosphorylation site on histone H3 coupled with mitotic chromosome condensation. J Biol Chem. 274(36),25543-9.

Gottschalk AJ., Timinszky G., Kong SE., Jin J., Cai Y., Swanson SK., Washburn MP., Florens L., Ladurner AG., Conaway JW., Conaway RC. (2009). Poly(ADP-ribosyl)ation directs recruitment and activation of an ATP-dependent chromatin remodeler. Proc Natl Acad Sci U S A.106(33),13770-4.

Greaves Ian K., Rangasamy D., Ridgway P., and Tremethick DJ. (2007). H2A.Z contributes to the unique 3D structure of the centromere. Proc Natl Acad Sci USA 104 (2),525-530.

Griffin WC., Gao J., Byrd AK., Chib S., Raney KD. (2017). A biochemical and biophysical model of G-quadruplex DNA recognition by positive coactivator of transcription 4. J Biol Chem. 292(23),9567-9582.

Grigoryev SA. (2001). Higher-order folding of heterochromatin: protein bridges span the nucleosome arrays. Biochem Cell Biol. 79,227–241.

Grigoryev SA., Woodcock CL. (1998). Chromatin structure in granulocytes. A link between tight compaction and accumulation of a heterochromatin-associated protein (MENT). J Biol Chem.273,3082–3089.

Grigoryev SA., Solovieva VO., Spirin KS., Krasheninnikov IA. (1992). A novel nonhistone protein (MENT) promotes nuclear collapse at the terminal stage of avian erythropoiesis. Exp Cell Res.198,268–275.

Grigoryev S.A., Bascom G., Buckwalter J.M., Schubert M.B., Woodcock C.L., Schlick T. (2016). Hierarchical looping of zigzag nucleosome chains in metaphase chromosomes. Proc. Natl. Acad. Sci. U. S. A. 113,1238–1243.

Grönroos E., Hellman U., Heldin CH. and Ericsson J. (2002) Control of Smad7 stability by competition between acetylation and ubiquitination. Mol Cell.10,483-493.

Guastafierro T., Catizone A., Calabrese R., Zampieri M., Martella O., Bacalini MG., Reale A., Di Girolamo M., Miccheli M., Farrar D., Klenova E., Ciccarone F., Caiafa P. (2013). ADP-ribose polymer depletion leads to nuclear Ctcf re-localization and chromatin rearrangement. Biochem J.449(3),623-30.

Gu W., and Roeder R G. (1997). Activation of p53 sequence-specific DNA binding by acetylation of the p53 C-terminal domain. Cell. 90(4),595-606.

Haile D. T., and Parvin J. D. (1999). Activation of transcription in vitro by the BRCA1 carboxyl-terminal domain. J. Biol. Chem. 274, 2113-2117.

Haince J. F., Kozlov, S., Dawson V. L., Dawson T. M., Hendzel M. J., Lavin M. F., and Poirier G. G. (2007). Ataxia telangiectasia mutated (ATM) signaling network is modulated by a novel poly(ADP-ribose)-dependent pathway in the early response to DNA-damaging agents. J. Biol. Chem. 282,16441–16453.

Haince J. F., McDonald D., Rodrigue A., Dery U., Masson J. Y., Hendzel M. J., and Poirier G. G. (2008). PARP1-dependent kinetics of recruitment of MRE11 and NBS1 proteins to multiple DNA damage sites. J. Biol. Chem. 283, 1197–1208.

Hale TK., Contreras A., Morrison AJ., Herrera RE. (2006). Phosphorylation of the Linker Histone H1 by CDK Regulates its binding to HP1alpha. Mol Cell.22,693–699.

Hamamori Y., Sartorelli V., Ogryzko V., Puri PL., Wu HY., Wang JY., Nakatani Y., Kedes L. (1999). Regulation of histone acetyltransferases p300 and PCAF by the bHLH protein twist and adenoviral oncoprotein E1A. Cell.96(3),405-13.

Hamilton C., Hayward RL., Gilbert N. (2011). Global chromatin fibre compaction in response to DNA damage. Biochem Biophys Res Commun.414(4),820-5.

Hanes SD. (2014). The Ess1 prolyl isomerase: traffc cop of the RNA polymerase II transcription cycle. Biochim Biophys Acta.1839,316–333.

Hansson ML., Popko-Scibor AE., Saint Just Ribeiro M., Dancy BM., Lindberg MJ., Cole PA., Wallberg AE. (2009). The transcriptional coactivator MAML1 regulates p300 autoacetylation and HAT activity. Nucleic Acids Res.37(9),2996-3006.

Hanzlikova H., Gittens W., Krejcikova K., Zeng Z. and Caldecott K. W. (2017). Overlapping roles for PARP1and PARP2 in the recruitment of endogenous XRCC1 and PNKP into oxidized chromatin. Nucleic Acids Res.45, 2546–2557.

Happel N., Doenecke D. (2009). Histone H1 and its isoforms: contribution to chromatin structure and function. Gene.431,1–12.

Hayakawa F., Towatari M., Ozawa Y., Tomita A., Privalsky ML., and Saito H. (2004). Functional regulation of GATA-2 by acetylation. J Leukoc Biol. 75,529-540.

Hechtman JF., Beasley MB., Kinoshita Y., Ko HM., Hao K., Burstein DE. (2013). Promyelocytic leukemia zinc finger and histone H1.5 differentially stain low- and high-grade pulmonary neuroendocrine tumors: a pilot immunohistochemical study. Hum Pathol.44(7),1400-5.

Hendrich B., Bird A. (1998). Identification and characterization of a family of mammalian methyl-CpG binding proteins. Mol Cell Biol.18(11),6538-47.

Henry NL., Bushnell DA., Kornberg RD. (1996). A yeast transcriptional stimulatory protein similar to human PC4. J Biol Chem.271(36),21842-7.

Henry KW., Wyce A., Lo WS., Duggan LJ., Emre NC., Kao CF., Pillus L., Shilatifard A., Osley MA., Berger SL. (2003). Transcriptional activation via sequential histone H2B ubiquitylation and deubiquitylation, mediated by SAGA-associated Ubp8. Genes Dev.17(21),2648-63.

Hergeth SP., Schneider R. (2015). The H1 linker histones: multifunctional proteins beyond the nucleosomal core particle. EMBO Rep.16(11),1439-53.

Herman JG., Baylin SB. (2003). Gene silencing in cancer in association with promoter hypermethylation. N Engl J Med. 349,2042–2054.

Herz HM., Hu D., Shilatifard A. (2014). Enhancer malfunction in cancer. Mol Cell.53,859–866.

Hill DA., Reeves R. (1997). Competition between HMG-I(Y), HMG-1 and histone H1 on four-way junction DNA. Nucleic Acids Res.25,3523.

Hill DA., Pedulla ML., Reeves R. (1999). Directional binding of HMG-I(Y) on four-way junction DNA and the molecular basis for competitive binding with HMG-1 and histone H1. Nucleic Acids Res.27,2135–2144.

Hirota T., Lipp J. J., Toh B. H., and Peters J. M. (2005). Histone H3 serine 10 phosphorylation by Aurora B causes HP1 dissociation from heterochromatin. Nature.438, 1176-1180.

Hizume K., Yoshimura S. H., and Takeyasu K. (2005). Linker Histone H1 per se can Induce Three-Dimensional Folding of Chromatin Fiber. Biochemistry. 44, 12978-12989.

Hoch DA., Stratton JJ., Gloss LM. (2007). Protein-protein Forster resonance energy transfer analysis of nucleosome core particles containing H2A and H2A.Z. J Mol Biol. 371,971–988.

Hochegger H., Dejsuphong D., Fukushima T., Morrison C., Sonoda E., Schreiber V., Zhao GY., Saberi A., Masutani M., Adachi N., Koyama H., de Murcia G., Takeda S. (2006). Parp-1 protects homologous recombination from interference by Ku and Ligase IV in vertebrate cells. EMBO J. 25(6),1305-14.

Holloway A. F., Occhiodoro F., Mittler G., Meisterernst M., and Shannon M. F. (2000). Functional interaction between the HIV transactivator Tat and the transcriptional coactivator PC4 in T cells. J. Biol. Chem. 275, 21668-21677.

Horike S., Cai S., Miyano M., Cheng JF., Kohwi-Shigematsu T. (2003). Loss of silent-chromatin looping and impaired imprinting of DLX5 in Rett syndrome. Nat Genet.37(1),31-40.

Huang B., Yang XD., Zhou MM., Ozato K. and Chen LF. (2009). Brd4 coactivates transcriptional activation of NF-kappaB via specific binding to acetylated RelA. Mol Cell Biol 29:1375-1387.

Huang J., Zhao Y., Huang D., Liu H., Justin N., Zhao W., Liu J., Peng Y. (2012). Structural features of the single-stranded DNA-binding protein MoSub1 from Magnaporthe oryzae. Acta Crystallogr D Biol Crystallogr.68,1071-6.

Hubbert C., Guardiola A., Shao R., Kawaguchi Y., Ito A., Nixon A., Yoshida M., Wang XF. and Yao TP. (2002). HDAC6 is a microtubule-associated deacetylase. Nature 417:455-458.

Hu J., Zhang Y., Zhao L., Frock RL., Du Z., Meyers RM., Meng FL., Schatz DG., Alt FW. (2015). Chromosomal Loop Domains Direct the Recombination of Antigen Receptor Genes. Cell.163,947–959.

Hupp TR., Sparks A., Lane DP. (1995). Small peptides activate the latent sequence-specific DNA binding function of p53. Cell.83(2),237-45.

Hurd PJ., Bannister AJ., Halls K., Dawson MA., Vermeulen M., Olsen JV., Ismail H., Somers J., Mann M., Owen-Hughes T., Gout I., Kouzarides T. (2012). Phosphorylation of histone H3 Thr-45 is linked to apoptosis. J Biol Chem.284(24),16575-83.

Huth JR., Bewley CA., Nissen MS., Evans JN., Reeves R., Gronenborn AM., Clore GM. (1997). The solution structure of an HMG-I(Y)-DNA complex defines a new architectural minor groove binding motif. Nat Struct Biol.4,657.

Hu X., Zhang C., Zhang Y., Hong CS., Chen W., Shen W., Wang H., He J., Chen P., Zhou Y., Shi C., Chu T. (2017). Down regulation of human positive coactivator 4

suppress tumorigenesis and lung metastasis of osteosarcoma. Oncotarget.8(32),53210-53225.

Hsu DS., Wang HJ., Tai SK., Chou CH., Hsieh CH., Chiu PH., Chen NJ. and Yang MH (2014). Acetylation of snail modulates the cytokinome of cancer cells to enhance the recruitment of macrophages. Cancer Cell 26:534-548.

Iaconelli J., Huang JH., Berkovitch SS., Chattopadhyay S., Mazitschek R., Schreiber SL., Haggarty SJ., Karmacharya R. (2015). HDAC6 inhibitors modulate Lys49 acetylation and membrane localization of β-catenin in human iPSC-derived neuronal cells. ACS Chem Biol.10,883-890.

Ikenoue T., Inoki K., Zhao B. and Guan KL. (2008) PTEN acetylation modulates its interaction with PDZ domain. Cancer Res 68:6908-6912.

Inoue Y., Itoh Y., Abe K., Okamoto T., Daitoku H., Fukamizu A., Onozaki K. and Hayashi H. (2007). Smad3 is acetylated by p300/CBP to regulate its transactivation activity. Oncogene 26:500-508.

Istomina NE., Shushanov SS., Springhetti EM., Karpov VL., Krasheninnikov IA., Stevens K., Zaret KS., Singh PB., Grigoryev SA. (2003). Insulation of the chicken beta-globin chromosomal domain from a chromatin-condensing protein, MENT. Mol Cell Biol.23(18),6455-68.

Ito A., Kawaguchi Y., Lai CH., Kovacs JJ., Higashimoto Y., Appella E. and Yao TP. (2002). MDM2-HDAC1-mediated deacetylation of p53 is required for its degradation. EMBO J.21,6236-6245.

Jackson DA., Pombo A. (1998). Replicon clusters are stable units of chromosome structure: evidence that nuclear organization contributes to the efficient activation and propagation of S phase in human cells. J Cell Biol. 140,1285–1295.

Jamai A., Imoberdorf RM., Strubin M. (2007). Continuous histone H2B and transcription-dependent histone H3 exchange in yeast cells outside of replication. Mol Cell. 25,345–355.

Jenuwein T., Allis CD. (2001). Translating the histone code. Science.293(5532),1074-80.

Jeong JW., Bae MK., Ahn MY., Kim SH., Sohn TK., Bae MH., Yoo MA., Song EJ., Lee KJ., Kim KW. (2002). Regulation and destabilization of HIF-1alpha by ARD1-mediated acetylation. Cell 111,709-720.

Ji X., Dadon DB., Powell BE., Fan ZP., Borges-Rivera D., Shachar S., Weintraub AS., Hnisz D., Pegoraro G., Lee TI., Misteli T., Jaenisch R., Young Richard A. (2016). 3D Chromosome Regulatory Landscape of Human Pluripotent Cells. Cell Stem Cell.18,262–275.

Jo J., Hwang S., Kim HJ., Hong S., Lee JE., Lee SG., Baek A., Han H., Lee JI., Lee I., Lee DR. (2016). An integrated systems biology approach identifies positive cofactor 4 as a factor that increases reprogramming efficiency. Nucleic Acids Res.44(3),1203-15.

John S., Reeves RB., Lin JX., Child R., Leiden JM., Thompson CB., Leonard WJ. (1995). Regulation of celltype-specific interleukin-2 receptor alpha-chain gene expression: potential role of physical interactions between Elf-1, HMG-I(Y), and NF-kappa B family proteins. Mol Cell Biol.15,1786.

John S., Robbins CM., Leonard WJ. (1996). An IL-2 response element in the human IL-2 receptor alpha chain promoter is a composite element that binds Stat5, Elf-1, HMG-I(Y) and a GATA family protein. EMBO J.15,5627.

Jones PA., Laird PW. (1999). Cancer epigenetics comes of age. Nat Genet.21,163–167.

Jonker HR., Wechselberger RW., Pinkse M., Kaptein R., Folkers GE. (2006). Gradual phosphorylation regulates PC4 coactivator function. FEBS J.273,1430-1444.

Ju BG., Solum D., Song EJ., Lee KJ., Rose DW., Glass CK., Rosenfeld MG. (2004). Activating the PARP-1 sensor component of the groucho/TLE1 corepressor complex mediates a CaMKinase II delta dependent neurogenic gene activation pathway. Cell.119,815–829.

Jung BP., Jugloff DG., Zhang G., Logan R., Brown S., Eubanks JH. (2003). The expression of methyl CpG binding factor MeCP2 correlates with cellular differentiation in the developing rat brain and in cultured cells. J Neurobiol.55(1),86-96.

Kadota S., Nagata K. (2014). Silencing of IFN-stimulated gene transcription is regulated by histone H1 and its chaperone TAF-I. Nucleic Acids Res.42(12),7642-53.

Kagey MH., Newman JJ., Bilodeau S., Zhan Y., Orlando DA., van Berkum NL., Ebmeier CC., Goossens J., Rahl PB., Levine SS., Taatjes DJ., Dekker J., Young RA. (2010). Mediator and cohesin connect gene expression and chromatin architecture. Nature. 467,430–435.

Kaiser, K., Stelzer, G., and Meisterernst, M. (1995). The coactivator p15 (PC4) initiates transcriptional activation during TFIIA-TFIID-promoter complex formation. EMBO J.14, 3520-3527.

Kannan P., and Tainsky M. A. (1999). Coactivator PC4 mediates AP-2 transcriptional activity and suppresses ras-induced transformation dependent on AP-2 transcriptional interference. Mol. Cell Biol. 19, 899-908.

Kappes F., Burger K., Baack M., Fackelmayer FO., Gruss C. (2001). Subcellular localization of the human proto-oncogene protein DEK. J Biol Chem.276,26317–23.

Kappes F., Scholten I., Richter N., Gruss C., and Waldmann T. (2004a). Functional domains of the ubiquitous chromatin protein DEK. Mol. Cell. Biol. 24, 6000–6010.

Kappes F., Damoc C., Knippers R., Przybylski M., Pinna L.A., and Gruss, C. (2004b). Phosphorylation by protein kinase CK2 changes the DNA binding properties of the human chromatin protein DEK. Mol. Cell. Biol.24,6011–6020.

Kappes F., Fahrer J., Khodadoust M.S., Tabbert A., Strasser C., Mor-Vaknin N., Moreno-Villanueva M., Bürkle A., Markovitz D.M., and Ferrando-May E. (2008). DEK is a poly(ADP-ribose) acceptor in apoptosis and mediates resistance to genotoxic stress. Mol. Cell. Biol.28,3245–3257.

Kappes F., Waldmann T., Mathew V., Yu J., Zhang L., Khodadoust M.S., Chinnaiyan A.M., Luger K., Erhardt S., Schneider R., and Markovitz D.M. (2011). The DEK oncoprotein is a Su(var) that is essential to heterochromatin integrity. Genes Dev. 25,673–678.

Kavanaugh GM., Wise-Draper TM., Morreale RJ., Morrison MA., Gole B., Schwemberger S., Tichy ED., Lu L., Babcock GF., Wells JM., Drissi R., Bissler JJ., Stambrook PJ., Andreassen PR., Wiesmüller L., Wells SI. (2011). The human DEK oncogene regulates DNA damage response signaling and repair. Nucleic Acids Res.39(17),7465-76.

Kaypee S., Sudarshan D., Shanmugam MK., Mukherjee D., Sethi G., Kundu TK. (2016). Aberrant lysine acetylation in tumorigenesis: Implications in the development of therapeutics. Pharmacol Ther.162,98-119.

Kaypee S., Sahadevan S. A., Patil S., Ghosh P., Roy N. S., Roy S., and Kundu T. K. (2018). Mutant and wild-type tumor suppressor p53 induces p300 autoacetylation. iScience 4, 260–272.

Kaypee S., Sahadevan SA., Sudarshan D., Halder Sinha S., Patil S., Senapati P., Kodaganur GS., Mohiyuddin A., Dasgupta D., Kundu TK. (2018). Oligomers of human histone chaperone NPM1 alter p300/KAT3B folding to induce autoacetylation. Biochim Biophys Acta Gen Subj.1862(8),1729-1741.

Khachaturov V., Xiao GQ., Kinoshita Y., Unger PD., Burstein DE. (2014). Histone H1.5, a novel prostatic cancer marker: an immunohistochemical study. Hum Pathol.45(10),2115-9.

Kiernan R., Bres V., Ng RW., Coudart MP., El Messaoudi S., Sardet C., Jin DY., Emiliani S., and Benkirane M. (2003a). Post-activation turn-off of NF-kappa B-dependent transcription is regulated by acetylation of p65. Journal of Biol.Chem.278,2758-2766.

Kim MY., Ann EJ., Kim JY., Mo JS., Park JH., Kim SY., Seo MS., Park HS. (2007) Tip60 histone acetyltransferase acts as a negative regulator of Notch1 signaling by means of acetylation. Mol Cell Biol 27:6506-6519.

Kim JM., Kim K., Schmidt T., Punj V., Tucker H., Rice JC., Ulmer TS., An W. (2015). Cooperation between SMYD3 and PC4 drives a distinct transcriptional program in cancer cells. Nucleic Acids Res.43(18),8868-83.

Kim MY., Mauro S., Gevry N., Lis JT., Kraus WL. (2004). NAD+-dependent modulation of chromatin structure and transcription by nucleosome binding properties of PARP-1. Cell.119,803–814.

Kirschmann DA., Lininger RA, Gardner LM., Seftor EA., Odero VA., Ainsztein AM., Earnshaw WC., Wallrath LL., Hendrix MJ. (2000). Down-regulation of HP1Hsalpha expression is associated with the metastatic phenotype in breast cancer. Cancer Res.60(13):3359-63.

Kishi N., Macklis JD. (2004). MECP2 is progressively expressed in post-migratory neurons and is involved in neuronal maturation rather than cell fate decisions. Mol Cell Neurosci.27(3),306-21.

Kishore AH., Batta K., Das C., Agarwal S., Kundu TK. (2007). p53 regulates its own activator: transcriptional co-activator PC4, a new p53-responsive gene. Biochem J.406(3),437-44.

Klosin A., Oltsch F., Harmon T., Honigmann A., Jülicher F., Hyman AA., Zechner C. (2020). Phase separation provides a mechanism to reduce noise in cells. Science.367(6476),464-468.

Kokura K., Kaul S.C., Wadhwa R., Nomura T., Khan M.M., Shinagawa T., Yasukawa T., Colmenares C., Ishii S. (2001). The Ski protein family is required for MeCP2-mediated transcriptional repression. J. Biol. Chem.276, 34115–34121.

Knaus R., Pollock R., Guarente L. (1996). Yeast SUB1 is a suppressor of TFIIB mutations and has homology to the human co-activator PC4. EMBO J.15(8),1933-40.

Kornberg R.D. (1974). Chromatin structure: a repeating unit of histones and DNA. Science.184, 868–871.

Korner U., Bustin M., Scheer U., Hock R. (2003). Developmental role of HMGN proteins in Xenopus laevis. Mech Dev.120,1177.

Kosak ST, Skok JA, Medina KL., Riblet R., Beau Michelle M Le., Fisher A G., Singh H. (2002). Subnuclear compartmentalization of immunoglobulin loci during lymphocyte development. Science 296,158-162.

Kostova NN., Srebreva LN., Milev AD., Bogdanova OG., Rundquist I., Lindner HH., Markov DV. (2005). Immunohistochemical demonstration of histone H1(0) in human breast carcinoma. Histochem Cell Biol.124(5),435-43.

Koutzamani E., Laborg H., Sarg B., Lindner HH., Rundquist I. (2002). Linker histone subtype composition and affinity for chromatin in situ in nucleated mature erythrocytes. J Biol Chem.277,44688–44694.

Kovacs JJ., Cohen TJ. and Yao TP. (2005). Chaperoning steroid hormone signaling via reversible acetylation. Nucl Recept Signal.3,e004.

Kraus WL. (2008). Transcriptional control by PARP-1: chromatin modulation, enhancer-binding, coregulation, and insulation. Curr Opin Cell Biol.20,294–302.

Kretzschmar M., Kaiser K., Lottspeich F., Meisterernst M. (1994). A novel mediator of class II gene transcription with homology to viral immediate-early transcriptional regulators. Cell.78(3),525–534.

Krietsch J., Rouleau M., Pic É., Ethier C., Dawson TM., Dawson VL., Masson JY., Poirier GG., Gagné JP. (2013). Reprogramming cellular events by poly(ADP-ribose)-binding proteins. Mol Aspects Med.34(6),1066-87.

Krishnakumar R., Gamble MJ., Frizzell KM., Berrocal JG., Kininis M., Kraus WL. (2008). Reciprocal binding of PARP-1 and histone H1 at promoters specifies transcriptional outcomes. Science.319(5864),r819-21.

Krishnakumar R., Kraus WL. (2010). PARP-1 regulates chromatin structure and transcription through a KDM5B-dependent pathway. Mol Cell. 39(5),736-49.

Kruithof M., Chien F-T., Routh A., Logie C., Rhodes D., Noort J van. (2009). Single-molecule force spectroscopy reveals a highly compliant helical folding for the 30-nm chromatin fiber. Nat Struct Mol Biol 16(5),534-40.

Kumar B. R., Swaminathan V., Banerjee S., and Kundu T. K. (2001). p300-mediated acetylation of human transcriptional coactivator PC4 is inhibited by phosphorylation. J Biol Chem. 276,16804-16809.

Kuniyasu H, Chihara Y, Kondo H. Differential effects between amphoterin and advanced glycation end products on colon cancer cells. (2003). Int J Cancer.104(6),722-7.

Kuzmichev A., Jenuwein T., Tempst P., Reinberg D. (2004). Different EZH2-containing complexes target methylation of histone H1 or nucleosomal histone H3. Mol Cell.14(2),183-93.

Lada AG., Kliver SF., Dhar A., Polev DE., Masharsky AE., Rogozin IB., Pavlov YI. (2015). Disruption of transcriptional coactivator Sub1 leads to genome-wide re-distribution of clustered mutations induced by APOBEC in active yeast genes. PLoS Genet.11,e1005217.

Laitinen J., Sistonen L., Alitalo K., Hölttä E. (1995). Cell transformation by c-Ha-rasVal12 oncogene is accompanied by a decrease in histone H1 zero and an increase in nucleosomal repeat length. J Cell Biochem. 57(1):1-11.

Landau DA., Wu CJ. (2013). Chronic lymphocytic leukemia: molecular heterogeneity revealed by high-throughput genomics. Genome Med.5(5):47.

Larson A.G., Elnatan D., Keenen M.M., Trnka M.J., Johnston J.B., Burlingame A.L., Agard D.A., Redding S., Narlikar G.J. (2017). Liquid droplet formation by HP1α suggests a role for phase separation in heterochromatin. Nature. 547,236-240.

Laybourn PJ., Kadonaga JT. (1991). Role of nucleosomal cores and histone H1 in regulation of transcription by RNA polymerase II. Science. 254(5029),238-45.

Lee DH., Ryu HW., Kim GW., Kwon SH. (2019). Comparison of three heterochromatin protein 1 homologs in Drosophila. J Cell Sci. 132(3),jcs222729.

Lee H., Habas R., Abate-Shen C. (2004). MSX1 cooperates with histone H1b for inhibition of transcription and myogenesis. Science.304(5677),1675-8.

Lee K K., Haraguchi T., Lee R S., Koujin T., Hiraoka Y., Wilson KL. (2001). Distinct functional domains in emerin bind lamin A and DNA-bridging protein BAF. J Cell Sci. 114, 4567-73.

Lee YH., Liu X., Qiu F., O'Connor TR., Yen Y., Ann DK. (2015). HP1β is a biomarker for breast cancer prognosis and PARP inhibitor therapy. PLoS One.10(3):e0121207.

Le Hir H., Izaurralde E., Maquat LE., Moore MJ. (2000). The spliceosome deposits multiple proteins 20-24 nucleotides upstream of mRNA exon–exon junctions. EMBO J .19,6860–6869.

Le Hir H., Gatfield D., Izaurralde E., Moore MJ. (2010). The exon-exon junction complex provides a binding platform for factors involved in mRNA export and nonsense-mediated mRNA decay. EMBO J. 20,4987–97.

Lehtonen S., Lehtonen E. (2001). HMG-17 is an early marker of inductive interactions in the developing mouse kidney. Differentiation.67,154.

Lepack AE., Werner CT., Stewart AF., Fulton SL., Zhong P., Farrelly LA., Smith ACW., Ramakrishnan A., Lyu Y., Bastle RM., Martin JA., Mitra S., O'Connor RM., Wang ZJ., Molina H., Turecki G., Shen L., Yan Z., Calipari ES., Dietz DM., Kenny PJ., Maze I. (2020). Dopaminylation of histone H3 in ventral tegmental area regulates cocaine seeking. Science.368(6487),197-201.

Levy L., Wei Y., Labalette C., Wu Y., Renard CA., Buendia MA. and Neuveut C. (2004) Acetylation of beta-catenin by p300 regulates beta-catenin-Tcf4 interaction. Mol Cell Biol 24:3404-3414.

Lieberman-Aiden E., van Berkum N. L., Williams L., Imakaev M., Ragoczy T., Telling A., Amit I., Lajoie B. R., Sabo P. J., Dorschner M. O., Sandstrom R., Bernstein B., Bender M. A., Groudine M., Gnirke A., Stamatoyannopoulos J., Mirny L. A., Lander E. S., Dekker J. (2009). Comprehensive mapping of long-range interactions reveals folding principles of the human genome. Science 326, 289–293.

Li, B., Pattenden, S.G., Lee, D., Gutierrez, J., Chen, J., Seidel, C., Gerton, J., and Workman, J.L. (2005). Preferential occupancy of histone variant H2AZ at inactive promoters influences local histone modifications and chromatin remodeling. Proc. Natl. Acad. Sci.USA 102, 18385–18390.

Li G., Reinberg D. (2011). Chromatin higher-order structures and gene regulation. Curr Opin Genet Dev 21,175-186.

Li H., Kaminski MS., Li Y., Yildiz M., Ouillette P., Jones S., Fox H., Jacobi K., Saiya-Cork K., Bixby D., Lebovic D., Roulston D., Shedden K., Sabel M., Marentette L., Cimmino V., Chang AE., Malek SN. (2014). Mutations in linker histone genes HIST1H1 B, C, D, and E; OCT2 (POU2F2); IRF8; and ARID1A underlying the pathogenesis of follicular lymphoma. Blood.,123(10):1487-98.

Li JY, Patterson M, Mikkola HK, Lowry WE, Kurdistani SK. (2012). Dynamic distribution of linker histone H1.5 in cellular differentiation. PLoS Genet. 8(8):e1002879.

Lim JH, Catez F, Birger Y, West KL, Prymakowska-Bosak M, Postnikov YV, Bustin M. (2004). Chromosomal protein HMGN1 modulates histone H3 phosphorylation. Mol Cell.15(4):573-84.

Lim JH., West KL., Rubinstein Y., Bergel M., Postnikov YV., Bustin M. (2005). Chromosomal protein HMGN1 enhances the acetylation of lysine 14 in histone H3. EMBO J.24(17),3038-48.

Linhoff MW., Garg SK., Mandel G. (2015). A high-resolution imaging approach to investigate chromatin architecture in complex tissues. Cell.163,246–55.

Lin L., Piao J., Gao W., Piao Y., Jin G., Ma Y., Li J., Lin Z. (2013). DEK over expression as an independent biomarker for poor prognosis in colorectal cancer. BMC Cancer.13:366.

Liu B., Yang R., Wong KA., Getman C., Stein N., Teitell MA., Cheng G., Wu H., Shuai K. (2005). Negative regulation of NF-kappaB signaling by PIAS1. Mol Cell Biol.25(3),1113-23.

Liu BL., Cheng JX., Zhang X., Wang R., Zhang W., Lin H., Xiao X., Cai S., Chen XY., Cheng H. (2010). Global histone modification patterns as prognostic markers to classify glioma patients. Cancer Epidemiol Biomarkers Prev.19(11),2888-96.

Liu M., Huang F., Zhang D., Ju J., Wu XB., Wang Y., Wang Y., Wu Y., Nie M., Li Z., Ma C., Chen X., Zhou JY., Tan R., Yang BL., Zen K., Zhang CY., Chen YG., Zhao Q. (2015). Heterochromatin protein HP1γ promotes colorectal cancer progression and is regulated by miR-30a. Cancer Res.75(21),4593-604.

Li W., Chen P., Yu J., Dong L., Liang D., Feng J., Yan J., Wang PY., Li Q., Zhang Z., Li M., Li G. (2016). FACT Remodels the Tetranucleosomal Unit of Chromatin Fibers for Gene Transcription. Mol Cell.64(1),120-133.

Li Y., Sabari BR., Panchenko T., Wen H., Zhao D., Guan H., Wan L., Huang H., Tang Z., Zhao Y., Roeder RG., Shi X., Allis CD., Li H. (2016). Molecular Coupling of Histone Crotonylation and Active Transcription by AF9 YEATS Domain. Mol Cell. 62(2),181-193.

Li Y., Li Z., Dong L., Tang M., Zhang P., Zhang C., Cao Z., Zhu Q., Chen Y., Wang H., Wang T., Lv D., Wang L., Zhao Y., Yang Y., Wang H., Zhang H., Roeder RG., Zhu

WG. (2018). Histone H1 acetylation at lysine 85 regulates chromatin condensation and genome stability upon DNA damage. Nucleic Acids Res.46(15),7716-7730.

Lohr JG., Stojanov P., Lawrence MS., Auclair D., Chapuy B., Sougnez C., Cruz-Gordillo P, Knoechel B., Asmann YW., Slager SL., Novak AJ., Dogan A., Ansell SM., Link BK., Zou L., Gould J., Saksena G., Stransky N., Rangel-Escareño C., Fernandez-Lopez JC., Hidalgo-Miranda A., Melendez-Zajgla J., Hernández-Lemus E., Schwarz-Cruz y Celis A., Imaz-Rosshandler I., Ojesina AI., Jung J., Pedamallu CS., Lander ES., Habermann TM., Cerhan JR., Shipp MA., Getz G., Golub TR. (2012). Discovery and prioritization of somatic mutations in diffuse large B-cell lymphoma (DLBCL) by whole-exome sequencing. Proc Natl Acad Sci U S A.109(10):3879-84.

Lopez CR., Singh S., Hambarde S., Griffin WC., Gao J., Chib S., Yu Y., Ira G., Raney KD., Kim N. (2017). Yeast Sub1 and human PC4 are G-quadruplex binding proteins that suppress genome instability at co-transcriptionally formed G4 DNA. Nucleic Acids Res.45(10),5850-5862.

Lucas JS., Zhang Y., Dudko OK., Murre C. (2014). 3D trajectories adopted by coding and regulatory DNA elements: first-passage times for genomic interactions. Cell. 158,339–352.

Luger K., Rechsteiner T. J., Flaus A. J., Waye M. M., and Richmond T. J. (1997). Characterization of nucleosome core particles containing histone proteins made in bacteria. J Mol Biol 272, 301-311.

Luger K., Richmond TJ. (1998). The histone tails of the nucleosome. Curr Opin Genet Dev.8,140–146.

Luger K., Dechassa ML., Tremethick D J. (2012). Nat Rev Mol Cell Biol. 13(7),436–447.

Lührs H., Hock R., Schauber J., Weihrauch M., Harrer M., Melcher R., Scheppach W., Bustin M., and Menzel T. (2002) Modulation of HMG-N2 binding to chromatin by butyrate-induced acetylation in human colon adenocarcinoma cells. Int J Cancer.97,567-573.

Luijsterburg MS., Lindh M., Acs K., Vrouwe MG., Pines A., van Attikum H., Mullenders LH., Dantuma NP. (2012). DDB2 promotes chromatin decondensation at UV-induced DNA damage. J Cell Biol.197(2),267-81.

Lukásová E., Koristek Z., Falk M., Kozubek S., Grigoryev S., Kozubek M., Ondrej V., Kroupová I. (2005). Methylation of histones in myeloid leukemias as a potential marker of granulocyte abnormalities. J Leukoc Biol. 77(1),100-11.

Lunyak V.V., Burgess R., Prefontaine G.G., Nelson C., Sze S.H., Chenoweth J., Schwartz P., Pevzner P.A., Glass C., Mandel G., Rosenfeld MG. (2002). Corepressor-dependent silencing of chromosomal regions encoding neuronal genes. Science.298, 1747–1752.

Lupiáñez D.G., Kraft K., Heinrich V., Krawitz P., Brancati F., Klopocki E., Horn D., Kayserili H., Opitz J.M., Laxova R. (2015). Disruptions of topological chromatin domains cause pathogenic rewiring of gene-enhancer interactions. Cell.161,1012–1025.

Luo P., Zhang C., Liao F., Chen L., Liu Z., Long L., Jiang Z., Wang Y., Wang Z., Liu Z., Miao H., Shi C. (2019). Transcriptional positive cofactor 4 promotes breast cancer proliferation and metastasis through c-Myc mediated Warburg effect. Cell Commun Signal.17(1),36.

Lu X., Wontakal SN., Emelyanov AV., Morcillo P., Konev AY., Fyodorov DV., Skoultchi AI. (2009). Linker histone H1 is essential for Drosophila development, the establishment of pericentric heterochromatin, and a normal polytene chromosome structure. Genes Dev.23(4),452–65.

Lu X., Wontakal SN., Kavi H., Kim BJ., Guzzardo PM., Emelyanov AV., Xu N., Hannon GJ., Zavadil J., Fyodorov DV., Skoultchi AI. (2013). Drosophila H1 regulates the genetic activity of heterochromatin by recruitment of Su(var)3-9. Science.340(6128),78–81.

Lyst M.J., Ekiert R., Ebert D.H., Merusi C., Nowak J., Selfridge J., Guy J., Kastan N.R., Robinson N.D., de Lima Alves F. (2013). Rett syndrome mutations abolish the interaction of MeCP2 with the NCoR/SMRT co-repressor. Nat. Neurosci. 16, 898–902.

Machida S., Takizawa Y., Ishimaru M., Sugita Y., Sekine S., Nakayama JI., Wolf M., Kurumizaka H. (2018). Structural Basis of Heterochromatin Formation by Human HP1. Mol Cell. 69(3),385-397.

Ma C., Nie XG., Wang YL., Liu XH., Liang X., Zhou QL., Wu DP. (2019). CBX3 predicts an unfavorable prognosis and promotes tumorigenesis in osteosarcoma. Mol Med Rep. 19(5):4205-4212.

Ma H., Samarabandu J., Devdhar RS., Acharya R., Cheng PC., Meng C., Berezney R. (1998). Spatial and temporal dynamics of DNA replication sites in mammalian cells. J Cell Biol. 143,1415–1425.

Maeshima K., Imai R., Tamura S., Nozaki T. (2014). Chromatin as dynamic 10-nm fibers. Chromosoma.123(3),225-37.

Mahy NL., Perry PE., Bickmore WA., (2002). Gene density and transcription influence the localization of chromatin outside of chromosome territories detectable by FISH. J Cell Biol. 159(5),753-63.

Maier VK., Chioda M., Rhodes D., Becker PB. (2008). ACF catalyses chromatosome movements in chromatin fibres. EMBO J.27(6),817-26.

Malewicz M., Kadkhodaei B., Kee N., Volakakis N., Hellman U., Viktorsson K., Leung CY., Chen B., Lewensohn R., van Gent DC., Chen DJ., Perlmann T. (2011). Essential role for DNA-PK-mediated phosphorylation of NR4A nuclear orphan receptors in DNA double-strand break repair. Genes Dev. 25(19),2031-40.

Malik S., Guermah M., and Roeder R. G. (1998). A dynamic model for PC4 coactivator function in RNA polymerase II transcription. Proc Natl Acad Sci U S A.95, 2192-2197.

Maloney A., Clarke PA., Naaby-Hansen S., Stein R., Koopman JO., Akpan A., Yang A., Zvelebil M., Cramer R., Stimson L., Aherne W., Banerji U., Judson I., Sharp S., Powers M., deBilly E., Salmons J., Walton M., Burlingame A., Waterfield M., Workman P. (2007). Gene and protein expression profiling of human ovarian cancer cells treated with the heat shock protein 90 inhibitor 17-allylamino-17-demethoxygeldanamycin. Cancer Res.67(7),3239-53.

Manuyakorn A., Paulus R., Farrell J., Dawson NA., Tze S., Cheung-Lau G., Hines OJ., Reber H., Seligson DB., Horvath S., Kurdistani SK., Guha C., Dawson DW. (2010). Cellular histone modification patterns predict prognosis and treatment response in resectable pancreatic adenocarcinoma: results from RTOG 9704. J Clin Oncol.28,1358-1365.

Margueron R., Reinberg D. (2011). The Polycomb complex PRC2 and its mark in life. Nature.469(7330),343-9.

Martinez-Balbas MA., Bauer UM., Nielsen SJ., Brehm A., and Kouzarides T. (2000). Regulation of E2F1 activity by acetylation. EMBO J.19,662-671.

Martianov I., Brancorsini S., Catena R., Gansmuller A., Kotaja N., Parvinen M., Sassone-Corsi P., Davidson I. (2005). Polar nuclear localization of H1T2, a histone H1 variant, required for spermatid elongation and DNA condensation during spermiogenesis. Proc Natl Acad Sci USA. 102,2808-2813.

Matrka MC., Hennigan RF., Kappes F., DeLay ML., Lambert PF., Aronow BJ., Wells SI. (2015). DEK over-expression promotes mitotic defects and micronucleus formation. Cell Cycle.14(24):3939-53.

Marzio G., Wagener C., Gutierrez MI., Cartwright P., Helin K., and Giacca M. (2000). E2F family members are differentially regulated by reversible acetylation. J Biol Chem. 275,10887-10892.

Matsuyama A., Shimazu T., Sumida Y., Saito A., Yoshimatsu Y., Seigneurin-Berny D., Osada H., Komatsu Y., Nishino N., Khochbin S., Horinouchi S. and Yoshida M. (2002). *In vivo* destabilization of dynamic microtubules by HDAC6-mediated deacetylation. EMBO J 21:6820-6831.

McGarvey T., Rosonina E., McCracken S., Li Q., Arnaout R., Mientjes E., Nickerson JA., Awrey D., Greenblatt J., Grosveld G., Blencowe BJ. (2000). The acute myeloid leukemia-associated protein, DEK, forms a splicing-dependent interaction with exon-product complexes. J Cell Biol.150(2),309-20.

McGowan S., Buckle AM., Irving JA., Ong PC., Bashtannyk-Puhalovich TA., Kan WT., Henderson KN., Bulynko YA., Popova EY., Smith AI., Bottomley SP., Rossjohn J., Grigoryev SA., Pike RN., Whisstock JC. (2006). X-ray crystal structure of MENT:

evidence for functional loop-sheet polymers in chromatin condensation. EMBO J.25(13),3144-55.

Medrzycki M., Zhang Y., McDonald JF, Fan Y. (2012). Profiling of linker histone variants in ovarian cancer. Front Biosci (Landmark Ed).1;17:396-406.

Medrzycki M., Zhang Y., Zhang W., Cao K., Pan C., Lailler N., McDonald JF., Bouhassira EE., Fan Y. (2014). Histone h1.3 suppresses h19 noncoding RNA expression and cell growth of ovarian cancer cells. Cancer Res.74(22),6463-73.

Mele M., and Rinn John L. (2016). "Cat's cradling" the 3D genome by the act of lncRNA transcription. Mol Cell 62,657–664.

Merika M., Williams AJ., Chen G., Collins T., Thanos D. (1998). Recruitment of CBP/p300 by the IFN beta enhanceosome is required for synergistic activation of transcription. Mol Cell.1,277.

Merika M., Thanos D. (2001). Enhanceosomes. Curr Opin Genet Dev.11,205.

Messner S., Altmeyer M., Zhao H., Pozivil A., Roschitzki B., Gehrig P., Rutishauser D., Huang D., Caflisch A., Hottiger MO. (2010). PARP1 ADP-ribosylates lysine residues of the core histone tails. Nucleic Acids Res.38(19),6350-62.

Millán-Ariño L., Islam AB., Izquierdo-Bouldstridge A., Mayor R., Terme JM., Luque N., Sancho M., López-Bigas N., Jordan A. (2014). Mapping of six somatic linker histone H1 variants in human breast cancer cells uncovers specific features of H1.2. Nucleic Acids Res.42(7),4474-93.

Mirzabekov AD., Pruss DV., Ebralidse KK. (1990). Chromatin superstructure-dependent crosslinking with DNA of the histone H5 residues Thr1, His25 and His62. J. Mol. Biol.211,479-491.

Misteli T., Gunjan, A., Hock R., Bustin M., and Brown D. T. (2000). Dynamic binding of histone H1 to chromatin in living cells. Nature. 408, 877-881.

Mondal P., Saleem S., Sikder S., Kundu TK., Biswas SC., Roy S. (2019). Multifunctional transcriptional coactivator PC4 is a global co-regulator of p53-dependent stress response and gene regulation. J Biochem.166(5),403-413.

Morgan MA., Shilatifard A. (2015). Chromatin signatures of cancer. Genes Dev.29(3),238-49.

Morin RD., Johnson NA., Severson TM., Mungall AJ., An J., Goya R., Paul JE., Boyle M., Woolcock BW., Kuchenbauer F., Yap D., Humphries RK., Griffith OL., Shah S., Zhu H., Kimbara M., Shashkin P., Charlot JF., Tcherpakov M., Corbett R., Tam A., Varhol R., Smailus D., Moksa M., Zhao Y., Delaney A., Qian H., Birol I., Schein J., Moore R., Holt R., Horsman DE., Connors JM., Jones S., Aparicio S., Hirst M., Gascoyne RD., Marra MA. (2010. Somatic mutations altering EZH2 (Tyr641) in follicular and diffuse large B-cell lymphomas of germinal-center origin. Nat Genet.42(2),181-5.

Mortusewicz O., Roth W., Li N., Cardoso M. C., Meisterernst M., and Leonhardt H. (2008). Recruitment of RNA polymerase II cofactor PC4 to DNA damage sites. J Cell Biol.183, 769-776.

Mortusewicz O., Evers B., Helleday T. (2016). PC4 promotes genome stability and DNA repair through binding of ssDNA at DNA damage sites. Oncogene.35(6),761-70.

Mujtaba S., He Y., Zeng L., Yan S., Plotnikova O., Sachchidanand, Sanchez R., Zeleznik-Le NJ., Ronai Z. and Zhou MM. (2004). Structural mechanism of the bromodomain of the coactivator CBP in p53 transcriptional activation. Mol Cell 13:251-263.

Mukhopadhyay D., Dasso M. (2007). Modification in reverse: the SUMO proteases. Trends Biochem Sci.32(6),286-95.

Müller S., Ronfani L., Bianchi ME. (2004). Regulated expression and subcellular localization of HMGB1, a chromatin protein with a cytokine function. J Intern Med. 255(3),332-43.

Munshi N., Merika M., Yie J., Senger K., Chen G., and Thanos D. (1998). Acetylation of HMG I(Y) by CBP turns off IFN beta expression by disrupting the enhanceosome. Mol Cell. 2,457-467.

Munshi N, Yie Y, Merika M, Senger K, Lomvardas S, Agalioti T, Thanos D. (1999). The IFN-beta enhancer: a paradigm for understanding activation and repression of inducible gene expression. Cold Spring Harb Symp Quant Biol.64,149-59.

Munshi N., Agalioti T., Lomvardas S., Merika M., Chen G., Thanos D. (2001). Coordination of a transcriptional switch by HMGI(Y) acetylation. Science 293,1133-1136.

Murga M., Jaco I., Fan Y., Soria R., Martinez-Pastor B., Cuadrado M., Yang S-M., Blasco M A., Skoultchi A I., Fernandez-Capetillo O. (2007). Global chromatin compaction limits the strength of the DNA damage response. J Cell Biol. 178(7),1101-1108.

Nan, X., Ng, H.H., Johnson, C.A., Laherty C.D., Turner B.M., Eisenman R.N., Bird A. (1998). Transcriptional repression by the methyl-CpG-binding protein MeCP2 involves a histone deacetylase complex. Nature. 393, 386–389.

Neupane M., Clark AP., Landini S., Birkbak NJ., Eklund AC., Lim E., Culhane AC., Barry WT., Schumacher SE., Beroukhim R., Szallasi Z., Vidal M., Hill DE., Silver DP. (2016). MECP2 Is a Frequently Amplified Oncogene with a Novel Epigenetic Mechanism That Mimics the Role of Activated RAS in Malignancy. Cancer Discov.6(1),45-58.

Nielsen AL., Oulad-Abdelghani M., Ortiz JA., Remboutsika E., Chambon P., Losson R. (2001). Heterochromatin formation in mammalian cells: interaction between histones and HP1 proteins. Mol Cell.7(4),729-39.

Nikitina T., Shi X., Ghosh R.P., Horowitz-Scherer R.A., Hansen J.C., Woodcock C.L. (2007). Multiple modes of interaction between the methylated DNA binding protein MeCP2 and chromatin. Mol. Cell. Biol. 27, 864–877.

Nissen MS., Reeves R. (1995). Changes in superhelicity are introduced into closed circular DNA by binding of high mobility group protein I/Y. J Biol Chem.270,4355.

Noordermeer D., Branco Miguel R., Splinter E., Klous P., IJcken W van., Swagemakers S., Koutsourakis M., Spek P van der., Pombo A., Laat W de. (2008). Transcription and Chromatin Organization of a Housekeeping Gene Cluster Containing an Integrated β-Globin Locus Control Region. PLoS Genet 4(3), e1000016.

Nora EP., Lajoie BR., Schulz EG., Giorgetti L., Okamoto I., Servant N., Piolot T., van Berkum NL., Meisig J., Sedat J., Gribnau J., Barillot E., Blüthgen N., Dekker J., Heard E. (2012). Spatial partitioning of the regulatory landscape of the X-inactivation centre. Nature. 485,381–385.

Norwood LE., Moss TJ., Margaryan NV., Cook SL., Wright L., Seftor EA., Hendrix MJ., Kirschmann DA., Wallrath LL. (2006). A requirement for dimerization of HP1Hsalpha in suppression of breast cancer invasion. J Biol Chem. 281(27),18668-76.

Nguyen DX., Baglia LA., Huang SM., Baker CM. and McCance DJ. (2004). Acetylation regulates the differentiation-specific functions of the retinoblastoma protein. EMBO J 23:1609-1618.

North BJ., Marshall BL., Borra MT., Denu JM. and Verdin E. (2003). The human Sir2 ortholog, SIRT2, is an NAD+-dependent tubulin deacetylase. Mol Cell 11:437-444.

Ochiai K., Yamaoka M., Swaminathan A., Shima H., Hiura H., Matsumoto M., Kurotaki D., Nakabayashi J., Funayama R., Nakayama K., Arima T., Ikawa T., Tamura T., Sciammas R., Bouvet P., Kundu TK., Igarashi K. (2020). Chromatin Protein PC4 Orchestrates B Cell Differentiation by Collaborating with IKAROS and IRF4. Cell Rep.33(12),108517.

Ohkuni K., Yamashita I. (2000). A transcriptional autoregulatory loop for KIN28-CCL1 and SRB10-SRB11, each encoding RNA polymerase II CTD kinase-cyclin pair, stimulates the meiotic development of S. cerevisiae. Yeast.16,829–846.

Olins A.L. and Olins D.E. (1974). Spheroid chromatin units (v bodies). Science. 183, 330–332.

Olson C.O., Zachariah R.M., Ezeonwuka C.D., Liyanage, V.R., Rastegar M. (2014). Brain region-specific expression of MeCP2 isoforms correlates with DNA methylation within Mecp2 regulatory elements. PLoS ONE. 9, e90645.

Ong PC., Golding SJ., Pearce MC., Irving JA., Grigoryev SA., Pike D., Langendorf CG., Bashtannyk-Puhalovich TA., Bottomley SP., Whisstock JC., Pike RN., McGowan S. (2009). Conformational change in the chromatin remodelling protein MENT. PLoS One.4(3),e4727.

Okosun J., Bödör C., Wang J., Araf S., Yang CY., Pan C., Boller S., Cittaro D., Bozek M., Iqbal S., Matthews J., Wrench D., Marzec J., Tawana K., Popov N., O'Riain C., O'Shea D., Carlotti E., Davies A., Lawrie CH., Matolcsy A., Calaminici M., Norton A., Byers RJ., Mein C., Stupka E., Lister TA., Lenz G., Montoto S., Gribben JG., Fan Y., Grosschedl R., Chelala C., Fitzgibbon J. (2014). Integrated genomic analysis identifies recurrent mutations and evolution patterns driving the initiation and progression of follicular lymphoma. Nat Genet.46(2):176-181.

Okamura S., Ng CC., Koyama K., Takei Y., Arakawa H., Monden M., Nakamura Y. (1999). Identification of seven genes regulated by wild-type p53 in a colon cancer cell line carrying a well-controlled wild-type p53 expression system. Oncol Res.11(6):281-5.

Okumura K., Mendoza M., Bachoo RM., DePinho RA., Cavenee WK. Furnari FB. (2006). PCAF modulates PTEN activity. J Biol Chem.281,26562-26568.

Paeschke K., Bochman ML., Garcia PD., Cejka P., Friedman KL., Kowalczykowski SC., Zakian VA. (2013). Pif1 family helicases suppress genome instability at G-quadruplex motifs. Nature.497,458–462.

Pan Z. Q., Ge H., Amin A. A., and Hurwitz J. (1996). Transcription-positive cofactor 4 forms complexes with HSSB (RPA) on single-stranded DNA and influences HSSB-dependent enzymatic synthesis of simian virus 40 DNA. J. Biol.Chem. 271, 22111-22116.

Pash JM., Alfonso PJ., Bustin M. (1993). Aberrant expression of high mobility group chromosomal protein 14 affects cellular differentiation. J Biol Chem.268,13632.

Pasheva E., Sarov M., Bidjekov K., Ugrinova I., Sarg B., Lindner H. and Pashev IG. (2004). *In vitro* acetylation of HMGB-1 and -2 proteins by CBP: the role of the acidic tail. Biochemistry 43:2935-2940.

Patel JH., Du Y., Ard PG, Phillips C.., Carella B., Chen CJ., Rakowski C., Chatterjee C., Lieberman PM., Lane WS., Blobel GA. and McMahon SB. (2004). The c-MYC oncoprotein is a substrate of the acetyltransferases hGCN5/PCAF and TIP60. Mol Cell Biol.24,10826-10834.

Pavan Kumar P., Bischof O., Purbey P., Notani D., Urlaub H., Dejean A., Galande S. (2007). Functional interaction between PML and SATB1 regulates chromatin-loop architecture and transcription of the MHC class I locus. Nat. Cell Biol. 9,45–56.

Peters AH., O'Carroll D., Scherthan H., Mechtler K., Sauer S., Schöfer C., Weipoltshammer K., Pagani M., Lachner M., Kohlmaier A., Opravil S., Doyle M., Sibilia M., Jenuwein T. (2001). Loss of the Suv39h histone methyltransferases impairs mammalian heterochromatin and genome stability. Cell.107(3),323-37.

Phair RD., Scaffidi P., Elbi C., Vecerova J., Dey A., Ozato K., Brown DT., Hager G., Bustin M., Misteli T. (2004). Global nature of dynamic protein-chromatin interactions

in vivo: three-dimensional genome scanning and dynamic interaction networks of chromatin proteins. Mol Cell Biol.24,6393.

Phillips-Cremins JE., Corces VG. (2013). Chromatin insulators: linking genome organization to cellular function. Mol Cell. 50,461–474.

Phillips-Cremins JE., Sauria ME., Sanyal A., Gerasimova TI., Lajoie BR., Bell JS., Ong CT., Hookway TA., Guo C., Sun Y., Bland MJ., Wagstaff W., Dalton S., McDevitt TC., Sen R., Dekker J., Taylor J., Corces VG. (2013). Architectural protein subclasses shape 3D organization of genomes during lineage commitment. Cell.153,1281–1295.

Pierantoni GM., Conte A., Rinaldo C., Tornincasa M., Gerlini R., Valente D., Izzo A., Fusco A. (2016). Hmga1 null mouse embryonic fibroblasts display downregulation of spindle assembly checkpoint gene expression associated to nuclear and karyotypic abnormalities. Cell Cycle.15(6):812-8.

Pil PM., Lippard SJ. (1992). Specific binding of chromosomal protein HMG1 to DNA damaged by the anticancer drug cisplatin. Science. 256,234.

Pines A., Vrouwe MG., Marteijn JA., Typas D., Luijsterburg MS., Cansoy M., Hensbergen P., Deelder A., de Groot A., Matsumoto S., Sugasawa K., Thoma N., Vermeulen W., Vrieling H., Mullenders L. (2012). PARP1 promotes nucleotide excision repair through DDB2 stabilization and recruitment of ALC1. J Cell Biol.199(2),235-49.

Poirier MG., Bussiek M., Langowski J., Widom J. (2008). Spontaneous access to DNA target sites in folded chromatin fibers. J. Mol. Biol. 379,772–786.

Polesskaya A., Duquet A., Naguibneva I., Weise C., Vervisch A., Bengal E., Hucho F., Robin P., HarelBellan A. (2000). CREB-binding protein/p300 activates MyoD by acetylation. J Biol Chem.275,34359-34364.
Polito P., Dal Cin P., Kazmierczak B., Rogalla P., Bullerdiek J., Van den Berghe H. (1999). Deletion of HMG17 in uterine leiomyomas with ring chromosome 1. Cancer Genet Cytogenet.108(2):107-9.

Pope BD., Ryba T., Dileep V., Yue F., Wu W., Denas O., Vera DL., Wang Y., Hansen RS., Canfield TK., Thurman Robert E., Cheng Y., Gülsoy G., Dennis Jonathan H., Snyder Michael P., Stamatoyannopoulos John A., Taylor J., Hardison Ross C., Kahveci T., Ren B., Gilbert David M. (2014). Topologically associating domains are stable units of replication-timing regulation. Nature.515,402–405.

Popova EY., Claxton DF., Lukasova E., Bird PI., Grigoryev SA. (2006). Epigenetic heterochromatin markers distinguish terminally differentiated leukocytes from incompletely differentiated leukemia cells in human blood. Exp Hematol.;34(4):453-62.

Popova EY., Grigoryev SA., Fan Y., Skoultchi AI., Zhang SS., Barnstable CJ. (2013). Developmentally regulated linker histone H1c promotes heterochromatin condensation and mediates structural integrity of rod photoreceptors in mouse retina. J Biol Chem. 288,17895-17907.

Pruss D., Reeves R., Bushman FD., Wolffe AP. (1994). The influence of DNA and nucleosome structure on integration events directed by HIV integrase. J Biol Chem.269,25031.

Qian D., Zhang B., Zeng XL., Le Blanc JM., Guo YH., Xue C., Jiang C., Wang HH., Zhao TS., Meng MB., Zhao LJ., Hao JH., Wang P., Xie D., Lu B., Yuan ZY. (2014). Inhibition of human positive cofactor 4 radiosensitizes human esophageal squmaous cell carcinoma cells by suppressing XLF-mediated nonhomologous end joining. Cell Death Dis.5(10),e1461.

Qiu Y., Zhao Y., Becker M., John S., Parekh BS., Huang S., Hendarwanto A., Martinez ED., Chen Y., Lu H., Adkins NL., Stavreva DA., Wiench M., Georgel PT., Schiltz RL.,Hager GL. (2006). HDAC1 acetylation is linked to progressive modulation of steroid receptor-induced gene transcription. Mol Cell.22,669-679.

Rao SSP., Huntley MH., Durand NC., Stamenova EK., Bochkov ID., Robinson JT., Sanborn AL., Machol I.,Omer AD., Lander ES., Aiden EL.(2014). A 3D Map of the Human Genome at Kilobase Resolution Reveals Principles of Chromatin Looping. Cell. 159(7),1665-80.

Ray Chaudhuri A., Nussenzweig A. (2017). The multifaceted roles of PARP1 in DNA repair and chromatin remodelling. Nat Rev Mol Cell Biol.18(10),610-621.

Reeves R., Nissen MS. (1990). The A.T-DNA-binding domain of mammalian high mobility group I chromosomal proteins. A novel peptide motif for recognizing DNA structure. J Biol Chem.265,8573.

Reeves R., Nissen MS. (1993). Interaction of high mobility group-I (Y) nonhistone proteins with nucleosome core particles. J Biol Chem.268,21137.

Reeves R., Wolffe AP. (1996). Substrate structure influences binding of the non-histone protein HMG-I(Y) to free nucleosomal DNA. Biochemistry.35,5063.

Reeves R., Leonard WJ., Nissen MS. (2000). Binding of HMG-I(Y) imparts architectural specificity to a positioned nucleosome on the promoter of the human interleukin-2 receptor alpha gene. Mol Cell Biol.20,4666.

Reeves R., Beckerbauer L. (2001). HMGI/Y proteins: flexible regulators of transcription and chromatin structure. Biochim Biophys Acta.1519,13–29.

Reeves R. (2010). HMG Nuclear Proteins: Linking Chromatin Structure to Cellular Phenotype. Biochim Biophys Acta.1799,1-2.

Reeves R., Adair JE. (2005). Role of high mobility group (HMG) chromatin proteins in DNA repair. DNA Repair (Amst).4(8),926-38.

Reddy KL., Rovani M K., Wohlwill A., Katzen A., Storti Robert V. (2006).
The Drosophila Par domain protein I gene, Pdp1, is a regulator of larval growth, mitosis and endoreplication. Dev Biol. 289(1),100-14.

Reddy K. L., Zullo J. M., Bertolino E., Singh H. (2008). Transcriptional repression mediated by repositioning of genes to the nuclear lamina. Nature 452,243–247.

Ribeyre C., Lopes J., Boule JB., Piazza A., Guedin A., Zakian VA., Mergny JL., Nicolas A. (2009). The yeast Pif1 helicase prevents genomic instability caused by G-quadruplex-forming CEB1 sequences *in vivo*. PLoS Genet.5, e1000475.

Ricci MA., Manzo C., García-Parajo MF., Lakadamyali M., Cosma MP. (2015). Chromatin fibers are formed by heterogeneous groups of nucleosomes *in vivo*. Cell.160(6),1145-58.

Richmond TJ., Davey CA. (2003). The structure of DNA in the nucleosome core. Nature. 423,145–150.

Riveiro-Falkenbach E., Soengas MS. (2010). Control of tumorigenesis and chemoresistance by the DEK oncogene. Clin Cancer Res.16(11),2932-8.

Robinson PJJ., Rhodes D. (2006). Structure of the ‘30 nm' chromatin fibre: a key role for the linker histone. Curr Opin Struct Biol 16,336–343.

Robu M., Shah RG., Petitclerc N., Brind'Amour J., Kandan-Kulangara F., Shah GM. (2013). Role of poly(ADP-ribose) polymerase-1 in the removal of UV-induced DNA lesions by nucleotide excision repair. Proc Natl Acad Sci U S A.110(5),1658-63.

Rohs R.,West SM., Sosinsky A., Liu P., Mann R S., and Honig B. (2009). The role of DNA shape in protein-DNA recognition. Nature 461,1248–1253.

Rossetto D., Avvakumov N., Côté J. (2012). Histone phosphorylation: a chromatin modification involved in diverse nuclear events. Epigenetics.7(10),1098-108.

Roth SY., Allis CD. (1992). Chromatin condensation: does histone H1 dephosphorylation play a role? Trends Biochem Sci.17,93-8.

Ruginis T., Taglia L., Matusiak D., Lee BS., Benya RV. (2006). Consequence of gastrin-releasing peptide receptor activation in a human colon cancer cell line: a proteomic approach. J Proteome Res.5(6),1460-8.

Ryan D.P. and Tremethick D.J. (2018). The interplay between H2A.Z and H3K9 methylation in regulating HP1α binding to linker histone-containing chromatin. Nucleic Acids Res.46(18),9353-9366.

Sabari BR., Zhang D., Allis CD., Zhao Y. (2017). Metabolic regulation of gene expression through histone acylations. Nat Rev Mol Cell Biol.18(2),90-101.

Samavarchi-Tehrani P., Golipour A., David L., Sung HK., Beyer TA., Datti A., Woltjen K., Nagy A., Wrana JL. (2010). Functional genomics reveals a BMP-driven mesenchymal-to-epithelial transition in the initiation of somatic cell reprogramming. Cell Stem Cell.7(1),64-77.

Sanborn AL., Rao SS., Huang SC., Durand NC., Huntley MH., Jewett AI., Bochkov ID., Chinnappan D., Cutkosky A., Li J., Geeting KP., Gnirke A., Melnikov A., McKenna D., Stamenova Elena K., Lander Eric S., Aiden EL. (2015). Chromatin extrusion explains key features of loop and domain formation in wild-type and engineered genomes. Proc Natl Acad Sci USA.112, E6456–6465.

Sancho M., Diani E., Beato M., Jordan A. (2008). Depletion of human histone H1 variants uncovers specific roles in gene expression and cell growth. PLoS Genet.4(10), e1000227.

Sandén C., Gullberg U. (2015). The DEK oncoprotein and its emerging roles in gene regulation. Leukemia.29(8),1632-6.

Sang B., Sun J., Yang D., Xu Z., Wei Y. (2019). Ras-AKT signaling represses the phosphorylation of histone H1.5 at threonine 10 via GSK3 to promote the progression of glioma. Artif Cells Nanomed Biotechnol.47(1):2882-2890.

Sanulli S., Trnka MJ., Dharmarajan V., Tibble RW., Pascal BD., Burlingame AL., Griffin PR., Gross JD., Narlikar GJ. (2019). HP1 reshapes nucleosome core to promote phase separation of heterochromatin. Nature. 575(7782),390-394.

Sartorelli V., Puri PL., Hamamori Y., Ogryzko V., Chung G., Nakatani Y., Wang JY., Kedes L. (1999). Acetylation of MyoD directed by PCAF is necessary for the execution of the muscle program. Mol Cell. 4,725-734.

Saunders C.J., Minassian B.E., Chow E.W., Zhao W., Vincent J.B. (2009). Novel exon 1 mutations in MECP2 implicate isoform MeCP2_e1 in classical Rett syndrome. Am. J. Med. Genet. Part A 149, 1019–1023.

Sawatsubashi S., Murata T., Lim J., Fujiki R., Ito S., Suzuki E., Tanabe M., Zhao Y., Kimura S., Fujiyama S., Ueda T., Umetsu D., Ito T., Takeyama K., Kato S. (2010). A histone chaperone, DEK, transcriptionally coactivates a nuclear receptor. Genes Dev.24(2),159-70.

Scaffidi P. (2016) Histone H1 alterations in cancer. Biochim Biophys Acta.,1859(3):533-9.

Scaffidi P., Misteli T., Bianchi ME. Release of chromatin protein HMGB1 by necrotic cells triggers inflammation. Nature.418,191.

Schang LM., Hwang GJ., Dynlacht BD., Speicher DW., Bantly A., Schaffer PA., Shilatifard A., Ge H., Shiekhattar R. (2000). Human PC4 is a substrate-specifc inhibitor of RNA polymerase II phosphorylation. J Biol Chem. 275,6071–6074.

Schmidt A., Zhang H., Cardoso M C. (20200. MeCP2 and Chromatin Compartmentalization. Cells.9, 878.

Sdek P., Oyama K., Angelis E., Chan SS., Schenke-Layland K., MacLellan WR. (2013). Epigenetic regulation of myogenic gene expression by heterochromatin protein 1 alpha. PLoS One.8(3),e58319.

Seitan VC., Faure AJ., Zhan Y., McCord RP., Lajoie BR., Ing-Simmons E., Lenhard B., Giorgetti L., Heard E., Fisher AG., Flicek P., Dekker J., Merkenschlager M. (2013). Cohesin-based chromatin interactions enable regulated gene expression within preexisting architectural compartments. Genome Res. 23,2066–2077.

Seligson DB., Horvath S., Shi T., Yu H., Tze S., Grunstein M. and Kurdistani SK. (2005). Global histone modification patterns predict risk of prostate cancer recurrence. Nature.435,1262-1266.

Selvi B R., Pradhan SK., Shandilya J., Das C., Sailaja BS., Shankar G N., Gadad SS., Reddy A., Dasgupta D., Kundu TK. (2009). Sanguinarine interacts with chromatin, modulates epigenetic modifications, and transcription in the context of chromatin. Chem Biol.16,203-216.

Sen N., Hara MR., Kornberg MD., Cascio MB., Bae BI., Shahani N., Thomas B., Dawson TM., Dawson VL., Snyder SH., Sawa A. (2008). Nitric oxide-induced nuclear GAPDH activates p300/CBP and mediates apoptosis. Nat Cell Biol.10(7),866-73.

Serrano A., Rodríguez-Corsino M., Losada A. (2009). Heterochromatin protein 1 (HP1) proteins do not drive pericentromeric cohesin enrichment in human cells. PLoS One.4(4), e5118.

Sexton T., Yaffe E., Kenigsberg E., Bantignies F., Leblanc B., Hoichman M., Parrinello H., Tanay A., Cavalli G. (2012). Three-dimensional folding and functional organization principles of the Drosophila genome. Cell. 148,458–472.

Shakya A., Park S., Rana N., King JT. (2020). Liquid-Liquid Phase Separation of Histone Proteins in Cells: Role in Chromatin Organization. Biophys J. 118(3),753-764.

Shandilya J., Swaminathan V., Gadad S.S., Choudhari R., Kodaganur G.S., and Kundu T.K. (2009). Acetylated NPM1 localizes in the nucleoplasm and regulates transcriptional activation of genes implicated in oral cancer manifestation. Mol Cell Biol. 29, 5115-5127.

Sharma GG., Hwang KK., Pandita RK., Gupta A., Dhar S., Parenteau J., Agarwal M., Worman HJ., Wellinger RJ., Pandita TK. (2003). Human heterochromatin protein 1 isoforms HP1(Hsalpha) and HP1(Hsbeta) interfere with hTERT-telomere interactions and correlate with changes in cell growth and response to ionizing radiation. Mol Cell Biol.23(22),8363-76.

Sheikh T.I., de Paz A.M., Akhtar S., Ausió J., Vincent J.B. (2017). MeCP2_E1 N-terminal modifications affect its degradation rate and are disrupted by the Ala2Val Rett mutation. Hum. Mol. Genet. 26, 4132–4141.

Shiio Y., Eisenman RN. (2003). Histone sumoylation is associated with transcriptional repression. Proc Natl Acad Sci U S A. 100(23),13225-30.

Sikder S., Kumari S., Mustafi P., Sen S., Singhal NB., Chellappan S., Godbole M., Chandrani P., Dutt A., Gopinath KS., Kundu TK. (2019). Nonhistone human chromatin

protein PC4 is critical for genomic integrity and negatively regulates autophagy. FEBS J.10(64),6855-6869.

Sikder S., Kumari S., Kumar M., Sen S., Singhal NB., Chellappan S., Godbole M., Chandrani P., Dutt A., Gopinath KS., Kundu TK. (2019). Chromatin protein PC4 is downregulated in breast cancer to promote disease progression: Implications of miR-29a. Oncotarget.10(64),6855-6869.

Sikorski TW., Ficarro SB., Holik J., Kim T., Rando OJ., Marto JA., Buratowski S. (2011). Sub1 and RPA associate with RNA polymerase II at different stages of transcription. Mol Cell.44(3),397-409.

Silverman GA., Bird PI., Carrell RW., Church FC., Coughlin PB., Gettins PG., Irving JA., Lomas DA., Luke CJ., Moyer RW., Pemberton PA., Remold-O'Donnell E., Salvesen GS., Travis J., Whisstock JC. (2001). The serpins are an expanding superfamily of structurally similar but functionally diverse proteins. Evolution, mechanism of inhibition, novel functions, and a revised nomenclature. J Biol Chem.276(36),33293-6.

Simpson RT. (1978). Structure of the chromatosome, a chromatin particle containing 160 base pairs of DNA and all the histones. Biochemistry.17,5524-31.

Simonsson M., Heldin CH., Ericsson J. and Grönroos E. (2005). The balance between acetylation and deacetylation controls Smad7 stability. J Biol Chem.280:21797-21803.

Singleton MK., Gonzales ML., Leung KN., Yasui DH., Schroeder DI., Dunaway K., LaSalle JM. (2011). MeCP2 is required for global heterochromatic and nucleolar changes during activity-dependent neuronal maturation. Neurobiol Dis.43(1),190-200.

Sjöblom T., Jones S., Wood LD., Parsons DW., Lin J., Barber TD., Mandelker D., Leary RJ., Ptak J., Silliman N., Szabo S., Buckhaults P., Farrell C., Meeh P., Markowitz SD., Willis J., Dawson D, Willson JK, Gazdar AF, Hartigan J, Wu L, Liu C, Parmigiani G, Park BH., Bachman KE., Papadopoulos N., Vogelstein B., Kinzler KW., Velculescu VE. (2006) The consensus coding sequences of human breast and colorectal cancers. Science.;314(5797):268-74.

Skene P.J., Illingworth R.S., Webb S., Kerr A.R., James K.D., Turner D.J., Andrews R., Bird A.P. (2010). Neuronal MeCP2 is expressed at near histone-octamer levels and globally alters the chromatin state. Mol. Cell. 37, 457–468.

Sykes SM., Mellert HS., Holbert MA., Li K., Marmorstein R., Lane WS. and McMahon SB. (2006). Acetylation of the p53 DNA-binding domain regulates apoptosis induction. Mol Cell 24:841-851.

Smeenk G., Wiegant WW., Marteijn JA., Luijsterburg MS., Sroczynski N., Costelloe T., Romeijn RJ., Pastink A., Mailand N., Vermeulen W., van Attikum H. (2013). Poly(ADP-ribosyl)ation links the chromatin remodeler SMARCA5/SNF2H to RNF168-dependent DNA damage signaling. J Cell Sci. 126,889-903.

Smith E., Lin C., Shilatifard A. (2011). The super elongation complex (SEC) and MLL in development and disease. Genes Dev.25,661–672.

Soares LM., Zanier K., Mackereth C., Sattler M., Valcarcel J. (2006). Intron removal requires proofreading of U2AF/3' splice site recognition by DEK. Science.312,1961–1965.

Soekarman D., von Lindern M., Daenen S., de Jong B., Fonatsch C., Heinze B., Bartram C., Hagemeijer A., and Grosveld G. (1992). The translocation (6;9) (p23;q34) shows consistent rearrangement of two genes and defines a myeloproliferative disorder with specific clinical features. Blood. 79,2990–2997.

Sofueva S., Yaffe E., Chan WC., Georgopoulou D., Vietri Rudan M., Mira-Bontenbal H., Pollard SM., Schroth GP., Tanay A., Hadjur S. (2013). Cohesin-mediated interactions organize chromosomal domain architecture. EMBO J. 32,3119–3129.

Solier S., Sordet O., Kohn KW., Pommier Y. (2009). Death receptor-induced activation of the Chk2- and histone H2AX-associated DNA damage response pathways. Mol Cell Biol.29,68-82.

Song F., Chen P., Sun D., Wang M., Dong L., Liang D., Xu R.M., Zhu P. and Li G. (2014). Cryo-EM study of the chromatin fiber reveals a double helix twisted by tetranucleosomal units. Science. 344,376–380.

Springhetti EM., Istomina NE., Whisstock JC., Nikitina T., Woodcock CL., Grigoryev SA. (2003). Role of the M-loop and reactive center loop domains in the folding and bridging of nucleosome arrays by MENT. J Biol Chem. 278,43384–43393.

Squazzo SL., Costa PJ., Lindstrom DL., Kumer KE., Simic R., Jennings JL., Link AJ., Arndt KM., Hartzog GA. (2002). The Paf1 complex physically and functionally associates with transcription elongation factors *in vivo*. EMBO J. 21(7),1764-74.

Sun J., Wei HM., Xu J., Chang JF., Yang Z., Ren X., Lv WW., Liu LP., Pan LX., Wang X., Qiao HH., Zhu B., Ji JY., Yan D., Xie T., Sun FL., Ni JQ. (2015). Histone H1-mediated epigenetic regulation controls germline stem cell self-renewal by modulating H4K16 acetylation. Nat Commun.6,8856.

Su X., Yang Y., Ma L., Luo P., Shen K., Dai H., Jiang Y., Shuai L., Liu Z., You J., Min K., Shi C., Chen Z. (2020). Human Positive Coactivator 4 Affects the Progression and Prognosis of Pancreatic Ductal Adenocarcinoma via the mTOR/P70s6k Signaling Pathway. Onco Targets Ther.13,12213-12223.

Sun ZW., Allis CD. (2002). Ubiquitination of histone H2B regulates H3 methylation and gene silencing in yeast. Nature. 418(6893),104-8.

Suzuki M., Yamada T., Kihara-Negishi F., Sakurai T., Oikawa T. (2003). Direct association between PU.1 and MeCP2 that recruits mSin3A-HDAC complex for PU.1-mediated transcriptional repression. Oncogene.22, 8688–8698.

Steeg PS., Ouatas T., Halverson D., Palmieri D., Salerno M. (2003). Metastasis suppressor genes: basic biology and potential clinical use. Clin Breast Cancer. 4(1),51-62.

Steigemann B., Schulz A., Werten S. (2013). Bacteriophage T5 encodes a homolog of the eukaryotic transcription coactivator PC4 implicated in recombination-dependent DNA replication. J Mol Biol.425(22),4125-33.

Steliou K., Boosalis MS., Perrine SP., Sangerman J., Faller DV. (2012). Butyrate histone deacetylase inhibitors. Biores Open Access.1(4),192-8.

Sterner R., Vidali G. and Allfrey VG. (1979). Studies of acetylation and deacetylation in high mobility group proteins. Identification of the sites of acetylation in HMG-1. J Biol Chem 254:11577-1158.

Strom AR., Emelyanov AV., Mir M., Fyodorov DV., Darzacq X., Karpen GH. (2017). Phase separation drives heterochromatin domain formation. Nature. 547(7662),241-245.

Strukov YG., Belmont AS. (2009). Mitotic Chromosome Structure: Reproducibility of Folding and Symmetry between Sister Chromatids. Biophys J. 96(4),1617–1628.

Struhl K. (1998). Histone acetylation and transcriptional regulatory mechanisms. Genes Dev. 12,599-606.

Swaminathan A., Delage H., Chatterjee S., Belgarbi-Dutron L., Cassel R., Martinez N., Cosquer B., Kumari S., Mongelard F., Lannes B., Cassel JC., Boutillier AL., Bouvet P., Kundu TK. (2016). Transcriptional Coactivator and Chromatin Protein PC4 Is Involved in Hippocampal Neurogenesis and Spatial Memory Extinction. J Biol Chem.291(39),20303-14.

Syed SH., Goutte-Gattat D., Becker N., Meyer S., Shukla MS., Hayes JJ.,Everaers R., Angelov D., Bednar J., Dimitrov S. (2010). Single-base resolution mapping of H1-nucleosome interactions and 3D organization of the nucleosome. Proc Natl Acad Sci USA.107,9620-9625.

Tabbert A., Kappes F., Knippers R., Kellermann J., Lottspeich F., Ferrando-May E. (2006). Hypophosphorylation of the architectural chromatin protein DEK in death-receptor-induced apoptosis revealed by the isotope coded protein label proteomic platform. Proteomics.6(21),5758-72.

Taguchi A., Blood DC., del Toro G., Canet A., Lee DC., Qu W., Tanji N., Lu Y., Lalla E., Fu C., Hofmann MA., Kislinger T., Ingram M., Lu A., Tanaka H., Hori O., Ogawa S., Stern DM., Schmidt AM. (2000). Blockade of RAGE-amphoterin signalling suppresses tumour growth and metastases. Nature.405(6784),354-60.

Tai CI., Ying QL. (2013).Gbx2, a LIF/Stat3 target, promotes reprogramming to and retention of the pluripotent ground state. J Cell Sci.126,1093-8.

Talbert PB., Henikoff S. (2017). Histone variants on the move: substrates for chromatin dynamics. Nat Rev Mol Cell Biol.18(2),115-126.

Tanaka M., Hennebold JD., Macfarlane J., Adashi EY. (2001). A mammalian oocyte-specific linker histone gene H1oo: homology with the genes for the oocyte-specific cleavage stage histone (cs-H1) of sea urchin and the B4/H1M histone of the frog. Development.128,655 – 664.

Tang Y., Luo J., Zhang W. and Gu W. (2006). Tip60-dependent acetylation of p53 modulates the decision between cell-cycle arrest and apoptosis. Mol Cell 24:827-839.

Tang Y., Tian XC. JAK-STAT3 and somatic cell reprogramming. JAKSTAT.2(4),e24935.

Tan M., Luo H., Lee S., Jin F., Yang J. S., Montellier E., Buchou T., Cheng Z., Rousseaux S., Rajagopal N., Lu Z., Ye Z., Zhu Q., Wysocka J., Ye Y., Khochbin S., Ren B., Zhao Y. (2011). Identification of 67 histone marks and histone lysine crotonylation as a new type of histone modification. Cell. 146, 1016–1028.

Tavenet A., Suleau A., Dubreuil G., Ferrari R., Ducrot C., Michaut M., Aude JC., Dieci G., Lefebvre O., Conesa C., Acker J. (2009). Genome-wide location analysis reveals a role for Sub1 in RNA polymerase III transcription. Proc Natl Acad Sci USA.106,14265–14270.

Taylor GC., Eskeland R., Hekimoglu-Balkan B., Pradeepa MM. and Bickmore WA. (2013). H4K16acetylation marks active genes and enhancers of embryonic stem cells, but does not alter chromatin compaction. Genome Res.23,2053-2065.

Teloni F., and Altmeyer M. (2016). Readers of poly(ADP-ribose):designed to be fit for purpose. Nucleic Acids Res. 44,993–1006.

Terme JM., Sesé B., Millán-Ariño L., Mayor R., Izpisúa Belmonte JC., Barrero MJ., Jordan A. (2011). Histone H1 variants are differentially expressed and incorporated into chromatin during differentiation and reprogramming to pluripotency. J Biol Chem. 286(41),35347-57.

Thanos D., Maniatis T. (1995). Virus induction of human IFN beta gene expression requires the assembly of an enhanceosome. Cell.83,1091–1100.

Thevenet L., Méjean C., Moniot B., Bonneaud N., Galéotti N., Aldrian-Herrada G., Poulat F., Berta P., Benkirane M., Boizet-Bonhoure B. (2004). Regulation of human SRY subcellular distribution by its acetylation/deacetylation. EMBO J.23,3336-3345.

Thomas J. O. (1999). Histone H1: location and role. Curr. Opin. Cell Biol.11, 312-317.

Thomas JO., Travers AA. (2001). HMG1 and 2, and related 'architectural' DNA-binding proteins. Trends Biochem Sci.26,167.

Tie F., Banerjee R., Fu C., Stratton CA., Fang M, Harte PJ. (2016). Polycomb inhibits histone acetylation by CBP by binding directly to its catalytic domain. Proc Natl Acad Sci U S A.113(6),E744-53.

Tims HS., Gurunathan K., Levitus M., Widom J. (2011). Dynamics of nucleosome invasion by DNA binding proteins. J Mol Biol 411,430–448.

Torres CM., Biran A., Burney MJ., Patel H., Henser-Brownhill T., Cohen AS., Li Y., Ben-Hamo R., Nye E., Spencer-Dene B., Chakravarty P., Efroni S., Matthews N., Misteli T., Meshorer E., Scaffidi P. (2016). The linker histone H1.0 generates epigenetic and functional intratumor heterogeneity. Science.353(6307):aaf1644.

Tremethick DJ. (2007). Higher-order structures of chromatin: the elusive 30 nm fiber. Review Cell 128(4),651-4.

Trieschmann L., Alfonso PJ., Crippa MP., Wolffe AP., Bustin M. (1995). Incorporation of chromosomal proteins HMG-14/HMG-17 into nascent nucleosomes induces an extended chromatin conformation and enhances the utilization of active transcription complexes. EMBO J .14,1478.

Trojer P., Zhang J., Yonezawa M., Schmidt A., Zheng H., Jenuwein T., Reinberg D. (2015). Dynamic Histone H1 Isotype 4 Methylation and Demethylation by Histone Lysine Methyltransferase G9a/KMT1C and the Jumonji Domain-containing JMJD2/KDM4 Proteins. J Biol Chem. 284(13),8395-405.

Tzao C., Tung HJ., Jin JS., Sun GH., Hsu HS., Chen BH., Yu CP. and Lee SC. (2009). Prognostic significance of global histone modifications in resected squamous cell carcinoma of the esophagus. Mod Pathol.22,252-260.

Uchimura Y., Ichimura T., Uwada J., Tachibana T., Sugahara S., Nakao M., Saitoh H. (2006). Involvement of SUMO modification in MBD1- and MCAF1-mediated heterochromatin formation. J Biol Chem. 281(32),23180-90.

Ujvari A., Luse DS. (2006). RNA emerging from the active site of RNA polymerase II interacts with the Rpb7 subunit. Nat Struct Mol Biol.13,49–54.

Van Den Broeck A., Brambilla E., Moro-Sibilot D., Lantuejoul S., Brambilla C., Eymin B., Khochbin S. and Gazzeri S. (2008). Loss of histone H4K20 trimethylation occurs in preneoplasia and influences prognosis of non-small cell lung cancer. Clin Cancer Res.14,7237-7245.

Van Rechem C., Whetstine JR. (2014). Examining the impact of gene variants on histone lysine methylation. Biochim Biophys Acta.1839,1463–1476.

Varghese F., Bukhari AB., Malhotra R., De A. (2014). IHC Profiler: An open-source plugin for the quantitative evaluation and automated scoring of immunohistochemistry images of human tissue samples. PLoS One.9(5)e96801.

Venkatesh S., Workman JL. (2015). Histone exchange, chromatin structure and the regulation of transcription. Nat Rev Mol Cell Biol.16(3),178-89.

Vervoorts J., Lüscher-Firzlaff JM., Rottmann S., Lilischkis R., Walsemann G., Dohmann K., Austen M. and Lüscher B. (2003). Stimulation of c-MYC transcriptional activity and acetylation by recruitment of the cofactor CBP. EMBO Rep 4:484-490.

Vietri Rudan M., Barrington C., Henderson S., Ernst C., Odom DT., Tanay A., Hadjur S. (2015). Comparative HiC reveals that CTCF underlies evolution of chromosomal domain architecture. Cell Rep.10,1297–1309.

Vietri Rudan M., Hadjur S. (2015). Genetic Tailors: CTCF and Cohesin Shape the Genome During Evolution. Trends Genet. 31,651–660.

Vicent GP., Koop R., Beato M. (2002). Complex role of histone H1 in transactivation of MMTV promoter chromatin by progesterone receptor. J Steroid Biochem Mol Biol.83,15-23.

von Lindern M., Poustka A., Lerach H., and Grosveld G. (1990). The (6;9) chromosome translocation, associated with a specific subtype of acute nonlymphocytic leukemia, leads to aberrant transcription of a target gene on 9q34. Mol. Cell. Biol.10,4016–4026.

Vujatovic O., Zaragoza K., Vaquero A., Reina O., Bernués J., Azorín F. (2012). Nucleic Acids Res.40(12),5402-14.

Wacker DA., Ruhl DD., Balagamwala EH., Hope KM., Zhang T., Kraus WL. (2007). The DNA binding and catalytic domains of poly(ADP-ribose) polymerase 1 cooperate in the regulation of chromatin structure and transcription. Mol Cell Biol. 27,7475–7485.

Waidmann S., Kusenda B., Mayerhofer J., Mechtler K., Jonak C. (2014). A DEK domain-containing protein modulates chromatin structure and function in Arabidopsis. Plant Cell.26(11),4328-44.

Waldmann T., Eckerich C., Baack M., and Gruss C. (2002). The ubiquitous chromatin protein DEK alters the structure of DNA by introducing positive supercoils. J. Biol. Chem. 277,24988–24994.

Wang C., Fu M., Angeletti RH., Siconolfi-Baez L., Reutens AT., Albanese C., Lisanti MP., Katzenellenbogen BS., Kato S., Hopp T., Fuqua SA., Lopez GN., Kushner PJ., Pestell RG. (2001). Direct acetylation of the estrogen receptor alpha hinge region by p300 regulates transactivation and hormone sensitivity. J Biol Chem. 276,18375-18383.

Wang JY., Sarker AH., Cooper PK., Volkert MR. (2004). The single strand DNA binding activity of human PC4 prevents mutagenesis and killing by oxidative DNA damage. Mol Cell Biol.24,6084–6093.

Wang T., Chuffart F., Bourova-Flin E., Wang J., Mi J., Rousseaux S., Khochbin S. (2019). Histone variants: critical determinants in tumour heterogeneity. Front Med. 13(3):289-297.

Wang Z., Roeder RG. (1998). DNA topoisomerase I and PC4 can interact with human TFIIIC to promote both accurate termination and transcription reinitiation by RNA polymerase III. Mol Cell.1,749–757.

Wasenius VM., Hemmer S.., Kettunen E., Knuutila S., Franssila K., Joensuu H. (2003). Hepatocyte growth factor receptor, matrix metalloproteinase-11, tissue inhibitor of metalloproteinase-1, and fibronectin are up-regulated in papillary thyroid carcinoma: a cDNA and tissue microarray study. Clin Cancer Res.9(1):68-75.

Wasylishen AR., Kalkat M., Kim SS., Pandyra A., Chan PK., Oliveri S., Sedivy E., Konforte D., Bros C., Raught B. and Penn LZ (2014). MYC activity is negatively regulated by a C-terminal lysine cluster. Oncogene 33:1066-1072.

Watrin E., Kaiser FJ., Wendt KS. (2016). Gene regulation and chromatin organization: relevance of cohesion mutations to human disease. Curr Opin Genet Dev. 37,59–66.

Werten S., Kohler C., Bayer NJ., Steinmetz I., Hinrichs W. (2016). Structural analysis and knock-out of a Burkholderia pseudomallei homolog of the eukaryotic transcription coactivator PC4. Gene.577(2),140-7.

West KL. (2004). HMGN proteins play roles in DNA repair and gene expression in mammalian cells. Biochem Soc Trans.32,918.

Wise-Draper T.M., Mintz-Cole R.A., Morris T.A., Simpson D.S., Wikenheiser-Brokamp K.A., Currier M.A., Cripe T.P., Grosveld G.C., and Wells S.I. (2009). Overexpression of the cellular DEK protein promotes epithelial transformation *in vitro* and *in vivo.* Cancer Res. 69,1792–1799.

White AE., Hieb AR., Luger K. (2016). A quantitative investigation of linker histone interactions with nucleosomes and chromatin. Sci Rep. 6,19122.

Williams KA., Lee M., Winter JM., Gildea DE., Calagua C., Curry NL., Lichtenberg J., Ye H., Crawford NPS. (2018). Prostate cancer susceptibility gene HIST1H1A is a modulator of androgen receptor signaling and epithelial to mesenchymal transition. Oncotarget;9(47):28532-28546.

Williams SP., Athey BD., Muglia LJ., Schappe RS., Gough AH., Langmore JP. (1986). Chromatin fibers are left-handed double helices with diameter and mass per unit length that depend on linker length. Biophys J.49(1),233-48.

Wolffe A. P., Khochbin S., and. Dimitrov S. (1997). What do linker histones do in chromatin? Bioessays. 19, 249-255.

Woodcock CL., Skoultchi AI., Fan Y. (2006). Role of linker histone in chromatin structure and function: H1 stoichiometry and nucleosome repeat
length. Chromosome Res. 14,17-25.

Wreggett K A., Hill F., James P S., Hutchings A., Butcher G W., Singh P B. (1994). A mammalian homologue of Drosophila heterochromatin protein 1 (HP1) is a component of constitutive heterochromatin. Cytogenet Cell Genet.66(2),99-103.

Wright RH., Lioutas A., Le Dily F., Soronellas D., Pohl A., Bonet J., Nacht AS., Samino S., Font-Mateu J., Vicent GP., Wierer M., Trabado MA., Schelhorn C., Carolis C., Macias MJ., Yanes O., Oliva B., Beato M. (2016). ADP-ribose-derived nuclear ATP synthesis by NUDIX5 is required for chromatin remodeling. Science.352(6290),1221-5.

Xiao Y., Wang J., Qin Y., Xuan Y., Jia Y., Hu W., Yu W., Dai M., Li Z., Yi C., Zhao S., Li M., Du S., Cheng W., Xiao X., Chen Y., Wu T., Meng S., Yuan Y., Liu Q., Huang W., Guo W., Wang S. and Deng W. (2015). Ku80 cooperates with CBP to promote COX-2 expression and tumor growth. Oncotarget 6:8046-8061.

Xu Y., Sumter TF., Bhattacharya R., Tesfaye A., Fuchs EJ., Wood LJ., Huso DL., Resar LM. (2004). The HMG-I oncogene causes highly penetrant, aggressive lymphoid malignancy in transgenic mice and is overexpressed in human leukemia. Cancer Res. 64(10):3371-5.

Yamagata T., Mitani K., Oda H., Suzuki T., Honda H., Asai T., Maki K., Nakamoto T., Hirai H. (2000). Acetylation of GATA-3 affects T-cell survival and homing to secondary lymphoid organs. EMBO J. 19,4676-4687.

Yamazaki H., Iwano T., Otsuka S., Kagawa Y., Hoshino Y., Hosoya K., Okumura M., Takagi S. (2015). SiRNA knockdown of the DEK nuclear protein mRNA enhances apoptosis and chemosensitivity of canine transitional cell carcinoma cells. Vet J.204(1),60-5.

Yang CS., Lopez CG., Rana TM. (2011). Discovery of nonsteroidal anti-inflammatory drug and anticancer drug enhancing reprogramming and induced pluripotent stem cell generation. Stem Cells.29(10),1528-36.

Yang MH., Nickerson S., Kim ET., Liot C., Laurent G., Spang R., Philips MR., Shan Y., Shaw DE., Bar-Sagi D., Haigis MC., Haigis KM. (2012). Regulation of RAS oncogenicity by acetylation. Proc Natl Acad Sci U S A 109:10843-10848.

Yang SM., Kim BJ., Norwood Toro L., Skoultchi AI. (2013). H1 linker histone promotes epigenetic silencing by regulating both DNA methylation and histone H3 methylation. Proc Natl Acad Sci U S A.110(5),1708-13.

Yang Y., Liu K., Liang Y., Chen Y. and Gong Y. (2015). Histone acetyltransferase inhibitor C646 reverses epithelial to mesenchymal transition of human peritoneal mesothelial cells via blocking TGF-beta1/Smad3 signaling pathway in vitro. Int J Clin Exp Pathol 8:2746-2754.

Yao YL., Yang WM., and Seto E. (2001). Regulation of transcription factor YY1 by acetylation and deacetylation. Mol Cell Biol. 21,5979-5991.

Yie J., Senger K., Thanos D. (1999). Mechanism by which the IFN-beta enhanceosome activates transcription. Proc Natl Acad Sci USA.96,13108.

Yi SA., Ryu HW., Lee DH., Han JW., Kwon SH. (2014). HP1β suppresses metastasis of human cancer cells by decreasing the expression and activation of MMP2. Int J Oncol. 45(6):2541-8.

Yu L., Volkert MR. (2013). Differential requirement for SUB1 in chromosomal and plasmid double-strand DNA break repair. PLoS One 8, e58015.

Yuan ZL., Guan YJ., Chatterjee D., and Chin YE. (2005). Stat3 dimerization regulated by reversible acetylation of a single lysine residue. Science. 307,269-273.

Zaidi MR., Okada Y., Chada KK. (2006). Misexpression of full-length HMGA2 induces benign mesenchymal tumors in mice. Cancer Res. 66(15):7453-9.

Zhang K., Faiola F. and Martinez E. (2005). Six lysine residues on c-Myc are direct substrates for acetylation by p300. Biochem Biophys Res Commun. 336:274-280.

Zhang T., Liu X., Chen X., Wang J., Wang Y., Qian D., Pang Q., Wang P. (2018). Inhibition of PC4 radiosensitizes non-small cell lung cancer by transcriptionally suppressing XLF. Cancer Med.7(4),1326-1337.

Zhao LY., Tong DD., Xue M., Ma HL., Liu SY., Yang J., Liu YX., Guo B., Ni L., Liu LY., Qin YN., Wang LM., Zhao XG., Huang C. (2017). MeCP2, a target of miR-638, facilitates gastric cancer cell proliferation through activation of the MEK1/2-ERK1/2 signaling pathway by upregulating GIT1. Oncogenesis.6(7),e368.

Zhao P., Kavarthapu R., Anbazhagan R., Liao M., Dufau ML. (2018). Interaction of positive coactivator 4 with histone 3.3 protein is essential for transcriptional activation of the luteinizing hormone receptor gene. Biochim Biophys Acta Gene Regul Mech.1861(10),971-981.

Zhao T., Qiu B., Zhou S., Ding G., Cao L., Wu Z. (2019). Expression of DEK in pancreatic cancer and its correlation with clinicopathological features and prognosis. J Cancer. 10(4):911-917.

Zhou BR., Feng H., Kato H., Dai L., Yang Y., Zhou Y., Bai Y. (2013). Structural insights into the histone H1-nucleosome complex. Proc Natl Acad Sci USA.110,19390-19395.

Zhou BR., Jiang J., Feng H., Ghirlando R., Xiao TS., Bai Y. (2015). Structural mechanisms of nucleosome recognition by linker histones. Mol Cell. 59,628–638.

Zhou BR., Feng H., Ghirlando R., Li S., Schwieters CD., Bai Y. (2016). A Small Number of Residues Can Determine if Linker Histones Are Bound On or Off Dyad in the Chromatosome. J Mol Biol.428(20),3948-3959.

Zhou Y., Gerrard DL., Wang J., Li T., Yang Y., Fritz AJ., Rajendran M., Fu X., Stein G., Schiff R., Lin S., Frietze S., Jin VX. (2019). Temporal dynamic reorganization of 3D chromatin architecture in hormone-induced breast cancer and endocrine resistance. Nat Commun.10(1),1522.

Zlatanova J., Caiafa P., and Van Holde, K. (200). Linker histone binding and displacement: versatile mechanism for transcriptional regulation. FASEB J. 14, 1697-1704.

Zuin J., Dixon JR., van der Reijden MI., Ye Z., Kolovos P., Brouwer RW., van de Corput MP., van de Werken HJ., Knoch TA., van IWF., Grosveld Frank G., Ren B., Wendt KS. (2014). Cohesin and CTCF differentially affect chromatin architecture and gene expression in human cells. Proc Natl Acad Sci U S A.111,996–1001.